University of Nottingham
UK | CHINA | MALAYSIA

‘Identification of bioactive lipids associated with osteoarthritis pain and pathology through targeted lipidomic analyses’

James Turnbull, BSc (Hons)

Thesis submitted to the University of Nottingham for the degree of Doctor of Philosophy

May 2023

Supervised by: Professors Victoria Chapman,

David A. Barrett, & Ana M. Valdes

Supported by: NIHR Nottingham Biomedical Research Centre

Abstract

Osteoarthritis (OA) is the leading cause of disability in the older population and is characterised by the degradation of the affected joint and development of chronic pain. There are currently no approved treatments that halt or reverse the joint pathology, and current treatments for associated pain are unsuitable for long-term treatment. There is also the need to identify those at high risk of developing OA that would benefit from early intervention. The oxylipins are oxidised lipid metabolites of polyunsaturated fatty acids (PUFAs), which play a central role in the regulation of the inflammatory response. They have also been reported to be involved in pain signalling and so present as attractive potential biomarkers and therapeutic targets for OA. This thesis aimed to develop methods to quantify a panel of pro- and anti-inflammatory oxylipins in biological samples using liquid chromatography-mass spectrometry (LC-MS/MS); and apply this method to clinical and pre-clinical studies involving participants with OA and animal models of the disease. The LC-MS/MS method developed covered the omega-3 and omega-6 PUFAs and many of their metabolites including eicosanoids, docosanoids, and endocannabinoids. The method was optimised over a 25 minute run time which allowed good separation of isomeric compounds and was sensitive into the picomolar range. Application of the method to plasma and serum collected from healthy volunteers (n=10) found significantly high levels of many oxylipins in serum compared to plasma. In a longitudinal study of healthy young adults who had suffered acute knee injury and are at high risk of developing OA in the future (n=47), levels of omega-3 PUFAs and their metabolites were significantly higher immediately after injury compared to later time points and controls. The opposite was observed for pro-inflammatory eicosanoids, which were significantly lower immediately after injury compared to later time points. At two years after injury, levels of the DHETs (metabolites of soluble epoxide hydrolase (sEH)) were associated with worse knee symptom scores. Measuring the oxylipins in a community cohort of people with varying levels knee pain and OA (n=154) identified metabolites of LOX and CYP450 as being associated with radiographic OA. Levels of 8,9-EET, 14,15-DHET, 12-HpETE, and

AEA were also associated with measures of self reported pain. Stratification of participants based pain and radiographic OA scores showed significantly higher levels of several EETs, 14- & 17-HDHA, and the HETEs. Baseline levels of 8,9-EET, 5-HETE, and 5,6-DHET were also associated with pain scores collected at 3 years follow-up. Using the destabilisation of the medial meniscus (DMM) model of OA, oxylipins were measured at 4, 8, and 12 weeks post model induction. Levels of prostaglandins, HETEs, EETs, and 12-HpETE were associated with synovitis and cartilage degradation scores at 4 and 8 weeks post-surgery; and levels of 17-HDHA were associated with less pain at 16-weeks post-injury. Targeting the sEH enzyme in the DMM model using an inhibitor called TPPU showed complete reversal of pain behaviour, decreased levels of DHETs, and increased EET:DHET ratios. Levels of 8,9-DHET were also associated with worse pain scores. During the COVID-19 pandemic the method was repurposed and serum from n=50 patients were measured for their oxylipin profile. Levels of both pro- and anti-inflammatory oxylipins were significantly higher in COVID-19 patients compared to controls. There were significant positive correlations between specialised pro-resolving mediators (SPMs), pro-inflammatory bioactive lipids, and anti-spike antibody binding. Levels of linoleic acid and 5,6-DHET were significantly lower in SARS-CoV-2 patients who died. These studies suggest a role of the oxylipins in OA pathology and associated pain phenotypes, and identify potential targets for therapeutic intervention for both joint pathology and pain. Through validation in replication cohorts, there is also the potential of using key oxylipins identified here, to predict future pain score. Future studies should look at the difference between serum/plasma and synovial fluid profiles of oxylipins in people with OA which may gave further mechanistic insight into their role in the pathogenesis of OA.

Accepted Publications

James Turnbull, Rakesh Jha, Catherine A. Ortori, Eleanor Lunt, Patrick J. Tighe, William L. Irving, Sameer A. Gohir, Dong-Hyun Kim, Ana M. Valdes, Alexander W. Tarr, David A. Barrett, Victoria Chapman. **Serum levels of pro-inflammatory lipid mediators and specialized pro-resolving molecule pathways are greatly increased in SARS-CoV-2 patients and correlate with markers of the adaptive immune response.** Journal of Infectious Diseases. 2022. DOI: 10.1093/infdis/jiab632

Peter R. W. Gowler, James Turnbull, Mohsen Shahtaheri, Sameer Gohir, Tony Kelly, Cindy McReynolds, Yang Jun, Rakesh R. Jha, Gwen S Fernandes, Weiya Zhang, Michael Doherty, David A. Walsh, Bruce D. Hammock, Ana M. Valdes, David A. Barrett, Victoria Chapman. **Clinical and preclinical evidence for roles of soluble epoxide hydrolase in osteoarthritis knee pain.** Arthritis Rheumatol. 2021. doi: 10.1002/art.42000.

Amrita Vijay, Afroditi Kouraki, Sameer Gohir, James Turnbull, Anthony Kelly, David A. Barrett, William Bulsiewicz, Ana M. Valdes. **The anti-inflammatory effect of bacterial short chain fatty acids is partially mediated by endocannabinoids.** Gut Microbes. 2021. https://doi.org/10.1080/19490976.2021.1997559

Robert E. Turnbull, Katrin N. Sander, James Turnbull, David A. Barrett, Alison H. Goodall. **Profiling eicosanoids released from platelets activated through GPVI: the role of COX-1 and 12-LOX.** Prostaglandins Other Lipid Mediat. 2021. DOI: 10.1016/j.prostaglandins.2021.106607

Sara V. Goncalves, Peter R. W. Gowler, Stephen G Woodhams; James Turnbull, Gareth J. Hathway, Victoria Chapman. **The challenges of treating osteoarthritis pain and opportunities for novel peripherally directed therapeutic strategies**. Neuropharmacology. 2022. https://doi.org/10.1016/j.neuropharm.2022.109075

Peter R. W. Gowler, James Turnbull, Mohsen Shahtaheri, Emma Jackson, Grace Keenan, David Walsh, David Barrett, Victoria Chapman. **Interplay between cellular changes in the knee joint, circulating lipids and pain behaviours in a slowly progressing murine model of osteoarthritis**. European Journal of Pain. 2022. https://doi.org/10.1002/ejp.2036

Submitted Manuscripts

James Turnbull, Rakesh R. Jha, Dong-Hyun Kim, David A. Barrett, Ana M. Valdes, Jennifer Alderson, Andrew Williams, Tonia L. Vincent, Fiona E. Watt, Victoria Chapman. **The impact of acute knee injury in active healthy adults on serum levels of pro- and anti-inflammatory lipid mediators and associations with knee pain.** [American Journal of Sports Medicine].

Amrita Vijay, Afroditi Kouraki, Cristina Menni, James Turnbull, Victoria Chapman, Tim D. Spector, Ana M. Valdes. **Dietary fibre supplementation increases circulating endocannabinoid levels in middle aged individuals. [**Food & Function].

Susan J. Franks, Peter R.W. Gowler, Joanne L. Dunster, James Turnbull, Sameer A. Gohir, Anthony Kelly, Ana M. Valdes, John R. King, David A. Barrett, V. Chapman, Simon Preston. **Mathematical Model for Metabolism of DHA.**

Manuscripts in preparation

James Turnbull, Rakesh R. Jha, Peter R. W. Gowler, Dong-Hyun Kim, David A. Barrett, David A. Walsh, Ana M. Valdes, Victoria Chapman. **Associations between serum oxylipin levels with measures of pain and pathology in osteoarthritis patients.** [Target: Annals of Rheumatic Diseases]

James Turnbull, Rakesh R Jha, Catharine A. Ortori, Dong-Hyun Kim, Ana M Valdes, Victoria Chapman, & David A Barrett. **Comprehensive comparison of oxylipin profiles in human serum and plasma.** [Target: Journal of Lipid Research]

Peter R. W. Gowler, James Turnbull, Rakesh R. Jha, Asta Tranholm, Paul Millns, Tony Kelly, Sameer Gohir, Susan Franks, David Onion, David A. Barrett, Ana Valdes, and Victoria Chapman. **Identification of genes associated with 17-HDHA expression in circulating monocytes in people with osteoarthritis pain.**

Declaration

The content of this thesis is the presentation of original research, and has not been submitted anywhere else for any other qualification. The contribution of others to the work presented here is detailed in relevant chapters. This work was carried out at the University of Nottingham, under the supervision of Professors Victoria Chapman (School of Life Sciences), David Barrett (School of Pharmacy), and Ana Valdes (School of Medicine).

Acknowledgements

I would firstly like to thank the NIHR for funding the studentship that supported me through this PhD. I would like to give a huge thank you to my supervisors Vicky Chapman, Dave Barrett, Ana Valdes, and Dong-Hyun Kim for their on-going support and encouragement throughout this PhD. I am grateful to the members of the Pain Centre versus arthritis and the Centre for Analytical Bioscience for their support and friendship over the years. In particular, I would like to thank Cath Ortori and Rakesh Jha from the CAB group for their help with the analytical aspects of the project, and to Peter Gowler from the Pain Centre for working with me on the pre-clinical studies. This thesis have involved working with many collaborators, to whom I am very grateful for their enthusiasm and support of my work. I am also grateful to all the participants involved in the clinical studies presented in this thesis, for giving up their time and donation of samples for this research. I would finally like to thank all my friends and family for their encouragement and support over the past four years, particularly my partner Tom for always keeping me positive and motivated.

Key Abbreviations

AA – arachidonic acid

COX -cyclooxygenase

CYP450 – cytochrome P450

DHA – docosahexaenoic acid

DHET - dihydroxyeicosatrienoic acid

EET - epoxyeicosatrienoic acid

EPA – eicosapentaenoic acid

HETE – hydroxyeicosatetraenoic acids

HODE - hydroxyoctadecadienoic acid

HPLC – High-performance liquid chromatography

KL – Kellgren-Lawrence

LA – linoleic acid

LC – liquid chromatography

LC-MS/MS – liquid chromatography-mass spectrometry

LOQ – Limit of quantification

LOX - lipoxygenase

LX - lipoxin

Mar - maresin

MRM – Multiple reaction monitoring

MS – mass spectrometry

NRS – Numerical rating scale

NSAID – Non-steroidal anti-inflammatory drug

OA – Osteoarthritis

oxoODE - oxo-octadecadienoic acid

PG - prostaglandin

PUFA – polyunsaturated fatty acid

QST – Quantitative sensory testing

Rv - resolvin

sEH – soluble epoxide hydrolase

SPE – solid phase extraction

SPM – specialised pro-resolving mediator

TPPU - N-[1-(1-oxopropyl)-4-piperidinyl]-N’-[4-(trifluoromethoxy)phenyl)-urea

TX – thromboxane

Table of Contents

Contents

Chapter One

General Introduction

1.1 Osteoarthritis

Worldwide, the leading cause of disability in the middle-aged and older population is osteoarthritis (OA) which is estimated to affect over 303 million people across the globe (Abate, Abebe et al. 2018). In the UK alone, approximately one in ten adults have symptomatic, clinically diagnosed OA, with the knee being the most common joint affected (Swain, Sarmanova et al. 2020). This widespread disease can affect people of any age and have huge impact on quality of life, however is most prevalent in the older population and has a higher frequency in women (Hame and Alexander 2013). OA is defined by breakdown of cartilage in the joint leading to narrowing of joint space, inflammation of the synovium, and formation of bone spurs (Figure 1). Hallmark symptoms of OA include chronic pain, joint stiffness, loss of mobility, and muscle weakness. These symptoms often lead to people with OA also suffering a sequelae of conditions including depression, anxiety, and social isolation - which can in turn perpetuate symptoms of OA (Sharma, Kudesia et al. 2016). OA is generally caused by long-term 'wear and tear' or trauma to the joint, and is also a common co-morbidity to other diseases such as obesity, cardiovascular disease, and diabetes (Swain, Kamps et al. 2022). Although any joint can be affected, the most common joints to exhibit OA are the knee, hip, hand, foot, and spine (Johnson and Hunter 2014). The focus of this thesis will be on the knee joint and associated pain.

Currently the physiological and biochemical changes that occur during the pathogenesis of this disease are poorly understood, and there are currently no approved therapies that stop the progression of, or reverse OA joint pathology. It is becoming accepted that although the phenotype presented in later stages of OA is common across OA sufferers, the underlining causes driving the pathology may differ. This would implicate that more targeted therapies would need to be developed in order to treat the particular underlying pathological mechanisms driving the progression of OA in a particular patient (Blaker, Clarke et al. 2017).

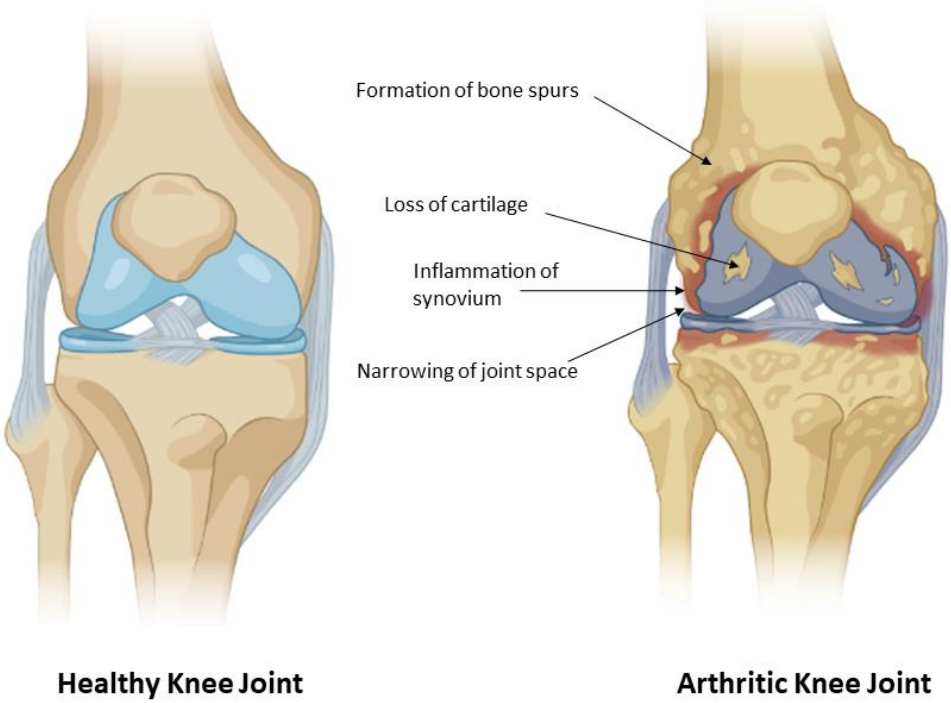

Figure 1. Comparative diagram of a healthy and osteoarthritic knee joints. Made using biorender.com

Chronic pain is a defining feature of OA, as there are currently no approved treatments that target the underlying causes of OA in the joint, the focus of treating patients currently relies on treating the symptomatic pain associated with the disease and improving the general physical and mental health of patients. Physiotherapy is often coupled with treating pain pharmacologically, which includes opioid-based and non-steroidal anti-inflammatory drugs (NSAIDs) painkillers, which also carry their own adverse side effects (da Costa, Pereira et al. 2021). Surgical interventions, which include osteotomy, joint fusion, joint distraction, and joint replacement are often performed in severe cases of OA (Bijlsma, Berenbaum et al. 2011) and are also combined with traditional analgesics during recovery.

Osteoarthritis results in significant cost for health service through care, individuals through loss of earning, and to employers. In the UK the estimated annualeconomic cost of arthritis to the NHS was £10.2 billion (Versus Arthritis, 2021). As an aging population, and with risk factors of OA such as obesity on

the rise, the prevalence of OA is only set to increase - putting an even higher demand on healthcare providers worldwide and posing a pressing socio-economic problem (Long, Liu et al. 2022). An increased understanding of the morphology and molecular aetiology that drives the pathogenesis of OA is essential for the future development of novel therapeutic approaches to treat OA.

1.2 The therapeutic potential of Bioactive Lipid Mediators

'Bioactive lipids' is a diverse term that encompasses various families of lipid molecules that have a diverse range of physiological and pathological functions in living organisms (Park, Choi et al. 2021). The focus of this thesis is on the oxylipins, which are oxidised metabolites of omega-3 and omega-6 polyunsaturated fatty acids (PUFAs). Due to their significant involvement in cellular signalling and mediation of biological processes, these lipids, along with their biosynthetic and metabolic pathways are potential therapeutic targets for the treatment of a wide range of diseases. One of the most studied biological processes involving the oxylipins is inflammation - the bodies' response to pathogenic invasion and tissue damage. The oxylipins are central in the regulation of the initiation, propagation, and resolution phases of inflammation (Figure 2) (Chiurchiù, Leuti et al. 2018). It is hypothesised that dysregulation of this carefully coordinated response could be a driving mechanism for chronic inflammatory diseases such as, arthritis, cancer, Alzheimer's disease, diabetes, and cardiovascular disease (Chiurchiù, Leuti et al. 2018). Therefore, the need to understand the complex roles and actions of individual lipids in biological processes, along with the changes occur in the lipidome in specific diseases proves a challenging but worthwhile area of research.

This thesis will focus mainly on two of the omega-6 and two of the omega-3 polyunsaturated fatty acids (PUFAs) and their downstream metabolites. The omega-6 PUFAs include arachidonic acid (AA) and linoleic acid (LA), which are 20 and 18 carbon long fatty acid chains respectively, and in general are the precursors to pro-inflammatory metabolites, traditionally called eicosanoids

(Dusting and Stewart 1990). The omega-3 PUFAs eicosapentaenoic acid (EPA) and docosahexaenoic acid (DHA) which are 20 and 22 carbons long respectively (Figure 3) are precursors to the anti-inflammatory and pro-resolution metabolites called the specialised pro-resolving mediators (SPMs). The balance of these pathways is thought to be a key regulator of the inflammatory response with dysregulation contributing to chronic inflammatory diseases.

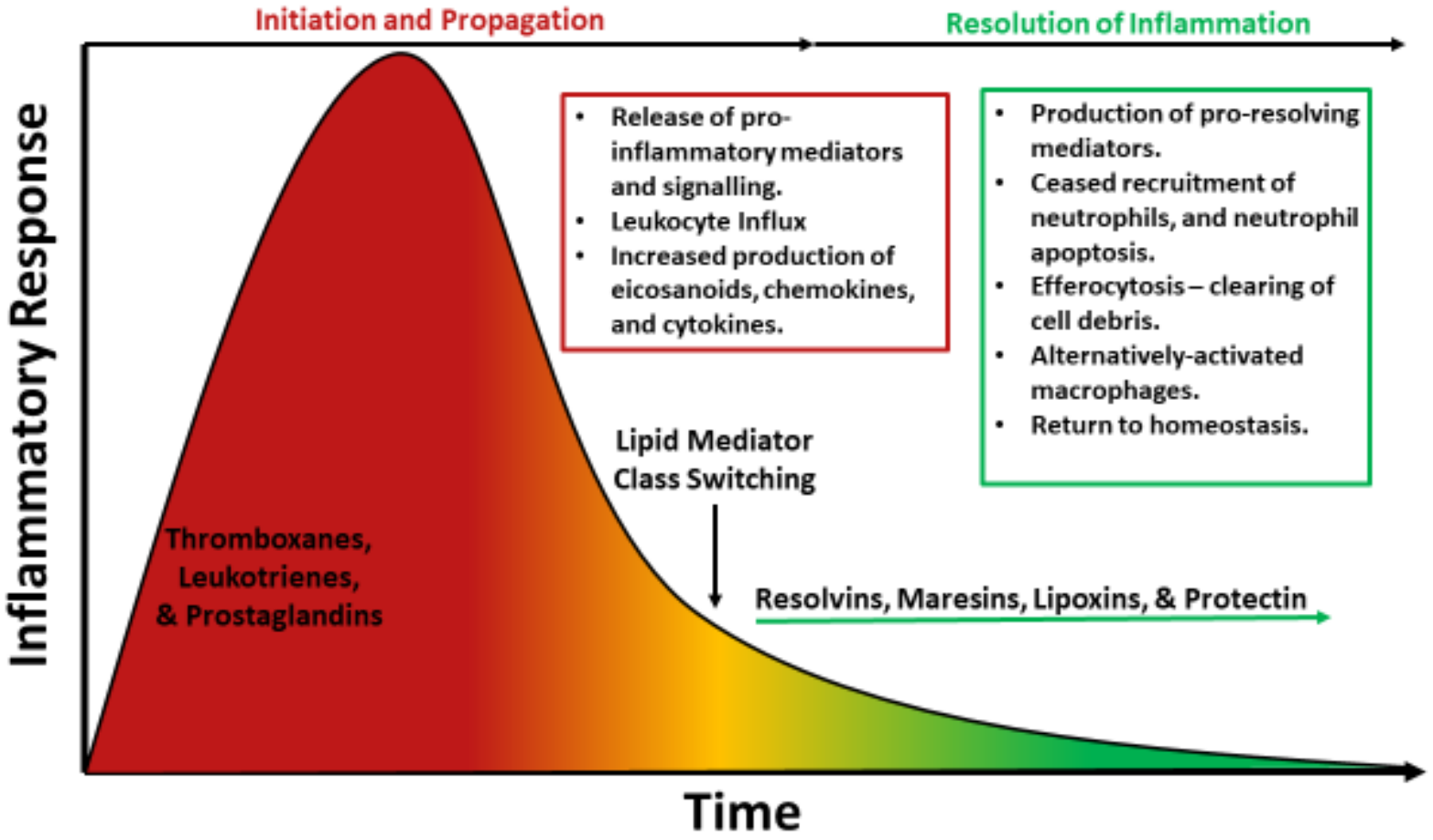

Figure 2. Reported roles of key lipid mediators involved in the inflammatory response. Adapted from (Serhan 2017)

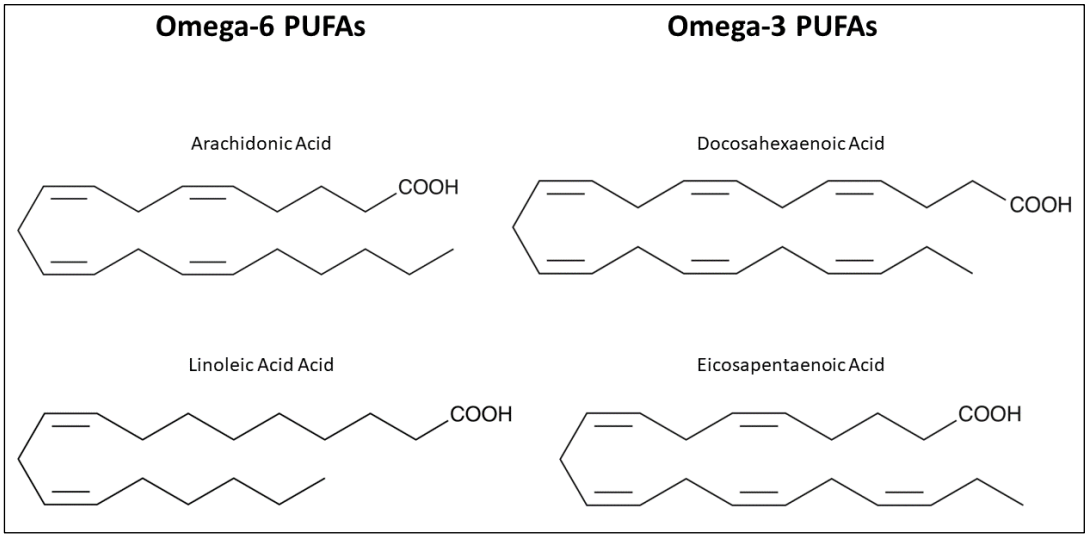

Figure 3. Structures of omega-6 (AA and LA) and omega-3 (EPA and DHA) PUFAs.

The first sub-class of oxylipins to be studied for their role in inflammation were the eicosanoids; derived in the most part from AA, this sub group of lipids includes the prostaglandins, leukotrienes, and thromboxanes (Figure 4). Their role in the initiation of inflammation was extensively investigated and led to the development of NSAIDs that inhibit the COX enzymes – an enzyme responsible for the production of some pro-inflammatory eicosanoids. Although effective at reducing acute inflammation, such as in response to pathogens or trauma; the use of these drugs long-term to treat chronic inflammatory is far from ideal. Side effects of these drugs include heart attack, gastro-intestinal bleeds, and kidney disease (Chiurchiu, Leuti, & Maccarrone, 2018). Thus, the need to understand the cellular mechanisms surrounding chronic inflammatory diseases is crucial in the process of developing effective treatments.

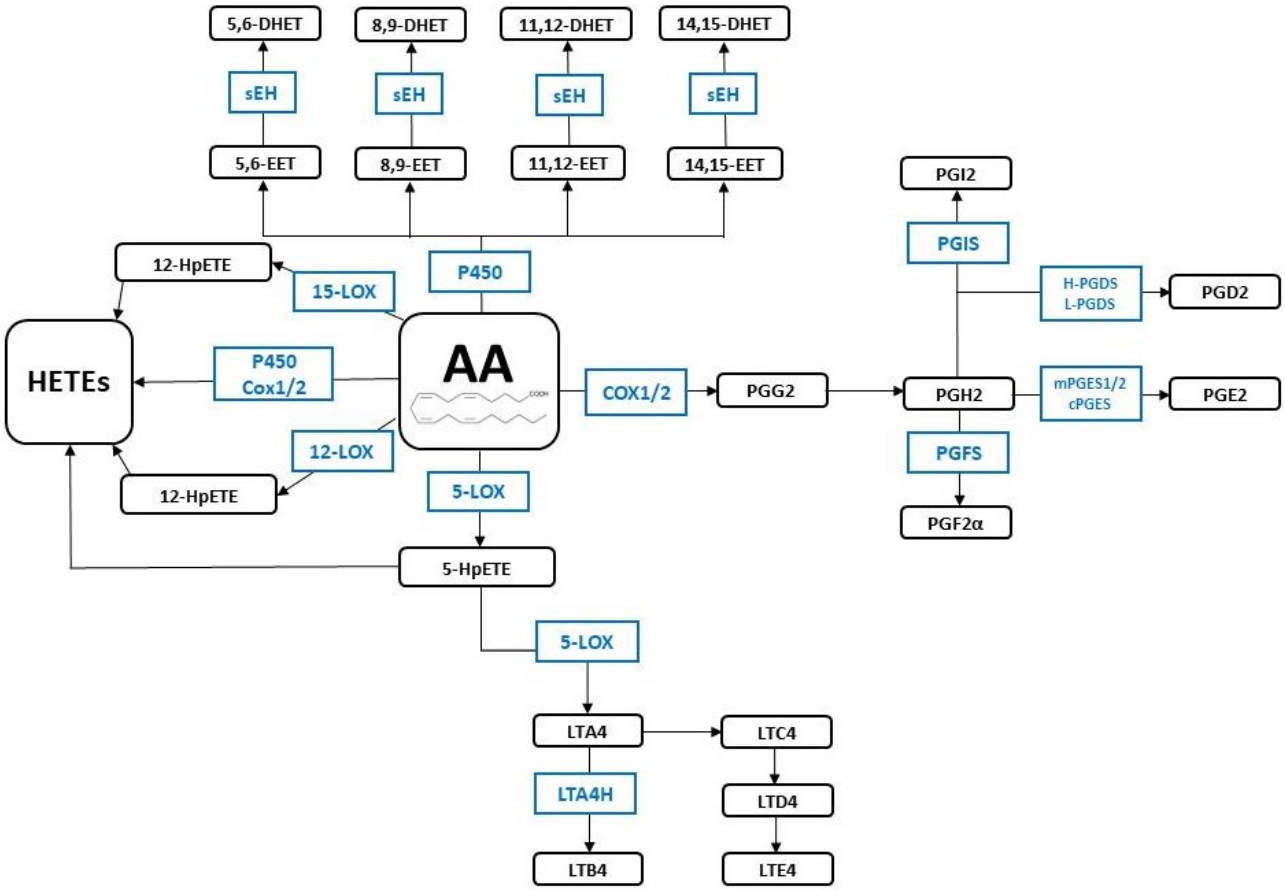

Figure 4. Pathway diagram of arachidonic acid cascade, highlighting key lipid mediators and enzymatic pathways.

Until the early 2000s, the resolution of inflammation was thought to be a passive process involving the gradual dispersal of pro-inflammatory cytokines and lipid mediators. It wasn't until Serhan and colleagues suggested that resolution was an active process involving its own collection of anti-inflammatory or 'pro-resolution' mediators and cells that the passive process was questioned (Serhan, Hong et al. 2002). Extensive studies by Serhan and colleagues have led to the discovery of lipid classes with pro-resolution properties, appropriately termed 'resolvins'. Closely followed by discovery of the maresin (Serhan, Yang et al. 2009) and protectin (Serhan, Gotlinger et al. 2006) lipid classes. The pathways that produce the SPMs share some common enzymes with those of the classical eicosanoids including LOX enzymes and CYP450, however COX-1/2 is not currently thought to be involved in these pathways. The unearthing of these lipids and their pathways (Figure 5) unveiled many new potential drug targets and analogues that could potentially harness the body's own resolution mechanisms and may have less risk of adverse side-effects. This quickly became a keen area of interest for researchers of inflammation and related diseases whose focus now is to develop pharmaceuticals that drive the body's own internal biochemical pathways down a pro-resolution path. These agonists have been coined 'immunoresolvents' by the Serhan group, and show potential in treatment of a wide variety of inflammatory diseases (Serhan 2017).

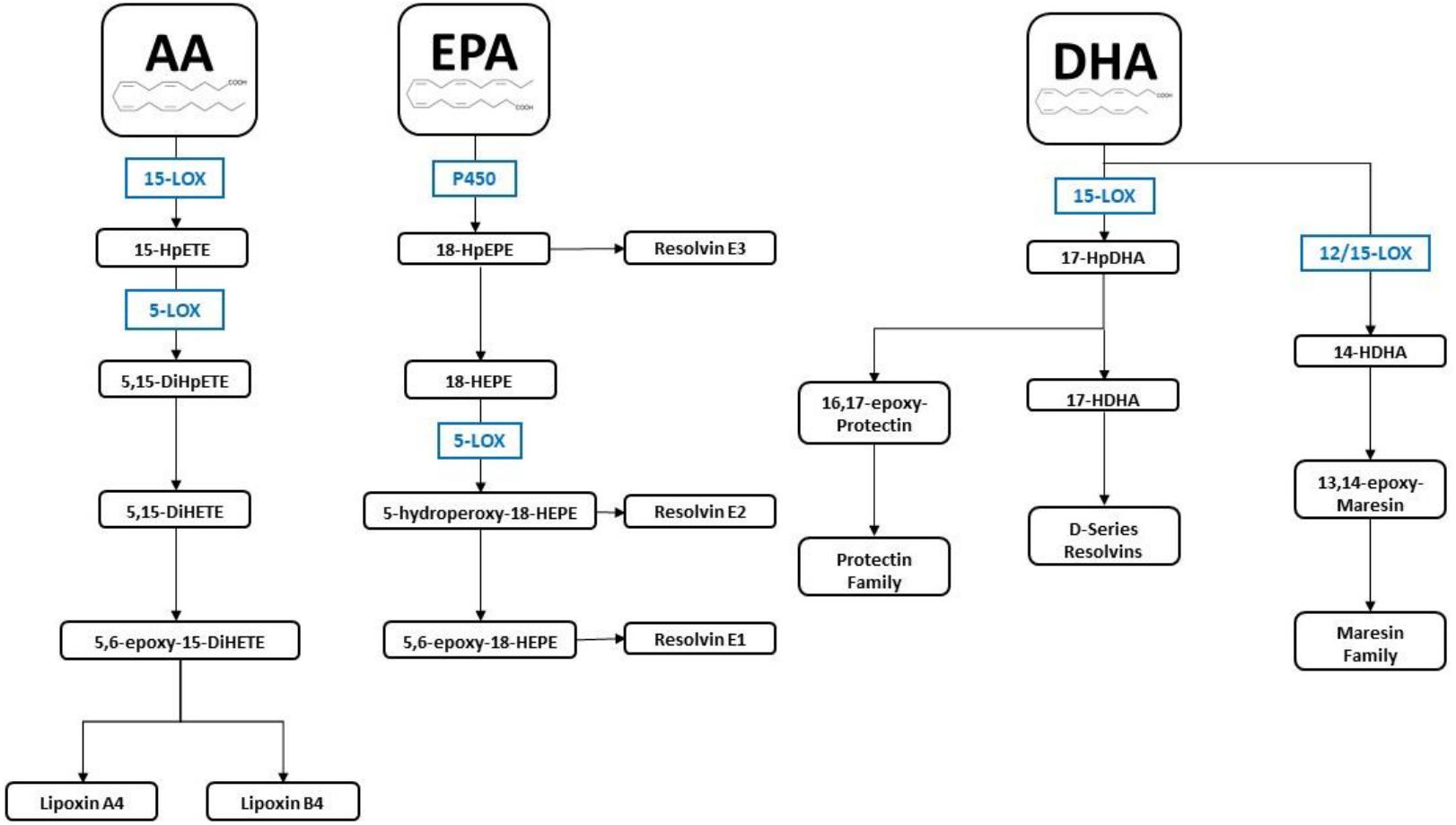

Figure 5. Pathway diagram of the synthesis of specialised pro-resolving mediators (SPMs) highlighting key lipid mediators and enzymatic pathways.

1.3 Roles of oxylipins in pain

1.3.1 Metabolites of Arachidonic Acid

Arachidonic acid is a 20-carbon omega-6 fatty acid found ubiquitously in mammalian cells. Under normal physiological conditions AA is membrane-bound, however, in response to inflammatory stimuli AA is released from the membrane by phospholipases (Gijón and Leslie 1999). This free AA is the precursor for a range of important lipid mediators known as the eicosanoids generated by three distinct enzymatic pathways; the cyclooxygenase (COX) pathway (Ricciotti and FitzGerald 2011), the lipoxygenase (LOX) pathway, and the cytochrome P450 (CYP450) pathway (Roman 2002).

1.3.2 Prostanoids

The prostanoids are pro-nociceptive and pro-inflammatory metabolites of AA downstream of the COX pathway (Jang, Kim et al. 2020). Following the phospholipase A2 mediated release of AA from the plasma membrane it is converted to prostaglandin H2 (PGH2) by COX1/2, before being transformed into prostaglandin E2 (PGE2), prostaglandin D2 (PGD2), prostacyclin (PGI2), prostaglandin F2α, (PGF2α), and thromboxane A2 (TXA2) by specific synthases (Ricciotti and FitzGerald 2011). The prostaglandins and thromboxane A2 are collectively known as the prostanoids. These metabolites all exert their effects through G protein-coupled receptors, specifically the PGD2 receptors (DP1 & DP2), the 4 PGE2 receptors (EP1, EP2, EP3, EP4), the PGF receptor (FP), the PGI receptor (IP), and the TXA receptor (TP) (Narumiya and FitzGerald 2001, Pettipher 2008). The prostanoids are well established as important nociceptive mediators, indeed aspirin, the first NSAID to be synthesised in the late 1800's, reduces pain and inflammation through inhibition of prostaglandin production by irreversible acetylation of the cyclooxygenases (COX) (Smith & Willis, 1971).

More recently synthesised NSAIDs share this same mode of action, blocking prostaglandin production through COX inhibition (Shen 1972).

Under normal physiological conditions COX-1 is stably expressed in both the dorsal horn of the spinal cord (Ebersberger, Grubb et al. 1999) and small diameter nociceptive neurons (Chopra, Giblett et al. 2000). Conversely COX2 is not thought to be constitutively expressed in these tissues but is rather inducible by inflammation (Beiche, Scheuerer et al. 1996, Ebersberger, Grubb et al. 1999). A recent study investigated the expression of precursor PUFAs and oxylipins across the pain pathway in rats (Domenichiello, Sapio et al. 2021). Under basal conditions, the prostanoid pre-cursor AA was predominantly expressed in the DRG and the dorsal horn of the spinal cord, whilst in the hind paw linoleic acid was more abundant (Domenichiello, Sapio et al. 2021). This study also highlighted the expression of the prostaglandin synthases which mediate the conversion of PGH2 to the different prostaglandins and thromboxanes. The results of these analysis showed that Ptges3 (a prostaglandin E synthase) was highly expressed across all aspects of the pain pathway, whilst Prostaglandin D2 synthase (Ptgds) was more abundantly expressed in the DRG and dorsal horn than the peripheral tissues (Domenichiello, Sapio et al. 2021). In these normal physiological conditions, PGE2 was highly expressed in both the hind-paw and the dorsal horn, whilst Thromboxane B2 (TXB2) was more abundantly expressed in the dorsal horn compared to the hind-paw (Domenichiello, Sapio et al. 2021). Following intra-plantar injection of carrageenan to induce inflammation and pain there were significant alterations in the local expression of these enzymes, COX2 expression increased 10-fold within the first hour, prostaglandin E synthases and prostaglandin I synthases were upregulated 4-hours post-injection, whilst thromboxane A synthase 1 (Tbaxas1) mRNA was upregulated from 24 hours post-injection (Domenichiello, Sapio et al. 2021). These data, alongside previous research that demonstrates the production of the prostaglandins by invading immune cells (Ma and Quirion 2005) highlights how the

machinery underlying prostanoid signalling is ubiquitous across the pain pathway.

PGE2 is a key peripheral nociceptive mediator, its effects are partly mediated by its ability to alter ion channel activity and subsequently alter neuronal sensitivity. It has been demonstrated to augment tetrodotoxin-resistant (TTX-R) Na^+ channel currents (England, Bevan et al. 1996), as well as inhibiting K_{Ca} channel mediated slow after-hyperpolarisation currents (Fowler, Wonderlin et al. 1985). The PGE2 induced enhancement of the firing frequency of small DRG neurons is also dependent on the activity of hyperpolarization-activated and cyclic nucleotide-gated (HCN) channels (Momin, Cadiou et al. 2008). PGE2 has also been demonstrated to increase the intracellular Cl^- concentration in DRG neurons which correlated with an increase in the expression of the Na^+-K^+-Cl^- co-transporter NKCC1 (Funk, Woitecki et al. 2008). Alongside these effects on ion channels PGE2 has also been shown to augment the activity of peripheral transducers such as P2X (Hamilton, Wade et al. 1999, Wang, Li et al. 2007), TRPA1 (Dall'Acqua, Bonet et al. 2014) and TRPV1 channels (Pitchford and Levine 1991, Moriyama, Higashi et al. 2005). In cultured rat DRG neurons, PGE2 was demonstrated to enhance the expression of the substance P (SP) receptor neurokinin 1 (NK1) (Banchet, Scholze et al. 2003). Other prostanoids also appear to display pro-nociceptive effects in the periphery but have not been researched as extensively as PGE2, with PGI2 being shown to decrease neuronal nociceptive threshold (Taiwo, Bjerknes et al. 1989), and potentiating TRPV1 activity (Pitchford and Levine 1991, Moriyama, Higashi et al. 2005), and PGD2 altering TTX-R Na^+ channels (Ebersberger, Natura et al. 2011)

Microglial activation is an important contributor to the maintenance of chronic pain in the dorsal horn of the spinal cord (Hains and Waxman 2006). Activated microglia produce and release PGE2 (Akundi, Candelario-Jalil et al. 2005), which directly affects the excitability of dorsal horn neurons

through the EP2 receptor (Zhao, Waxman et al. 2007). In nerve injury models in the rat PGD2 synthase is upregulated in dorsal horn microglia, suggesting an increase in the synthesis of PGD2 (Kanda, Kobayashi et al. 2013). Administration of a DP2 receptor antagonist attenuated nerve injury induced mechanical allodynia, supporting a contribution (Kanda, Kobayashi et al. 2013). Experiments in mice lacking L-PGDS confirmed that spinal cord PGD2 signalling is essential for the allodynia induced by PGE2 (Eguchi, Minami et al. 1999).

The effects of pharmacological agents targeted towards the prostanoid receptors support the role of these lipids as pro-nociceptive mediators. EP1, EP2, and EP4 antagonists have all been demonstrated to reduce inflammatory pain (Sekiguchi, Otoshi et al. 2011, Araldi, Ferrari et al. 2013). Agonists of the DP1 receptor increased DRG excitability by increasing TTX-resistant Na^+ channels (Ebersberger, Natura et al. 2011).

This evidence collectively highlights the critical importance of the prostanoids in the nociceptive pathway, however, as previously mentioned classical NSAIDs are not wholly efficacious over long-term use and are associated with adverse events. A significant amount of research has been focussed on either altering the pharmacology of NSAIDs to reduce the severity of these adverse events or inhibiting other aspects of the prostanoid signalling cascade in an attempt to produce robust analgesia. One strategy has been to co-administer an NSAID with a proton pump inhibitor, which are prescribed for gastro-intestinal (GI) diseases (Washio, Esaki et al. 2016, Rodríguez, Lanas et al. 2020). Whilst there is evidence that this combination treatment may protect against upper GI damage, it might actually worsen outcomes on the lower GI tract . Others have focussed on NSAIDs which release nitric oxide (NO) or hydrogen sulphide (H_2S), both of which are thought to have protective effects in the GI tract (Fiorucci, Distrutti et al. 2006). Naproxinod, an NO-releasing naproxen, reached clinical trials but was found not to be superior to naproxen so was

eventually withdrawn (Schnitzer, Hochberg et al. 2011). H_2S-releasing molecules such as the H_2S-naproxen compound, ATB-346 have now entered into clinical trials (Wallace, Nagy et al. 2020). Others have developed NSAIDS that release both NO and H_2S such as AVT-18A (Kashfi, Chattopadhyay et al. 2015) or NBS-1120 (Kodela, Chattopadhyay et al. 2015) which have both shown promising results in rats. Recent work has started to investigate intervening in the prostanoid pathways at different point. A study in dogs with spontaneous OA showed promising results from the inhibition of microsomal PGE Synthase-1 (mPGES1) which mediates the synthesis of PGE2 from PGH2 (Robertson-Plouch, Stille et al. 2017). Inhibition of prostanoid signalling can have important analgesic benefits, however, more work is needed to fully develop compounds which are safe and efficacious for chronic usage.

Leukotrienes

Leukotrienes are metabolites of the arachidonic acid cascade with a key role in driving inflammation. They are produced following two consecutive dioxygenation reactions catalysed by the 5-lipoxygenase (5-LOX) enzyme, this pathway was first identified in leukocytes where 5-LOX is highly expressed (Salmon and Higgs 1987). The production of leukotrienes is usually accompanied by prostaglandin synthesis and the release of histamine (Haeggstrom 2018). This sub-class of lipids has primarily been studied for their involvement in the pathogenesis of inflammatory diseases such as asthma and cardiovascular disease (Sasaki and Yokomizo 2019). However, in the last decade the potential pro-nociceptive roles of this class of lipids has been studied. Okubo et al detected increased expression of 5-LOX and FLAP, key enzymes in the production of leukotrienes, in the spinal microglia following spared nerve injury (SNI) surgery in rats (Okubo, Yamanaka et al. 2010). The biological effects of LTB4 are mediated mainly through its receptor BLT1, Ashara et al investigated the role of this pathway in a formalin induced model of pain. In both BLT1 knockout mice and in mice

pre-treated with a BLT1 inhibitor, they observed reduced nociception following injection with formalin (Asahara, Ito et al. 2015).

Hydroxyeicosatrienoic Acids (HETEs)

A separate and distinct class of lipid mediators, the hydroxyeicosatrienoic acids (HETEs), are also the product of the LOX pathway. The intermediary mediators hydroperoxyeicosatetraenoic acids (HpETEs) are produced from arachidonic acid by LOX enzymes before being reduced by the glutathione peroxidase system to the HETEs (Needleman, Truk et al. 1986). Separately, the formation of the 19- and 20- HETEs are catalysed by the CYP450 pathway (Roman 2002).

The chemical structure of the HPETEs is similar to the TRPV1 agonist capsaicin, and there is evidence that this class of lipid mediators may act as endogenous TRPV1 agonists. In primary rat DRG cultures and HEK cells expressing TRPV1, 12-(S)-HPETE, 15-(S)-HPETE, 5-(S)-HETE, and 15-(S)-HETE activated capsaicin sensitive channels, with the TRPV1 antagonist capsazepine blocking this effect (Hwang, Cho et al. 2000). Similarly, the CYP450 derived 20-HETE potentiates the TRPV1 response to capsaicin (Wen, Östman et al. 2012). 12-HPETE and 12-HETE increase afferent renal nerve activity via TRPV1 activation (Xie and Wang 2011). Collectively these studies support a potential role of local HETEs increasing peripheral primary afferent activity via TRPV1 activation leading to increased pain responses. Indeed, in a model of chronic osteoarthritis pain in the rat 12-HETE was upregulated in the knee joint, and 15-HETE was upregulated in the DRGs compared to saline controls (Wong, Sagar et al. 2014, Kelly, Chapman et al. 2015). In a model of UVB-induced inflammatory pain there was an increase in 5-HETE levels in the injured skin whilst simultaneously 12-HETE was upregulated in the DRGs in both rats and mice (Sisignano, Angioni et al. 2013). Interestingly, intra-plantar injection of 5-HETE in mice and 20-HETE in rats was sufficient to reduce mechanical withdrawal thresholds indicating

a painful response to their administration (Sisignano, Angioni et al. 2013, Hwang, Wagner et al. 2017). A recent study also suggested that 12-HETE and 15-HETE are able to suppress both the delta opioid receptor (DOR) and kappa opioid receptor (KOR) systems following inflammation (Sullivan, Chavera et al. 2017).

The pro-nociceptive roles of the leukotrienes and the HETEs alongside the potential contributions of the leukotrienes to the adverse effects of NSAIDs has led to development of joint COX-LOX inhibitors (Burnett and Levy 2012). One such drug was Licofelone which was found to produce a similar analgesia to naproxen (Gaur, Kori et al. 2009). However, despite completing phase III clinical trials in OA patients Licofelone has still not undergone regulatory submission yet.

Lipoxins

Unlike most of the other arachidonic acid metabolite sub-classes, the lipoxins have anti-inflammatory and analgesic bioactivity. Downstream of LTA4, Lipoxin A4 (LXA4) and Lipoxin B4 (LXB4) are produced by the combined action of 12/15-LOX and 5-LOX (Serhan and Samuelsson 1988). Cell types which possess both lipoxygenases are limited and therefore the production of lipoxins results primarily from transcellular metabolism (Sala, Folco et al. 2010) . Together with the resolvins, maresins, and protectins, which will be discussed elsewhere in this review, they make up the group termed specialised pro-resolving mediators (SPMs). These lipids share the physiological function of dampening the pro-inflammatory response and initiating the resolution phase and the return to tissue homeostasis. In a spinal hemisection model of pain in Wistar rats, exogenously dosed LXA4 reduced mechanical hypersensitivity through modulation of microglial activation and TNF-α release (Martini, Berta et al. 2016). LXA4 was also found to inhibit NLRP3 activation by regulating the JNK/beclin1/PI3KC3 pathway in rats with non-compressive disc herniation (Jin, Xie et al. 2020).

Analogues of lipoxins have been investigated for their analgesic potential. Lipoxin analogues successfully provided inhibited pain response in model of cancer induced bone pain, here through suppression of pro-inflammatory cytokines (Hu, Mao-Ying et al. 2012). Studies using the analogue aspirin triggered lipoxin (ATL) established that repeated intrathecal injection of ATL attenuated chronic constriction injury (CCI)-induced thermal hyperalgesia through inhibition of the NALP1 inflammasome (Li, Tian et al. 2013). Follow-up studies further revealed that ATL administration attenuated the development of morphine tolerance though inhibiting Akt phosphorylation and causing a subsequent decrease in capsase-1 cleavage, NALP1 activation, and IL1β production (Tian, Liu et al. 2015). Several lipoxin mimetics have been synthesised and assessed for their anti-inflammatory properties however their efficacy in modulating pain is yet to be investigated (de Gaetano, Butler et al. 2019).

Epoxyeicosatrienoic Acids (EETs)

AA is oxidised by the cytochrome P450s (CYP) (Roman 2002), to produce the epoxyeicosatrienoic acids (EETs) (Zeldin 2001). The EETs are short-lived *in vivo*, being rapidly hydrolysed by the enzyme soluble epoxide hydrolase (sEH) into the dihydroxyeicosatrienoic acids (DHETs) (Zeldin 2001). Like the lipoxins the EETs also appear to have an anti-inflammatory role (Fleming 2007, Bystrom, Wray et al. 2011, Bystrom, Thomson et al. 2013). These anti-inflammatory effects are thought to be mediated by inhibition of Nf-kB nuclear translocation thereby inhibiting the downstream production of pro-inflammatory cytokines (Node, Huo et al. 1999). The role of the EETs in modulating nociceptive responses have been of recent interest. Intra-plantar administration of the EETs acutely reverses carrageen-induced pain in rats (Morisseau, Inceoglu et al. 2010), whilst topical administration of the EETs prophylactically reduced responses in models of inflammatory pain in rats (Inceoglu, Schmelzer et al. 2007). These data suggest that the EETs may act peripherally as anti-hyperalgesic molecules. However, *in vitro* data have

suggested that high concentrations of 8,9-EET can induce calcium influx in a small subset of DRG neurons (Brenneis, Sisignano et al. 2011), suggesting that the role of these bioactive lipids in mediating nociception might not be straight forward.

The development of a range of sEH inhibitors which aim to stabilise *in vivo* levels of the EETs has allowed researchers to investigate the potential anti-nociceptive and anti-inflammatoy roles of these lipids more thoroughly. Initial studies using sEH inhibitors focussed on their anti-inflammatory potential, with small molecule inhibitors of sEH reducing lipopolysaccharide (LPS) induced lethality and circulating levels of pro-inflammatory cytokines in mice (Schmelzer, Kubala et al. 2005). Subsequently, sEH inhibitors have been shown to both prophylactically and therapeutically reverse inflammation induced pain in rats following topical and systemic applications (Schmelzer, Kubala et al. 2005, Inceoglu, Schmelzer et al. 2007, Rose, Morisseau et al. 2010, Inceoglu, Wagner et al. 2011, Wagner, Inceoglu et al. 2013). There is evidence that EETs have a role in modulating nociception separate from their anti-inflammatory actions, as sEH inhibitors also reduce neuropathic pain behaviour in mice and rat models of diabetic neuropathy (Inceoglu, Jinks et al. 2008, Wagner, Inceoglu et al. 2013, Wagner, Yang et al. 2014, Inceoglu, Bettaieb et al. 2015). In the absence of allodynia or hyperalgesia the administration of sEH inhibitors have not been shown to alter acute nociceptive responses (Inceoglu, Jinks et al. 2006, Inceoglu, Wagner et al. 2011, Wagner, Inceoglu et al. 2013). This implies that the EETs and DHETs are not involved in the processing of normal nociceptive stimuli and are instead involved in the maladaptive processes that underlie inflammatory and neuropathic pain states. Indeed, the magnitude of the analgesic effect of the sEH inhibitors appears to be larger in response to more painful stimuli (Inceoglu, Wagner et al. 2011).

The mechanism (s) through which sEH inhibitors produce analgesia is yet to be elucidated. sEH inhibition maintains plasma levels of the EETs whilst decreasing plasma levels of the DHETs (Wagner, Inceoglu et al. 2013). In

addition, sEH inhibitors also regulate other metabolites of the AA cascade, reducing levels of both PGD2 and PGE2 in inflammatory pain states (Inceoglu, Jinks et al. 2006, Wagner, Inceoglu et al. 2013). sEH inhibition also reduces spinal levels of COX2 mRNA following intra-plantar injection of LPS in rats, which may also underpin the effects of the sEH inhibitors on the prostaglandins (Inceoglu, Jinks et al. 2008). However, the analgesic properties of sEH inhibitors does not appear to be entirely mediated by their effects on COX2 expression as they have been shown to reverse the pain induced by direct administration of PGE2 in rats (Inceoglu, Wagner et al. 2011). sEH inhibitors also modulate the expression of the LOX metabolites, the HODEs and the HETEs, which may play an important role in their analgesic effects (Schmelzer, Kubala et al. 2005).

The EETs interact with a small number of proteins, notably peroxisome proliferator-activated receptor gamma (PPARγ) (Liu, Zhang et al. 2005, Samokhvalov, Vriend et al. 2014), which is known to reduce inflammatory and neuropathic pain, and PPARγ regulated transcription is key in reducing microglia activation and oxidative stress (Bernando and Minghetti 2006, Morgenweck, Abdel-aleem et al. 2010, Morgenweck, Griggs et al. 2013, Mansouri, Naghizadeh et al. 2017, Khasabova, Khasabov et al. 2019). Although PPARγ activation by the EETs may contribute to the underlying analgesic effects of sEH inhibitors, direct effects of EET on PPARγ and pain are still to be elucidated. The EETs also have affinity for translocator protein (TSPO) which is a mitochondrial protein important in the synthesis of steroids (Inceoglu, Jinks et al. 2008). Ligands of TSPO alleviate inflammatory pain, so it may be hypothesised that EETs interactions with TSPO could mediate an increase in steroidogenesis subsequently leading to analgesia (Bressan, Farges et al. 2003, Inceoglu, Jinks et al. 2008). Indeed, sEH inhibitors have been shown to increase spinal mRNA levels of the steroidogenesis marker, steroidogenic acute regulatory protein (StARD1) in inflammatory conditions (Inceoglu, Jinks et al. 2008). Likewise in a pre-clinical model of post-stroke pain 14,15-EET reduced pain via enhanced

allopregnanolone production and subsequent γ-aminobutyric acid A receptor ($GABA_AR$) signalling (Chen, Li et al. 2019). The secondary messenger cAMP also appears to play an important role in mediating the analgesic effects of sEH inhibitors, especially their effects on steroidogenesis. In naïve rats sEH inhibitors were found to increase basal nociceptive thresholds in the presence of elevated cAMP induced by administration of a phosphodiesterase 4 (PDE4) inhibitor (Inceoglu, Wagner et al. 2011). In naïve rats co-administration of the cAMP analogue 8-Br cAMP and the EETs or a sEH inhibitor resulted in significant increases in spinal StARD1 mRNA expression (Inceoglu, Jinks et al. 2008).

These data suggest that the EETs may modulate nociception through at least two pathways, indirectly through downregulation of COX2 signalling, as well as through cAMP dependent steroidogenesis. However, more work is still needed to fully understand the mechanisms underlying the anti-nociceptive properties of the EETs. There is also the question of whether the DHETs are just non-active end-products of this enzymatic pathway or if they have their own pro-nociceptive activities.

Soluble epoxide hydrolase inhibitors have undergone phase I clinical trials and have been shown to be well-tolerated and produce sustained inhibition of the enzyme (Lazaar, Yang et al. 2016). They are now undergoing clinical trial for the treatment of neuropathic pain (clinicaltrials.gov: NCT04228302).

Metabolites of EPA and DHA

Resolvins

The omega-3 PUFAs EPA and DHA are metabolized into a series of specialised pro-resolution lipid mediators (Lu, Hong et al. 2005). The first group of pro-resolution mediators demonstrated to be derived from EPA

and DHA are the resolvins; which can be further classified based on whether they were derived from EPA (E-series) or DHA (D-series) (Serhan, Hong et al. 2002). The resolvins play an active role in driving the resolution of inflammation by inhibiting production of pro-inflammatory mediators, and stimulating the removal of macrophages from the site of injury (Recchiuti and Serhan 2012). The D series resolvins are formed following a series of oxygenations mediated by 15-LOX and then 5-Lox whilst the E series resolvins are endogenously synthesised by CYP450 and then 5-Lox (Serhan and Levy 2018). The initial stages of DHA and EPA metabolism to form the resolvins can also be mediated by aspirin acetylated COX2 (Serhan, Hong et al. 2002). The resolvins exert their effects through different receptors; resolvin D1 (RvD1) binds and activates *N*-formyl peptide receptor 2 (ALX), and G protein-coupled receptor 32 (GPR32), RvD2 via GPR18, resolvins E1 (RvE1) and E2 (RvE2) bind to chemerin receptor 1 (ChemR1), and leukotriene B4 receptor (BLT-1)(Serhan and Petasis 2011, Chiang, Dalli et al. 2015).

Alongside their role as endogenous anti-inflammatory mediators, recent work has investigated the resolvins as analgesic agents. Localised administration of RvD1 and RvE1 has been found to significantly reduce carrageenan-induced inflammatory pain in mice by attenuating the inflammatory response (Ji, Park et al. 2010). Interestingly, spinal administration of RvE1 was found to reduce the second phase of formalin induced pain, thought to be maintained by central spinal mechanisms, suggesting that the analgesic effects of the resolvins can be mediated by effects on spinal activity (Ji, Park et al. 2010). Indeed, spinal administration of RvD1 was found to inhibit the response of wide dynamic response neurons in the hind-paw carrageenan model of inflammation in the rat (Meesawatsom, Burston et al. 2016). Spinal pre-treatment of RvE1 was also found to attenuate neuropathic pain in mice through the prevention of spinal microgliosis (Xu, Berta et al. 2013). Intrathecal pre-treatment of RvD1 was found to prevent the onset of post-surgical pain in rats, but when

administered after surgery RvD1 only produced a transient analgesia, indicating that the resolvins might be key mediators in the early stages of pain chronification (Huang, Wang et al. 2011). Encouragingly, the resolvins have been shown to have a lower effective analgesic dose range compared to COX inhibitors and morphine in both rats and mice (Xu, Berta et al. 2013, Fonseca, Orlando et al. 2017). It is important to note that there is some evidence for sexual divergence in the analgesia produced by the resolvins, whilst RvD1 and RvD2 have been shown to inhibit both neuropathic and inflammatory pain equally in male and female mice, RvD5 only reduced neuropathic and inflammatory pain in male mice but had no effects in female (Luo, Gu et al. 2019).

The mechanisms underlying resolvin induced analgesia have started to be investigated. In cultured primary sensory mouse neurons RvD2 and RvE1 have been shown to have inhibit transient receptor potential vanilloid channel 1 (TRPV1) activity whilst both RvD2 and RvD1 were found to inhibit TRP ankyrin 1 (TRPA1) activity (Park, Xu et al. 2011). Intra-thecal administration of RvD1 has also been shown to block the phosphorylation of *N*-methyl-D-aspartate (NMDA) receptors in a model of chronic pancreatitis in rats (Quan-Xin, Fan et al. 2012).

The resolvins are potent endogenous analgesic mediators, however they have extremely short half-lives *in vivo* which may complicate any potential clinical applications they may have. The administration of the D-series resolvin precursor 17-hydroxy docosahexaenoic acid (HDHA) may be able to overcome this limitation. Both prophylactic and therapeutic treatment with 17-HDHA potently attenuated pain in CFA induced inflammatory arthritis in rats (Lima-Garcia, Dutra et al. 2011). Similarly, systemic application of 17-HDHA has also been shown to reduce osteoarthritis pain in a chemical and surgical rat model (Huang, Burston et al. 2017). This analgesia appeared to be mediated by a reduction in spinal astrogliosis in the chemical model of OA (Huang, Burston et al. 2017). Clinical research

suggests that circulating concentrations of this resolvin precursor may be a biomarker for pain (Valdes, Ravipati et al. 2017). Thermal pain thresholds were found to be higher in people with lower serum concentrations of 17-HDHA, whilst in people with OA higher serum concentrations of 17-HDHA were associated with less OA pain (Valdes, Ravipati et al. 2017).

Maresins

Maresin 1 and Maresin 2 are macrophage derived metabolites of DHA and are part of the SPMs. The maresins are produced by enzymatic hydrolysis of 14-HDHA, an intermediate metabolite formed from epoxidation of DHA. Although it is currently unclear the role maresins play in the pain pathway, exogenous administration of Maresin 1 (Mar1) has been studied as a potential analgesic in a range of animal models. Serhan et al found Mar1 reduced pain in both inflammatory and chemotherapy induced neuropathic pain models (Serhan, Dalli et al. 2012), dose-dependently inhibited TRPV1 currents in neurons, and inhibited capsaicin induced inward currents. Studies by Fattori et al using carrageenan and CFA-induced mechanical hyperalgesia also reported a reduction of pain upon Maresin 1 administration (Fattori, Pinho-Ribeiro et al. 2019). Recent work has shown that Mar1 can also reduce inflammatory arthritis pain in mice, these data suggest that the analgesic effects are as a result of a Mar1 induced decrease in macrophage recruitment (Allen, Montague-Cardoso et al. 2020). Although it has not been studied as in depth as maresin 1, maresin 2 is reported to be anti-inflammatory and pro-resolving which suggests it may have potential as an analgesic for inflammatory pain (Deng, Wang et al. 2014, Rodriguez and Spur 2015). The role of maresins specifically in inflammatory pain has been reviewed recently elsewhere (Hwang, Chung et al. 2019).

Protectin D1

The final member of the SPMs is protectin D1 (PD1) which is derived from docosapentaenoic acid (Dalli and Serhan 2019). Despite not being as extensively researched as the resolvins, PD1 has been identified as a key anti-inflammatory and anti-nociceptive mediator. PD1 has recently been shown to mediate some of its effects through the GPCR GPR37 expressed by macrophages (Bang, Xie et al. 2018). This work showed that PD1 enhanced phagocytosis by macrophages via GPR37, and that GPR37$^{-/-}$ mice showed prolonged mechanical allodynia and thermal hyperalgesia following inflammatory insult (Bang, Xie et al. 2018). These data suggest a neuro-immune mechanism behind the resolution of inflammatory pain. However, there is evidence that PD1 can also have more direct effects on nociceptors, having been demonstrated to prevent TNF-α and TRPV1 mediated spinal cord synaptic plasticity (Park, Lü et al. 2011). *In vivo* behavioural experiments showed that intra-thecal and intra-plantar PD1 can robustly reduce intra-thecal TNF-α and peripheral capsaicin induced pain behaviours respectively (Park, Lü et al. 2011). PD1 has also been demonstrated to protect against neuropathic pain in mice in two models of neuropathic pain when administered both locally and systemically (Xu, Liu et al. 2013). It was shown that PD1 prevented the onset of nerve damage induced spinal long term-potentiation as well as reducing the associated microgliosis and astrogliosis in the dorsal horn. Of interest for the potential of PD1 or mimetics as a therapeutic agent are the robust analgesic effects of PD1 on neuropathic pain that were seen in this study (Xu, Liu et al. 2013).

Chronic pain is a global public health concern that affects a significant proportion of the population (Murray, Barber et al. 2015). Unfortunately, current pharmacological treatments for chronic pain are either not efficacious in the long term or are associated with adverse effects. There is a clear need for improved analgesic agents to tackle the growing issue of chronic pain (Yekkirala, Roberson et al. 2017). The studies explored in this

review have demonstrated the importance of n-3 and n-6 derived lipid metabolites to the pain pathway, which may pave the way for the development of novel pharmacological drugs for the treatment of chronic pain.

It is well known that the prostanoids are potent pro-nociceptive mediators. Reducing their production through inhibition of COX1/2, the mechanism of action of classical NSAIDs, is also well known to produce substantial acute analgesia (Attiq, Jalil et al. 2018). Long term usage of these drugs is associated with adverse events in the gastric pathway (Lazzaroni and Bianchi Porro 2004). Recent work has focussed on the addition of H_2S and NO moieties to NSAIDs in the hope that reducing the associated adverse effects will allow for people to take these analgesics in the long term. Omega-6 derived products of the LOX pathway such as the HETEs and the leukotrienes are also thought to be pro-nociceptive. This has led to the development of joint COX-LOX inhibitors to inhibit these pro-nociceptive pathways. Currently none of these compounds have reached the market.

Due to the complexity of the metabolic pathways that underlie the synthesis of these pro-nociceptive lipids, it might be preferable to target enzymes or receptors which are more specific to actions of these mediators rather than inhibiting the actions of COX1/2 or the LOXs which both mediate the synthesis of a large number of lipid mediators. A targeted approach may lead to the development of effective analgesics with a reduced side effect profile. Further work is therefore needed to fully elucidate the mechanisms of actions of these n-6 derived pro-nociceptive mediators.

It is also important to realise that these lipid mediators may have different actions at different levels of the pain pathway. Until recently our understanding of the expression of the oxylipins, their precursors, and the proteins that mediate their biosynthesis remained incomplete. Using mass-spectrometry and RNA sequencing Domenichiello and colleagues have started to characterise the distribution of these key elements in the oxylipin

molecular pathways in the pain circuitry of rats (Domenichiello, Sapio et al. 2021). Furthering our understanding of how lipid synthesis and metabolism differs at the distinct levels of the pain pathway will be invaluable for the development of future pharmacological agents.

Recent studies described in this review suggest that novel therapeutic agents for the treatment of pain may be found by harnessing the potential of endogenous anti-inflammatory and anti-nociceptive pathways. There is substantial evidence that the n-6 derived EETs and lipoxins, and the n-3 derived resolvins, maresins, and protectins all display potent anti-inflammatory and anti-nociceptive properties. Chronic pain may in part be the result of a deficiency in the resolution pathways which curtail the inflammatory response (Lawrence and Gilroy 2007). Pharmacological agents which augment these endogenous resolution pathways may be able to promote the resolution of this chronic inflammation and consequently produce substantial anaesthesia. Several of these endogenous anti-inflammatory lipid mediators may also have direct effects on nociceptors, so the development of mimetic compounds may also provide an interesting novel therapeutic option.

1.4 Lipid Quantification

The ability to accurately identify and confidently quantify bioactive lipids is essential in understanding their physiological function, the roles they play in pathogenesis of diseases, and the effect of pharmaceuticals designed to inhibit or enhance their concentrations or bioactivity.To identify any lipidomic changes that occur in the pathogenesis of OA, suitable analytical techniques must be used that offer the appropriate sensitivity whist maintaining specificity between analytes. Targeted liquid chromatography-tandem mass spectrometry (LC-MS/MS) analysis is by far the most widely accepted and used technique for this task, allowing the researchers to quantitatively measure several families of lipids in each sample (Köfeler,

Fauland et al. 2012). The advantage of targeted analysis is that we can focus the mass spectrometer's capabilities onto select transitions, greatly increasing the sensitivity and specificity of the assay by filtering and fragmenting the ions that enter the mass spectrometer using the triple quadrupole instrumentation.

Triple quadrupole mass spectrometry has been used for analysis of mixtures and structure elucidation since the 1970s (Yost & Enke, 1979). For each analyte of interest, ionisation occurs and a precursor molecular ion is generated and enters the MS. The first quadrupole (Q1) has the role of filtering the ions entering the MS from the source, allowing only ions with a pre-programmed *m/z* ratio to pass through Q1 and on into Q2. However, if these are ions generated from a complex biological sample such as blood plasma which contains many thousands of different small molecules the likelihood of generating a precursor ion that is specific to a single analyte of interest is nigh on impossible. Therefore, fragmentation of each precursor ion by collision induced dissociation (CID) is performed in Q2, which allows product ions to be generated which exploit the structural differences between analytes; this proves essential when investigating isobaric species – that are structurally different molecules but have the same molecular weight. This leaves the role of Q3 to filter specific product ions to the detector and again, reduce the effect of matrix ions giving background noise. Below in Figure 2 is a schematic diagram of the selection, fragmentation, and detection process in a triple quadrupole MS system.

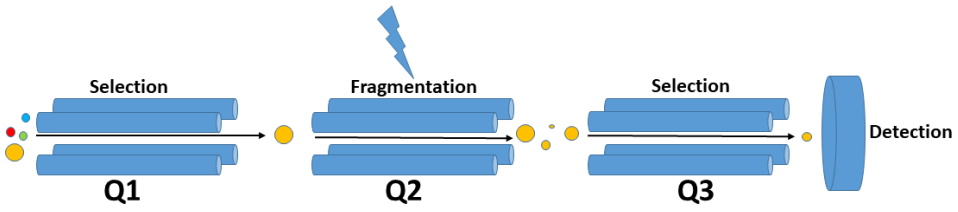

Figure 6. Schematic diagram of triple quadrupole mass spectrometer.

First used in the literature in 2001, 'lipidomics' is the study of lipids using MS technologies (Rustam & Reid, 2018). Analysing bioactive lipids via MS raises several complications. As many of the lipids within a single class are

isomers of one another, often having very slight structural changes and identical fragmentation patterns. This means that identification of specific analytes frequently requires an additional level of mass spectrometry or chromatographic separation to accurately recognise and quantify individual lipid species. This has been a long-standing problem in bioactive lipid analysis where there has been a history of misidentified lipid species (Liebisch, Ejsing et al. 2015, Koelmel, Ulmer et al. 2017, Köfeler, Eichmann et al. 2021, Gill and Contag 2022).

Mass Spectrometry monitoring of lipid product ions is typically combined with liquid chromatography, which retains and separates analytes by time based on their physiochemical properties prior to entering the MS. Chromatographic separation aims to remove matrix components that are not of interest and provide a specific retention time for each analyte of interest. With lipids, long conjugated hydrophobic carbon chains in the structure of analytes makes reverse-phase chromatography the most popular high-performance liquid chromatography (HPLC) separation method. This is where a hydrophobic stationary phase is used, such as a C8 or C18 packed column, which retain lipids on column. Gradient elution using a mix of aqueous and organic mobile phases is generally used to give sufficient separation by time to give confident identification in a mixture (Yamada et al, 2013). To achieve improved sensitivity and separation, traditional HPLC is now being replaced with ultra-HPLC (UHPLC). This technique operates at higher pressure than traditional HPLC and allows for lower particle sizes in columns, this in turn improves separation between analytes and can reduce analysis time and volume of sample required.

In many assays for bioactive compounds the straightforward combination of liquid chromatography and mass spectrometry would be enough to be confident in the identity of each analyte detected. However, the structural similarity of the lipids within the same classes of oxylipins means that analytes have extremely similar physicochemical properties. This results in chromatograms that are often complex and ambiguous – making confident

identification of the exact lipid species difficult to achieve. The quality of bioactive lipid analysis can be enhanced by using state-of-the-art LC-MS/MS instrumentation, focusing on the advanced capabilities of the MS system to use scheduled data acquisition, multiple monitoring of product ions for each analyte, and analysing prepared standard mixes of disambiguated lipids. To improve levels of confidence in the measured biological concentrations and identities of each bioactive lipid it is essential to use accepted bioanalytical method validation and quality control processes during development and application of a new method. Achieving improved LC-MS/MS sensitivity, separation and resolution of over 60 bioactive lipids was a critical objective for the generation of high-quality lipid profiling data for the clinical and pre-clinical studies planned for this thesis.

Aims

The overall aims of this project were to:

i) develop and validate a targeted UHPLC-MS/MS method for the quantification of more than 67 oxylipins in plasma/serum;
ii) apply this method to the analysis of clinical samples collected from people who have, or are at high risk of developing OA;
iii) identify relationships between oxylipins and clinical features of OA;
iv) identify potential targets for therapeutic intervention and potential biomarkers of disease progression;
v) investigate the effects of targeting oxylipins pathways in animal models of OA.

Chapter Two:

Development of a targeted LC-MS/MS assay for oxylipins: validation and detailed assessment of plasma and serum lipid profiles

Acknowledgements

I would like to thank Cath Ortori for her help in the initial stages of method development and helping with any issues with the mass spec. I would also like to thank Rakesh Jha for helping with this study including helping with extraction of samples from volunteers, performing validation experiments together, and performing the MVA for these samples.

The data presented in this chapter are currently being prepared into the manuscript:

James Turnbull, Rakesh R Jha, Catharine A. Ortori, Dong-Hyun Kim, Ana M Valdes, Victoria Chapman, & David A Barrett. **Comprehensive comparison of oxylipin profiles in human serum and plasma**. [Target: Journal of Lipid Research]

Abstract

In this chapter, a quantitative LC-MS/MS method for 67 oxylipins in human serum and plasma was developed and validated using the internationally accepted FDA bioanalytical method guidelines. For all the measured oxylipins the accuracy, precision, recovery, linearity, limit of quantification and matrix effects were measured. The new method was then applied to plasma and serum samples which were collected from healthy volunteers (n=10) along with plasma and serum from people with osteoarthritis (n=31). The serum levels of many oxylipins, particularly the AA derived COX-1/2 and CYP450 metabolites, were significantly higher compared to plasma (either fresh or standing), including the HETEs, PGs, TXs, and EETs. However, the levels of the majority of oxylipins were comparable between fresh and standing plasma, suggesting stability of these analytes in heparinised whole blood for 45 mins at room temperature before centrifugation. These data show that careful consideration should be made when planning sample collection and choice of matrix, as this can influence the oxylipin profile..

2.1 Introduction

2.1.1 Lipidomics

To be able to study the role of lipid mediators in the pathophysiology of OA we require analytical methods that can accurately and reliably measure their concentration in a matrix of choice. Liquid chromatography coupled with triple quadrupole mass spectrometry (LC-MS/MS) is the most suitable and widely used method of quantification of these lipid mediators – offering sensitivity, specificity, and the ability to measure many different lipids simultaneously in a single analysis (Liakh, Pakiet et al. 2020). Generally speaking, there are two approaches to lipidomics analysis, untargeted (or global) (Smirnov, Mazin et al. 2021) and targeted (Xu, Hu et al. 2020). Untargeted lipidomics aims to look at the lipidome as a whole and covers various classes of lipids such as fatty acids, triglycerides, phospholipids, and sterols. Untargeted analyses tend to use accurate mass instrumentation and processing software to perform lipid identification and relative quantification. Targeted analysis is performed when a particular set of analytes of interest are known, and analysis of samples is usually performed alongside reference standards of target compounds. In contrast to untargeted analysis, this allows quantitative measurements of analytes using extracted calibration and deuterated internal standards. In the case of the oxylipins, targeted analysis largely overcomes potential problems of identity due to the structural similarity between different lipids within the same sub-class, eg the prostaglandins, and also allows increased sensitivity of the method by filtering out background ions that are not of interest. Numerous methods have been reported for oxylipins measurements and applied to various studies and matrices, that have been reviewed in detail elsewhere (Chhonker, Bala et al. 2018). Many assays focus on particular classes of lipid mediators, such as the eicosanoids or endocannabinoids, whereas others aim to cover multiple classes of both pro- and anti-inflammatory mediators in order to gain a more comprehensive understanding of changes in the lipidome in study samples.

2.1.2 Analytical Challenges

Quantification of bioactive lipids using LC-MS/MS raises several analytical challenges that must be overcome. Due to the structural similarity of analytes, particularly

within the same family of lipids, analytes are often isobaric (share the same exact mass), have identical fragmentation patterns and extremely similar physiochemical properties. Where unique fragment ions cannot be generated by MS ionisation, sufficient chromatographic separation must be achieved in order to accurately assign peak identities. By nature, the majority of lipid mediators are present at extremely low endogenous concentrations, in the low nanomolar or picomolar range in biofluids or tissues (Dyall, Balas et al. 2022) which is close to the limit of sensitivity of current quantitative analytical methods. In order to gain appropriate sensitivity and specificity within a reasonable sample throughput of these lipids it is important to carefully optimise mass spectrometry and chromatographic parameters such as peak separation, dwell time, and extraction procedure. Improvements in mass spectrometry technologies in recent years have allowed an increased number of analytes to be measured simultaneously whilst also maintaining suitable sensitivity and specificity. This is helped with the use of scheduled multiple reaction monitoring (MRM) procedures to monitor two transitions for each analyte within a given time window (eg. 2 min) whilst maintaining optimum cycle and dwell times.

2.1.3 Method Validation

To ensure that the method is performing accurately and reliably, validation experiments are performed to assess various measures of performance. Typically, in regulated LC-MS/MS studies these experiments are conducted to FDA/MHRA regulatory standards (2018, Kaza, Karaźniewicz-Łada et al. 2019). However, these regulatory guidelines are designed for novel small molecule drugs, rather than endogenous compounds, which only have guidance limited to using analyte-free matrix for calibration and QC samples. The need to validate the method is extremely important to ensure that the method is performing correctly, it also allows direct comparisons to be made between samples from different analytical runs, assuming each run meets analytical requirements for reporting.

2.1.4 Measuring Oxylipins in Blood

The choice of matrix to profile for lipids is important when considering different biological questions, such as the mechanistic roles of oxylipins in local tissue environment versus systemic circulating roles. Analysis of homogenised tissue aims

to assess local concentrations of lipid mediators, however measuring blood from experimental animals or human patients allows quantification of systemic or circulating levels of analytes. Blood is much more accessible and routinely collected in clinical studies, compared to tissue and other matrices such as synovial fluid. Blood samples are almost always prepared to remove red blood cells to give either plasma (by addition of an anti-coagulant) or serum (allowing blood to clot) followed by centrifugation of blood and to pellet cells and retrieving the remaining supernatant for lipidomic investigations. Studies often prepare either plasma or serum for analysis, however the effect that the coagulation process has on individual lipid concentrations is not fully understood (in sera samples compared with plasma) or the effect that different anti-coagulants have on the concentration of oxylipins in the sample once the blood is collected. Previous studies has found different overall oxylipins profiles between plasma, serum, and urine (Wolfer, Gaudin et al. 2015), differences between plasma and serum levels of some HETEs and PUFAs (Ishikawa, Maekawa et al. 2014), and changes in lipidome with use of different anti-coagulants (Moren, Lhomme et al. 2016). The study in this chapter will focus on the differences in lipid profiles between blood plasma and serum. The process of coagulation involves the activation of platelets which can produce lipid mediators, particularly the eicosanoids downstream of arachidonic acid (Turnbull, Sander et al. 2022). Furthermore, phospholipase A2 (PLA2), which plays an important role in the coagulation process, also converts phospholipid bound PUFAs into their free fatty acid form. These increased levels of free PUFAs could then be further metabolised into oxylipins metabolites through key enzymatic pathways that are also known to be activated during coagulation such as COX-2. Therefore, to gain the most accurate overview of circulating lipid mediators in the blood, we must minimize the effect of sample collection and preparation steps that can influence their concentration and introduce unwanted variability between sample collection..

The aims of this chapter were to:

i) develop and validate a targeted LC-MS/MS method to quantify oxylipins in biofluids;

ii) apply this method to the analysis of plasma and serum collected from the same healthy volunteers in a well-controlled study;

iii) apply this method to the analysis of plasma and serum collected from a 'typical' clinical study of people with OA;

iv) identify key lipid metabolism pathways which may be affected by the coagulation process;

v) assess whether oxylipins levels are correlated between plasma and serum.

2.2 Materials and Methods

2.2.1 Materials

HPLC grade acetonitrile, butylated hydroxytoluene (BHT), ethanol, ethyl acetate, formic acid, bovine serum albumin (BSA) and methanol were purchased from Fisher Scientific (Waltham, MA, USA). Lipid reference standards were purchased from Cayman Chemicals (Ann Arbour, MI, USA.) and stored in ethanol at -80°C (Appendix 1). Solid phase extraction (SPE) cartridges (Strata-X polymeric reversed phase, 33µm, 200 mg/6 mL) were purchased from Phenomenex (Torrance, CA, USA). An Acquity BEH C18 Column with guard column was purchased from Waters (Milford, MA, USA).

Participant Characteristics

The healthy volunteers recruited to donate blood for this study had a median age of 25.5, were 70% female, and had a median BMI of 21.2. The people with OA where both plasma and serum samples were collected, had a median age of 65, were 58% female, and had a median BMI of 30.2 (Table 1).

Table 1. Characteristics of participants.

	Healthy Volunteers	People with OA
n	10	31
Age (median (IQR))	25.5 (22.8-28)	65.0 (57.0-69.0)
Sex (% Female)	70.0%	58.1%
BMI (median (IQR))	21.2 (19.8-25.9)	30.2 (26.9-32.4)

2.2.2 Preparation of Plasma and Serum

Whole blood was collected from healthy volunteers (n=10) for preparation of both plasma and serum at the same time (Figure 1). Volunteers were non-fasted and whole blood was collected between 9:00-11:00. Ethical approval for collection of blood from healthy volunteers was obtained from the University of Nottingham's Faculty of Medicine and Health Sciences Research Ethics Committee (Reference number: 432-1912).

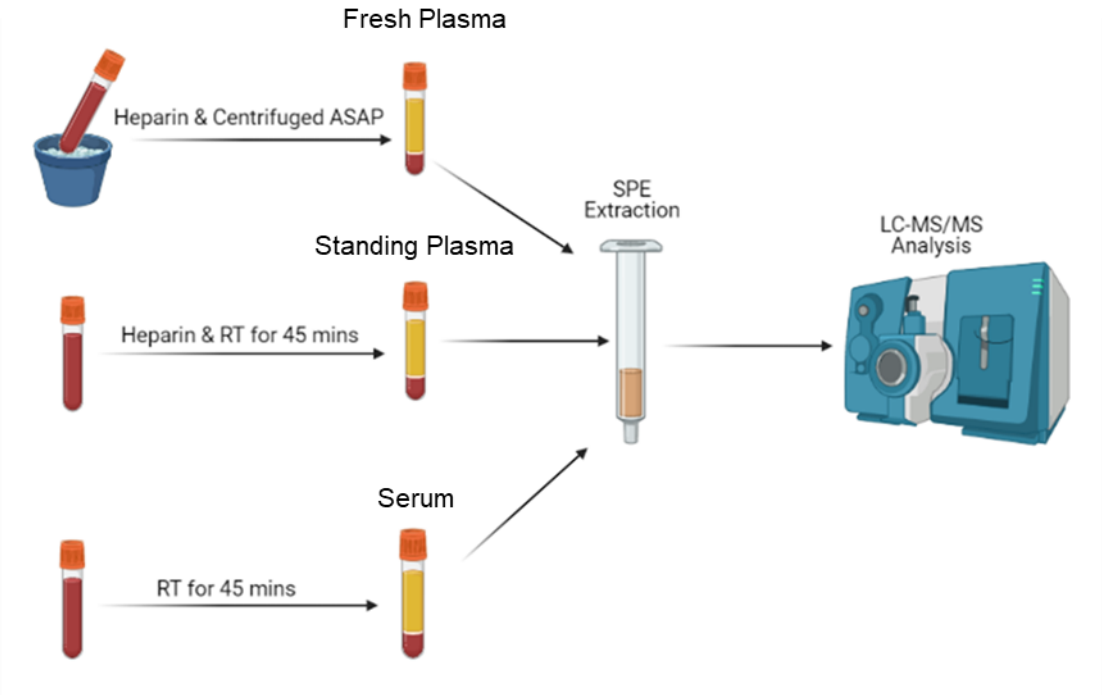

Figure 1. Study design for the collection of blood and preparation of fresh plasma, standing plasma, and serum from blood collected from healthy volunteers.

For plasma preparation, two aliquots of whole blood were collected in heparinised tubes (BD Vacutainer, NJ, USA). One aliquot was stored on ice immediately and was centrifuged within 5 mins of collection at 2000g for 15 mins at 4°C and the plasma removed and stored at -80°C (fresh plasma). The second aliquot of heparinised blood was left standing at room temperature for 45 mins to mimic the conditions used for serum collection, and then centrifuged at 2000g for 15 mins at 4°C (referred to as "standing plasma" throughout this chapter).

For serum preparation, whole blood was collected in serum separator tubes and allowed to clot at room temperature for 45 mins. Whole blood was then centrifuged at 2000g for 15 mins at 4°C and the serum removed and stored at -80°C.

2.2.3 Calibration and Internal Standards Preparation

Calibration standards containing all target analytes were prepared at a range of concentrations reflecting the known biological levels of each lipid. Due to the varying ranges of biological concentrations of lipid mediators, analytes were separated into four groups with the calibration line covering an appropriate range of molar concentrations. Reference standards were diluted with ethanol to working stock

solutions and further diluted in 4% BSA (PBS). 11-point calibration curves were prepared for oxylipins, SPMs, and endocannabinoids, spiked to cover ranges of 0.02-500 nM, 0.002-50 nM, and 0.1-2500 nM, respectively. Several deuterated internal standards were used to compensate for any variation in extraction or analysis across analytical runs. Commercial stock solutions of prostaglandin D2-d_5, 15-HETE-d_8, resolvin D5-d_4, arachidonic acid-d_8, and anandamide-d_8 were diluted and mixed to produce an internal standard working solution. The internal standards were selected to cover the main structural groups of oxylipins and applied to these groups during data analysis (Section 2.2.4). The internal standard mixture was spiked into each sample and QC standard during the extraction procedure, which is described in further detail below.

2.2.4 Sample preparation and extraction

Samples were stored at -80°C prior to analysis. Samples were thawed on ice and 400 µL of sample was spiked with 40 µL of the internal standard mix (AA-d8 (1.7 µM), PGD2-d4 (0.2 µM), and 15-HETE-d8 (1.3 µM), RvD2-d4 (0.2 µM), and AEA-d8 (0.8 µM)). 800 µL of precipitation solvent was added to each sample (ethanol, formic acid, and BHT: 1000:3:0.75 v/v/v), and vortex mixed for 10 mins followed by 10 minute centrifugation at 2000 g and 4°C. Supernatants were transferred to fresh tubes and diluted in 3 mL of distilled water. Solid phase extraction (SPE) cartridges were conditioned with 100% and 25% ethanol then were loaded with diluted samples. Cartridges were washed with water (10 mL) and 25% ethanol (5 mL), and analytes were eluted in ethyl acetate (5 mL). Ethyl acetate was then evaporated from samples under N_2 gas to dryness. Samples were then reconstituted in 100 µL of 50:50 methanol:H_20, vortexed mixed and then centrifuged before finally being transferred to amber glass vials for analysis.

2.2.5 LC-MS/MS Instrumentation

Lipidomic analysis was carried out using an Applied Biosystem MDS SCIEX 6500+ Q-Trap hybrid triple-quadrupole–linear ion trap mass spectrometer equipped with an electrospray ionisation (ESI) interface and coupled with a ExionLC™ Series UHPLC (Applied Biosystem, Foster City, CA, USA). The HPLC Column used was Acquity UPLC BEH C18 1.7 µm (150 x 2.1 mm) with guard column (Acquity UPLC BEH C18 1.7 µm,

VanGuard Pre-Column 2.1 x 5 mm) and maintained at 40°C. Autosampler temperature was maintained at 4°C throughout analysis. Aqueous mobile phase was 0.02% formic acid in water; the organic mobile phase was 0.02% formic acid in methanol:acetonitrile (1:4, v/v) and maintained a flow rate of 0.3 mL/min for 25 mins. Quantification of each analyte was calculated using a fully extracted calibration standard curve. Correction was made for the exact aliquoted sample volume (in case the standard 400 µL volume was not available) to calculate a final concentration of each individual lipid present in all samples. Quantification was performed using MultiQuant V.3.0.3 software. Identification of each compound in samples was confirmed by LC retention times, corresponding secondary product ion transition, and presence in a solution of 'unambiguous analytes'. The solutions of 'unambiguous analytes' are a set of four different solutions where analytes which could easily be confused are spiked into different solutions, eg. PGD1 is present in group 1 only and PGE2 is present in group 2 only. This approach was used to add confidence to peak identification of co-eluting or isobaric lipids. The peak area ratio of each analyte (analyte:IS) was used to calculate the molar concentration using the calibration standard curve.

2.2.6 Validation Experiments

As analytes are endogenous to biological matrices, the widely-used pseudo plasma matrix of 4% BSA in PBS was used for the preparation of calibration standards and blank samples. The developed and optimised method was assessed for assay precision, accuracy, recovery, matrix effects, and ion suppression. Quality control (QC) samples, both endogenous and spiked, were analysed for precision and accuracy (n=6) with acceptance criteria of <15% CV. Recovery of analytes through SPE was assessed using extracted QCs and an unextracted calibration line.

Accuracy and Precision

Accuracy and precision are important aspects of analytical method validation and experiments were conducted by spiking known concentrations of the standards mix to the sample matrix (at least n=6 per day of extraction). Accuracy was calculated to find the out the closeness of the measured outcome to the expected concentration of the spiked analyte concentration. An experiment for precision was done to assess

any bias or unwanted variations in peak areas as a result of the sample extraction process. Some (n=6) replicate samples were spiked with known concentration of the standards and variation in the response was checked for same day (inter-day precision) and different day (intra-day precision) and results were reported in terms of percentage relative standard deviation (%CV).

Recovery through Solid Phase Extraction

A recovery experiment was carried out by spiking three different (High (500 nM), Medium (50 nM) and Low (5 nM)) known concentrations of standards mix to the sample matrix and compared with the endogenous levels of the lipids in the same samples. Percent recovery was calculated as ratio of the difference in the lipid concentration of the spiked and endogenous levels to the spiked concentration of the individual lipid mediators.

Matrix Effects

The constituents of matrices other that the analyte of interest may have some effect on the extraction efficiency of the desired analyte which may increase or decrease the actual response of these analytes and these effects are termed as matrix effects. Matrix effects were evaluated as mean percent deviation by spiking known concentration of analytes in pseudo as well as sample matrix.

Lower Limit of Quantification (LLOQ)

For this study and throughout this thesis, the lowest standard on the calibration was regarded as the limit of quantification where signal:noise >5. If any background contamination was observed and was consistent across samples, the LLOQ was set at 4 times higher than the response of contamination. Where analytes were detected but were below the LLOQ, these were reported as BLQ. For some statistical analyses where a zero value cannot be used (and only for this purpose), samples that had BLQ reported were given a nominal value of 10% of the LLOQ.

Run Acceptance Criteria

Each sample analysis run was assessed carefully to ensure it met the acceptance criteria below. Data were processed blinded to sample groups. The internal standard response plot gives an initial overview of the consistency of the extraction and LC-

MS/MS process, and was used to identify any samples where there were higher than expected levels of variability, typically introduced during the extraction process. The %CV of calculated concentration of QCs (typically n=6 per day of extraction) was deemed acceptable at <15%; where %CV was 15-20% this was accepted or rejected following careful review of peak integration of samples. Up to one outlier QC per six QCs was acceptable to be removed if identified as a statistical outlier using Grubbs test. Where samples were analysed in batches (eg. three batches), the %CV for each individual batch (eg. n=6 QCs) was calculated and for whole sample set (eg. n=18), to give an overview of individual batch and whole run variability. Where run acceptance criteria were not met, data were not reported and the sample extracts were re-analysed on the LC-MS/MS.

Enhanced product Ion scans

Enhanced product ion (EPI) scans enable the capture of a detailed fragment ion spectrum of a specific lipid peak in a sample, significantly increasing the confidence in identity. EPI scans were performed on pooled serum extracts alongside authentic reference standards to confirm peak identity by spectral matching. These EPI scans were obtained from human serum samples as listed in Chapter 6. Matched chromatograms and spectra for SPMs are detailed in the thesis appendix.

Statistical analysis

The concentration for each individual analyte obtained from LC-MS/MS analysis were taken into account for statistical analysis. Plasma, standing plasma, and serum were the three groups of samples subject to statistical analysis. Groups were assessed for normal distribution. Differences between groups were assessed using a paired t-test. Univariate and correlation analyses were performed using GraphPad Prism (Version 8.2.1) and multivariate analysis were performed using Metaboanalyst version 4.0 (https://www.metaboanalyst.ca/) where principal component analysis (PCA) was performed for data visualization. Partial least square discrimination analysis (PLS-DA) was used to identify the important lipid mediators differentiating the groups. The PLS-DA model was validated in terms of R2, Q2 and accuracy and by performing cross validation. The PLS-DA model was validated in terms of R2, Q2 and accuracy and by

performing cross validation used cut-off value of variable importance in projection (VIP) >1.0 to identify the discriminatory lipid mediators.

Analytical strategy

The overall analytical approach for the method development and optimisation included the following stages to:

- Generate a comprehensive MRM method for a range of oxylipins that included transitions that gave appropriate sensitivity and specificity.
- Optimise chromatography to obtain baseline separation of oxylipin isomers, whist ensuring throughput is fit for purpose.
- Utilise scheduled MRM to improve the amount of data point collected for peaks, and improve overall peak shape.
- Ensure the method is performing to analytical standards by conducting validation experiments.

2.3 Results

2.3.1 Optimisation and validation of LC-MS/MS method

Optimisation of MS Parameters

Each analyte of interest was individually infused at a concentration of 100 nM directly into the MS for optimisation of MS parameters and selection of product ions. Optimisation of declustering potential (DE), collision energy (CE), and exiting potential (CXP) was performed for each analyte individually (Table 2). For the majority of analytes, two product ions were incorporated into the MRM method. This was required specifically to separate structurally similar lipids within the same class, which produce ions that have the same precursor ion, and often the same most sensitive product ion. Monitoring a second product ion that was perhaps less sensitive, but was unique to the analyte, added to the confident allocation of peak identities in the complex chromatograms that were obtained in these analyses.

Table 2. Monitored transitions and optimised MS parameters (declustering potential (DP), collision energy (CE), and exciting potential (CXP)) for each analyte. Oxylipins highlighted blue are AA and LA derived classic eicosanoids, highlighted orange are the DHA and EPA derived SPMs and intermediates, and highlighted green are the endocannabinoids. A list of full oxylipin names, structures and HMDB IDs are detailed in the thesis appendix.

Analyte	Q1	Q3 (1)	Q3 (2)	DP (V)	CE (V)	CXP (V)
AA-d8	311	267	-	-140	-20	-15
AA	303	259	205	-105	-18	-15
TXB2	369	169	195	-22	-65	-19
11-dehydroxy-TX B2	367	305	349	-22	-85	-17
PGE2	351	315	271	-16	-35	-19
PGD2	351	315	271	-14	-30	-17
6-Keto-PG-F1α	369	351	325	-32	-55	-19
PGD2-d4	355	319	-	-16	-50	-19
LTE4	438	333	-	-55	-24	-19
LTB4	335	195	-	-75	-22	-23
6-trans-LTB4	335	195	128	-105	-22	-11
6-trans-12-epi-LTB4	335	195	129	-100	-20	-23
5-HETE	319	114	257	-35	-18	-15
8-HETE	319	257	154	-20	-20	-13
9-HETE	319	151	166	-55	-18	-17
11-HETE	319	167	-	-35	-20	-19
12-HETE	319	179	208	-60	-20	-21

15-HETE	319	301	219	-15	-14	-19
15-HETE-d8	327	309	-	-85	-26	-15
16-HETE	319	301	233	-45	-16	-15
19-HETE	319	275	301	-80	-22	-15
20-HETE	319	301	275	-25	-20	-17
5-HpETE	317	203	273	-40	-24	-23
12-HpETE	317	273	153	-40	-22	-13
5,6-EET	319	191	-	-30	-14	-17
8,9-EET	319	155	301	-40	-16	-13
11,12-EET	319	178	167	-40	-16	-23
14,15-EET	319	301	219	-45	-14	-27
5,6-DHET	337	145	319	-85	-24	-18
8,9-DHET	337	126	185	-75	-26	-15
11,12-DHET	337	167	169	-80	-24	-19
14,15-DHET	337	207	129	-90	-24	-11
5(S),6(R)-DiHETE	335	114	144	-45	-20	-13
5,12-DiHETE	335	195	128	-55	-26	-13
5,15-DiHETE	335	173	114	-45	-20	-9
8,9-DiHETE	335	127	185	-80	-26	-15
8,15-DiHETE	335	317	126	-60	-20	-19
Linoleic Acid	279	279	261	-105	-26	-13
9-HODE	295	171	-	-80	-24	-19
13-HODE	295	195	-	-40	-14	-19
9-OxoODE	293	185	125	-80	-28	-21
13-OxoODE	293	133	195	-80	-28	-13
DHA	326	283	-	-65	-14	-15
17-HDHA	343	281	201	-55	-16	-17
14-HDHA	343	205	281	-70	-16	-17
EPA	301	257	203	-5	-15	-13
18-HEPE	317	299	215	-40	-14	-17
10,17-DiHDHA	359	153	256	-65	-22	-19
Resolvin D1	375	141	215	-40	-20	-15
Resolvin D2	375	175	140	-28	-45	-19
Resolvin D3	375	147	115	-75	-24	-17
Resolvin D4	375	100	130	-55	-22	-11
Resolvin D5	359	199	140	-45	-20	-11
Resolvin D2-d5	380	174	141	-30	-40	-19
Protectin D1	359	153	206	-65	-22	-17
Resolvin E1	349	195	161	-85	-22	-17
17-oxo-DHA	341	297	184	-60	-16	-17
Lipoxin A4	351	115	217	-18	-45	-13
Lipoxin B4	351	220	255	-55	-20	-19
Lipoxin A5	349	114	233	-40	-18	-13
Maresin 1	359	177	122	-50	-22	-21
Maresin 2	359	221	232	-35	-16	-25
PEA	300	62	-	25	17	8
OEA	326	62	-	71	37	8
2AG	379	287	-	46	19	16
AEA	438	62	-	25	61	8
AEA-d8	356	63	-	25	41	8

Source parameters were optimised by infusing AA directly into source and adjusting parameters to give optimum response (Table 3).

Table 3. Optimised front-end MS parameters presented in arbitrary units (except ion spray voltage).

Source Parameters	Values
Curtain gas (CUR)	10
Ion spray voltage (IS)	-4200 V
Nebulizer gas (GS1)	30
Heating gas (GS2)	20
Temperature (TEM)	450
Collision associated dissociation gas (CAD)	6
Interface Heater	On

Optimisation of Chromatography

The chromatography optimised was based on previous lipid methods developed in our group using traditional HPLC and a QTrap 4000 (Zhang, Pearson et al. 2007, Wong, Sagar et al. 2014). Although several comparable methods have been reported that separate similar groups of lipids over LC runs < 10 mins (Wang, Armando et al. 2014, Wolfer, Gaudin et al. 2015) the need for the developed method to have a high level of confidence in quantifying structurally similar lipids meant that a large number of transitions would be required for this MRM method compared with the previously published methods. The increased cycle time was projected to result in very low dwell times for each transition (5 ms or less) which may not be achievable even on the fastest of modern MS instruments given the number of analytes to be measured (>65). Initial experiments confirmed this problem and demonstrated reduced sensitivity and poor chromatographic peak shapes when trying to use these very low dwell times. To resolve this problem it was decided to take full advantage of the scheduled MRM protocol available in the QTRAP MS instrument. This required the extension to a 25 minute run time enabling the separation of analytes as much as possible. This allowed for increased dwell times, and hence much improved sensitivity, for each transition across an acquisition window of 120 seconds. This window accommodates any shifts in retention time and sufficient background noise to allow realistic signal to noise calculations.

The starting flow rate was 300 µl/min, with a gradient elution separating analytes over a 25 minute run time. The percentage of organic gradient used was optimised as follows: 0 min - 35%, 7 min - 60%, 14 min - 60%, 18 min - 100%, 21 min - 100%, 21.2 min - 35%, and 24 min - 35% (Figure 2). A 100% organic was period was used at the end of each analysis in order to remove any retained lipids from the column before the analysis of the next sample. Figure 3 shows the chromatographic separation of a comprehensive profile of analyte classes that are incorporated in this method.

The gradient and run time used was optimised to allow sufficient baseline resolution of isomeric lipids that share fragment ions, including prostaglandin E2 & D2 and 14- & 17-HDHA (Figure 4). In particular the plateau between 7 and 14 mins allowed the separation of multiple co-eluting enzymes which under linear gradient elution did not achieve baseline separation.

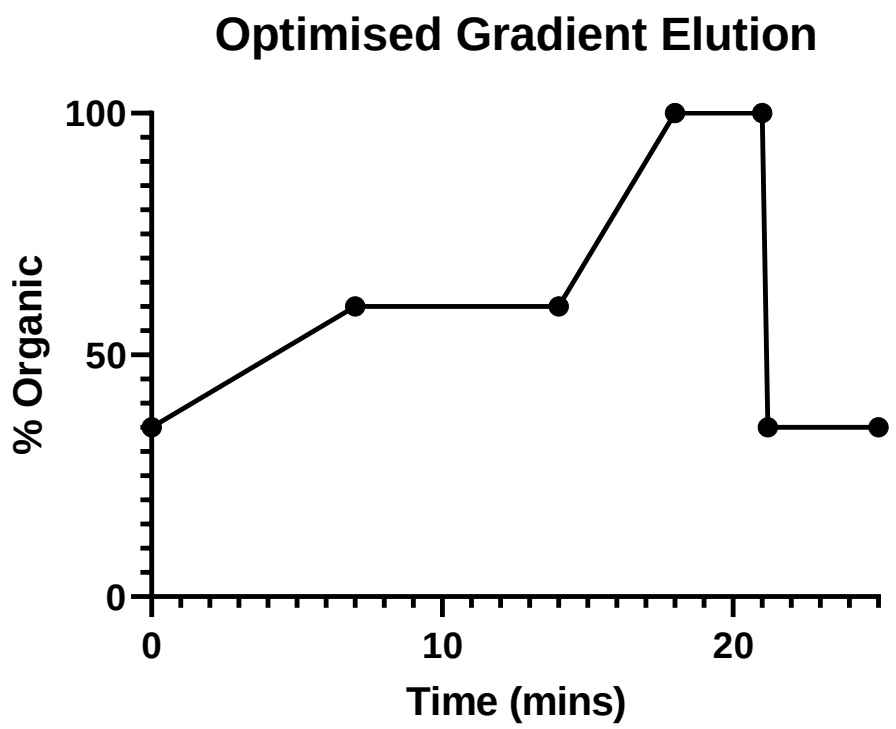

Figure 2. Optimised gradient elution for separation of oxylipins over a 25 minute runtime. The gradient starts with an initial slope which then plateaus for several minutes to allow optimum separation of analytes. This is followed by further slope to elute the most non-polar analytes from column. A 100% organic wash was then used to elute any further non-polar compounds still on column. The %organic is then returned to the initial 35% to allow for equilibration before the next sample is injected. .

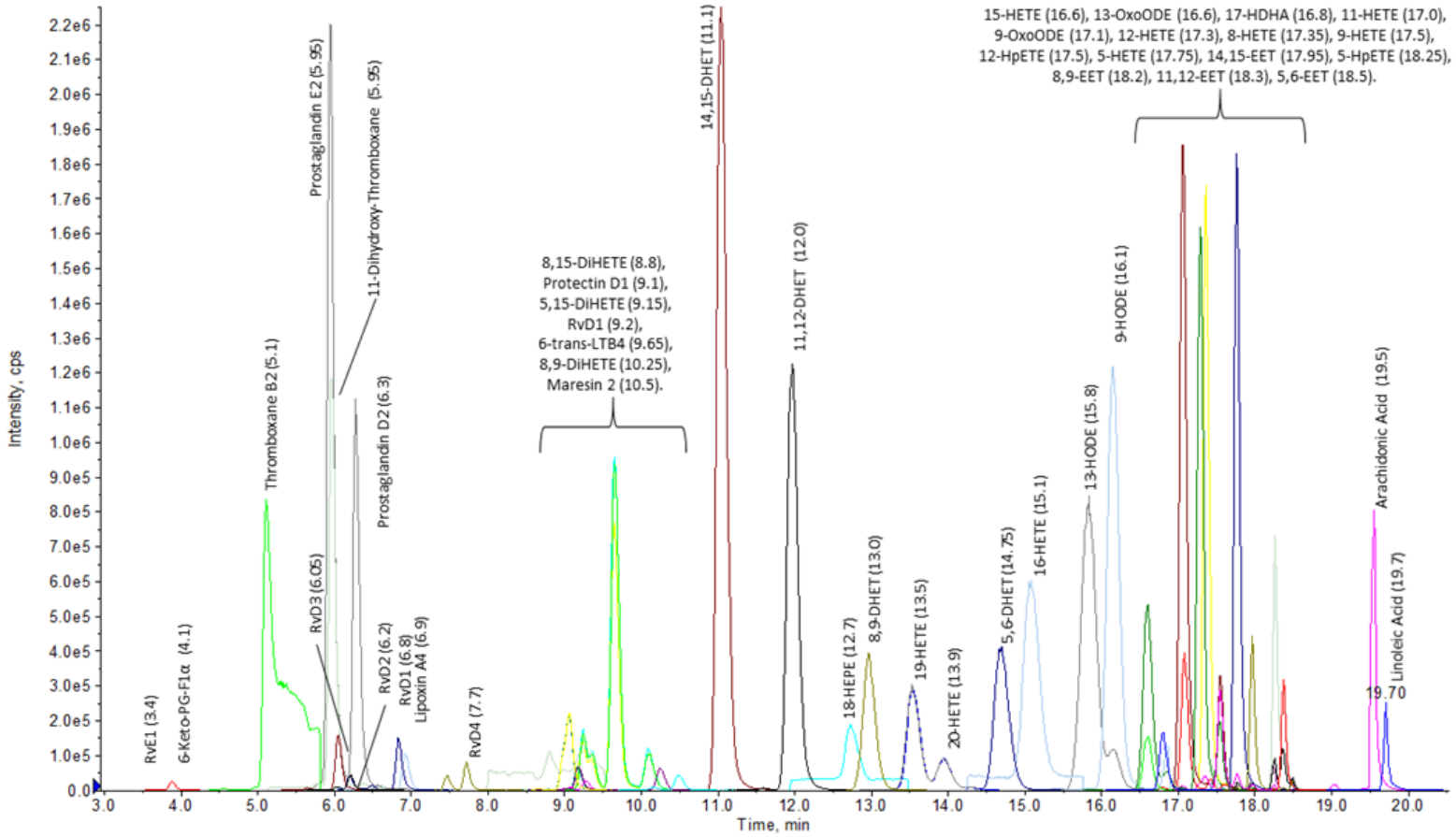

Figure 3. Extracted ion chromatographic separation of oxylipins measured using LC-MS/MS over a 25 min run time.

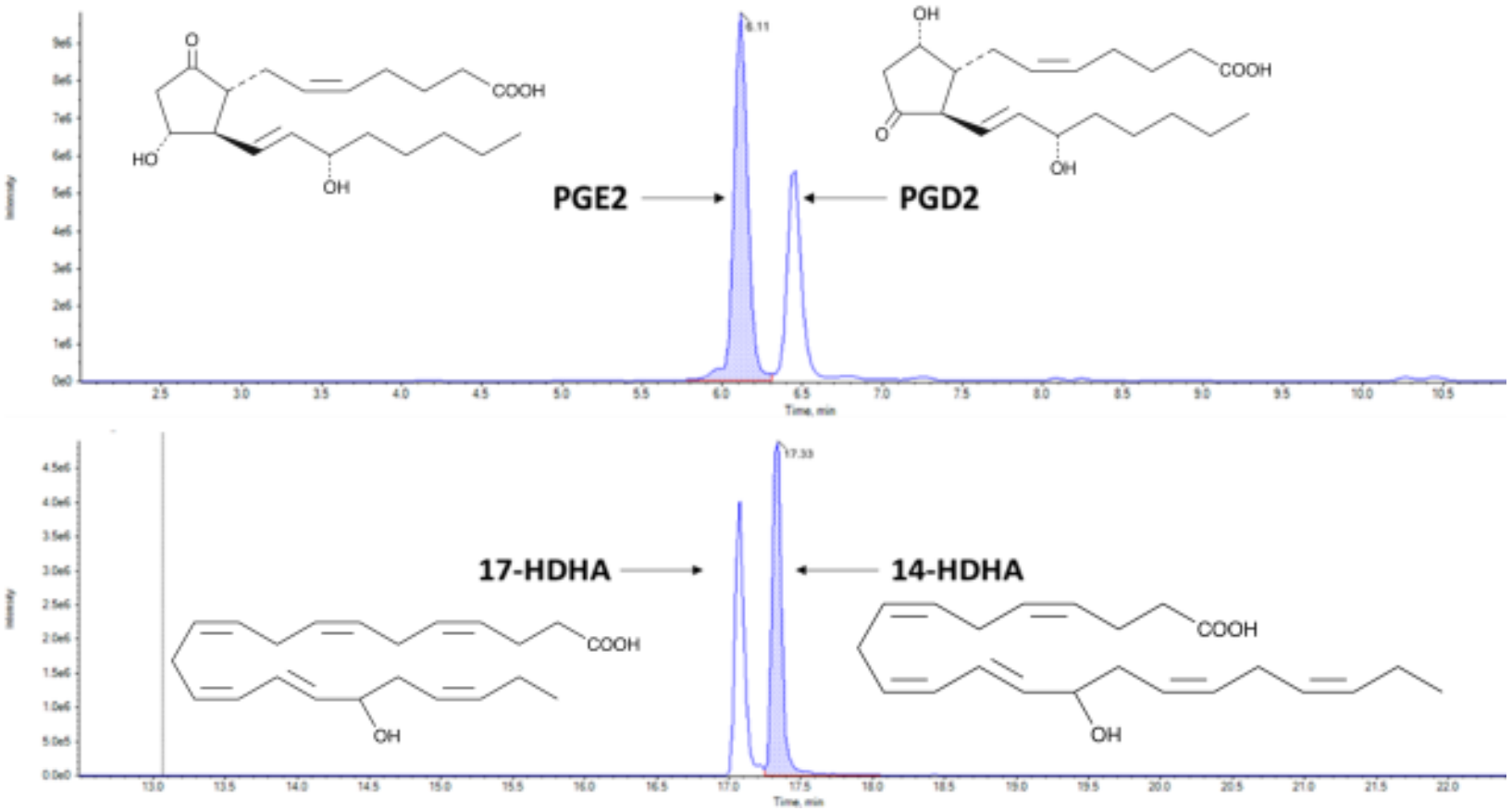

Figure 4. Example chromatographic separation between structural isomers PGE2 and PGD2, and between 14-HDHA and 17-HDHA. Ion chromatographs show successful baseline separation between each example of isomers, and added structural diagrams shows the similarity in structure between isomers.

Scheduled MRM

Scheduled multiple reaction monitoring (sMRM) containing two transitions per analyte over a 120 second acquisition window, covering both positive and negative ionisation modes was used to measure 68 lipid mediators (Figure 4). Due to the large number of transitions of this method, dwell time and cycle time were optimised using sMRM. Each peak was assigned a two-minute window where the analyte transitions would be monitored. This allowed higher dwell times to be set for each transition without compromising on the overall cycle time of the method. The two-minute window also allowed enough time either side of the analyte peak to assess the background noise levels (important for correct peak integration) and assign appropriate LOQ. For most oxylipins, the addition of sMRM improved peak shape, the number of data point across each peak, and reduced background noise. Figure 5 shows an example of the improvements to the 8,9-DHET peak.

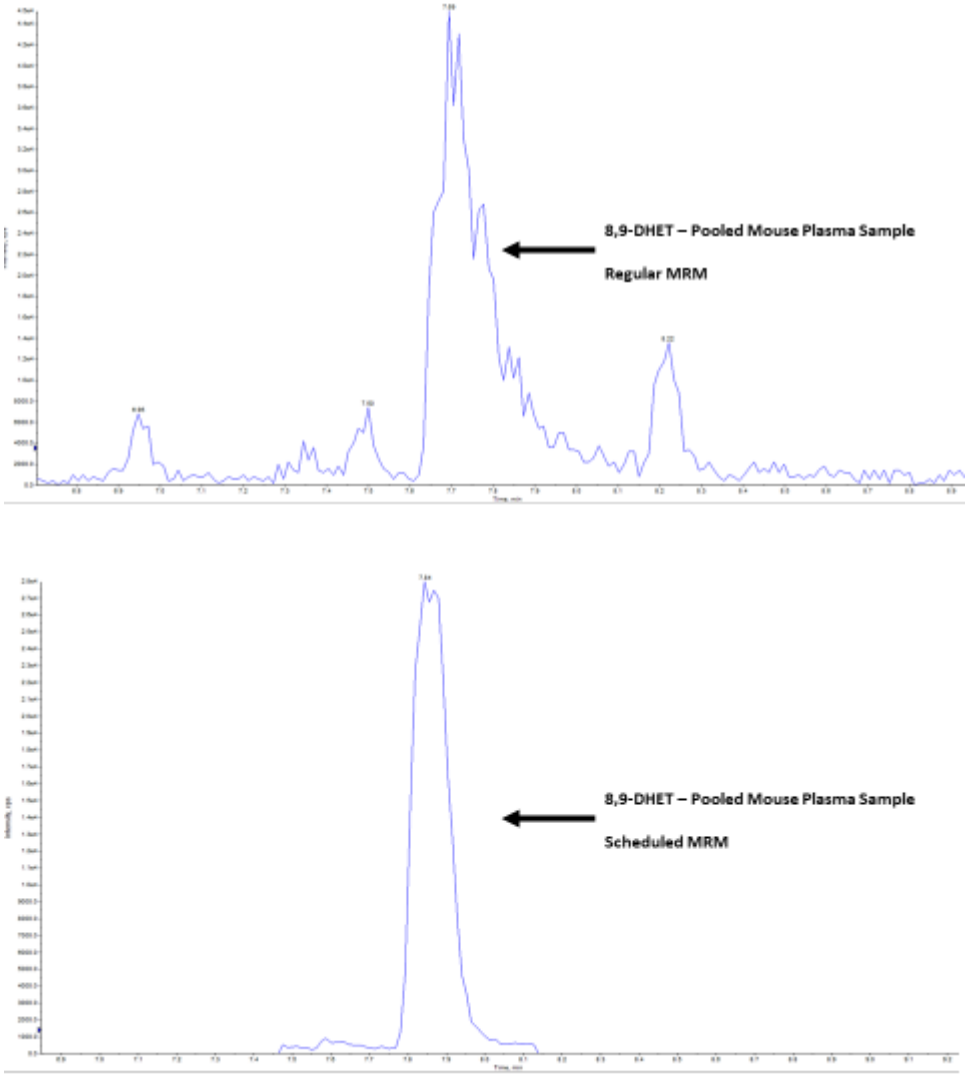

Figure 5. Example chromatograms of 8,9-DHET in pooled mouse plasma with and without the sMRM. sMRM was used for each transition over a 120 sec window and allowed for the optimisation of dwell times to a 1 sec cycle time.

Method Validation

Overall, all analytes showed good accuracy and precision with the majority within 15% variation (Table 4). The correlation coefficients (r^2) in the validation ranged from 0.8920 to 0.9987, showing good linearity across the range of quantification. Recoveries were greater than 50% for the majority of the analytes, showing that the extraction process was generally efficient for most analytes. The lipids 19-HETE, 10,17-DiHDHA, and LxA4 gave recovery values below 50%, but these recoveries were reproducible and did not affect the quantification of these lipids. The metabolites of LA, the HODEs and oxoODEs, give high levels of recovery in these experiments. The

matrix effect calculated showed a wide range of responses. Matrix effects are particularly difficult to calculate for endogenous compounds as they are by nature present in the matrix. The benefit of using a calibration line which is extracted alongside the samples is that in routine quantification recovery and matrix effects are accounted for during the quantification process. Through each set of study samples in this thesis, LLOQ, R^2, accuracy, and precision were calculated to ensure method performance was acceptable.

Table 4. Validation Table of 52 compounds that underwent full validation. *n=6 for QC samples were used for each experiment.*

Lipids	LLOQ (nM)	R^2	Recovery (%)			Matrix Effect (%)	Accuracy (%)	Precision (%CV)
			Low (5 nM)	Medium (50 nM)	High (500 nM)			
AA	500	0.988	127.90	130.00	114.40	58.14	96.27	3.67
TxB2	0.02	0.995	82.40	102.20	96.40	53.30	99.35	23.96
PGE2	0.02	0.998	106.30	106.70	105.60	64.31	109.58	3.71
PGD2	0.02	0.997	114.10	94.70	95.00	54.05	103.34	4.89
LTB4	0.02	0.995	116.20	86.20	93.80	64.15	104.04	5.72
5-HETE	0.02	0.944	123.90	118.10	112.50	20.98	136.91	6.13
8-HETE	0.02	0.983	125.90	119.90	107.40	22.85	79.17	3.31
9-HETE	0.02	0.994	86.30	103.70	70.60	25.91	106.83	12.00
11- HETE	0.02	0.969	119.40	105.50	75.60	27.57	96.30	2.22
12-HETE	0.02	0.929	102.20	124.60	63.80	22.04	121.69	3.53
15-HETE	0.02	0.996	159.00	177.30	119.90	28.23	100.03	3.74
16-HETE	0.5	0.998	109.60	115.60	114.80	44.41	103.38	2.05
19-HETE	5	0.994	28.50	104.00	125.10	44.49	103.36	8.86
20-HETE	0.1	0.997	104.20	108.70	117.60	42.21	108.66	6.45
12-HpETE	0.02	0.929	76.10	85.90	150.90	113.51	60.82	2.36
5,6-EET	0.02	0.985	131.30	103.50	68.50	23.58	112.21	12.91
8,9-EET	0.02	0.984	83.60	96.20	50.60	24.76	86.46	9.00
11,12-EET	0.02	0.959	95.10	92.50	63.30	23.51	102.99	5.91
14,15-EET	0.02	0.993	170.40	172.60	104.50	28.93	99.96	7.83
5,6-DHET	0.02	0.990	107.90	102.10	118.50	43.04	111.15	3.73
8,9-DHET	0.02	0.997	109.10	99.70	122.40	31.17	105.32	3.77
11,12-DHET	0.02	0.995	125.00	95.70	128.40	43.02	91.05	2.73
14,15-DHET	0.02	0.993	110.70	104.40	125.30	44.94	109.37	4.23
5(S),6(R)-DiHETE	0.004	0.995	80.70	78.60	80.10	26.16	102.11	20.82
5,12-DiHETE	0.002	0.956	63.00	89.20	88.00	36.68	106.77	4.59
5,15-DiHETE	0.004	0.998	136.30	78.00	73.40	27.17	90.21	9.77
8,9-DiHETE	0.5	0.993	160.30	92.50	81.00	16.90	102.89	9.22
8,15-DiHETE	0.004	0.998	78.00	103.30	93.50	36.80	110.28	1.42
Linoleic Acid	2500	0.995	99.40	131.60	127.80	54.97	104.37	2.01
9-HODE	0.5	0.998	276.10	255.10	196.50	50.28	104.90	3.71
13-HODE	0.5	0.995	151.70	212.80	161.80	33.13	96.20	2.32
9-OxoODE	0.5	0.984	250.70	208.80	102.50	25.94	123.73	12.02
13-OxoODE	0.5	0.987	162.20	246.00	442.40	203.37	111.40	7.54
DHA	500	0.919	117.00	128.60	114.30	65.33	100.56	4.75
17-HDHA	0.02	0.992	96.40	91.60	101.50	39.42	119.83	5.57
14-HDHA	0.02	0.995	91.90	109.60	104.20	31.81	101.03	2.27
EPA	500	0.892	112.20	148.60	141.50	54.96	101.12	9.22
18-HEPE	0.02	0.998	107.60	117.00	148.60	11.17	71.82	6.42
10,17-DiHDHA	0.002	0.985	8.33	12.39	10.83	4.47	121.28	11.03
Resolvin D1	0.002	0.989	112.20	94.00	98.90	30.84	77.37	2.37
Resolvin D2	0.004	0.983	120.10	118.20	100.40	38.61	75.60	10.16
Resolvin D3	0.01	0.966	114.90	89.40	82.20	29.33	83.19	8.46
Resolvin D5	0.1	0.923	118.80	87.00	89.20	30.16	69.86	9.92
Protectin D1	0.01	0.971	61.70	84.40	74.50	28.97	100.67	7.22
Lipoxin A4	0.01	0.976	50.00	43.80	16.70	24.81	110.17	11.17
Lipoxin B4	0.1	0.984	151.80	96.60	97.10	54.76	118.03	12.33
Maresin 1	0.1	0.992	55.00	102.90	89.00	30.53	104.35	21.09
Maresin 2	0.01	0.994	106.00	100.60	116.90	42.21	108.36	7.52
PEA	0.1	0.973	51.70	101.90	102.20	56.93	119.82	10.75
OEA	0.1	0.958	53.30	103.60	85.20	47.11	104.06	11.45
2AG	0.1	0.989	58.60	119.90	106.20	66.43	96.97	6.76
AEA	0.1	0.998	51.10	122.90	97.20	47.71	98.95	2.83

2.3.2 Analysis of lipid profiles in human plasma and serum samples from healthy volunteers

Multivariate analysis shows plasma and serum have distinct oxylipin profiles

35 individual oxylipins were consistently detected in the serum and plasma samples and the measured concentrations of these analytes were used as a basis for further multivariate and univariate data analysis. PCA and PLS-DA were used for multivariate analysis of the plasma, standing plasma and serum samples data sets obtained from targeted lipidomic profiling where absolute concentration was taken as response for each variable (lipid mediators). A total cumulative variance of 55.3 % (component 1- 46 % and Component 2- 9.3 %) in PLS-DA analysis was obtained for these three groups where serum samples were clearly separated from the plasma and standing plasma samples (Figure 6A). Some differences were observed between the lipid profiles of fresh plasma and standing plasma but not as clearly separated as observed in serum samples. The PLS-DA model was validated to find out the prediction accuracy and fit of the model. The validation results indicated R2 = 0.95, Q2 = 0.73 and accuracy = 0.75 showing good fit of the developed model.

The discriminatory lipid mediators playing important role in separation of the three groups (fresh plasma, standing plasma, and serum samples) in PLS-DA analysis were found based on variable importance in projection (VIP). The lipid mediators having VIP>1.0 were identified as most important discriminatory lipids and found list of 18 lipid mediators (TxB2, 14, 15-DHET, 11, 12-DHET, 11-HETE, 8,9-DiHETE, 12-HpETE, 16-HETE, 8,9-DHET, 11,12-EET, 5,6-EET, LTB4, 12-HETE, AA, 8-HETE, 8,9-EET, PGE2, 5-HETE and 5,6-DHET) having VIP>1.0 where most of them were arachidonic acid and their metabolites (Figure 6B). These results give strong evidence for different oxylipin profiles for plasma and serum, but suggest that fresh and standing plasma share mostly similar profiles. These differences will be explored in more detail in the next section where individual oxylipin concentrations in each group are compared using matched-pair univariate analyses.

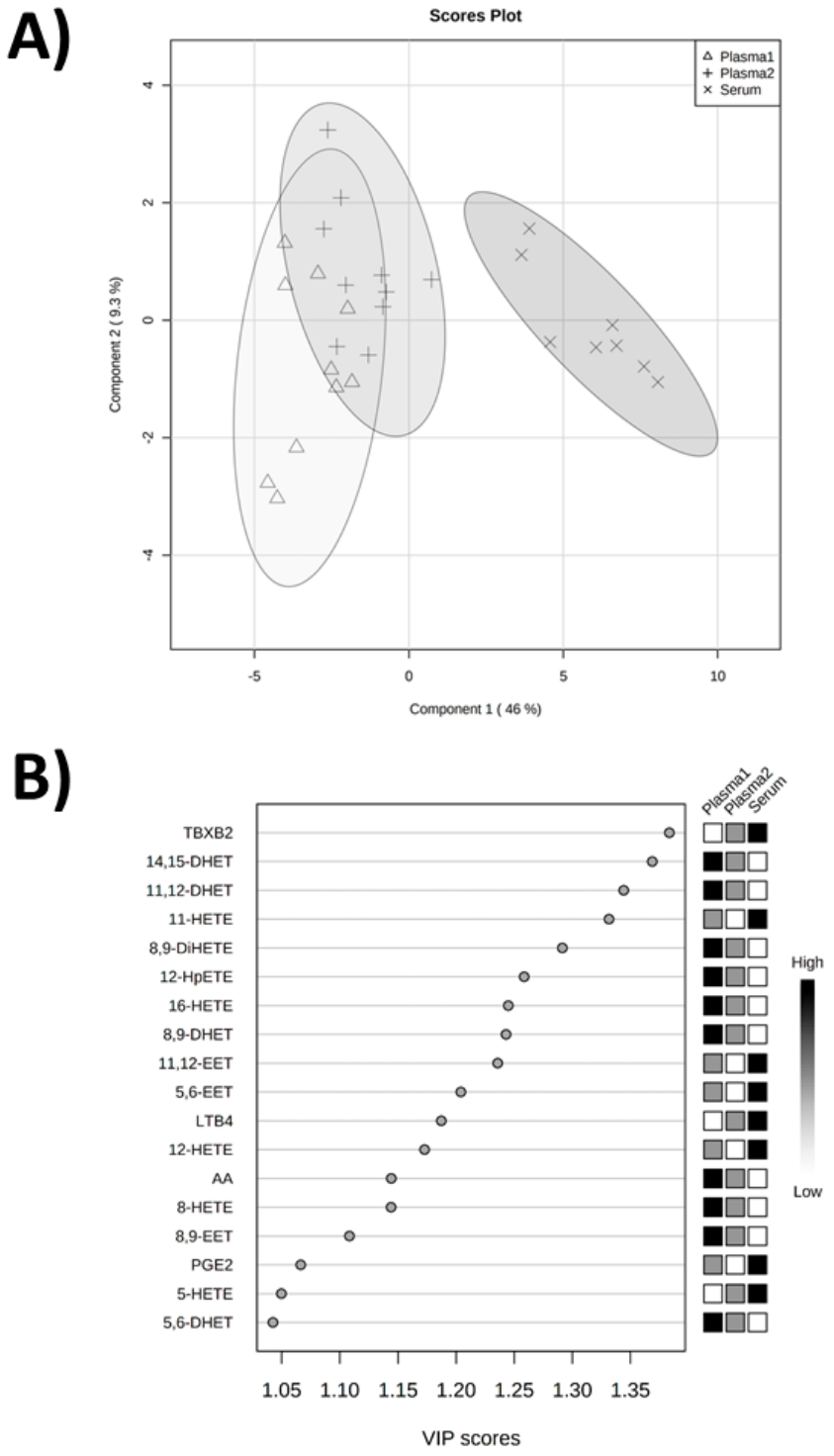

Figure 6. A) Partial least square discrimination analysis (PLS-DA) score plot for the fresh plasma (plasma 1), standing plasma (plasma 2) and serum samples obtained from the healthy volunteers (n = 10) showing three different clusters with R2 = 0.95, Q2 = 0.74 and accuracy = 0.75. B) Variable importance in projection (VIP) score plot showing the important lipid mediators responsible for the separation of the clusters of plasma, standing plasma and serum samples.

Comparison of human plasma and serum oxylipins levels in healthy volunteers

Comparison of the levels between plasma and serum collected from healthy volunteers showed that overall several lipids were significantly different between the matrices (Table 5). Of the PUFAs measured in this study (AA, LA, EPA, and DHA) only levels of AA were significantly different between matrices, being significantly higher in serum than both fresh and standing plasma (Table 5, Figure 7A). Levels of 11-dehydroxy-TX B2, PGD2, and LTB4 were only detectable in serum and were either not present or not detectable in plasma. Levels of TXB2 and PGE2 were detectable in both matrices and significantly higher in serum compared to both fresh and standing plasma (Figure 7 B-C, Table 5). The levels of all HETEs measured (5-, 8-, 11-, 12-, 15-, and 16-HETE) were all significantly higher in serum compared to both fresh and standing plasma (Figure 7D-I).

Table 5. Concentrations of lipid mediators quantified in human plasma and serum.

Lipid	Fresh Plasma			Serum			P Value (Paired t test)	Biosynthetic Enzymes
	Mean	±	SD	Mean	±	SD		
TBXB2	0.15	±	0.02	23.46	±	14.71	0.001	COX-1, COX-2, TXS
11-dehydroxy-TBXB2	Not Detected			0.35	±	0.20	-	COX-1, COX-2, TXS
PGE2	0.03	±	0.01	0.29	±	0.17	0.001	COX-1, COX-2, mPGES-1, mPGES-2, cPGES
PGD2	Not Detected			0.15	±	0.06	-	COX-1, COX-2, H-PGDS, L-PGDS
LTB4	Not Detected			1.84	±	1.51	-	5-LOX, LTA4H
5-HETE	0.20	±	0.10	2.59	±	2.12	0.007	5-LOX, LTA4H
8-HETE	0.13	±	0.04	0.24	±	0.10	0.002	8-LOX
11-HETE	0.11	±	0.04	1.19	±	0.65	0.001	COX-1/2 (precursor 11-HpETE minor COX reduction product)
12-HETE	1.78	±	0.96	24.78	±	18.51	0.005	12-LOX
15-HETE	0.80	±	0.34	3.76	±	1.89	0.001	15-LOX
16-HETE	0.15	±	0.05	0.18	±	0.04	0.015	CYP450
12-HpETE	0.32	±	0.17	0.59	±	0.21	0.001	12-LOX
5,6-EET	0.69	±	0.35	9.57	±	7.06	0.004	CYP450
5,6-DHET	0.10	±	0.05	0.12	±	0.06	0.001	CYP450, s-EH
8,9-DiHETE	0.02	±	0.01	0.02	±	0.01	0.762	
8,9-EET	0.11	±	0.04	0.20	±	0.07	0.001	CYP450
8,9-DHET	0.10	±	0.04	0.11	±	0.04	0.320	CYP450, s-EH
11,12-EET	2.06	±	1.20	32.49	±	23.84	0.004	CYP450
11,12-DHET	0.40	±	0.19	0.41	±	0.17	0.676	CYP450, s-EH
14,15-EET	0.69	±	0.38	3.98	±	2.10	0.001	CYP450
14,15-DHET	0.33	±	0.14	0.34	±	0.13	0.669	CYP450, s-EH
9-HODE	16.39	±	16.51	17.15	±	18.74	0.560	linoleate 9S-lipoxygenase
9-oxoODE	1.77	±	1.87	2.24	±	3.07	0.386	linoleate 9S-lipoxygenase
13-HODE	41.32	±	47.47	43.19	±	52.68	0.580	lipoxygenase, 15-LOX
13-oxoODE	11.34	±	13.52	11.96	±	13.39	0.791	lipoxygenase, 15-LOX
18-HEPE	0.14	±	0.13	0.14	±	0.13	0.013	CYP450, acetylated COX-2
17-HDHA	0.31	±	0.28	0.42	±	0.17	0.040	15-LOX
14-HDHA	1.38	±	3.13	1.61	±	0.65	0.814	15-LOX, 12-LOX
AEA	0.39	±	0.10	0.67	±	0.14	<0.0001	FAAH, NAPE-PLD
OEA	5.45	±	1.73	5.53	±	1.24	0.885	NAPE-PLD
2-AG	7.27	±	5.50	11.19	±	10.85	0.060	MAGL, DAGL
AA	9.93	±	4.29	19.17	±	7.17	0.001	linoleoyl-CoA desaturase, PLA2
LA	81.32	±	49.48	94.11	±	59.57	0.181	
EPA	2.31	±	2.60	2.47	±	2.11	0.523	
DHA	11.50	±	9.27	12.07	±	8.09	0.488	

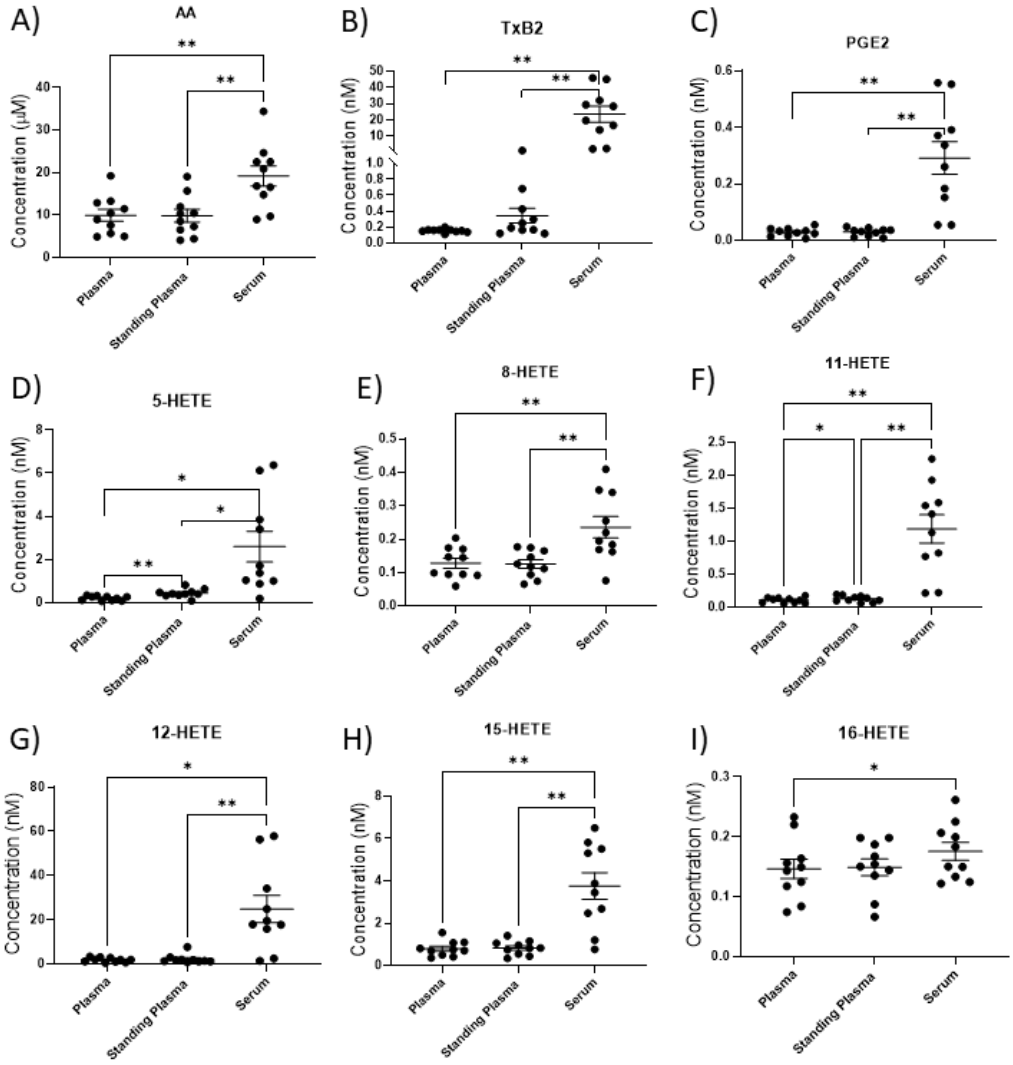

*Figure 7. Levels of A) AA and metabolites B) TXB2, C) PGE2, D) 5-HETE, E) 8-HETE, F) 11-HETE, G) 12-HETE, H) 15-HETE, and I) 16-HETE in fresh plasma, standing plasma, and serum from n=10 healthy volunteers. Data are presented as mean ± SEM. Significance was assessed using a repeated measures one-way ANOVA with Tukey's multiple comparisons test. *p=<0.05, **p=<0.01.*

The CYP450 metabolites of AA and EETs, showed higher levels in serum compared to both plasma groups but were stable between fresh and standing plasma (Figure 8 A-D). Their downstream sEH metabolites, the DHETs, showed that only levels of 5,6-DHET were significantly higher in serum compared to plasma, with 8,9-, 11,12-, and 14,15-DHET levels being consistent between all matrices (Table 5). Similarly, levels of LA and its metabolites 9-HODE, 13-HODE, 9-oxoODE, and 13-oxoODE were consistent between plasma and serum (Table 5).

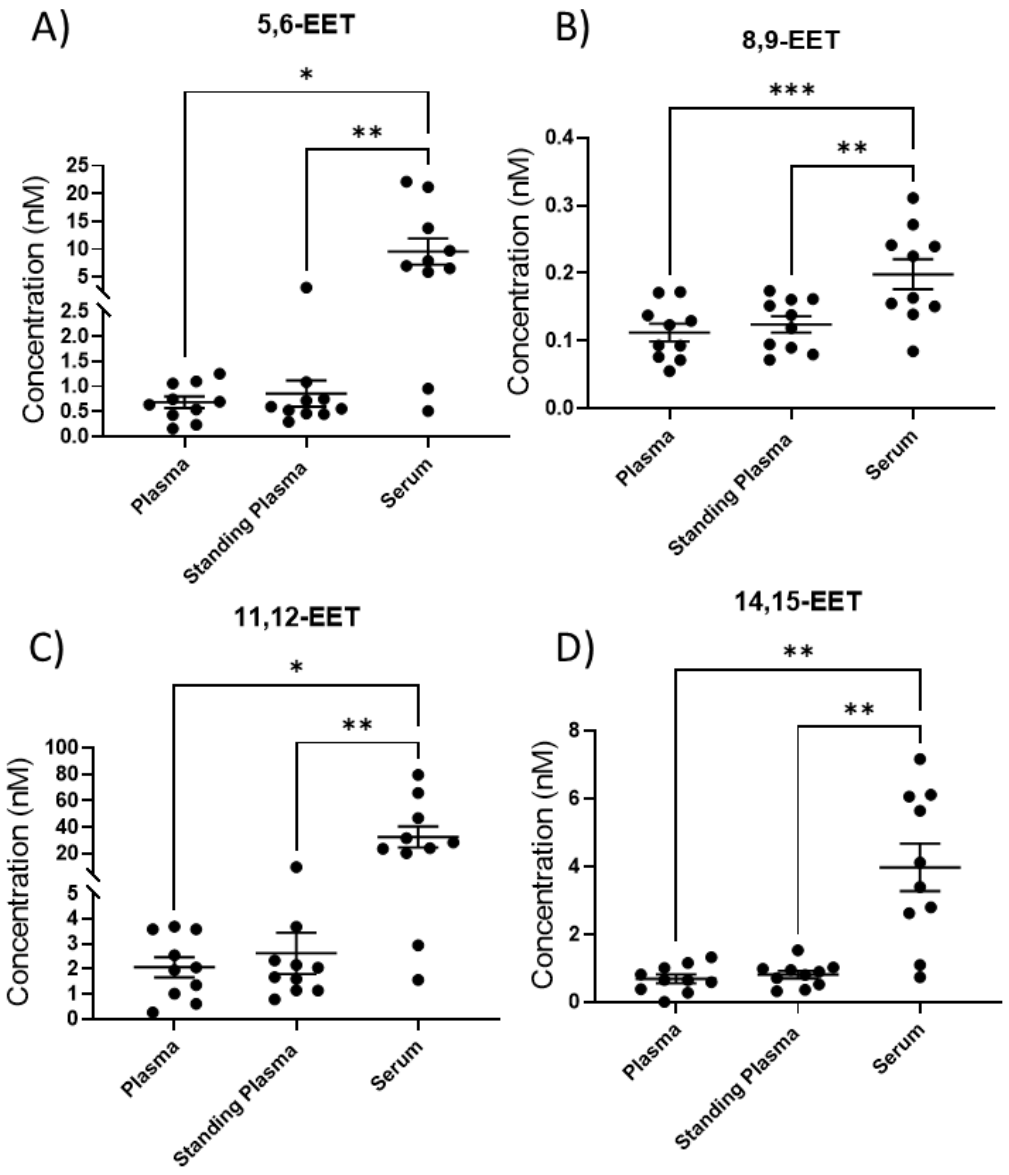

*Figure 8. Levels of A) 5,6-EET B) 8,9-EET, C) 11,12-EET , and D) 14,15-EET, in fresh plasma, standing plasma, and serum from n=10 healthy volunteers. Data are presented as mean ± SEM. Significance was assessed usinga repeated meansures one-way ANOVA with Tukey's multipule comparisons test. *p=<0.05, **p=<0.01.*

Levels of the endocannabinoid-like molecule OEA were stable across matrices, however AEA was significantly higher in both standing plasma and serum compared to fresh plasma. There were no significant changes between levels of 2-AG in fresh plasma compared to standing plasma or serum, however levels were significantly higher in serum compared to standing plasma (Table 5).

Comparison of plasma and serum oxylipin levels in human clinical samples from osteoarthritis patients

To investigate differences in oxylipin levels between plasma and serum in a clinical setting, blood samples were collected from a sub-set of osteoarthritis patients (n=31) recruited to the iBEAT-OA cohort. Blood samples were prepared into plasma and serum according to standard clinical practices, and their oxylipin profiles measured (Table 6). Overall, the differences seen between the oxylipin levels in the clinical setting mirror what is seen in the healthy volunteers but with notable exceptions. Firstly, levels of LA were significantly lower in the serum compared to plasma in the clinical cohort whereas in the healthy cohort these were stable. In contrast, the LA metabolites HODEs and oxoODEs were significantly increased in serum compared to plasma (Figure 9A-D). Levels of 14-HDHA, 8,9-DHET, and 11,12-DHET also showed increased levels in serum compared to plasma in the clinical cohort (Figure 9E-F). Finally, the levels of OEA were significantly higher in the serum compared to the plasma (Figure 9H).

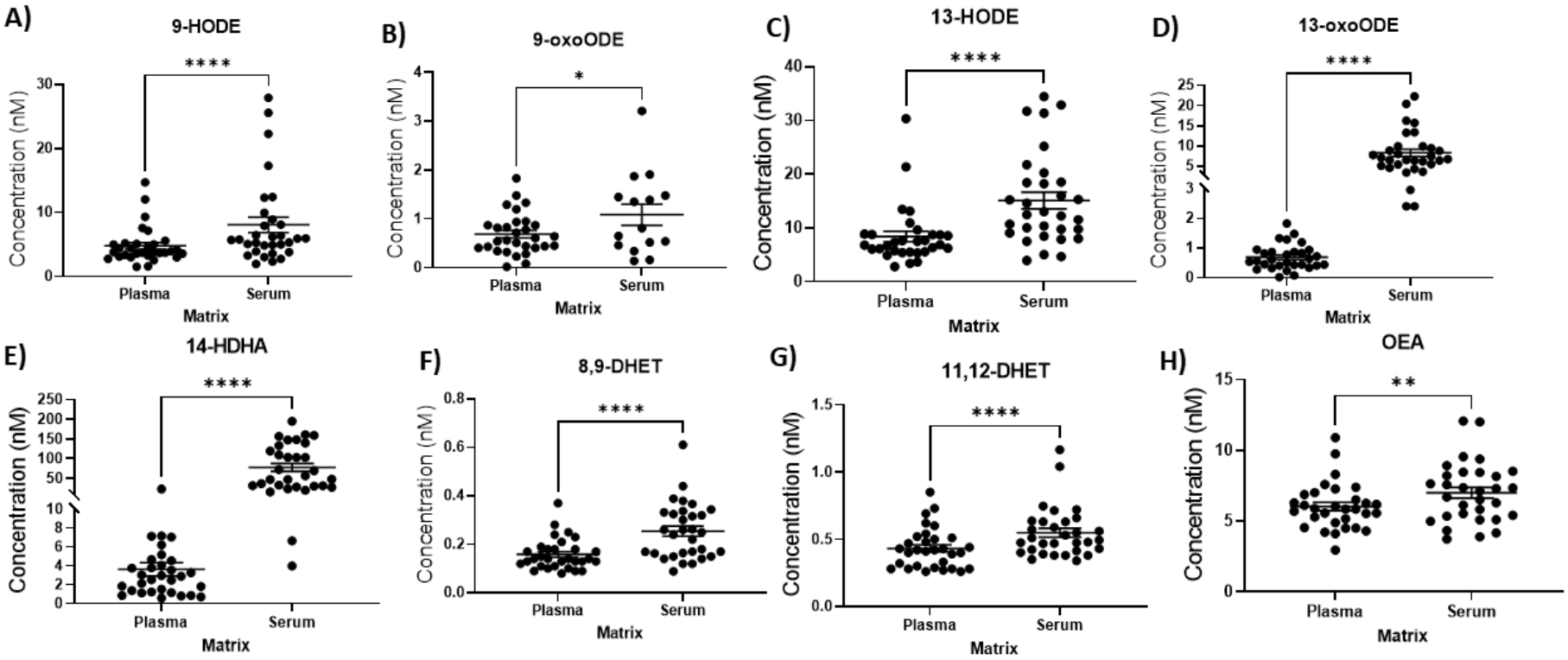

*Figure 9. Comparison of levels of A) 9-HODE; B) 9-oxoODE; C) 13-HODE; D) 13-oxoODE; E) 14-HDHA; F) 8,9-DHET; G) 11,12-DHET in plasma and serum collected from people with OA. Significance was assessed using Wilcoxon Test. . *p=<0.05, **p=<0.01, ***p=<0.001, ****p=<0.0001.*

Table 6. Concentrations of oxylipins measured in a clinical study of n=31 participants. Significant changes were assessed using a paired t-test.

Lipid	Plasma			Serum			P Value	Fold Change
	Mean (nM)	±	SD	Mean (nM)	±	SD		
TXB2	0.44	±	0.61	27.61	±	40.00	<0.0001	62.8
11-dehydrox-TXB2	Not Detected			0.53	±	0.58	-	-
PGE2	0.04	±	0.04	0.42	±	0.47	<0.0001	10.7
PGD2	Not Detected			Not Detected			-	-
LTB4	0.06	±	0.05	0.78	±	0.99	<0.0001	12.5
5-HETE	0.52	±	0.20	4.89	±	9.72	<0.0001	9.3
8-HETE	3.92	±	2.64	1.48	±	1.57	0.0001	0.4
9-HETE	0.12	±	0.04	0.16	±	0.07	0.1248	1.3
11-HETE	0.21	±	0.07	2.87	±	3.55	<0.0001	14.0
15-HETE	1.02	±	0.34	9.83	±	9.08	<0.0001	9.6
16-HETE	0.14	±	0.03	0.20	±	0.05	<0.0001	1.4
19-HETE	0.56	±	0.30	0.34	±	0.25	0.0293	0.6
5,6-EET	1.07	±	0.48	1.02	±	0.99	0.8848	1.0
5,6-DHET	0.24	±	0.09	30.91	±	33.76	<0.0001	127.6
8,9-EET	0.46	±	0.17	1.56	±	1.99	0.0184	3.4
8,9-DHET	0.16	±	0.06	0.25	±	0.11	<0.0001	1.6
11,12-EET	1.55	±	0.58	2.43	±	3.94	>0.9999	1.6
11,12-DHET	0.43	±	0.15	0.55	±	0.18	<0.0001	1.3
14,15-EET	0.76	±	0.29	7.69	±	11.86	0.011	10.1
14,15-DHET	0.37	±	0.13	0.41	±	0.18	0.0627	1.1
9-HODE	4.79	±	2.78	8.08	±	6.52	<0.0001	1.7
9-oxo-ODE	0.69	±	0.41	1.09	±	0.81	0.0339	1.6
13-HODE	8.37	±	5.30	15.09	±	8.37	<0.0001	1.8
13-oxo-ODE	7.54	±	2.97	8.31	±	4.89	<0.0001	1.1
18-HEPE	0.22	±	0.11	0.73	±	0.72	<0.0001	3.4
17 HDHA	0.45	±	0.24	2.58	±	1.61	<0.0001	5.7
14-HDHA	3.61	±	3.90	77.25	±	55.25	<0.0001	21.4
AEA	1.30	±	0.38	1.20	±	0.66	0.4102	0.9
OEA	6.03	±	1.61	7.01	±	2.08	0.0016	1.2
PEA	7.99	±	2.00	25.70	±	28.96	0.0019	3.2
2-AG	50.84	±	30.45	50.84	±	23.72	0.839	1.0
AA (µM)	38.14	±	13.19	47.67	±	15.97	<0.0001	1.2
LA (µM)	357.28	±	133.57	244.83	±	117.50	<0.0001	0.7
EPA (µM)	16.66	±	10.30	25.37	±	12.99	0.0635	1.5
DHA (µM)	39.49	±	17.76	43.13	±	21.29	0.2556	1.1

Multivariate analysis shows plasma and serum have distinct oxylipin profiles in people with osteoarthritis

PLS-DA analysis was performed for the plasma and serum samples obtained from the people with osteoarthritis. In these sample sets, there were only two groups and PLS-DA analysis showed two different clusters for plasma and serum samples with total variance of 69 % (component 1- 45.1% and component 2- 24.4%) (Figure 10A). PLS-DA model was found to be fit through validation in terms of R2= 0.978, Q2= 964 and accuracy= 1.0 and analysis reveals clear difference in the lipidomic profile of plasma and serum sample. The VIP graph obtained from PLS-DA analysis provides the list of important lipid mediators involved in separation of the plasma and serum clusters. A total of 12 lipid mediators were identified (11-dehydroxy-TXB2, TXB2, 14-HDHA, PGE2, 19-HETE, 5,6-DHET, 11-HETE, 15-HETE, LTB4, 17-HDHA, 5-HETE and 9-oxoODE) as having VIP>1.0 and these are considered as key lipid mediators responsible for separation of the two clusters of the samples (Figure 10B). Most of the lipid mediators among these were pro-inflammatory and upregulated in the serum samples. The result of the multivariate analysis for osteoarthritis samples were in accordance with the univariate analysis as in the case of the healthy volunteers.

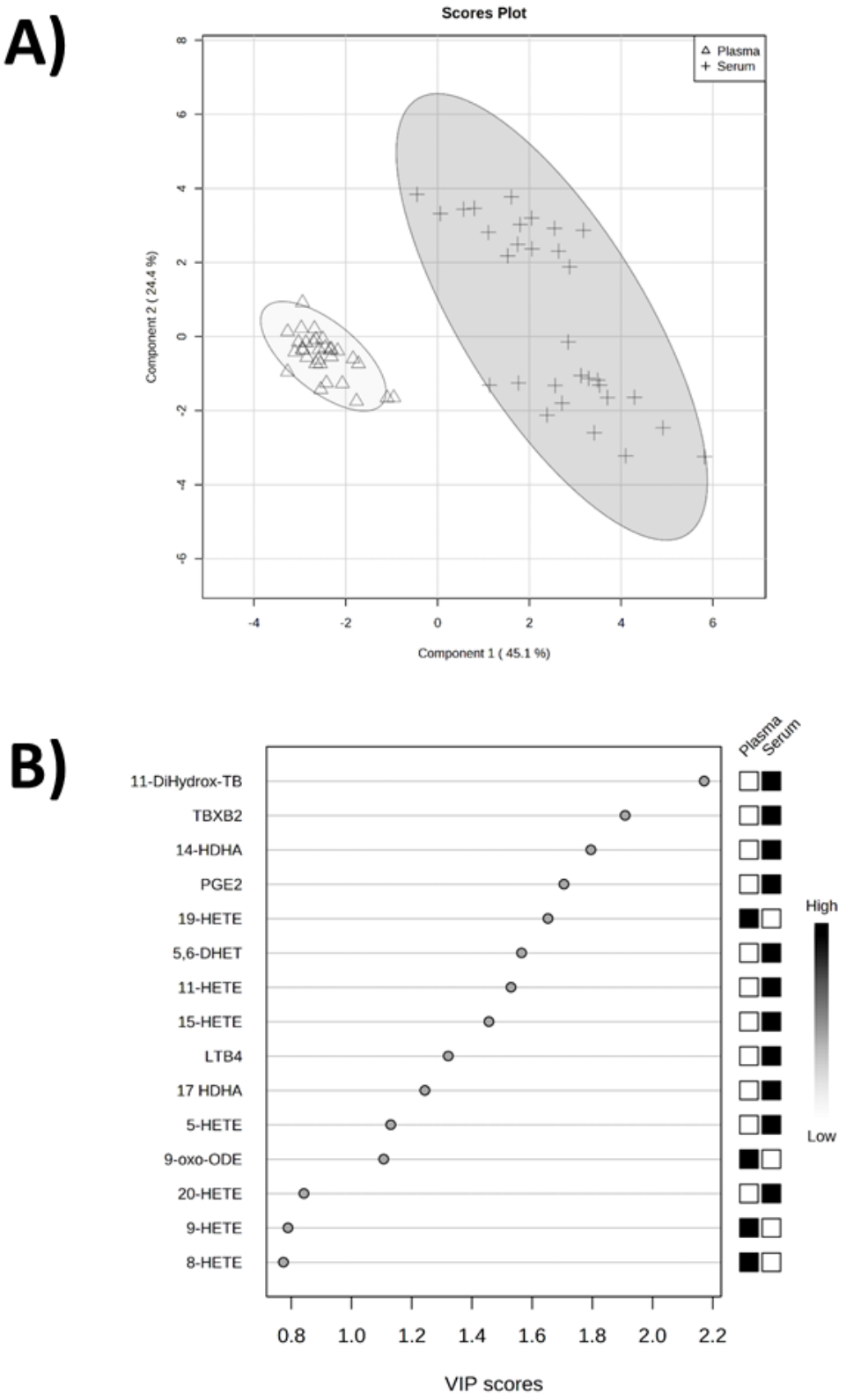

Figure 10. Partial least square discrimination analysis (PLS-DA) showing two different clusters for plasma and serum human clinical samples with R2= 0.978, Q2=0 964 and accuracy= 1.0. B) Variable importance in projection (VIP) score plot showing key maker compounds involved in separation of the plasma and serum clusters in PLS-DA model where 13 marker compounds have VIP>1.0.

Correlation between levels of oxylipins in serum and plasma in healthy volunteers and osteoarthritis patients

Correlation analysis was performed between levels of lipids measured in fresh plasma and serum in both cohorts which are summarised in Table 7. In healthy volunteers, levels of LA, DHA, and EPA were all significantly correlated between plasma and serum – whereas levels of AA were not. With the exception of 8-HETE and 16-HETE, all of the HETEs, PGs, and TXs were not correlated between matrices. The CYP450 metabolites of AA, the EETs, were also not correlated, with the exception of 8,9-EET. All of the DHETs (the sEH metabolites of the EETs) had levels which correlated between the matrices. This is also the case with the LA metabolites HODEs and oxoODEs, as well as the omega-3 PUFA metabolites 18-HEPE and 17-HDHA. Finally, of the endocannabinoids measured AEA and 2-AG were correlated – whereas OEA was not. In the clinical cohort, levels of AA, LA, DHA, TXB2, PGE2, 8,9-, 11,12-, & 14,15-DHET, endocannabinoidss, 18-HEPE, and 9-, & 13-HODE were correlated between plasma and serum.

Table 7. Correlation analyses performed between levels of plasma and serum collected in both healthy volunteers (n=10) and people with osteoarthritis (n=31). Significance was assessed using Pearson's test.

Lipid	Healthy Volunteers		Osteoarthritis Patients	
	R Value	P Value	R Value	P Value
AA	0.611	0.060	0.387	0.031
TBXB2	-0.153	0.674	0.375	0.041
PGE2	0.385	0.273	0.596	0.006
5-HETE	0.366	0.298	0.346	0.056
8-HETE	0.668	0.035	-0.123	0.510
11-HETE	0.161	0.657	0.210	0.256
15-HETE	0.534	0.112	0.196	0.291
16-HETE	0.81	0.005	0.306	0.094
5,6-EET	0.035	0.924	-0.019	0.916
8,9-EET	0.737	0.015	-0.043	0.818
11,12-EET	0.033	0.927	0.002	0.993
14,15-EET	0.439	0.204	0.150	0.420
5,6-DHET	0.976	<0.0001	0.102	0.587
8,9-DHET	0.707	0.022	0.535	0.002
11,12-DHET	0.925	0.0001	0.659	<0.0001
14,15-DHET	0.909	0.0003	0.743	<0.0001
AEA	0.745	0.013	0.394	0.028
OEA	0.329	0.354	0.656	<0.0001
2-AG	0.977	<0.0001	0.567	0.0009
LA	0.899	0.0004	0.486	0.006
9-HODE	0.985	<0.0001	0.7246	<0.0001
9-oxoODE	0.741	0.023	0.431	0.125
13-HODE	0.986	<0.0001	0.646	<0.0001
13-oxoODE	0.872	0.001	0.146	0.442
EPA	0.977	<0.0001	0.030	0.872
18-HEPE	0.981	<0.0001	0.584	0.0006
DHA	0.971	<0.0001	0.694	<0.0001
17-HDHA	0.911	0.0002	0.181	0.331
14-HDHA	0.532	0.113	0.140	0.452

2.4 Discussion

Although several comparable methods have been reported that separate similar groups of lipids over LC runs < 15 mins (Wang, Armando et al. 2014, Wolfer, Gaudin et al. 2015), the large number of transitions in this MRM method increased the cycle time significantly which meant dwell times for each transition had to be reduced which in turn reduced sensitivity and gave poor peak shape. To take full advantage of scheduled MRM, a 25 minute run time was used with aimed to separate analytes as much as possible, similar to other reported methods (Strassburg, Huijbrechts et al. 2012, Thakare, Chhonker et al. 2018, Hartling, Cremonesi et al. 2021). This allowed for increased dwell times for each transition across an acquisition window of 120 seconds. This window accommodates for any shifts in retention time and sufficient background noise to allow realistic signal to noise calculations. The experiments performed for the validation of the method showed that it was possible to accurately and reproducible quantify a panel of pro- and anti-inflammatory oxylipins in human plasma and serum.

The method developed met the main criteria of the FDA/MHRA guidelines for most analytes. The metabolites of LA, the HODE and oxoODEs, showed high levels of recovery. I believe this is due to high levels of background levels of these analytes in both the BSA and from the SPE cartridges. This prompted efforts to reduce this background, and with fresh stock of fatty acid free BSA levels of HODEs and oxoODEs were significantly reduced. The levels of oxylipins measured in healthy individuals were consistent with literature with most being in the picomolar and nanomolar range for most analytes and micromolar range for PUFAs (Zhang, Pearson et al. 2007, Mainka, Dalle et al. 2020, Rund, Nolte et al. 2020). The validation of the method provide confidence in the measurement of the oxylipins, and provides us with fully quantitative data which can be compared between studies within our research group and with other labs around the world.

In healthy volunteers and people with OA, 35 oxylipins across four different PUFA pathways were quantified in plasma and serum. Oxylipins that were not able to be detected in plasma or serum included the SPM molecules resolvins, maresins, lipoxins, and protectin D1 – although their precursors were detected. This is likely due to the low endogenous levels of SPMs in biological samples, particularly in plasma/serum, possibly due to a lack of high systemic inflammation in participants within this study – this is discussed in further detail in chapter seven. These data show clear differences in the levels of many oxylipins measured in

plasma and serum prepared from the same blood collection. The stability of most PUFA precursors between matrices suggests that changes are driven by activation/inhibition of downstream enzymatic pathways including COX-2 and CYP450.

The comparison of fresh plasma and serum in the healthy volunteers, and between plasma and serum in the clinical cohort, both showed that the AA derived metabolites had the most significant difference in levels between the matrices. It is likely that activation of PLA2 during coagulation of blood in pre-serum samples would increase circulating levels of AA through release from phospholipid membranes (Penzo, Petronilli et al. 2004), whereas in heparinised blood, heparin inhibits the activity of PLA2 which would prevent AA from being released (Dua and Cho 1994). The coagulation process also activates platelets which are a key source of oxylipin production, particularly the AA derived eicosanoids (Turnbull, Sander et al. 2022), whereas the omega-3 oxylipins are reported to mediate platelet function (Yamaguchi, Stanger et al. 2021). The oxylipins that show the most dramatic difference are produced through COX1/2 and CYP450 pathways, whereas sEH and LOX pathway metabolites appear to be more stable between matrices. The clinical cohort did show significant differences between levels of the omega-3 metabolites, which were generally not observed in the healthy cohort. This difference between cohorts is likely to be due to differences in the time of blood standing before preparation into plasma and serum between cohorts, with the healthy volunteers samples adhering strictly to the scheduled protocol compared with the OA cohort representing what happens in a realistic clinical environment. The comparison of fresh and standing plasma in healthy volunteers showed that the majority of analytes were stable in heparinised whole blood for 45 minutes at room temperature. This is useful to know for clinical sample collection and processing procedures, as processing times can vary considerably between samples, and there is often a delay between blood collection and centrifugation.

Investigating the correlation between plasma and serum levels of oxylipins showed that the 50-60% of oxylipins showed correlation between matrices. Again, the oxylipins showing the strongest correlation were generally derived from LA, EPA, and DHA, with the exception of the DHETs and endocannabinoids. This indicates that although the levels of oxylipins may differ between matrices, for those oxylipins that show correlation, the serum levels are still representative of the circulating blood levels. For those where levels do not correlate

between plasma and serum, higher levels in serum are unlikelyto be representative of the *in vivo* levels and there is risk of misinterpretation of findings that may not be biologically relevant due to *ex vivo* changes during coagulation.

This study has several limitations, firstly there was a modest number of participants in the healthy cohort – however these participants were all of a similar age & BMI. Information on the medication use of the clinical cohort was not provided, which may have influence over these results. All participant were not supplementing with omega-3 fatty acids within 1 month of blood sample collection, however other dietary sources of fatty acids were not accounted for. Only one anticoagulant was investigated for plasma preparation which mean these results are only descriptive of heparinised plasma, and further investigation looking at other anti-coagulants such as EDTA and citrate is required. Only one coagulation time point was included for serum samples which was 45 minutes, although this is the standard time allowed for clotting, clinical studies report an array of coagulation times ranging from 10 minutes to several hours. Efforts should be made across the lipid analysis community (and bioanalysis as a whole) to ensure that sample preparation procedures and appropriately documented including reporting: serum or plasma; time allowed for clotting in serum; anti-coagulant used for plasma; time taken between collect and centrifugation; stored on ice / at RT prior to centrifugation; and temperature of centrifuge and long term storage freezer. This hopefully will lead to standardised methods which will minimise variation between samples and allow for more realistic comparisons between studies and labs.

Overall, these data show that careful consideration should be made when planning sample collection and choice of matrix as the oxylipin profile does differ between plasma and serum. Heparinised whole blood generally showed stability of oxylipins at room temperature for 45 minutes, which is beneficial knowledge for investigators, particularly in a clinical setting. These results also warrant further work investigation into the effect of different anti-coagulants on the plasma oxylipin profile, and non-standard coagulation times on serum lipid profiles.

Chapter Three

The impact of acute knee injury in active healthy adults on serum levels of oxylipins

Acknowledgements

This study was conducted in collaboration with Dr. Fiona Watt and Prof. Tonia Vincent and their team at the Kennedy Institute of Rheumatology, at the University of Oxford. Participant recruitment, sample collection, and clinical phenotyping was performed by the team at Oxford University. A sub-cohort of the participant samples available were selected for lipidomic analysis, which was carried out at University of Nottingham.

This work is currently under review as the following manuscript:

James Turnbull, Rakesh R. Jha, Dong-Hyun Kim, David A. Barrett, Ana M. Valdes, Jennifer Alderson, Andrew Williams, Tonia L. Vincent, Fiona E. Watt, Victoria Chapman. **The impact of acute knee injury in active healthy adults on serum levels of pro- and anti-inflammatory lipid mediators and associations with knee pain.** [American Journal of Sports Medicine]

Abstract

Despite acute knee injury being a major risk factor for osteoarthritis (OA), the factors that initiate and / or maintain this risk for longer-term knee pain are poorly understood. It was hypothesised that there would be associations between systemic levels of oxylipins and knee symptoms longitudinally following acute knee injury. An assay of 41 oxylipins (quantified by LC-MS/MS) was carried out in sera of i) 47 individuals (median age 28) (sampled within 8 weeks of acute knee injury, at 3 months and 2 years post-injury) and with paired Knee Injury and Osteoarthritis Outcome Scores (KOOS)-4 ii) age-and sex-matched controls. Levels of omega-3 polyunsaturated fatty acids (PUFAs) eicosapentaenoic acid (EPA; p=<0.0001) and docosahexaenoic acid (DHA; p=<0.0001) and the pro-resolution metabolites 17-, and 14-hydroxydocosahexaenoic acid (HDHA) were all significantly greater at the time of injury compared with later times, and were also higher than in healthy controls. Pro-inflammatory prostaglandins (E2 and D2), leukotriene B4 and thromboxane B2 were significantly lower at the time of injury compared to later times. 2 years post-injury, greater levels of 8,9-, 11,12-, and 14,15-DHET were associated with worse knee pain/symptoms. The profile of pro-resolving versus pro-inflammatory lipids immediately following knee joint injury suggests a switch towards pro-resolution pathways, followed by a later activation of pro-inflammatory pathways. The association of DHETs with knee symptoms at 2 years post-injury may suggest a therapeutic potential of targeting relevant pathways to reduce knee pain.

3.1 Introduction

Knee injury is a complex pathology that can lead to chronic pain and is a major risk factor for osteoarthritis (OA) (Majewski, Susanne et al. 2006, Mahmoudian, Lohmander et al. 2021, Watt 2021). Common injuries known to predispose to OA include intraarticular ligament ruptures such as of the anterior cruciate ligament (ACL), acute meniscal tears, as well as intra-articular fracture (Majewski, Susanne et al. 2006). Typically, clinical studies investigating mechanisms of knee pain focus on individuals who have already developed chronic diseases such as knee OA. These people tend to be older in age with established disease and increased rates of associated co-morbidities, such as obesity, diabetes, hypertension, depression, and anxiety (Swain, Kamps et al. 2022). Studies examining initiating processes and biomarkers in this population are therefore challenging.

Understanding the molecular mechanisms that drive the transition from acute injury and whether its resolution is successful or leads to chronic joint pain and disease is important and currently unknown. Knowing the timing of an acute knee injury provides us with the potential to examine these processes including OA pathogenesis longitudinally. This may help to identify therapeutic options for preventing persistent knee pain, early disease or slowing its initiation or progression.

There is an immediate inflammatory response made in the joint by connective tissues to acute knee joint injury, in mice and humans. Previously, colleagues have reported increased levels of proteins in synovial fluid at the time of the knee join injury which were associated with greater levels of knee symptoms at that time, including interleukin-6 (IL-6), monocyte chemotactic protein 1, matrix metalloproteinase 3 (MMP-3), tissue inhibitor of metalloproteinases 1 (TIMP-1), activin A, and tumor necrosis factor–stimulated gene 6 (TSG-6), in the Knee Injury Cohort at Kennedy (KICK) study (Burleigh, Chanalaris et al. 2012, Watt, Ismail et al. 2013, Lieberthal, Sambamurthy et al. 2015). In addition, they found that elevated levels of MCP-1 and IL-6 in synovial fluid at the time of the injury were independently associated with worse knee injury and osteoarthritis

outcome (KOOS4) scores at 2 years following the injury (Watt, Paterson et al. 2016).

Whether pro- and anti-inflammatory oxylipins potentially play roles in the transition from acute knee injury to persistent knee pain or early osteoarthritis is unknown. To the best of current knowledge, lipid pathways have not been studied in the context of acute knee injury in a longitudinal study.

The aim of this study was to study circulating levels of a range of oxylipins longitudinally in individuals following acute knee injury compared to age and sex matched controls. The study then aimed to assess associations between levels of oxylipins and patient reported outcome scores (PROMs) calculated using the knee injury and osteoarthritis outcome score (KOOS) scale. This study was in the KICK cohort, which consisted of young, highly active people who were generally healthy other than having experienced an acute knee injury. The hypothesis was that there would be associations with some of these oxylipins and knee symptoms at the time of the injury and over 2 years.

3.2 Methods

3.2.1 Participants & Study Design

The KICK study recruited people between 2010 and 2014 from a population exposed to acute knee injury who were attending assessment at six hospitals and clinics in London, UK. Inclusion criteria were: clinically significant acute knee injury within 8 weeks of recruitment; aged 16–50 years; knee effusion, evident clinically or by MRI; and evidence of one or more specified structural injuries on MRI (meniscal tear, cruciate ligament rupture, collateral ligament tear, posterolateral corner injury, traumatic chondral defects, articular or periarticular fracture, patellofemoral dislocation, or tibiofemoral dislocation) within 8 weeks of post-injury visit. All participants gave written informed consent to participate before screening, according to the Declaration of Helsinki. South East London Research Ethics Committee 5, UK (REC 10/H0706/44), gave ethics approval. For the purposes of this study, a subgroup of 47 participants were selected from the KICK cohort. This was all participants who had a serum sample available from each of the immediately post-injury, 3 month and 2 year visits.

3.2.2 Healthy controls

Individuals gave consent for blood sampling (REC 11/H0711/17). They had no history of arthritis or knee pain and were approximately matched with the patients for age and sex.

3.2.3 Clinical Outcomes

The primary outcome measure in KICK was the Knee Injury and Osteoarthritis Outcome Score (KOOS), from which KOOS4, a single composite score, can be calculated (an average of 4 of the 5 KOOS subscales including pain, symptoms, sports/recreation, and quality of life) (Roos, Roos et al. 1998). The KOOS and Tegner score, a measure of activity (Briggs, Steadman et al. 2009), were collected at the immediately post-injury visit, which was within 8 weeks of injury, at 3 months and 2 years later (Table 1). Medical review including medication history was collected at each visit.

3.2.4 Biosamples

Venous blood was collected from participants in KICK at each study visit or for healthy controls at a single visit, into plain Vacutainer tubes. Blood was allowed to clot for 40 minutes and then centrifuged at 1600g for 15 minutes at 20°C prior to aliquoting supernatants into cryovials and storage at -80°C in monitored freezers until use.

3.2.5 Lipidomic Analysis

The method described in Chapter 2 were used for these samples. Sample were analysed across two batches for which each were extracted alongside (n=6) QC samples, and were analysed in a signle analytical run on LC-MS/MS.

3.2.6 Statistical Analysis

At the outset of the project, the following analyses were predefined:

- Is acute knee injury associated with changes in oxylipins (comparing to healthy, age, sex matched control data)?
- Do levels of oxylipins change over time following acute traumatic knee injury?
- Are levels of oxylipins associated with patient reported measurements of knee pain over 2 years?
- Are baseline levels of oxylipins associated with future KOOS4 following acute knee joint injury?

Differences between groups including healthy controls were assessed using either Kruskal-Wallis or Mann-Whitney test, depending on the normality of the data, and corrected for multiple comparisons. Differences between two time points in the injury cohort were tested using matched pairs analysis (Friedman test). Associations between circulating lipid levels with knee symptoms (KOOS-4) and activity (Tegner) scores were assessed by linear regression analyses using R programming software (www.r-project.org), and graphs and

descriptive analyses produced using GraphPad Prism (V7). A sensitivity analysis was performed, excluding those participants from the analyses who were either supplementing with omega-3 or taking a COX-2 inhibitor at the time of the blood sample. For some tests, groups were stratified based on the upper (75%) and lower (25%) percentiles of KOOS-4 score at 2 years. Multivariate analysis using Metaboanalyst V4.0 (https://www.metaboanalyst.ca/) was undertaken and principal component analysis (PCA) was performed for data visualisation. Partial least square discrimination analysis (PLS-DA) was performed to identify the key lipids involved in the separation between two time points after knee injury, immediately after injury and at 2 years after injury. A cross validation analysis was used to validate the developed PLS-DA model based on accuracy, R2 and Q2 scores and a permutation test. Lipids having Variable Importance in Projection (VIP) scores greater than 1 were recognized as playing a key role in cluster differentiation.

3.3 Results

3.3.1 Clinical Characteristics of Cohort

Of 150 participants in the KICK cohort, recruited within a median of 21 years from their acute knee injury, 47 participants met the criteria for this sub-study and had their serial serum samples processed for lipidomic analysis (Figure 1).

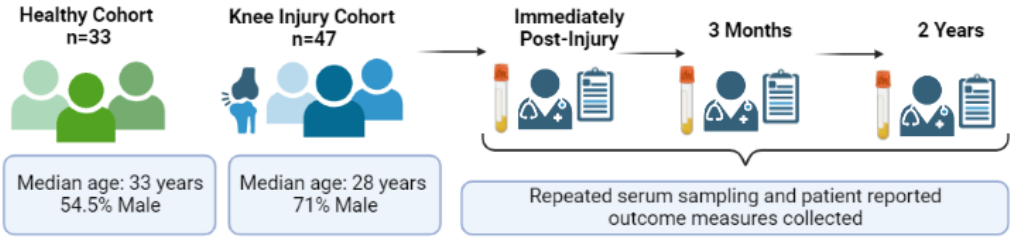

Figure 1. Workflow of study design including basic participant characteristics and data collected.

The mean age was 30, the majority of this subgroup were male (71%) and they were highly active prior to injury, being similar to the overall cohort (Table 1).

Table 1. Data shown are for characteristics of Knee Injury Cohort at Kennedy (KICK) participants included in this substudy based on our selection criteria; and for the age- & sex-matched controls.

	KICK	Healthy controls
No. of Participants	47	33
Age (median (IQR))	28.0 (21.0-41.2)	33.7 (21-59)
BMI (kg/m^2) (median (IQR))		
Sex: M/F (n,%)	32 (71%) / 13 (29%)	18 (54.5%) / 15 (45.5%)
KOOS-4 Score (median (IQR)):		-
Immediately post-injury	39.7 (27.5-48.1)	
3 Months	62.6 (51.4-71.6)	
2 Years	82.6 (68.6-90.9)	
Tegner Score: (median (IQR))		-
Pre-injury	8.5 (6-10)	
Immediately post-injury	2.0 (1-3)	
3 Months	4.0 (4-5)	
2 Years	6.0 (5-9)	

Overall, participants KOOS-4 score improved over time (Figure 2), however at 3 months and 2 years post-injury there are a significant number of participants

who had low KOOS-4 symptoms indicating on-going knee symptoms including chronic pain.

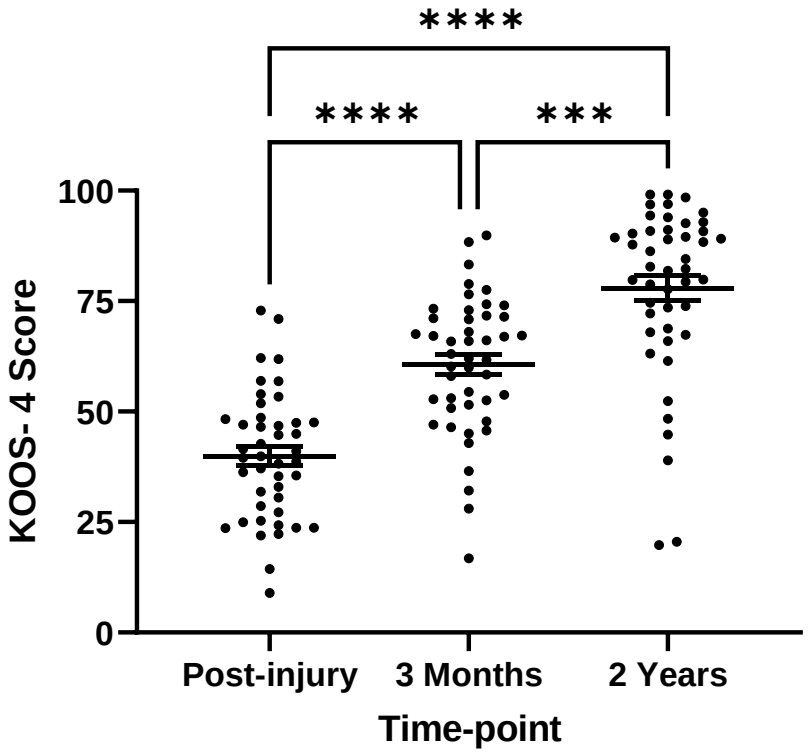

*Figure 2. KOOS-4 scores collected from participants of the KICK cohort immediately post-injury and at 3 months and 2 years post injury. Significance was assessed by Kruskal-Wallis test. ****p=<0.0001, ***p=0.0005. Data are shown as individual values with mean ± SEM for each group.*

3.3.2 Levels of pro-and anti-inflammatory oxylipins following acute knee injury

Levels of the oxylipins were quantified in the healthy control samples, and the KICK participant samples from the 3 visits (Table 2). 43 lipid metabolites met bioanalytical QC criteria for further analysis and their levels were compared between visits and to healthy controls.

Table 2. Bioactive lipid measurements for a panel of 41 lipids meeting QC requirements, quantified by LC-MS/MS are shown, for healthy controls and for participants in the KICK study who were sampled at three time points: immediately post-injury; 3 months; and 2 years after knee injury. Mean and standard deviations (SD) are given. Ratios between the EETs and their corresponding DHETs are also presented Concentrations are as stated in units, either nM or µM.

Lipid (concentration)	**Control (n=34)** Mean ± SD			**Immediately post-injury (n=47)** Mean ± SD			**3 Months (n=47)** Mean ± SD			**2 Years (n=47)** Mean ± SD		
5,6-EET (nM)	0.53	±	0.26	0.42	±	0.14	0.33	±	0.11	0.31	±	0.11
8,9-EET (nM)	2.02	±	5.33	0.95	±	0.57	0.90	±	0.85	0.84	±	0.58
11,12-EET (nM)	133.03	±	149.69	264.54	±	223.77	247.45	±	231.30	268.81	±	256.57
14,15-EET (nM)	0.63	±	0.31	0.64	±	0.24	0.43	±	0.20	0.39	±	0.19
5,6-DHET (nM)	0.72	±	0.82	0.53	±	0.31	0.36	±	0.23	0.33	±	0.16
8,9-DHET (nM)	0.26	±	0.13	0.32	±	0.24	0.24	±	0.12	0.22	±	0.09
11,12-DHET (nM)	0.58	±	0.17	0.94	±	0.52	0.60	±	0.30	0.58	±	0.21
14,15-DHET (nM)	0.51	±	0.13	0.76	±	0.42	0.54	±	0.25	0.52	±	0.15
5,6-Ratio	1.13	±	0.74	0.93	±	0.45	1.12	±	0.51	1.05	±	0.40
8,9-Ratio	5.76	±	10.93	3.69	±	2.70	4.24	±	4.08	4.00	±	2.24
11,12-Ratio	227.16	±	246.77	352.52	±	317.75	472.00	±	525.89	495.31	±	478.88
14,15-Ratio	1.24	±	0.53	0.95	±	0.36	0.83	±	0.35	0.77	±	0.30
TxB2 (nM)	39.69	±	43.11	28.71	±	23.40	57.39	±	52.07	52.96	±	46.35
11-dehy-TxB2 (nM)	0.48	±	0.64	0.57	±	0.67	1.20	±	1.24	1.25	±	1.28
PGE2 (nM)	0.44	±	0.50	0.59	±	0.46	0.85	±	0.73	0.83	±	0.72
PGD2 (nM)	0.43	±	0.72	0.11	±	0.06	0.20	±	0.13	0.18	±	0.12
LTB4 (nM)	1.56	±	2.25	0.65	±	0.94	2.03	±	3.00	1.93	±	2.72
16-HETE (nM)	0.24	±	0.06	0.25	±	0.07	0.23	±	0.08	0.23	±	0.06
11-HETE (nM)	4.36	±	7.79	2.05	±	1.46	3.14	±	2.56	2.88	±	2.24
15-HETE (nM)	12.21	±	19.51	8.50	±	6.01	10.61	±	8.15	10.77	±	9.14
8-HETE (nM)	2.05	±	5.34	1.01	±	0.62	0.98	±	0.92	0.93	±	0.68
12-HETE (nM)	129.87	±	142.16	269.76	±	220.40	245.09	±	219.92	269.16	±	247.69
5-HETE (nM)	20.05	±	70.97	1.57	±	0.85	2.78	±	7.09	1.66	±	1.49
12-HpETE (nM)	3.11	±	1.70	2.72	±	1.24	3.09	±	2.23	3.33	±	2.20
13-oxoODE (nM)	22.69	±	10.47	31.22	±	20.98	17.95	±	8.33	16.56	±	7.63
13-HODE (nM)	59.44	±	45.77	61.37	±	42.24	64.14	±	116.85	42.60	±	24.91
9-oxoODE (nM)	2.68	±	1.53	3.87	±	4.81	2.24	±	0.95	1.81	±	0.63
9-HODE (nM)	25.46	±	27.57	22.17	±	17.66	19.56	±	16.92	16.06	±	9.65
18-HEPE (nM)	0.97	±	2.00	1.46	±	1.30	1.05	±	0.91	0.72	±	0.48
17-HDHA (nM)	2.12	±	3.33	2.63	±	2.02	2.21	±	2.25	1.78	±	1.32
14-HDHA (nM)	14.03	±	14.54	45.95	±	48.05	30.64	±	41.67	28.58	±	28.09
5,12-DiHETE (nM)	1.59	±	2.33	0.75	±	1.06	2.23	±	3.42	2.21	±	3.23
8,9-DiHETE (nM)	0.06	±	0.04	0.12	±	0.08	0.10	±	0.12	0.06	±	0.04
2-AG (nM)	57.30	±	46.52	30.74	±	28.42	37.96	±	24.66	31.38	±	24.81
AEA (nM)	0.61	±	0.36	0.62	±	0.26	0.44	±	0.21	0.49	±	0.21
OEA (nM)	2.97	±	0.93	3.37	±	1.16	2.74	±	0.93	2.93	±	0.72
PEA (nM)	7.85	±	1.45	9.85	±	2.96	8.36	±	2.34	8.57	±	2.23
LA (µM)	272.78	±	112.93	690.38	±	289.17	344.01	±	228.74	277.99	±	121.66
AA (µM)	70.55	±	29.69	108.03	±	33.43	74.46	±	27.94	67.99	±	22.47
EPA (µM)	17.28	±	9.32	41.23	±	35.04	24.15	±	24.00	14.21	±	8.23
DHA (µM)	52.29	±	23.49	104.60	±	51.77	64.02	±	42.08	50.28	±	27.78

To assess whether analyses needed to be adjusted for age, sex, BMI, or activity linear regression analysis was performed between levels of lipid and these potential cofounders. After adjusting for multiple comparisons, none of the lipids were associated with any of the clinical characteristics (Table 3).

Table 3. Associations between serum lipid levels immediately post-injury with age, sex, and Tegner score, tested by univariate linear regression analysis between lipid levels and Tegner scores at 3 months and 2 years post-injury. Adjusting for multiple tests, statistical significance was assessed as p=<0.0012.

Lipid	Age		Sex		BMI (Post-Injury)		BMI (3 Months)		BMI (2 Years)		Tegner (Post-Injury)		Tegner (3 Months)		Tegner (2 Years)	
	R squared	P value	R squared	P value	R squared	P value	R squared	P value	R squared	P value	R squared	P value	R squared	P value	R squared	P value
5,6-EET	0.004	0.6830	0.001	0.8148	0.095	0.0395	0.117	0.0229	0.155	0.0082	0.011	0.4945	7.0E-05	0.9570	0.119	0.0205
8,9-EET	0.002	0.7758	0.045	0.1667	0.004	0.6718	0.040	0.1938	0.001	0.8338	0.021	0.3511	0.002	0.7637	0.011	0.4905
11,12-EET	1.89E-07	0.9978	0.043	0.1761	0.002	0.7531	0.002	0.7637	0.006	0.6070	0.009	0.5342	0.002	0.7961	0.010	0.5080
14,15-EET	0.016	0.4188	0.012	0.4823	0.044	0.1595	0.156	0.0079	0.021	0.3535	0.049	0.1488	4.28E-04	0.8940	0.091	0.0445
5,6-DHET	0.121	0.0209	0.036	0.2150	0.018	0.3680	0.291	0.0002	0.076	0.0703	0.008	0.5704	9.92E-04	0.8392	0.036	0.2124
8,9-DHET	0.053	0.1320	0.025	0.3028	0.003	0.7067	0.222	0.0012	0.016	0.4063	0.052	0.1358	0.001	0.8033	0.015	0.4252
11,12-DHET	0.083	0.0580	0.020	0.3624	0.009	0.5314	0.138	0.0129	0.013	0.4684	0.108	0.0295	0.012	0.4710	0.022	0.3271
14,15-DHET	0.076	0.0702	0.019	0.3697	0.006	0.6200	0.120	0.0215	0.010	0.5088	0.091	0.0466	0.014	0.4443	8.85E-04	0.8462
5,6-Ratio	0.131	0.0159	0.007	0.5956	0.024	0.3083	0.093	0.0444	0.001	0.8207	0.017	0.3988	0.004	0.6766	0.018	0.3811
8,9-Ratio	0.023	0.3270	0.002	0.7748	0.014	0.4369	0.003	0.7111	3.20E-04	0.9082	0.036	0.2146	0.007	0.5990	0.016	0.4056
11,12-Ratio	0.021	0.3469	0.027	0.2893	0.012	0.4711	0.002	0.7660	0.008	0.5597	0.016	0.4080	0.005	0.6550	0.008	0.5475
14,15-Ratio	0.066	0.0931	7.96E-04	0.8558	0.042	0.1741	0.034	0.2292	0.013	0.4698	0.016	0.4140	6.22E-04	0.8723	0.151	0.0084
TBXB2	0.029	0.2665	0.004	0.6926	0.033	0.2257	6.33E-05	0.9591	0.019	0.3717	0.010	0.5224	0.009	0.5326	0.007	0.5949
11-dehy-TBXB2	1.36E-04	0.9401	0.028	0.2794	0.013	0.4631	0.009	0.5732	0.011	0.5009	0.036	0.2193	0.004	0.6939	6.61E-04	0.8669
PGE2	0.008	0.5622	0.010	0.5190	8.04E-04	0.8621	0.005	0.6632	0.005	0.6702	0.008	0.5594	0.020	0.3544	0.009	0.5404
PGD2	0.037	0.2090	0.109	0.0286	0.004	0.7437	0.009	0.5595	0.017	0.4184	0.009	0.5374	0.010	0.5177	0.005	0.6364
LTB4	0.059	0.1132	0.100	0.0367	0.022	0.3317	4.41E-04	0.8924	0.020	0.3616	0.049	0.1475	0.018	0.3825	0.010	0.5138
16-HETE	0.121	0.0207	0.013	0.4542	4.17E-04	0.8928	0.011	0.4933	1.61E-04	0.9348	0.171	0.0053	2.38E-07	0.9975	0.010	0.5165
11-HETE	0.025	0.3089	0.009	0.5511	0.027	0.2751	0.005	0.6498	0.009	0.5503	0.017	0.4055	0.017	0.4036	5.44E-04	0.8792
15-HETE	0.003	0.7105	0.025	0.3040	0.016	0.3981	0.007	0.5935	0.008	0.5576	0.016	0.4195	0.013	0.4664	0.004	0.6666
8-HETE	3.06E-04	0.9102	0.058	0.1155	0.004	0.6764	0.036	0.2182	0.001	0.8294	0.020	0.3609	0.002	0.7549	0.009	0.5381
12-HETE	3.63E-05	0.9690	0.048	0.1516	0.001	0.8172	0.002	0.7732	0.005	0.6482	0.011	0.4928	0.002	0.7712	0.012	0.4713
5-HETE	6.55E-04	0.8691	0.028	0.2795	0.008	0.5447	0.046	0.1628	0.036	0.2178	0.035	0.2267	0.005	0.6630	0.012	0.4808
12-HpETE	1.79E-04	0.9313	0.143	0.0113	0.001	0.8327	0.002	0.7485	0.005	0.6495	0.057	0.1174	0.016	0.4071	0.037	0.2028
13-oxoODE	0.001	0.8083	0.078	0.0670	0.030	0.2505	0.057	0.1179	1.89E-04	0.9294	0.033	0.2404	5.77E-04	0.8770	0.056	0.1176
13-HODE	0.009	0.5316	0.016	0.4081	0.011	0.4978	0.006	0.6036	1.19E-05	0.9822	0.001	0.8173	0.002	0.7725	0.050	0.1410
9-oxoODE	0.019	0.3767	0.003	0.7089	0.004	0.6672	0.123	0.0199	0.017	0.4002	5.27E-06	0.9882	0.004	0.7016	0.002	0.7658
9-HODE	0.028	0.2744	0.002	0.7857	0.034	0.2288	0.039	0.1993	4.26E-05	0.9664	0.001	0.8297	0.006	0.6085	0.016	0.4028
18-HEPE	1.68E-04	0.9335	6.14E-05	0.9597	0.028	0.2681	0.170	0.0054	0.032	0.2430	0.036	0.2163	0.046	0.1623	0.099	0.0350
17-HDHA	0.002	0.7583	0.006	0.6218	0.031	0.2401	0.063	0.1017	4.88E-04	0.8868	0.004	0.7000	0.010	0.5197	0.031	0.2474
14-HDHA	0.007	0.5803	0.036	0.2195	0.002	0.7953	9.91E-04	0.8393	7.66E-04	0.8584	0.003	0.7188	0.010	0.5107	0.020	0.3509
5,12-DiHETE	0.054	0.1280	0.103	0.0338	0.022	0.3267	0.004	0.6943	0.026	0.3003	0.058	0.1165	0.022	0.3381	0.009	0.5354
8,9-DiHETE	0.025	0.3057	0.054	0.1282	2.98E-04	0.9136	0.184	0.0051	0.038	0.2146	0.003	0.7433	0.058	0.1155	0.001	0.8222
2-AG	0.020	0.3627	0.069	0.0840	0.251	0.0004	0.312	<0.0001	0.242	0.0007	0.021	0.3531	0.016	0.4163	0.002	0.7730
AEA	0.026	0.2958	0.010	0.5098	0.010	0.5039	2.12E-04	0.9253	5.88E-07	0.9961	0.042	0.1847	0.009	0.5413	0.087	0.0495
OEA	0.100	0.0365	0.008	0.5701	0.033	0.2288	0.072	0.0777	0.043	0.1788	0.078	0.0658	0.033	0.2395	0.022	0.3297
PEA	0.047	0.1566	0.017	0.3939	0.006	0.6087	0.184	0.0037	0.077	0.0691	0.104	0.0325	0.005	0.6541	3.11E-04	0.9085
LA	0.004	0.6823	0.093	0.0445	0.131	0.0134	0.137	0.0134	2.13E-04	0.9251	0.105	0.0320	0.003	0.7102	0.095	0.0396
AA	0.046	0.1622	0.001	0.8082	0.006	0.6164	0.167	0.0058	0.036	0.2187	0.095	0.0421	4.48E-04	0.8916	0.100	0.0342
EPA	0.032	0.2449	0.029	0.2699	0.005	0.6510	0.165	0.0062	0.004	0.6918	0.002	0.7511	0.098	0.0381	0.168	0.0052
DHA	0.017	0.3967	0.006	0.6262	0.004	0.6894	0.225	0.0011	0.002	0.7635	0.018	0.3907	0.085	0.0552	0.114	0.0235

In the earliest sample after injury, levels of the omega-3 PUFAs DHA and eicosapentaenoic acid (EPA), and their metabolites 14-hydroxy-docosahexaenoic acid (14-HDHA) and 18-hydroxy-eicosapentaenoic acid (18-HEPE), were significantly higher compared with healthy controls, and also compared with later times after injury (Figure 3A,C-E). In addition, levels of the DHA metabolite 17-HDHA were significantly higher in the earliest sample taken following injury, compared with healthy controls, but were not significantly different to controls at later times (Figure 2B). Any potential contribution of omega-3 supplementation or oral anti-inflammatory medication use on these levels were considered. Sensitivity analyses were carried out excluding participants who had supplemented/medicated within one month of the sample collection time point (for omega-3: immediately post-injury n=12, 3 months n=7, 2 year n=7; oral anti-inflammatories: post-injury n=28, 3 months n=13, 2 years n=8). Excluding these individuals did not change our findings (data not shown).

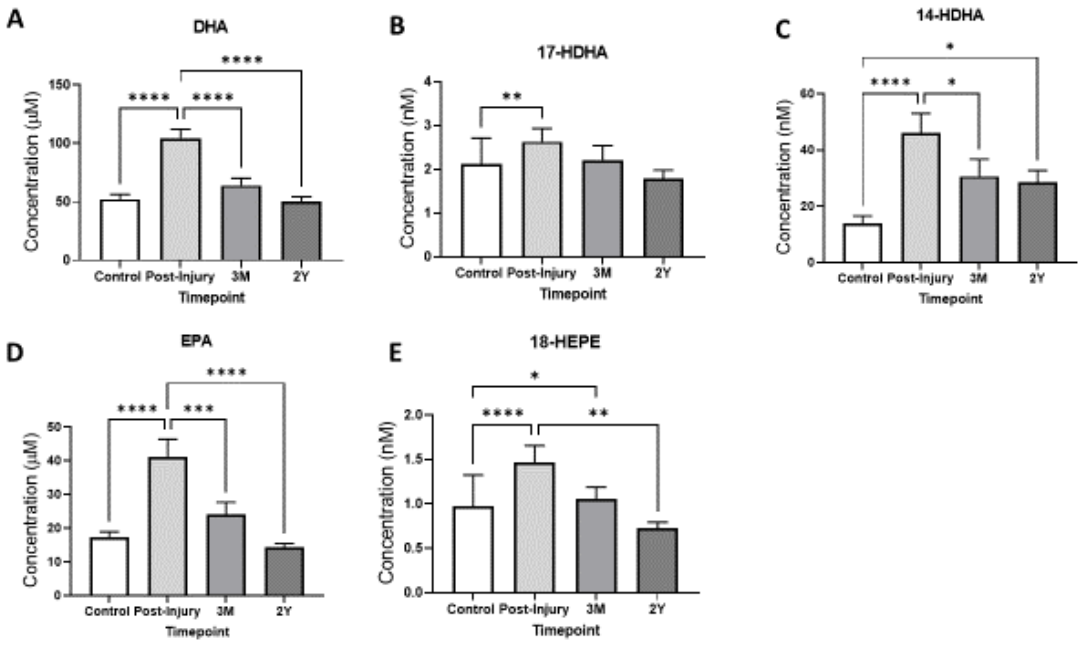

*Figure 3. Levels of omega-3 polyunsaturated fatty acids metabolites A) DHA, B) 17-HDHA, C) 14-HDHA, D) EPA, and E) 18-HEPE in controls (n=33), and in injury cohort (n=47) immediately post-injury and at 3 months and 2 years post-injury. Data are presented as mean ± SEM. Statistical analysis: Kruskal-Wallis test, adjusted for multiple comparisons using Dunn's test. *p=<0.05, **p=<0.01, ***p=<0.001, ****p=<0.0001.*

Serum levels of AA were higher in the earliest sample taken following knee joint injury compared to healthy controls, and compared to later times after injury (Figure 4A). Despite, this there were no differences in the levels of PGE2, prostaglandin D2 (PGD2), thromboxane B2 (TXB2), and 11-dehydroxy-TXB2 in the earliest sample taken following injury, compared to the healthy control group (Figure 4B-E). However, at 3 months and 2 years after injury, levels of PGE2 were significantly higher compared with levels in heathy controls (Figure 4B). In addition, following knee injury, levels of PGD2 and TXB2 were significantly higher at 3 months and 2 years, compared to the early post-injury levels (Figure 4C-D). Other differences of note were significantly higher levels of 11-dehydroxy-TXB2 at 3 months and 2 years, compared with the early post-injury levels and healthy controls (Figure 4E). Finally, levels of leukotriene B4 (LTB4) were significantly lower in the earliest sample taken following injury, when compared with the later times or with levels in healthy controls (Figure 4F).

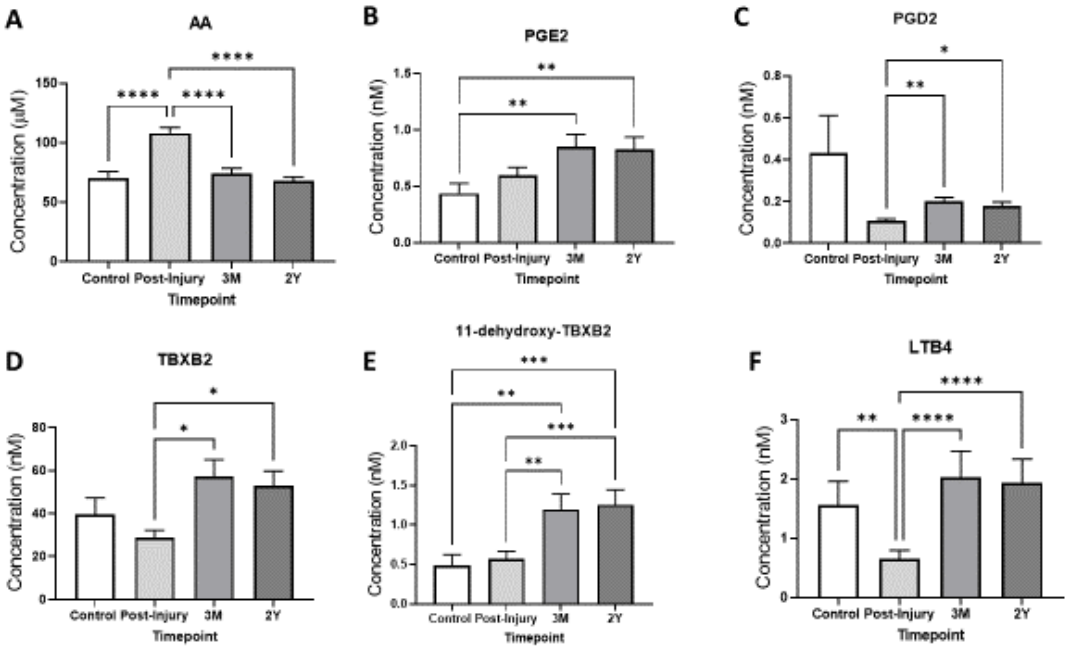

*Figure 4. Levels of omega-6 polyunsaturated fatty acid A) AA and its metabolites B) PGE2, C) PGD2, D) TXB2, E) 11-dehydroxy-TXB2, and F) LTB4 in controls (n=33), and in injury cohort (n=47) immediately post-injury and at 3 months and 2 years post-injury. Graphs are presented as mean ± SEM. Statistical analysis: Kruskal-Wallis test, adjusted for multiple comparisons using Dunn's test. *p=<0.05, **p=<0.01, ***p=<0.001, ****p=<0.0001.*

There were also significant differences in levels of the anti-inflammatory lipids epoxyeicosatrienoic acids (EETs) and their metabolites dihydroxyeicosatrienoic acids

(DHETs). At all time-points, levels of 5,6-EET were lower in those with injury compared with healthy controls (Fig 5A), with a similar pattern evident for 8,9-EET and 14,15-EET at the 3 month and 2 year time-points (Fig 5B&C). By contrast, levels of 11,12-EET were higher at all times after injury compared to the healthy controls (Fig 5D). Levels of 5,6-DHET, which is downstream of 5,6-EET, were lower than the healthy controls at all times after injury (Fig 5E). There were also significantly higher levels of 8,9-DHET in the earliest sample taken following injury, compared with samples at 3 months and 2 years, although these levels did not differ compared to controls (Figure 5F). Levels of 11,12- and 14,15-DHETs were also significantly higher in the earliest sample taken following injury, compared to healthy controls (Fig 5 G&H).

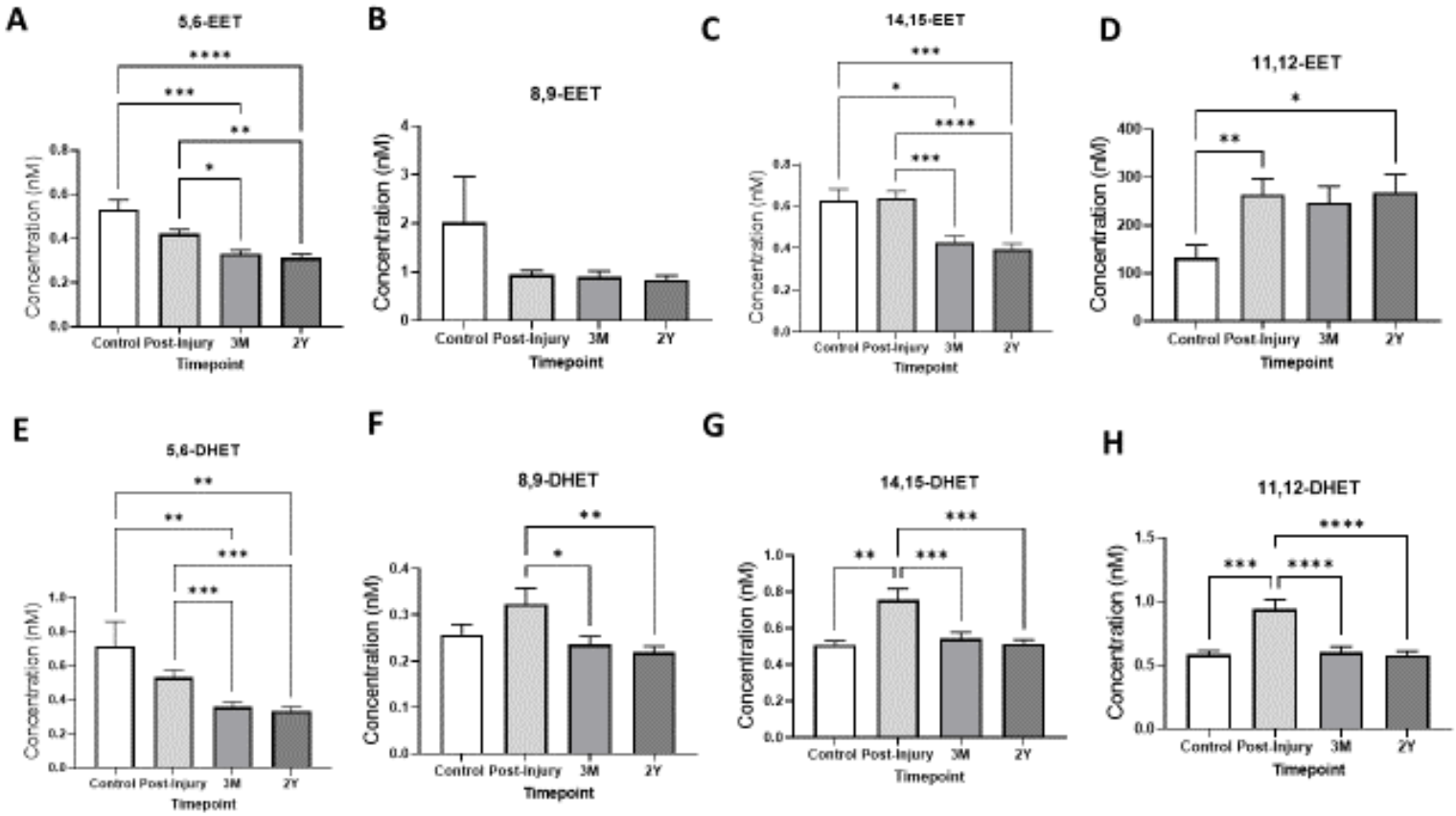

*Figure 5. Levels of CYP450 metabolites of AA A) 5,6-EET, B) 8,9-EET, C) 14,15-EET, D) 11,12-EET, and corresponding sEH metabolites E) 5,6-DHET, F) 8,9-DHET, G) 14,15-DHET, and H) 11,12-DHET in controls (n=33), and in injury cohort (n=47) immediately post-injury and at 3 months and 2 years post-injury. Graphs are presented as mean ± SEM. Statistical analysis: Kruskal-Wallis test, adjusted for multiple comparisons using Dunn's test. *p=<0.05, **p=<0.01, ***p=<0.001, ****p=<0.0001.*

There were some minor differences in levels of the endocannabinoid N-arachidonoylethanolamine (AEA) and related lipids (oleoylethanolamide (OEA) and N-palmitoylethanolamide (PEA)) between the groups, but no clear overall trend (Table 2). By contrast, levels of 2-arachidonoylglycerol (2-AG) were significantly lower in all groups post-injury compared to healthy controls (Table 2).

The levels of the linoleic acid (LA) metabolites 9-, and 13-hydroxyoctadecadienoic acid (HODE) were stable across groups, with the exception of lower levels of 13-HODE at 2 years compared to levels in the earliest sample taken following injury (Table 2). Their respective downstream metabolites 9-, and 13-oxoODE, showed higher levels in the earliest sample taken following injury, compared with either later times or controls (Table 2).

3.3.3 Distinct lipid profiles immediately post-injury and at 2 years by multivariate analysis

PLS-DA analysis of the lipid data revealed a clear difference in the serum lipid profiles between samples taken immediately and 2 years post-injury showing two different clusters (Figure 6A). The key lipids contributing to the separation were ranked by variable importance in projection (VIP) score (Figure 6B). 15 different lipids were identified as having VIP greater than 1.0 and these lipids were identified as most important lipid mediators involved in separation of the two groups where PUFAs were highest ranked. Apart from PUFAs, there were mostly pro-inflammatory lipid mediators in the top ranked list such as oxoODEs (9 and 13-oxoODEs), DHETs (5,6-DHET, 11,12-DHET and 14, 15-DHET), thromboxanes, PGD2, LTB4 and 5,12-DiHETE. The data of multivariate analysis were consistent with the overall findings of the univariate analysis for the lipid levels between the two groups.

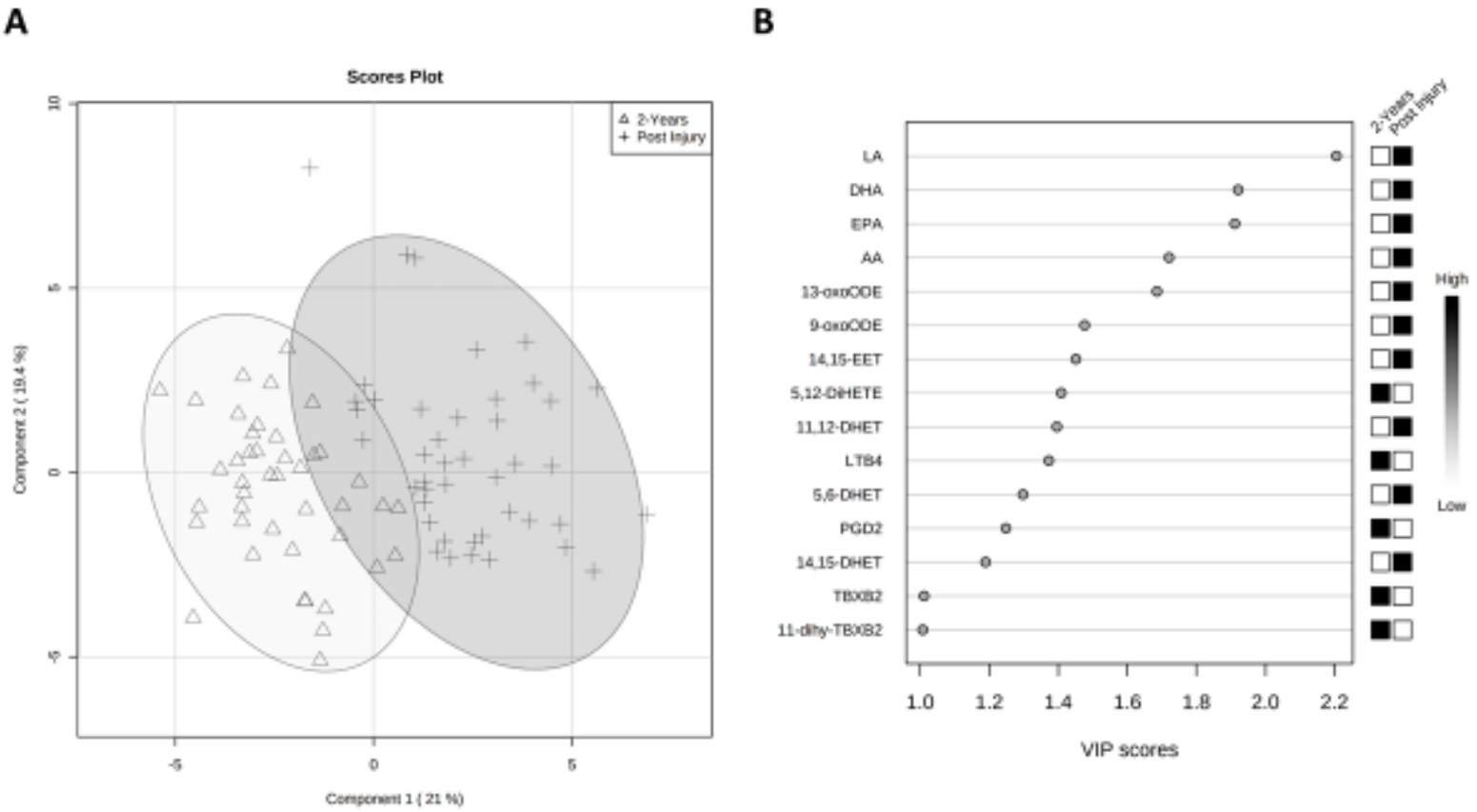

Figure 6. A) Partial least square discrimination analysis (PLS-DA) for the serum lipids quantified in KICK participants (n=47) showing two different clusters at two different time points (immediately post-injury and at 2 year), with R2 = 0.77, Q2 = 0.70 and Accuracy = 0.95. B) Variable importance in projection (VIP) scores indicating the 15 lipids above a threshold of VIP>1.0, considered as involved in the separation between the two time points.

3.3.4 Levels of DHETs and associations with persistent knee symptoms at 2 years

Univariate linear regression analyses were carried out to assess potential associations between serum levels of lipids and knee symptom scores assessed by KOOS-4 at each time point. At two years post-injury, there was an association between higher levels of 8,9-, 11,12-, and 14,15-DHET and worse knee symptoms (lower KOOS score), which remained after adjusting for multiple comparisons (Figure 7A-C). Although these associations may have been driven by unadjusted confounders such as age, sex, BMI or activity levels, exploratory univariate analyses to test for any associations between lipid levels and these clinical characteristics did not support these being a factor (Table 3). Finally, I investigated whether any of the lipids at the earliest time point following injury may predict future pain. In this cohort, there were no significant associations between lipid levels at the earliest time point post injury and KOOS-4 scores at 2 years post-injury.

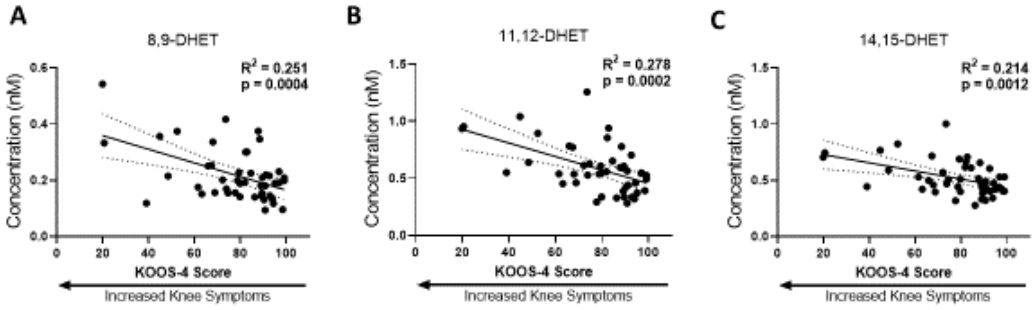

Figure 7. Linear regression analysis performed between knee osteoarthritis outcome score (KOOS-4) and levels of A) 8,9-DHET B) 11,12-DHET, and C) 14,15-DHET at 2 years post injury (n=46).

3.4 Discussion

The major finding of this study in young healthy individuals was that immediately following acute knee injury there is overall, in the majority of participants, an increase in the levels of the substrates for the two main resolution pathways, DHA and EPA, which then decline at 3 months and 2 years after injury. Support for activation of some of the resolution pathways in the majority of participants included a robust elevation in levels of molecular intermediates (18-HEPE, 14-, & 17-HDHA) at this early time after injury. These changes were not restricted to the DHA / EPA pathways, as levels of some of the EETs and their metabolites DHETs, which comprise another major anti-inflammatory pathway, were also altered immediately following injury in the majority of participants. EETs are derived from AA and immediately following injury levels of AA were also elevated. Interestingly, it was only at months to years after injury that levels of AA derived pro-inflammatory molecules such as the prostaglandins were elevated in the majority of participants. Levels of oxylipins quantified at the time of injury were not associated with subsequent knee symptoms at 2 years follow-up in this cohort. However, higher levels of 8,9-, 11,12-, and 14,15-DHET were cross-sectionally associated with having worse knee symptoms at two years following injury. As this longitudinal study is ongoing, further analysis will be performed between levels of oxylipins immediately after injury and outcomes scores and radiographic pathology scores at 5 years post-injury.

The observation of increased levels of the omega-3 PUFAs DHA and EPA and their metabolites (which are the precursors for the D and E series resolution molecules (Serhan and Levy 2018)) within 8 weeks of acute knee injury suggests that the biological response to this type of injury includes an activation of these pro-resolution pathways, which are known in other contexts to act to counter pro-inflammatory signalling and restore tissue homeostasis (Basil and Levy 2016). The profile of changes in levels of the anti-inflammatory EETs after joint injury compared to healthy controls and at later times after injury was more variable than the DHA/EPA pathway. Overall, it was notable that levels of DHET

(metabolites of the EETs generated by sEH) were more consistently altered between the different members of the EET family, with significant increases in levels of 8, 9-DHET, 11, 12-DHET and 14, 15-DHET immediately following injury compared to later times after injury, and in some cases also when compared with levels in healthy controls. These data suggest greater flux through this pathway immediately following joint injury.

When considering the trajectory of injury in this subset of the KICK participants, it is clear that there is a wide range of changes in symptoms over the 2 years, with the majority of participants showing a general improvement in KOOS-4 scores and increased levels of activity across the cohort, suggestive of a clinical recovery, consistent with the larger cohort (Garriga C 2021). The trajectory of recovery in these participants may at least in part be mediated by the magnitude of the activation of the resolution pathways, although this would require confirmation in a larger cohort. Overall, the findings of the univariate analysis were supported by principle component analysis of the entire dataset, which indicated that the main molecules driving the separation in lipid profile between samples collected immediately post-injury versus at 2 years from the same individuals were some of the precursors for the resolution molecules and a number of metabolites derived via the sEH pathway.

The profile of change in the levels of the classically pro-inflammatory metabolites of AA, including the PGs, TXs, and LTB4, was of reduced or unchanged levels immediately post-injury compared to controls, with levels elevated at later times after knee injury. Considering the data collectively, systemically there appears to be a shift in favour of the pro-resolution pathway lipids at early time points following injury, with lower levels of activation of the pro-inflammatory pathways, which if mirrored at the site of injury may aid tissue recovery. Previous studies in this cohort have also identified significantly lower serum levels of pro-inflammatory molecules (MCP-1, activin A, MMP-3, TIMP-1, and TSG-6) individuals post-injury compared with healthy controls including (Watt, Paterson et al. 2016). However, at the level of the synovial fluid levels of these pro-inflammatory molecules were higher immediately after

injury. Improved understanding of the relationship between synovial fluid, tissue and blood levels of these molecules, whether levels are independent of one another, or if a temporal/reciprocal relationship exists between the circulating and tissue environments in the overall inflammatory / resolution response is needed to maximise interpretation .

Levels of DHETs at the time of injury were not associated with symptoms two years later. However, at 2 years following injury levels of 8,9-, 11,12-, & 14,15-DHET were significantly associated with worse knee symptoms. No other oxylipins measured in this study were significantly associated with KOOS-4 score at any time point, after adjusting for multiple comparisons. These data lend further support to a role of the sEH pathway in the persistence of knee pain, in line with a previous report in older people with OA knee pain from our research group (Valdes, Ravipati et al. 2018). Experimental studies also support these clinical observations, and have suggested sEH inhibition as a therapeutic potential in canine OA (McReynolds, Hwang et al. 2019) as well as a rodent albumin-induced arthritis model (Teixeira, Abdalla et al. 2020). The findings of this current study support the further investigation of these pathways following acute knee injury and suggest that the outcome of current clinical trials of an sEH inhibitor for neuropathic pain (Hammock, McReynolds et al. 2021) may have wider relevance.

Limitations of this study include a modest sample size (albeit with resampling of the same individuals) and some sex imbalance between the injury and control group. Nevertheless, there were no substantial sex differences in these oxylipins based on this work. The subset of participants selected for this study who had attended in person for all study visits associated with blood sampling could have included some biases such as attrition bias and differential follow bias. For example, it is feasible that participants attending all visits were more likely to have knee symptoms. However, the data showed our group still exhibited a range of clinical outcomes at 2 years and that the baseline characteristics of this subgroup were largely similar to the overall cohort (Watt, Paterson et al. 2016), which was reassuring. Although longitudinal matched

paired analysis strengthened our statistical analysis, we cannot rule out the potential for confounding, such as from BMI, differences in physical activity levels between the injured group and control and dietary factors. It is of note that the control group could not be matched on physical activity, and given the nature of the injury cohort participants, were likely to differ substantially in terms of physical activity levels. In addition, although the final time-point of two years allowed the identification of participants with a substantial recovery in activity levels and improved knee symptoms and those who had not recovered clinically, later time-points would be required to understand the relationship between these pathways, and the development of OA after injury. The pathways that were studied are impacted upon, at least in part, by COX-2 activity and therefore the use of oral anti-inflammatories is an important consideration. Overall, the sensitivity analysis excluding participants' samples who were using NSAIDs (COX-2 or FAAH inhibitors) did not alter the findings of our study. Nevertheless, there were a high number of participants using NSAIDs post-injury, which could contribute to the complexity of the changes between the individual EET / DHET molecules, as some are metabolised by both sEH and COX-2 (Rand, Barnych et al. 2017). It is also of note that all except 2 participants underwent knee surgery between the post-injury and 3 month time points, which is a feature of this cohort (and many joint injury cohorts) and needs to be considered when interpreting 3 month and 2 year levels, but is at least relatively homogeneous in terms of exposure.

In conclusion, the profile of pro-resolving versus pro-inflammatory lipids immediately following knee joint injury suggests a switch in favour of the resolution pathways, followed by a later activation of pro-inflammatory pathways. The association of systemic levels of EET/DHET with increased knee symptoms at 2 years post-injury adds to the mounting clinical evidence for a role of the soluble epoxide hydrolase pathway in knee pain and supports the therapeutic potential of targeting this pathway to reduce future knee pain, consistent with other chronic pain states.

Chapter Four

Investigating associations between oxylipins and clinical phenotypes in people with osteoarthritis knee pain

Acknowledgements

This study was conducted on a clinical cohort set-up by colleagues in the School of Medicine (Mike Doherty, Dave Walsh, Ana Valdes, Weiya Zhang, & Gwen Fernandes) who performed sample collection and collection of clinical data and I would like to thanks for providing me with these samples and data. I would like to thank Rose Ferrands-Bentley for her help with the extraction of clinical data from databases. I would also like to thank all the participants for their involvement in this study, and donation of their blood samples.

Data reported in this chapter are currently being prepared into the manuscript:

James Turnbull, Rakesh R. Jha, Peter R. W. Gowler, Rose Ferrands-Bentley, Dong-Hyun Kim, David A. Barrett, Gwen S. Fernandes, Michael Doherty, Weiya Zhang, David A. Walsh, Ana M. Valdes, Victoria Chapman. **Associations between serum oxylipin levels with clinical measures of pain and radiographic osteoarthritis in people with knee pain.** [Target Journal: Annals of Rheumatic Diseases]

Abstract

Osteoarthritis (OA) is the fastest growing cause of chronic pain worldwide. Identifying molecules that predict the course of OA pain and / or pathology may aid both the development of new treatments and the appropriate early management of pain progression. Oxylipins are bioactive lipids with both pro- and anti-inflammatory effects, which support tissue repair and regulate pain signalling. In this study, it was investigated whether levels of pro- or anti-inflammatory oxylipins predict the progression of knee pain. Serum samples were collected from participants (n=154) from the Knee Pain in the Community Cohort (KPIC) who were clinically assessed at baseline and 3 years follow-up for pain phenotype. Radiographic OA scores and serum samples were collected at baseline. Serum levels of oxylipins were quantified using LC-MS/MS. Analyses were performed to identify relationships between serum levels of oxylipins with current knee pain and radiographic OA scores, and with pain scores at 3 years follow-up. Serum concentrations of multiple oxylipins, derived from two key enzymatic pathways, LOX and CYP450, were associated with current self-reported pain scores in a community cohort of participants with varying amounts of radiographic OA and knee pain, also reported were significant associations between serum levels of four oxylipins derived from two key enzymatic pathways, LOX and CYP450, and KL score. In our follow-up study, serum concentrations of 8,9-EET, 5,6-DHET, and 5-HETE were positively associated with future pain outcomes in this community cohort of knee pain participants with varying levels of radiographic OA. Our study has highlight the potential involvement of omega-3 and -6 PUFA derived oxylipins in both OA joint pathology and the associated pain phenotype, and point toward future potential therapeutic targets to treat symptomatic OA and the potential use of oxylipins as biomarkers for future pain.

4.1 Introduction

To follow on from the work in chapter three looking at the association of oxylipins with early outcomes following knee injury, this chapter will focus on an observational clinical study where oxylipins were measured in people from the knee pain in the community cohort (KPIC) who had varying severities of knee pain and radiographically defined OA (Fernandes, Sarmanova et al. 2017).

Previous studies by our team, and others, identified a potential role of two endogenous anti-inflammatory pathways, the specialised pro-resolution molecules (SPMs) and the soluble epoxide hydrolase (sEH) pathway in OA pain. Levels of an intermediate for some of the SPMs, 17-hydroxydocosahexaenoic acid (17-HDHA), but not the down-stream D-series or E-series resolvins measured (RvE1, RvD1-3, and RvD5), were associated with pain intensity in OA patients and heat pain thresholds in healthy volunteers (Valdes, Ravipati et al. 2017). This association between 17-HDHA and pain scores and pain sensitivity remained significant after adjusting for circulating levels of omega-3, and accounted for a larger proportion of pain sensitivity scores than omega-3 (2.07% of variance for omega-3, 3.05% for 17-HDHA after adjusting for age, sex, BMI). A role of the SPMs in OA and arthritis pain is further supported by the robust inhibitory effects of 17-HDHA on pain behaviour in experimental models of OA (Huang, Burston et al. 2017) and inflammatory arthritis (Lima-Garcia, Dutra et al. 2011).

The sEH pathway regulates levels of the endogenous anti-inflammatory epoxyeicosatrienoic acids (EETs), which are metabolised into their corresponding DHETs. In chapter three, serum levels of DHETs were shown to be associated with worse knee symptom scores at 2 years post knee injury, and a previous study from our group showed an association of synovial fluid levels of DHETs with radiographic OA progression (Valdes, Ravipati et al. 2018).

Currently, there are no approved treatments which halt or reverse the pathology in the joint developed during OA pathogenesis. Low-grade unresolved inflammation is a key mechanistic driver in the pathogenesis of OA (Robinson, Lepus et al. 2016). As the oxylipins are central mediators in the

inflammatory response, they present as potential targets for novel pharmacological interventions to treat the joint damage and/or associated pain, as well as potential biomarkers to monitor/predict disease progression.

The aim of this study was to investigate whether levels of pro- or anti-inflammatory oxylipins were associated with radiographic knee OA or knee pain, and whether baseline levels of oxylipins were able to predict the progression of knee pain associated with OA. In this study, levels of oxylipins were quantified in serum collected at baseline from participants with a range of pain and pathology score including pain questionnaires, quantitative sensory testing (QST), Kellgren and Lawrence (K/L), and ultrasound scores. Follow-up pain scores were also collected at a 3 year time point and potential associations between levels of oxylipins with pain and radiographic OA progression at baseline and with pain at 3 years later were investigated to assess the potential use of oxylipins as prognostic markers of chronic pain.

4.2 Methods

4.2.1 Participants

Participants (n=154) were recruited from the Knee Pain in the Community Cohort (KPIC) (Fernandes, Sarmanova et al. 2017), ethical approval was provided for this study by Nottingham University Hospitals NHS Trust and the Nottingham Research Ethics Committee 1 (Ref 14/EM/0015) and all participants provided written informed consent. Participants both with and without x-ray confirmed radiographic knee OA were included in this study (Table 1).

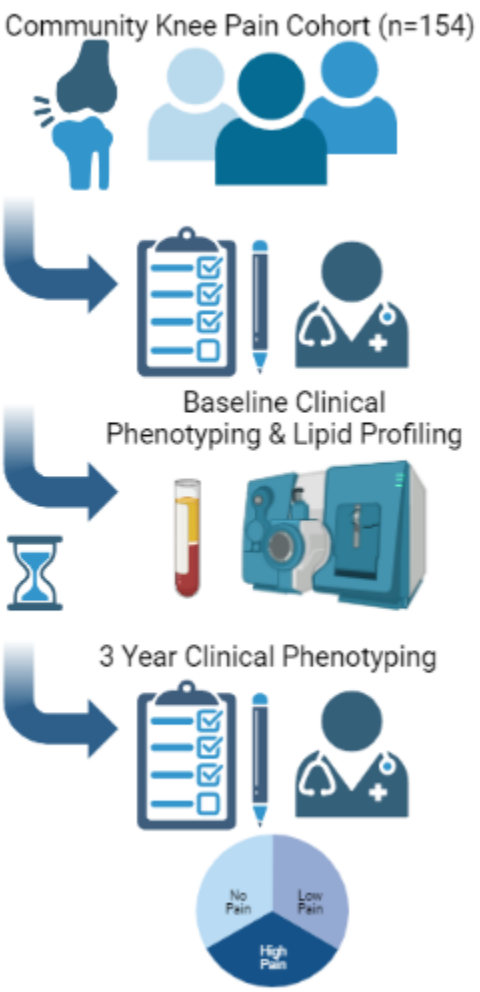

Figure 6. Graphical workflow of study design.

4.2.2 Patient and Public Involvement (PPI) Statement

A PPI group reviewed a lay summary of the proposed study and provided feedback through a focus group. They agreed that being able to predict future pain intensity is desirable if it would help with the clinical management of OA pain. This PPI group also suggested factors that might help incentivise help people to take part in these studies.

4.2.3 Collection of Self-Reported Pain

Self reported pain questionnaires were completed by participants at baseline and 3 years follow-up, where participants were asked the same three questions to score their pain on a visual analogue scale (VAS):

1. How would you rate your most painful knee pain on a 0-10 scale at the ***present time***, that is right now, where 0 is 'no pain' and 10 is 'pain as bad as could be'?
2. In the past month, how intense was your ***'worst knee pain'*** rated on a 0-10 scale, where 0 is 'no pain' and 10 is 'pain as bad as could be'?
3. In the past month, ***on average***, how intense was the pain in your most painful knee rated on a 0-10 scale, where 0 is 'no pain' and 10 is 'pain as bad as could be'?

The mean of the scores given for each question by each participant were also calculated for analysis. Change in pain between the two time points was also calculated based on the difference between the scores from question three.

4.2.4 Quantitative Sensory Testing (QST)

Participants were invited to participate in non-invasive QST which assessed sensitivity to standardised stimuli. This comprised assessment of mechanical pressure pain thresholds (PPT) at baseline and year 3 using a hand-held pressure algometer (Somedic AB, Sweden) that was connected to a computer (HP ProBook 4520 s). The algometer consisted of a rod with a circular end

($1cm^2$) that was placed perpendicular to the skin and pressure applied at a gradually increasing rate (standardised rate set at 30 kPa/s) until the participant indicated that the sensation had changed from pressure to pain by pressing a button.

4.2.5 Radiographs

Bilateral tibio-femoral and patellofemoral radiographs were taken using a standardised protocol (standing posterior-anterior (PA) and skyline views) and scored by two specifically trained raters. Grading of radiographs for changes of OA were completed according to the summated Kellgren and Lawrence (KL) score.

4.2.6 Ultrasound

Both knee joints were imaged using a Toshiba Aplio SSA-770A machine with a multi-frequency (7–12 MHz) linear array transducer. The same equipment and software was used throughout the whole study. The assessment was performed with knee flexion of approximately 20–30° and included the supra-patellar recess, medial and lateral tibio-femoral spaces.

4.2.7 Analysis of circulating levels of oxylipins by liquid chromatography with tandem mass spectrometry (LC-MS/MS)

Serum samples were collected from participants at baseline. Samples were extracted and analysed using the methods outlines in chapter 2. Samples were extracted in 3 batches, with n=6 QCs included for each. The sample extract were analysed in a single LC-MS/MS analytical run.

4.2.8 Data Analysis

Patient characteristics are presented as the median ± interquartile range. From the full cohort, patients were stratified based on KL and average NRS (item 3) scores into an No OA-Lower pain group (KL ≤1 & VAS ≤5) and an OA-Higher pain group (KL ≥2 & VAS ≥6). Concentrations of serum oxylipins were log-

transformed in order to achieve a normal distribution. Data were analysed in Prism (Graphpad v.8) or R (www.r-project.org). Linear regression analyses were used to identify associations between clinical characteristics and levels of oxylipins (adjusting for the 34 oxylipins quantified). Univariate analysis of a subset of the cohort compared levels of oxylipins between two groups (OA-higher pain: VAS > 6, KL > 2, n=45; No OA-lower pain: VAS <5, KL < 2, n =56) used a Mann-Whitney U test.

4.3 Results

4.3.1 Participant characteristics

A subset of participants of the KPIC cohort were recruited to this study which were selected based on availability of clinical data, and serum samples available at baseline. They had an average age of 61 yrs, and 61.7% were female (Table 1). 81 / 154 had a KL grade of 2 or above and 73 / 154 had a KL grade of below 2. 92 of 154 had an average VAS score of 5 or below and 62 of 154 had an average VAS score of below 5. For some analysis, participants included in this study were divided into two groups based on KL score and average VAS score, which were well matched for age, sex, and BMI (Table 1). Of the participants who were not stratified into early/OA-higher pains, n=36 had KL ≥2 & VAS ≤5 and n=17 had KL ≤1 & VAS ≥6.

Table 1. Clinical characteristics at baseline of the full cohort (n=154); early stage OA group (defined as having KL ≤1 and average VAS score of ≤5); advanced stage OA group (defined as having KL ≥2 and average VAS score ≥6); and participants whose clinical features did not place them in early or OA-higher pains. Data are presented as median [interquartile range]. BMI = Body mass index, VAS = visual analogue scale (based on question 3 of the questionnaire), KL = Kellgren-Lawrence radiographic grade.

	Full Cohort	**No OA-Lower Pain**	**OA-Higher Pain**	**Other**
No of Participants	154	56	45	53
Age	61[53-68]	57[52-67]	61[55-66]	64[57-70]
BMI (kg/m^2)	28[25-32]	27[24-31]	29[26-33]	28[25-33]
Sex (%F)	61.7%	62.5%	62.2%	61.2%
Average VAS	5[3-7]	3[2-4]	7[6-8.5]	5[3-6]
PDQ	6[3-10]	4[2-8]	11[8-14]	5[3-8]
KL Grade	2[0-3]	0[0-1]	3[2-3]	2[1-3]
Knee Effusion:				
Left Knee	3.3[0.5-5.7]	2.3[0-4.6]	4.4[2.8-6.7]	3.5[0-5.8]
Right Knee	3.2[1.1-5.7]	2.4[0-3.9]	5.4[2.8-8.5]	2.8[0-5.6]
Synovial Hypertrophy:				
Left Knee	0[0-3.4]	0[0-2.4]	1.8[0-5.2]	0[0-3.5]
Right Knee	0[0-2.4]	0[0-0.8]	2.1[0-4.9]	0[0-1.2]

4.3.2 Serum levels of oxylipins in participants with knee pain at baseline

Levels of oxylipins were quantified in the full cohort (Table 2). Linear regression analysis, after adjustment for multiple comparison, revealed significant associations between levels of DHA (positive) and TXB2 (negative) with age (Table 3), and a significant negative association between EPA and DHA with BMI. In addition, levels of 5,6-DHET were significantly lower in females (Table 3).

Table 2. Average concentration (nM) ± standard deviation of oxylipins quantified in serum in full cohort (n=154); early stage OA group (KL ≤1 & VAS ≤5); advanced OA group (KL ≥2 & VAS ≥6); and participants whose clinical features did not place them in early or OA-higher pains.

Lipid	Full Cohort (n=154)			No OA-lower pain (n=56)			OA-higher pain (n=45)			Other (n=53)		
	Mean (nM)	±	SD	Mean (nM)	±	SD	Mean (nM)	±	SD	Mean (nM)	±	SD
5,6-EET	24.18	±	42.25	11.37	±	17.78	40.11	±	56.17	27.20	±	43.45
5,6-DHET	0.58	±	0.41	0.56	±	0.36	0.61	±	0.46	0.60	±	0.40
5,6-Ratio	44.64	±	93.90	32.98	±	108.44	59.16	±	69.10	44.80	±	74.90
8,9-EET	0.77	±	1.04	0.49	±	0.49	1.11	±	1.38	0.76	±	0.96
8,9-DHET	0.35	±	0.19	0.35	±	0.18	0.35	±	0.20	0.34	±	0.27
8,9-Ratio	45.98	±	429.75	1.63	±	1.65	101.18	±	639.54	134.55	±	638.16
11,12-EET	125.11	±	220.71	59.67	±	94.27	206.54	±	293.79	142.62	±	226.11
11,12-DHET	0.84	±	0.47	0.85	±	0.45	0.82	±	0.49	0.88	±	0.49
11,12-Ratio	178.69	±	337.10	88.05	±	159.01	291.48	±	447.93	240.63	±	432.88
14,15-EET	0.30	±	0.17	0.29	±	0.18	0.31	±	0.15	0.25	±	0.13
14,15-DHET	0.53	±	0.53	0.54	±	0.63	0.52	±	0.38	0.54	±	0.39
14,15-Ratio	28.28	±	77.14	43.21	±	91.37	9.70	±	48.41	4.26	±	15.91
12-HpETE	3.55	±	2.09	2.94	±	1.14	4.32	±	2.68	3.27	±	1.98
TBXB2	12.46	±	21.23	8.88	±	11.86	16.93	±	28.30	13.39	±	24.70
PGE2	0.46	±	0.59	0.38	±	0.41	0.55	±	0.74	0.63	±	1.14
LTB4	0.50	±	0.97	0.40	±	0.71	0.61	±	1.20	0.65	±	0.94
20-HETE	43.19	±	78.08	19.78	±	31.37	72.31	±	104.54	47.50	±	74.00

18-HEPE	0.63	±	0.61	0.56	±	0.54	0.71	±	0.68	0.68	±	0.76
16-HETE	0.50	±	0.33	0.53	±	0.39	0.46	±	0.22	0.53	±	0.34
15-HETE	5.47	±	7.27	3.75	±	4.29	7.61	±	9.36	5.84	±	6.70
13-oxoODE	13.92	±	8.43	14.90	±	9.26	12.71	±	7.08	17.48	±	8.84
11-HETE	2.44	±	2.40	1.98	±	1.54	3.01	±	3.07	2.53	±	2.27
9-oxoODE	7.04	±	4.53	7.73	±	4.93	6.18	±	3.82	7.48	±	3.67
9-HODE	8.28	±	5.79	8.40	±	5.72	8.13	±	5.87	14.59	±	31.60
9-HETE	2.23	±	4.08	1.00	±	1.51	3.76	±	5.50	2.41	±	3.92
12-HETE	117.40	±	206.99	54.28	±	86.16	195.94	±	275.31	133.35	±	208.80
5-HETE	1.18	±	1.37	0.88	±	0.78	1.56	±	1.79	0.85	±	0.71
17-HDHA	1.24	±	1.66	0.78	±	0.75	1.80	±	2.22	1.67	±	2.61
14-HDHA	23.93	±	52.53	8.66	±	16.86	42.93	±	72.03	28.05	±	51.90
AEA	0.73	±	0.40	0.62	±	0.38	0.86	±	0.38	0.73	±	0.40
AA	13879.96	±	4958.74	12661.60	±	4411.58	15396.14	±	5179.13	13409.35	±	4829.68
LA	21896.43	±	9355.66	22250.42	±	10148.67	21455.91	±	8242.00	23235.95	±	9011.40
EPA	752.97	±	407.61	747.47	±	388.32	759.81	±	430.31	670.66	±	383.45
DHA	16327.41	±	7033.10	16083.18	±	6408.57	16631.35	±	7729.47	15453.54	±	6471.32

The relationship(s) between oxylipin levels and pain scores or K/L score at baseline were determined using linear regression analysis. Following adjustment for multiple comparison, baseline levels of 8,9-EET:DHET ratio, 9- and 15-HETE, and 14-HDHA were positively associated with K/L score (Table 3). There were no significant associations between serum levels of any lipids measured with knee effusion or synovial hypertrophy scores at baseline (data not shown). Following adjustment for multiple comparison, levels of 8,9-EET, 14,15-DHET, 12-HpETE, AEA were associated with the VAS score for 'how would you rate your pain at the present time?'. Levels of AEA also showed a significant positive association with PDQ scores at baseline (Table 4).

Table 3. Significant associations (linear regression analysis) between baseline serum levels of oxylipins with age, sex, BMI, and KL score in the full cohort of participants (n=154). Beta values show the direction and strength of the relationship between the two variables. P values were adjusted for multiple comparisons using Bonferroni correction.

Lipid	Age		Sex		BMI		KL	
	Beta	**P Value**	**Beta**	**P Value**	**Beta**	**P Value**	**Beta**	**P Value**
5,6-DHET	ns		-0.4497	0.00002	ns		ns	
8,9-EET:DHET Ratio	ns		ns		ns		0.5096	0.0014
TBXB2	-1.9758	0.0005	ns		ns		ns	
15-HETE	ns		ns		ns		0.7593	0.0013
9-HETE	ns		ns		ns		0.4671	0.0013
14-HDHA	ns		ns		ns		0.4829	0.0001
EPA	ns		ns		-7.5718	0.0001	ns	
DHA	13.3589	0.0009	ns		-9.6459	0.0002	ns	

To identify whether oxylipin levels differ between participants defined as being at an early stage (KL ≤ 1 and VAS ≤5) or an advanced stage of OA (KL ≥2 and VAS ≥6), a subset analysis of oxylipins was undertaken (Table 2). Levels of 5,6-, 8,9-, and 11,12-EET as well as their EET:DHET ratios were significantly higher in the OA-higher pain compared to No OA-lower pain (Figure 1 A-C). Levels of 17-HDHA and 14-HDHA were also significantly higher in the OA-higher pain compared to No OA-lower pain (Figure 1D).

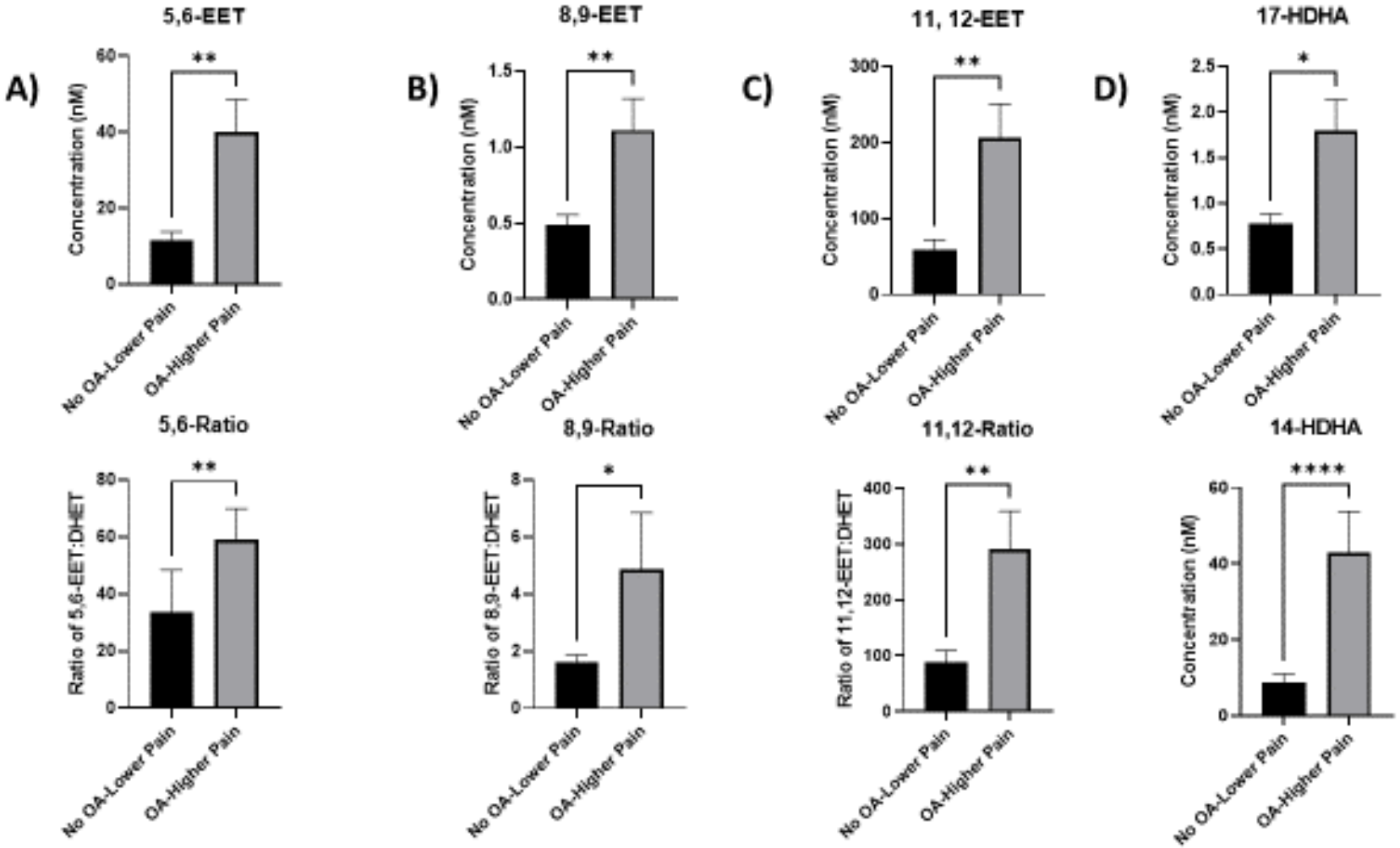

*Figure 2. Serum Concentration of EETs and ratio of EET/DHET concentration, A) 5, 6-EET & 5, 6-EET/DHET, B) 8, 9-EET & 8, 9-EET/DHET, C) 11, 12-EET & 11, 12-EET/DHET and intermediate metabolites of DHA D) 17-HDHA & 14-HDHA in baseline samples based on High KL High Pain (HKHP) Vs Low KL Low Pain (LKLP) group. Significance was assessed using Mann-Whitney test. *p=<0.05, **p=<0.01.*

Levels of 5-, 9-, 11-, 12-, 15-, and 20-HETE were also significantly higher in the OA-higher pain compared to No OA-lower pain (Figure 2 A-G). Finally, levels of 5,6-, 8,9-, & 11,12-EET; 5,6-, & 11,12-ratio; 14,15-DHET; 12-HpETE; 9-, 12-, & 20-HETE; 14-HDHA, and AEA were significantly associated with at least one of the 3 VAS scores, after adjusting for multiple comparisons (n=101, Table 4). Levels of AEA and 14,15-DHET were significantly associated with higher PDQ scores in this subset of participants, whereas the ratio of 14,15-EET:DHET was negatively associated with PDQ scores (Table 4).

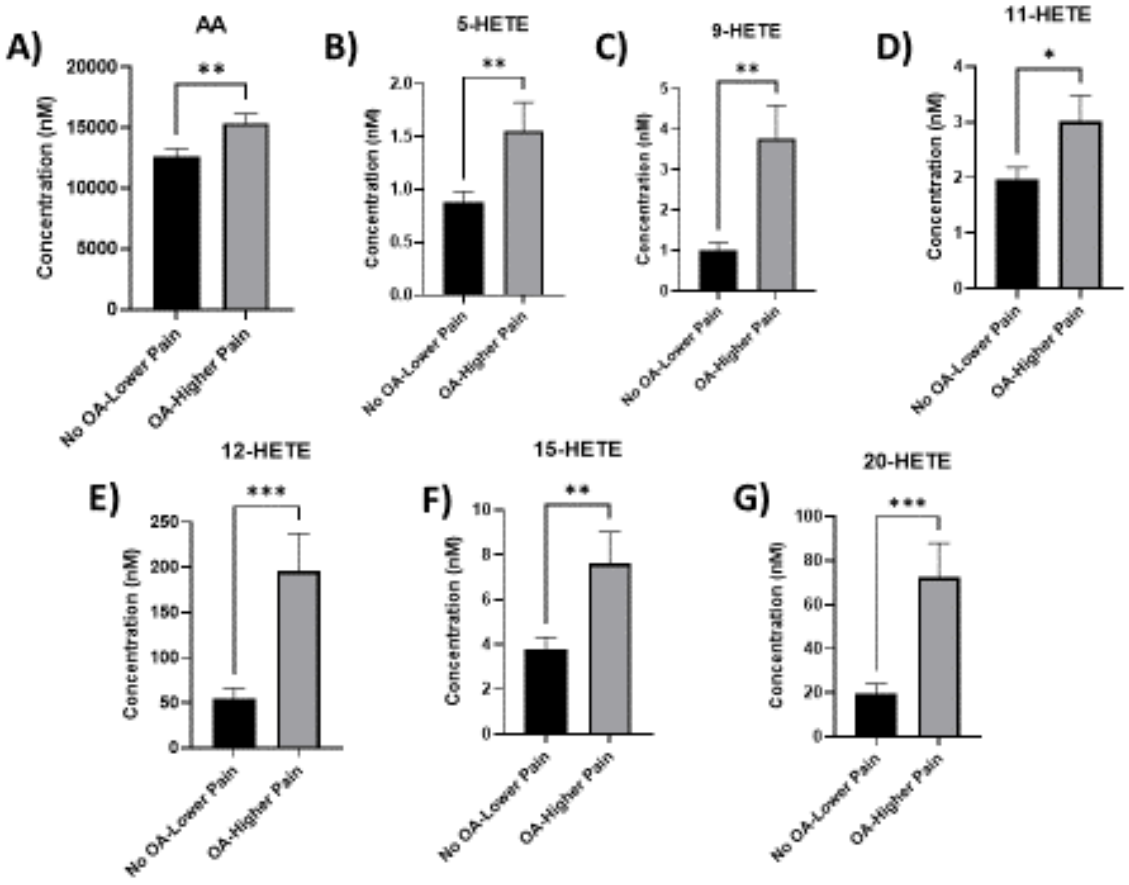

*Figure 3. Serum concentration of arachidonic acid and their metabolites (HETEs) A) AA, B) 5-HETE, C) 9-HETE, D) 11-HETE, E) 12-HETE, F) 15-HETE and G) 20-HETE in baseline samples based on High KL High Pain (HKHP) Vs Low KL Low Pain (LKLP) group. Significance was assessed using Mann-Whitney test. *p=<0.05, **p=<0.01, ***p=<0.001.*

Table 4. Significant associations (linear regression analysis), after adjusting for multiple comparisons, between baseline levels of oxylipins and baseline VAS scores for the full cohort (n=154), baseline VAS scores in the advanced / No OA-lower pain (n=101), and 3 year VAS scores in the full cohort (n=154). PainDETECT questionnaire scores… P values were adjusted for multiple comparisons using Bonferroni correction.

Lipid	Present Time (Q1)		Worst Pain (Q2)		Average Pain (Q3)		Mean of Q1-3		PDQ	
	Beta	p value	Beta	p value	Beta	P value	Beta	p value	Beta	P value
Baseline: Full Cohort										
8,9-DHET	1.809	0.0013	ns		ns		ns		ns	
14,15-DHET	0.827	0.0009	ns		ns		ns		ns	
12-HpETE	4.090	0.0002	ns		ns		ns		ns	
AEA	3.060	0.0004	ns		ns		ns		5.875	0.0008
Baseline: No OA- Lower pain and OA-Higher pain subgroups										
5,6-EET	ns		1.340	0.0002			1.249	0.0002	ns	
5,6-Ratio	ns		1.505	4.17E-05	1.210	0.0009	1.249	0.0003	ns	
8,9-EET	2.410	0.0009			2.132	0.0011	2.171	0.0006	ns	
11,12-EET	ns		1.310	0.0001	ns		1.178	0.0003	ns	
11,12-EET:DHET Ratio	ns		1.282	0.0002	ns		1.105	0.0007	ns	
14,15-DHET	1.006	0.0005	ns		ns		ns		2.019	0.0005
14,15-EET:DHET Ratio	ns		ns		ns		ns		-1.700	0.0006
12-HpETE	5.465	0.0003	4.718	0.0010	4.835	0.0002	5.030	0.0001	ns	
20-HETE	ns		1.388	5.56E-05	1.104	0.0010	1.262	8.78E-05	ns	
9-HETE	ns		1.435	0.0002	1.260	0.0008	1.340	0.0002	ns	
12-HETE	ns		1.323	9.54E-05	1.048	0.0014	1.193	0.0002	ns	
14-HDHA	1.368	0.0002	1.245	0.0003	1.285	0.0001	1.309	3.71E-05	ns	
AEA	4.491	6.43E-05	3.586	0.0008	4.356	1.88E-05	4.067	2.82E-05	9.146	4.89E-5
3 Year Follow-up: Full Cohort										
8,9-EET	ns		ns		2.166	0.0009	1.949	0.0012	ns	
5-HETE	ns		2.030	0.0008	ns		1.724	0.0010	ns	
8,9-EET + 5-HETE	0.062	0.0019	0.059	0.0002	0.062	0.0003	0.068	0.0002		

4.3.3 Associations of the baseline serum levels of oxylipins in participants at 3 year follow up

Next, it was investigated whether baseline lipids were associated with future pain VAS scores and the mean of those 3 questions (n=154). After adjusting for multiple comparisons, baseline levels of 8,9-EET were significantly (positive) associated with 3 year average pain score (Q3) and the mean of scores for Q1-3. Baseline levels of 5-HETE were significantly (positive) associated with worst pain score (Q2) and the mean of scores from Q1-3 (Table 4). However, there were no significant associations between baseline lipid levels and change in pain over the 3 years, after multiple comparisons (data not shown). Baseline levels of 5,6-DHET were also significantly (positive) associated with QST scores of the anterior tibialis at 3 years (beta value: 152.179, p value: 0.0003).

To further focus upon potential associations of baseline oxylipins with future pain, participants were stratified into three groups based on 3 year follow-up average pain scores (Q3). A response of 0 was categorised as 'no pain', a score of 1-5 was categorised as 'low pain'; and a score of 6-10 was categorised as 'high pain'. Univariate analysis was carried out to assess differences in the levels of baseline lipids between groups stratified based on 3 year pain (Table 5). Baseline levels of DHA were stable between the no and low pain groups, but significantly lower in the high pain group compared to low pain group at follow-up (Figure 3A).

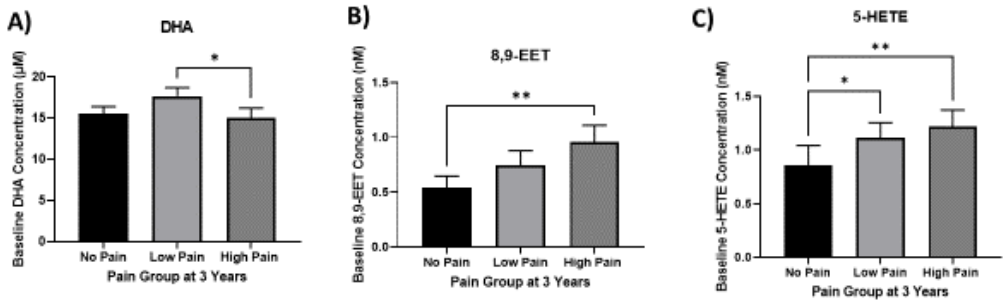

*Figure 4. Baseline serum levels of A) DHA, B) 8,9-EET, C) 5-HETE in groups based on 3 year follow-up pain scores from Q3 (average pain). No pain = score of 0; low pain = score 1-5; and high pain = score 6-10. Significance was assessed using Kurskal-Wallis Test with multiple comparisons. *p=<0.05, **p=<0.01.*

Baseline levels of 8,9-EET were significantly higher in the high pain group compared to the no pain group (Figure 3B), whereas levels of 14,15-EET were significantly higher in the low pain group compared to the no pain group (Table 2). Levels of 5-HETE were significantly higher in both the low and high pain group, compared the no pain groups (Figure 3C). Levels of 16-HETE were significantly higher in the low pain group compared to no pain group (Table 5). Of the other lipids measured, there were no significant differences in baseline lipid levels between the three groups at follow-up, however there were some general trends of higher levels in the higher pain group (including 17-, & 14-HDHA; 5,6-, & 11,12-EET; 14,15-DHET; 9-, 12-, 15-, & 2-HETE; and TXB2 (Table 5).

Table 5. Average concentration (nM) ± standard deviation of oxylipins quantified in serum samples at baseline in three groups based on numerical rating scale (NRS) item 3 scores at 3 years follow-up: No pain (NRS=0); Lower pain (NRS=1-5); and Higher pain (NRS=6-10).

	Lipid	No Pain at 3 Years			Lower Pain at 3 Years			Higher Pain at 3 Years		
		Mean	±	SD	Mean	±	SD	Mean	±	SD
Serum Lipid Concentration at Baseline (nM)	5,6-EET	14.91	±	27.66	24.78	±	42.48	32.61	±	46.10
	5,6-DHET	0.48	±	0.29	0.63	±	0.38	0.62	±	0.49
	5,6-Ratio	36.62	±	62.51	45.95	±	109.53	3113.10	±	20547.53
	8,9-EET	0.54	±	0.79	0.74	±	1.04	0.91	±	0.94
	8,9-DHET	0.31	±	0.23	0.36	±	0.20	0.36	±	0.23
	8,9-Ratio	165.67	±	812.43	8.93	±	51.82	54.68	±	336.01
	11,12-EET	80.64	±	156.30	127.82	±	217.69	170.87	±	243.84
	11,12-DHET	0.82	±	0.43	0.90	±	0.47	0.81	±	0.53
	11,12-Ratio	151.26	±	310.44	160.07	±	250.46	293.66	±	501.55
	14,15-EET	0.23	±	0.12	0.32	±	0.15	0.27	±	0.15
	14,15-DHET	0.46	±	0.46	0.52	±	0.48	0.62	±	0.45
	14,15-Ratio	24.86	±	74.85	28.72	±	73.89	1.33	±	3.71
	12-HpETE	2.89	±	1.52	3.36	±	1.87	3.83	±	2.01
	TBXB2	8.58	±	19.18	13.30	±	21.07	15.84	±	25.49
	PGE2	0.49	±	1.09	0.49	±	0.63	0.54	±	0.63
	LTB4	0.61	±	1.21	0.67	±	1.08	0.46	±	0.75
	20-HETE	27.06	±	51.81	45.87	±	81.90	55.73	±	77.75
	18-HEPE	0.54	±	0.56	0.70	±	0.70	0.72	±	0.73
	16-HETE	0.46	±	0.37	0.55	±	0.25	0.51	±	0.37
	15-HETE	4.01	±	5.27	5.63	±	6.86	6.87	±	8.03
	13-oxoODE	14.86	±	8.52	15.76	±	9.06	14.48	±	8.29
	11-HETE	1.85	±	1.39	2.52	±	2.42	2.85	±	2.54
	9-oxoODE	7.13	±	3.88	7.46	±	4.66	6.84	±	3.99
	9-HODE	9.73	±	11.06	9.09	±	6.09	12.38	±	31.95
	9-HETE	1.41	±	2.77	2.18	±	3.82	3.00	±	4.41
	12-HETE	77.39	±	154.05	118.13	±	194.48	157.95	±	221.48
	5-HETE	0.84	±	1.35	1.11	±	1.09	1.16	±	0.85
	17-HDHA	1.18	±	2.22	1.38	±	1.82	1.58	±	1.98
	14-HDHA	14.04	±	31.13	27.34	±	60.90	33.07	±	52.05
	AEA	0.68	±	0.38	0.73	±	0.45	0.78	±	0.36
	AA (μM)	12.46	±	4.44	14.42	±	4.76	14.30	±	5.50
	LA (μM)	23.14	±	10.45	22.92	±	8.08	22.07	±	10.34
	EPA (μM)	0.70	±	0.36	0.80	±	0.44	0.69	±	0.52
	DHA (μM)	15.65	±	5.86	17.68	±	7.76	15.18	±	8.54

4.5 Discussion

The aim of this study was to quantify pro- and anti-inflammatory oxylipins in a cohort of participants with varying amounts of radiographic OA and knee pain, in order to investigate the relationship between circulating levels of these lipid mediators with clinical features of OA. Linear regression analyses performed between levels of oxylipins with self-reported pain scores revealed several strong associations. Analyses also revealed significant associations between KL score and four oxylipins derived from two key enzymatic pathways. The relationship between baseline levels of oxylipins with self-reported pain scores collected 3 years later was also investigated, and revealed baseline levels of 8,9-EET and 5-HETE were associated with self-reported pain scores collected 3 years later.

In the full cohort, higher levels of 14-HDHA, 15-HETE, 9-HETE, and the ratio of 8,9-EET:DHET were significantly associated with higher KL scores. 14-HDHA and 15-HETE are both produced from their respective PUFA substrates (DHA and AA) via lipoxygenase enzymes (12/15-LOX), and both act as precursors to the specialised pro-resolving mediators maresins (14-HDHA) and lipoxins (15-HETE). Expression of 12/15-LOX in cartilage has previously been reported to increase during progression of DMM-induced, and aging OA in mice, and that 12/15-LOX knockout mice had more severe cartilage degeneration compared to wild type mice in both models (Habouri, El Mansouri et al. 2017). Further studies have also found that deletion of 12/15-LOX leads to uncontrolled inflammation and tissue damage in inflammatory models of arthritis (Kronke, Katzenbeisser et al. 2009). These studies suggests that the LOX pathways play a somewhat protective role in the joint, which may work to slow disease progression but is insufficient to halt the structural changes driving the disease completely. Future studies investigating the LOX pathway as a potential therapeutic target, could investigate whether LOX receptor agonists enhance these apparent protective roles and further slow the progression of OA in animal models, however given the diverse and somewhat paradoxical roles of

LOX enzymes (Ackermann, Hofheinz et al. 2017), targeting this pathway is likely to lead to off-target effects.

The second key enzymatic pathway to be identified in this study is the CYP450 pathway which converts AA into 9-HETE and 8,9-EET from which the EET:DHET ratio gives a rough overview of the pathway as a whole. The association of this pathway with KL score supports previous findings from our group, which showed association of synovial fluid levels of DHETs with radiographic knee OA over 3.3 years (Valdes, Ravipati et al. 2018). Given the anti-inflammatory role of the EETs, upregulation/increased activity of CYP450 could be an endogenous response to joint damage and associated inflammation.

Of the oxylipins associated with KL score, 15-HETE is the only lipid to be associated with KL only and not to any of the NRS items, suggesting the involvement in this This finding supports previously reported observation of higher plasma levels of 15-HETE in symptomatic OA patients compared to non-symptomatic controls (Attur, Krasnokutsky et al. 2015). Through further validation, these four oxylipins strongly associated with KL score could have further clinical potential as prognostic markers of disease progression and reduce the burden on radiography services.

Linear regression analysis performed between levels of oxylipins with different items of self reported pain in the full cohort revealed strong associations with two DHETs, AEA, and 12-HpETE. The associations of 8,9- and 14,15-DHET with NRS (item 1) in the full cohort support previous findings reported from our group and others, and adds further evidence to mounting support for targeting the sEH pathway to treat OA related pain (Valdes, Ravipati et al. 2018, McReynolds, Hwang et al. 2019, Hammock, McReynolds et al. 2021, Gowler, Turnbull et al. 2022) Intrestingly, AEA was associated with both NRS score (item 1) and with PDQ, which is designed to assess the neuropathic quality of pain, suggesting that it may be involved in multiple pain signalling pathways.

Changes in gene expression of AEA regulator enzymes and receptors have been reported to be altered at both the level of the spinal cord and joint tissue during different phases of OA in the MIA model (Bryk, Chwastek et al. 2020). 12-HpETE is a 12-LOX metabolite of AA and is a precursor to the hepoxilins (HXs, not measured in this study), which are reported to have roles in both inflammation and pain. Studies have shown that HXA3 and HXB3 are released from the spinal cord and directly activate TRPV1 and TRPA1, leading to hyperalgesia and allodynia (Gregus, Doolen et al. 2012, Kelly, Chapman et al. 2015), and given the reported increase in TRPV1 function in models of OA (Kelly, Chapman et al. 2015) this could add further support to the use of TRPV1 antagonists to treat OA pain.

Stratification of participants based on clinical criteria for radiographic OA and knee pain scores revealed further associations between levels of oxylipins and self-reported measures of pain, including the anti-inflammatory EETs and the pro-resolution pathway marker 14-HDHA. The association of these anti-inflammatory mediators with increased pain scores could point towards attempted activation of endogenous resolution pathways in response to joint damage and associated pain. 14-HDHA is an intermediary molecule in the DHA pathway and acts as a precursor to the maresins. Macrophages are mainly responsible for the production of maresins which act to increase the function of M2 macrophages, responsible for the release of anti-inflammatory cytokines and the resolution of inflammation (Hwang, Chung et al. 2019). Maresins and the more recently discovered maresin conjugates are also reported to have their own direct roles in modulating pain and promoting tissue repair (Dalli, Sanger et al. 2016, Tang, Wan et al. 2018).

These observations are also supported by univariate analyses between these groups were comparison shows significantly higher levels of EETs, EET:DHET ratios, HETEs, and HDHAs in OA-Higher pain groups compared to undefined joint damage-lower pain groups. These findings suggest increased systemic

activation of key lipid metabolic pathways in people with symptomatic OA, which may be an endogenous molecular response to limit disease progression and resolve persisting inflammation. In this study, 62.8% of participants reported improved average pain scores (item 3) at the 3 year time point compared to baseline, with a median improvement of 3 on the NRS scale. Of the remaining participants, 12.8% had no change in pain, and 24.3% had an increase in pain with a median increase of 2 on the NRS scale. Stratification of participants by improved, unchanged, or worsened pain over 3 years showed no differences in levels of baseline oxylipins through univariate analyses, as did linear regression analysis between baseline oxylipins levels and change in pain over 3 years.

Regression analysis performed between baseline levels of lipid mediators and pain scores at 3 year later revealed positive associations between 8,9-EET and 5-HETE with self-reported pain scores, and 5,6-DHET with QST scores. With replication in other cohorts, these data could have clinical implications as potential biomarkers of future pain, which would help identify those participants who could benefit most from clinical interventions. The associations of 8,9-EET and 5-HETE with future self-reported pain scores, and 5,6-DHET with future QST measurements could imply distinct roles for these lipids in both peripheral and centralised pain signalling.

Building on the linear regression analysis performed between baseline lipid levels and 3-year pain scores, the univariate analysis performed on baseline lipid levels between groups stratified by levels of pain at 3 years showed that those with higher pain at 3 year had significantly lower baseline levels of DHA than those with lower pain at 3 years. These data suggest that having higher levels of DHA could lead to lower pain in the future. A potential clinical implication here could be a dietary intervention aiming to increase the amount of DHA consumed by people with OA related knee pain, however further

studies are required in this area (Wu, Jain et al. 2015, Mustonen and Nieminen 2021).

The absence of follow-up KL scores means that it is not known to what extent OA progressed over the 3 years over the study, which is a limitation of this study. When looking at extreme groups, participants were excluded who did not fall into these categories based on their clinical characteristics. This group of participants are likely made up of people who either have non-symptomatic radiographic OA (n=36) or have non-OA related knee pain (n=17). These are important demographics of people suffering from OA and pain, however, this study was underpowered to investigate these groups individually so therefore have excluded these from some analyses. There is also a potential limitation of recruitment bias in this study, as participants were selected based on availability of serum samples and follow-up pain scores, there could be bias towards participants who are more proactive in managing their OA and pain which may not be representative of the wider population of people with OA. In this study, serum samples were analysed for their lipidomic profile, this gives a systemic profile of oxylipins but is unlikely to reflect the local oxylipin profile in the diseased joint. However, given the relative ease of serum collection compared to joint tissue/synovial fluid, our findings in serum give a strong rationale for further investigation of the potential of oxylipins as blood biomarkers of OA through further replication and validation studies.

These findings highlight the role of omega-3 and -6 PUFA derived oxylipins in both OA joint pathology and the associated pain phenotype, and point toward future potential therapeutic targets to treat symptomatic OA and the potential use of oxylipins as biomarkers for future pain.

Chapter Five

Investigating the effects of targeting soluble epoxide hydrolase in a mouse model of OA on plasma lipids

Acknowledgements

These studies were completed jointly by Dr Peter Gowler, and myself. All animal work, including dosing and pain behaviour was completed by Peter, lipidomic analysis was performed by myself, and equal contributions were made towards statistical analysis.

This project was also completed in part in collaboration with Prof. Bruce Hammock's research group at University of California Davis. Levels of TPPU were measured in dried blood spots from mice by the Hammock group.

Data from this chapter have been peer reviewed and reported in the manuscripts below:

Peter R. W. Gowler, James Turnbull, Mohsen Shahtaheri, Emma Jackson, Grace Keenan, David Walsh, David Barrett, Victoria Chapman. **Interplay between cellular changes in the knee joint, circulating lipids and pain behaviors in a slowly progressing murine model of osteoarthritis**. European Journal of Pain. doi.org/10.1002/ejp.2036.

Peter R. W. Gowler, James Turnbull, Mohsen Shahtaheri, Sameer Gohir, Tony Kelly, Cindy McReynolds, Yang Jun, Rakesh R. Jha, Gwen S Fernandes, Weiya Zhang, Michael Doherty, David A. Walsh, Bruce D. Hammock, Ana M. Valdes, David A. Barrett, Victoria Chapman. **Clinical and preclinical evidence for roles of soluble epoxide hydrolase in osteoarthritis knee pain.** Arthritis Rheumatol. 2021. doi: 10.1002/art.42000.

Abstract

Animal model of disease are essential to researchers to allow the study of disease mechanisms and to assess the suitability of potential treatment for the disease in an *in vivo* model. The destabilisation of the medial meniscus (DMM) model, is a slow progressing model which mimics the development of OA following acute knee injury. The soluble epoxide hydrolase pathway, which metabolises EETs to their corresponding diols, has been identified by studies in this thesis, and others, as a potential target for chronic knee pain. In these studies, the oxylipins were measured in mouse plasma collected at 3 key time points following DMM surgery (n=20 per time point, and their associations with features of OA investigated, including cartilage damage, synovitis, and pain behaviour. In a separate study, mice either received sham or DMM surgery and either dosed with a soluble epoxide hydrolase inhibitor (TPPU) or vehicle. In the DMM time point study, several oxylipins were associated with cartilage damage and synovitis at 4 and 8 weeks post-surgery, including the HETEs and EETs. At 16 weeks post-surgery, when pain behaviour had developed, levels of 17-HDHA were associated with lower pain behaviour. Dosing with TPPU showed attenuation of pain phenotype in mice that received DMM surgery compared to vehicle treated mice. This effect was seen both with intraperitoneal injection and repeated oral administration. Treatment with TPPU did not significantly increase the levels of the EETs, but did increase the ratios of EETs to their corresponding diols. This could be explained by feedback inhibition of EET production, or increased COX-2 metabolism of EETs to EHETs. Levels of 8,9-DHET were associated with pain behaviour, and the 8,9-EET:DHET ratio was associated with both cartilage damage and synovitis. These studies show good translation of the associations seen the clinical studies to a mouse model of OA, and show that targeting sEH to treat chronic OA pain is a promising strategy worth further investigation.

5.1 Introduction

In order to investigate the efficacy of potential pharmacological intervention for treatment of OA, we must have suitable animal models that mimic the pathology and associated pain phenotype seen in patients. Several models are validated to be used in order to model the OA phenotype in animals. Injection of monoiodoacetate (MIA), a glycolytic inhibitor, into the joint blocks aerobic glycolysis in chondrocytes. This causes deterioration of the extracellular matrix which leads to behavioural, histological and biochemical changes that mimic human OA (Pomonis, Boulet et al. 2005, Liu, Okun et al. 2011). Surgical models are also used to induce a OA phenotype in animal studies. The medial meniscal transection (MNX) involves the removal of the medial collateral ligament (MCL) which leads to rapid degradation of the joint and pain behaviour within 7 days of surgery (Gowler, Mapp et al. 2020). These studies used the DMM model as this mimics clinical meniscal injury, a known predisposing factor for the development of human OA, and permits the study of structural and biological changes over the course of the disease (Culley, Dragomir et al. 2014). The DMM model most closely mimics the OA phenotype of participants in the earlier chapter of this thesis, those who have sustained acute knee injury, and those with established knee OA phenotype.

One of the relatively more straightforward sub-pathways of the arachidonic acid cascade, is the cytochrome P450 (CYP 450) pathway involving the CYP2C and CYP2J epoxygenases. CYP450 monooxygenases are a large family of enzymes that oxidise many bioactive compounds *in vivo* and *in vitro.* Although many current therapeutics target the cyclooxygenase (COX) and lipoxygenase (LOX) pathways (Dannhardt and Kiefer 2001) of the arachidonic acid cascade, CYP450 has been somewhat overlooked for its therapeutic potential. Acting on arachidonate, specific CYP450 epoxygenases oxidise the double bonds to produce four epoxyeicosatrienoic acid (EET) metabolites: 5,6-EET; 8,9-EET; 11,12-EET; and 14,15-EET. These metabolites are structural isomers of one another and are named based on the position of the epoxide bond on the carbon chain (Spector and Kim 2015). The pro-inflammatory mediator 20-HETE

is also a product of CYP450 metabolism, however compounds that inhibit it's production have not been shown to be therapeutic in models of hypertension (Morisseau and Hammock 2013).

The EETs were first identified over 30 years ago and are reported to have high biological activity. Their role in physiology is focused on driving the tissue environment toward homeostasis (Morisseau and Hammock 2013). The EETs have potent anti-inflammatory and analgesic properties (Inceoglu, Jinks et al. 2008, Thomson, Askari et al. 2012). The exact mechanisms by which the EETs exert their bioactivity are not fully understood Spector et al (2004) reviewed current studies and summarised the effects of the EET's bioactivities which included inhibition of PGE2 production, decreased cytokine induced cell adhesion, and inhibition of platelet cyclooxygenases (Spector, Fang et al. 2004). Since then, there has been growing evidence of GPCR receptor involvement in EET mechanisms of action. One study screened 105 GPCRs against 14,15-EET and found responses from several prostaglandin receptors (PTGER2, PTGER4, PTGFR, PTGDR, PTGER3IV) – however out of the 105 GPCRs screened, none showed high affinity for 14,15-EET (Liu, Qian et al. 2017). It is likely that EETs have various molecular targets and their mechanisms may differ between tissues. There is an extensive amount of literature identifying the EET's involvement in many metabolic and inflammatory diseases including cardiovascular (Xu, Zhang et al. 2011), respiratory (Morin, Sirois et al. 2008), and neurodegenerative (Lakkappa, Krishnamurthy et al. 2016) diseases. Despite their high bioactivity, *in vivo* they are readily metabolised by soluble epoxide hydrolase (sEH) (Figure 1)(Morisseau and Hammock 2013), this makes enhancing their biological half-lives and bioactivity a potential therapeutic approach for a range of diseases.

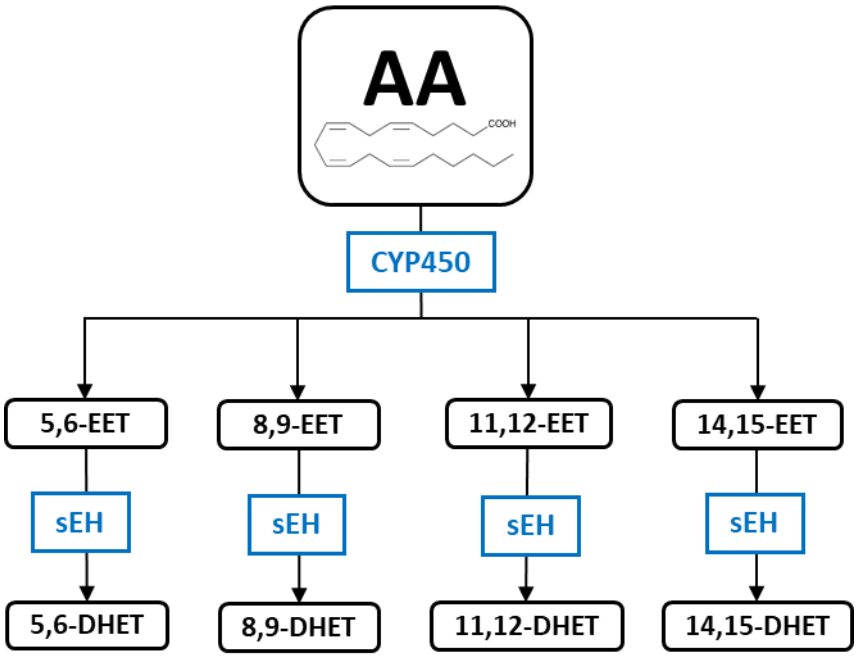

Figure 1. Production of EETs by CYP 450 epoxygenases, and metabolism to corresponding DHETs by soluble epoxide hydrolase.

Soluble epoxide hydrolase metabolises EETs to their corresponding dihydroxyeicosatrienoic acids (DHETs). sEH was first isolated from mouse liver tissue and originally identified as being involved in clearance of xenobiotics (Zeldin, Moomaw et al. 1996), and was later found to regulate levels of the EETs *in vivo* by Hammock and colleagues (Yu, Xu et al. 2000). The sEH enzyme is coded by the EPHX2 gene on chromosome 8 and is expressed in most mammalian tissues. The enzyme is formed of two 60-kDa monomers that form a homodimer, where epoxides bind specifically to the c-terminal domain where the epoxide bond is hydrolysed to two hydroxyl groups – forming a diol (He, Wang et al. 2016).

Originally the DHETs were thought to be biologically inactive stable metabolites of epoxide hydrolysis with no clinical relevance, however more recent research suggests that the DHETs may have pro-inflammatory and pro-nociceptive effects. *In vitro* and *in vivo* studies showed that DHETs contributed to monocyte chemoattractant 1 (MCP-1) induced monocyte chemotaxis – a key event in inflammation (Kundu, Roome et al. 2013).

The distinct anti-inflammatory properties of the EETs make the sEH pathway presents as an attractive target for pharmacological intervention that would increase levels of EETs and/or decreases levels of DHETs. The Hammock group at UC Davis have studied the soluble epoxide hydrolase enzyme extensively and have developed many compounds that act as inhibitors to its activity. These inhibitors have been tested as potential therapeutics for several inflammatory diseases such as heart disease (Qiu, Li et al. 2011), diabetes (Luria, Bettaieb et al. 2011) and canine osteoarthritis (McReynolds, Hwang et al. 2019)

TPPU is a potent sEH inhibitor that is commercially available. The structure of TPPU (Figure 2) is centred on a urea pharmacophore, with two electron withdrawing side groups. The hydrogens on the urea group are essential for binding to the aspartate moiety in the active site of sEH. The 4-trifluoromethoxy phenyl group on the molecule was added in order to increase the total *in vivo* exposure time (Ulu, Appt et al. 2012).

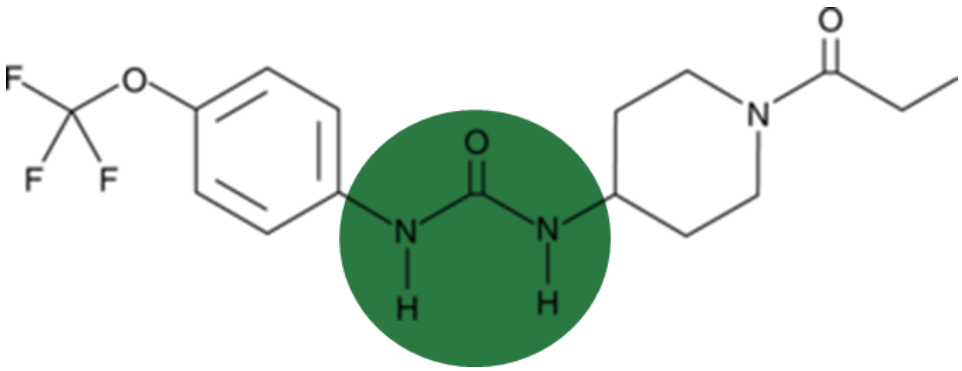

Figure 2. Chemical structure of N-[1-(1-oxopropyl)-4-piperidinyl]-N'-[4-(trifluoromethoxy)phenyl)-urea (TPPU). Urea pharmacophore is highlighted in green.

Inhibitors of sEH are generally fairly straightforward and inexpensive to produce (Rose, Morisseau et al. 2010) with the basic structure of the pharmacophore and side groups being a two-step synthesis. TPPU is a commercially available sEH inhibitor used in research due to its good potency, pharmacokinetics, and biological activity without apparent non-specific binding (Wan, Yang et al. 2019).

Investigating the efficacy of treating diseases where the hallmark is chronic pain with sEH inhibitors is particularly important. Current treatments for chronic pain such as opioids and non-steroidal anti-inflammatory drugs (NSAIDs) can be addictive, become ineffective, have severe adverse side effects, and are generally unsuitable for long-term use (Zhang, Robertson et al. 2019). In the case of OA, there are also no current therapeutics available that treat the progression of the joint pathology that underpins the disease.

The aim of these studies was to asses the relationship between oxylipins and OA phenotype in a model of OA and to evaluate the efficacy of acute and chronic administration of TPPU, a soluble epoxide hydrolase inhibitor, for its analgesic potential. This included investigating the compound's effect on pain behaviour, circulating oxylipins, and joint pathology.

5.2 Materials and Methods

5.2.1 Animals

All experiments using mice were carried out by Peter Gowler and performed in accordance with the United Kingdom Animals (Scientific Procedures) Act (1986). Adult male C57BL/6 (total n=60 timepoint study; n = 149, sEH study aged 10-11 weeks at time of model induction) were housed in individually ventilated cages in temperature controlled (20-23°C) rooms under a 12 hour light-dark cycle (7am- 7pm). Mice had access to standard rodent diet and water *ad libitum*.

5.2.2 Pain Behaviour

The experimenter was blinded to the experimental group mice were in throughout the duration of the study. Mice were randomly allocated to either the model or sham group by a third party, and then treatment groups were stratified by a third party to ensure balanced pain behaviour between groups. All mice were habituated to the behavioural test environments prior to assessment. Weight-bearing asymmetry between the ipsilateral (left) and contralateral (right) hind limbs as assessed by an incapacitance meter (Linton Instrumentation, Norfolk, United Kingdom) as previously described (Sagar, Burston et al. 2011). Hind paw mechanical withdrawal thresholds were assessed using von Frey monofilaments. The 50% withdrawal threshold was measured using the EC50 of log transformed responses to a battery of von Frey hairs as previously described (Hulse, Beazley-Long et al. 2014).

5.2.3 DMM Surgery (Time point Study)

Adult male C57BL/6J mice (n=60) were anaesthetised with 2% isoflurane before undergoing either DMM (n=30) or sham (n=30) surgery of the ipsilateral hindlimb as previously described (Ashraf, Radhi et al. 2019). Pain behaviour was measured at baseline and then once a week for up to 16 weeks post-surgery. At 4 weeks post-surgery, 20 mice were euthanised (DMM: n=10, sham: n=10) and blood samples were taken. At 8 weeks post-surgery, 20 mice were

euthanised (DMM: n=10, sham: n=10) and blood samples were taken. The last 20 mice were euthanised at 16 weeks post-surgery (DMM: n=10, sham: n=10) and blood samples were taken. The final groups sizes were therefore 4 weeks post-DMM (n=10), 4 weeks post-sham (n=10), 8 weeks post-DMM (n=10), 8 weeks post-sham (n=10), 16 weeks post-DMM (n=10), and 16 weeks post-sham (n=10). The length of the model allowed us to collect plasma samples at 4 weeks post-surgery when there is no significant pain nor pathology, 8 weeks post-surgery when there is significant pathology but no pain, and at 16 weeks post-surgery when there is both pain and pathology.

5.2.4 Joint Histology

Knee joints were dissected post-mortem and fixed in 10% neutral buffered formalin for 48 h, and then decalcified in a 10% EDTA (with 7.5% PVP) solution for 10 days before being processed with xylene and embedded in paraffin. Sagittal sections (5 μm) across the depth of the medial side of the joint were collected. Three sections per joint were then stained for haematoxylin and eosin (H&E) and three sections per joint were then stained for safranin O (Saf-O) as previously described (Ashraf, Radhi et al. 2019). Slides were blinded and then joint pathology was assessed by two independent scorers based on previously published scoring criteria (Ashraf, Radhi et al. 2019).

5.2.5 Acute TPPU Dosing Study

Adult male C57BL/6J mice (n=30) were anaesthetised with 2% isoflurane and underwent either destabilisation of the medial meniscus (DMM) (n =20) or sham (n=10) surgery of the ipsilateral hind limb as previously described (Ashraf, Radhi et al. 2019). Pain behaviour was measured at baseline and then once a week for 16 weeks post-surgery. At 16 weeks post-surgery mice received an i.p. injection of 3mg/kg TPPU (n=10) or vehicle (n=20). Pain behaviour was then measured at 1 hour and 3 hours post-injection. Mice were euthanised by i.p. injection of sodium pentobarbital and plasma was collected for lipid analysis. The final group sizes were sham + vehicle (n=10), DMM + vehicle (n=10), and DMM + TPPU (n=10).

5.2.6 Chronic TPPU Dosing Study

In a separate study, adult male C57BL/6J mice (n=28) were anaesthetised with 2% isoflurane and underwent either DMM (n=19) or sham (n=9) surgery of the ipsilateral hind limb as previously described (Ashraf, Radhi et al. 2019). Pain behaviour was then measured at baseline and then once a week for 16 weeks post-surgery. From 12 weeks post-surgery the drinking water in the cage was replaced with either 11mg/L TPPU in 1% PEG-400 (n = 15) in filtered water or 1% PEG-400 (n = 13) in filtered water. Based on the average volume of water consumed by mice per day it was estimated the dose to be approximately 3mg/kg TPPU. The water solution of TPPU and vehicle was replaced twice a week over the course of dosing. Blood (10 µL) was collected from the tail vein of mice before dosing, 2 weeks after dosing, and 4 weeks after dosing with TPPU or vehicle. At 16 weeks post-surgery mice were euthanised by i.p. injection of sodium pentobarbital, and plasma was collected for lipid analysis. The final group sizes were sham + vehicle (n = 4), sham + TPPU (n = 5), DMM + vehicle (n = 9), and DMM + TPPU (n = 10).

5.2.7 LC-MS/MS Lipidomic Analysis

Whole blood was collected from animals immediately following sacrifice and prepared into heparinised plasma before being stored at -80°C until analysis. Targeted lipidomic analysis was carried out on plasma samples collected from animals at the end of the study to measure systemic levels of EETs and DHETs, along with other lipid mediators. Chapter 2 provides details of the development and validation of the LC-MS/MS method used as well as sample preparation. The workflow of the study including lipidomic analysis is summarised below in Figure 3.

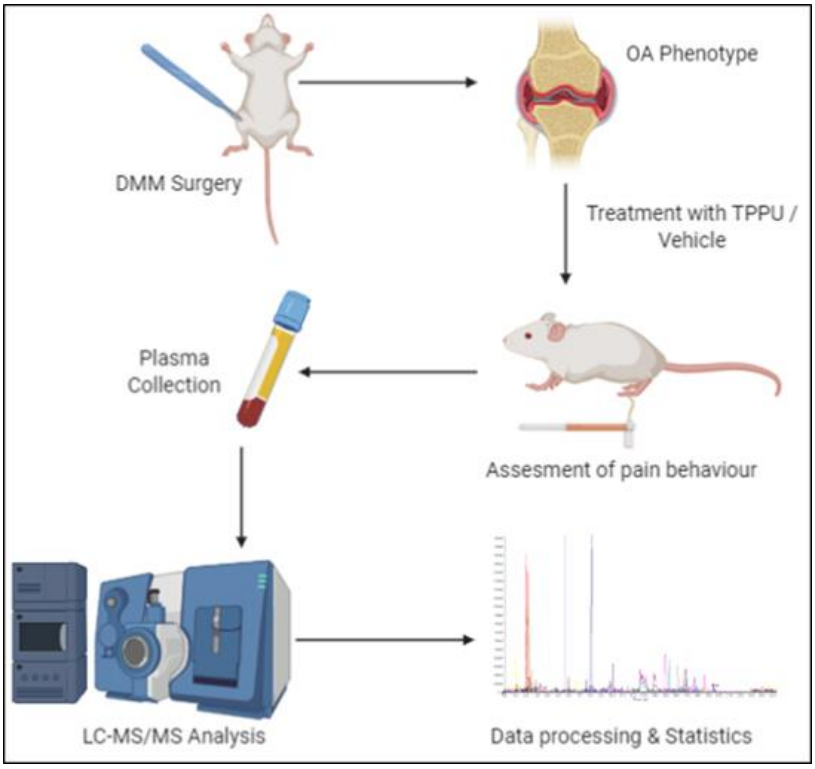

Figure 3. Visual summary of experimental workflow for lipidomic analysis. Made using biorender.com

5.2.8 Data and Statistical Analysis

All data were analysed and graphically presented using Prism v7 (Graphpad; San Diego, CA). Data were tested for normal distribution utilising the D'Agostino and Pearson normality test. If data were normally distributed, they were analysed with parametric tests, and if data were not normally distributed they were instead analysed with non-parametric tests. Differences in histological joint damage in DMM and sham mice were assessed by unpaired t-test. Changes in weight bearing asymmetry and ipsilateral hind-paw withdrawal thresholds were assessed by 2-way ANOVA with Bonferroni corrected multiple corrections. Analysis of the differing circulating levels of the EETs and DHETS, as well as TPPU's effects on histological joint damage was done by one-way ANOVA with Tukey's multiple comparisons. Correlation analysis between the circulating levels of the EETs and DHETs, and both pain scores and joint damage was done by Pearson's correlation test. Data presented as mean ± SEM.

5.3 Results

5.3.1 Plasma oxylipins in the DMM time point study

Plasma levels of 33 ω-3/ω-6 derived oxylipins were quantified at 4, 8, and 16-weeks post- surgery in the DMM model and sham controls (Table 1). There were no significant differences between levels of oxylipins between time points, however due to the lower n numbers in this study in comparison to clinical studies, it is likely that the study was underpowered to assess these differences. Therefore, I focused upon potential associations of oxylipins with joint pathology and pain behaviour and the different time points.

Table 1. Concentration of oxylipins quantified in plasma and associations with measures of pain behaviour at 4 weeks, 8 weeks, and 16 weeks post-surgery in sham and DMM mice.

Lipid	Lipid plasma concentration nM ± SD											
	Sham Week 4		DMM Week 4		Sham Week 8		DMM Week 8		Sham Week 16		DMM Week 16	
PGE2	1.00	0.71	0.53	0.21	0.53	0.44	0.67	0.45	0.69	0.22	0.57	0.33
PGD2	1.46	0.53	1.10	0.34	0.98	0.19	1.24	0.50	1.23	0.26	1.08	0.43
TxB B2	41.94	39.81	26.74	19.28	88.36	178.01	31.29	42.36	53.63	44.13	42.13	29.30
LTB4	6.66	3.91	5.59	3.09	4.18	2.20	4.11	2.94	4.81	2.80	6.52	3.92
6-T-LTB4	1.04	0.35	0.81	0.24	0.48	0.31	0.84	1.09	0.78	0.51	0.96	0.69
5-HETE	27.53	12.73	21.59	9.14	15.99	6.91	16.75	10.16	19.67	7.22	25.00	15.34
8-HETE	11.62	1.92	9.20	3.53	8.68	3.26	10.24	3.86	10.25	2.47	10.85	4.13
9-HETE	3.80	2.08	2.59	0.88	3.21	2.15	3.28	2.52	3.51	2.38	2.72	1.32
11-HETE	2.55	1.97	1.32	0.83	1.95	1.80	1.94	2.96	1.58	0.97	1.63	1.30
12-HETE	839.37	374.00	691.60	423.51	528.51	215.39	763.11	364.32	723.83	314.82	839.13	398.34
15-HETE	23.63	11.10	18.14	6.82	17.92	10.24	20.60	11.87	24.75	8.00	21.28	9.13
5-HpETE	13.91	3.50	13.32	4.52	15.76	7.14	18.15	8.29	28.78	37.32	12.44	1.00
12-HpETE	13.86	3.82	12.11	3.16	12.03	2.54	15.90	7.97	22.37	26.51	13.94	5.29
5,6-EET	15.44	8.67	13.25	8.89	14.59	7.77	28.06	48.20	21.95	13.95	23.03	13.45
8,9-EET	2.00	1.21	1.64	0.68	2.97	3.62	2.25	2.60	2.11	0.83	2.44	1.65
11,12-EET	5.93	2.90	4.21	1.53	5.11	3.95	4.76	4.04	4.83	2.19	5.03	2.89
14,15-EET	6.53	2.88	4.94	1.76	5.77	3.34	6.03	5.09	6.51	2.29	6.22	3.00
11,12-DHET	2.79	1.95	2.66	1.25	2.28	1.63	1.96	0.55	2.72	0.95	3.59	2.52
14,15-DHET	4.91	3.49	4.54	1.96	4.59	4.46	3.62	0.95	5.27	2.54	6.06	4.08
9-HODE	66.53	22.80	47.68	21.35	72.20	71.74	65.00	32.80	73.32	17.73	83.41	39.08
13-HODE	169.83	38.90	136.62	65.76	151.02	136.06	159.73	47.64	173.07	42.76	180.88	90.20
9-OxoODE	26.99	6.16	16.97	8.99	36.22	56.81	24.93	19.21	26.05	8.32	25.34	14.92
13-OxoODE	37.88	8.79	28.50	8.96	45.40	45.04	39.69	22.23	40.37	17.62	43.76	15.18
5,12-DiHETE	4.13	1.90	3.27	2.52	1.38	0.68	4.19	7.19	2.55	1.84	2.76	2.13
5,15-DiHETE	0.27	0.13	0.24	0.14	0.18	0.07	0.26	0.27	0.29	0.25	0.21	0.12
8,9-DiHETE	0.24	0.05	0.23	0.14	0.16	0.06	0.32	0.43	0.32	0.15	0.31	0.18
17-HDHA	7.65	2.17	5.87	2.10	7.29	5.97	8.04	3.93	7.90	2.26	6.55	2.91
RvD5	0.34	0.10	0.32	0.11	0.23	0.17	0.34	0.17	0.32	0.13	0.24	0.10
Maresin 2	1.11	0.43	0.98	0.36	0.82	0.24	1.45	1.37	1.52	1.57	0.88	0.30
2-AG	308.45	76.90	281.84	102.39	209.54	93.78	220.67	66.90	324.95	105.11	299.73	101.80
AEA	0.54	0.10	0.53	0.07	0.60	0.15	0.89	0.60	0.57	1.27	0.60	0.18
OEA	5.24	0.96	5.23	0.87	7.10	8.53	5.23	1.32	7.66	8.78	6.01	1.89
PEA	9.14	2.95	8.31	2.36	16.03	24.27	7.61	2.11	8.18	1.96	10.37	3.71

5.3.2 Associations at 4 weeks post-surgery

Cartilage damage score was moderately negatively correlated with plasma concentrations of PGE2, PGD2, 8-HETE and 12-HETE (Figure 4A-D). There was a moderate negative correlation of synovitis score with plasma 5-HETE (Figure 4E).

5.3.3 Associations at 8 weeks post-surgery

Structural and inflammatory changes in the knee joint were associated with plasma levels of oxylipins. Plasma 5-HETE was moderately negatively correlated with cartilage damage score (Figure 5A). There were significant moderate negative correlations between synovitis score and plasma levels of 5-HETE, 12-HpETE, maresin 2, 8,9-EET, 11,12-EET, and 14,15-EET(Figure 5B-G). There were no significant associations between plasma oxylipins and levels of the macrophage markers CD68 and CD206 in the synovium, nor with pain behaviour, at this time-point.

5.3.4 Associations at 16 weeks post-surgery

This was the first time-point that pain behaviour was significant in the DMM model compared with sham controls. There was a weak but significant positive correlation between higher plasma levels of 17-HDHA with less weight bearing asymmetry, indicative of less pain behaviour (Figure 6A). There were no significant associations between plasma concentrations of 17-HDHA and hind PWTs (Figure 6B). At this time-point, 9-oxoODE was moderately negatively correlated with cartilage damage. There were no significant associations between plasma oxylipins and the level of the macrophage markers CD68 and CD206 in the synovium.

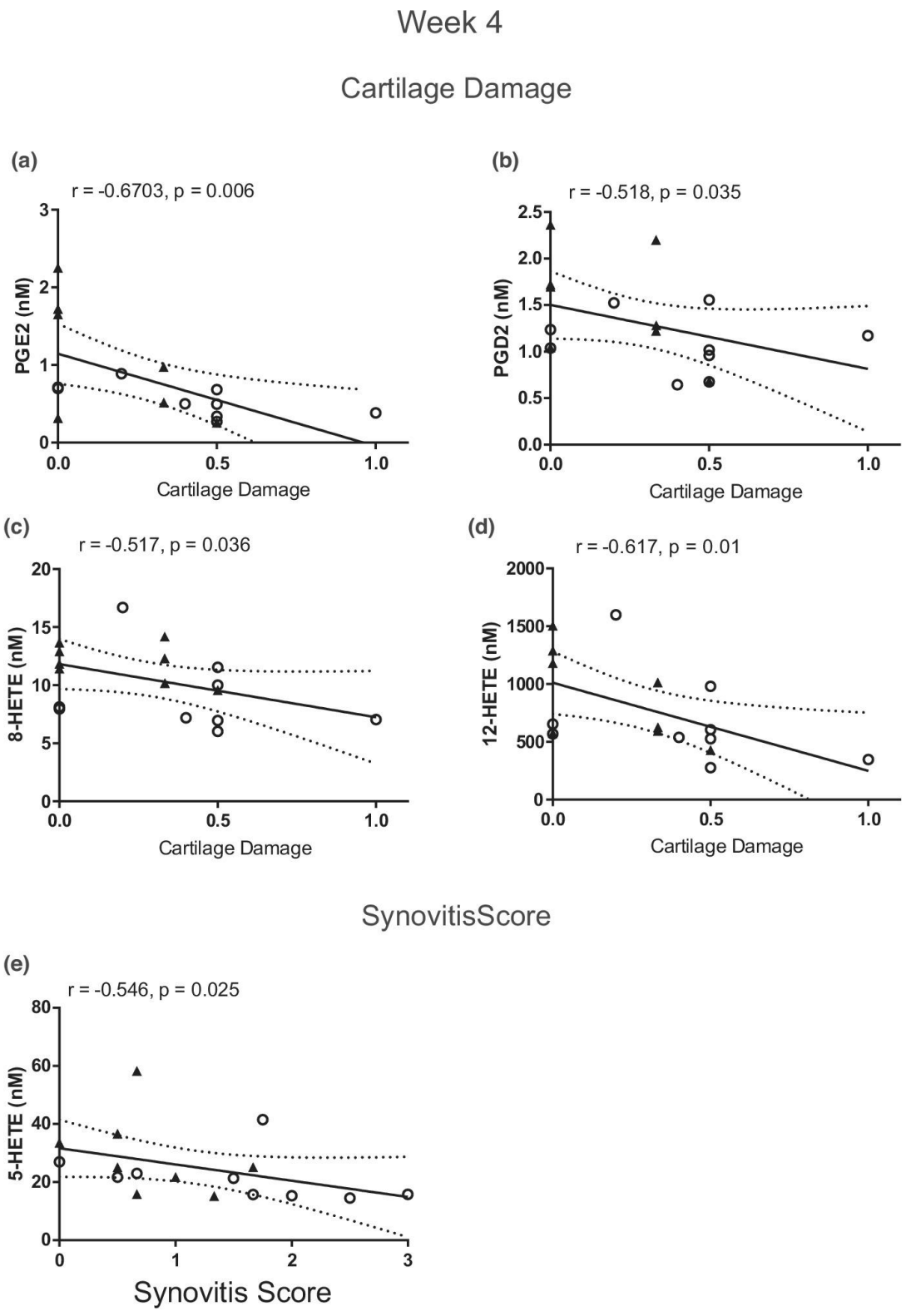

Figure 4. Correlation between cartilage damage and plasma concentrations of PGE2 (a), PGD2 (b), 8-HETE (c) and 12-HETE (d) in mice 4 weeks post-surgery. Correlation between synovitis score and plasma concentrations of 5-HETE (e) in mice 4 weeks post-surgery. The open circles represent DMM-operated mice, and the closed triangles represent sham-operated mice. Data analysed by Spearman's Rho.

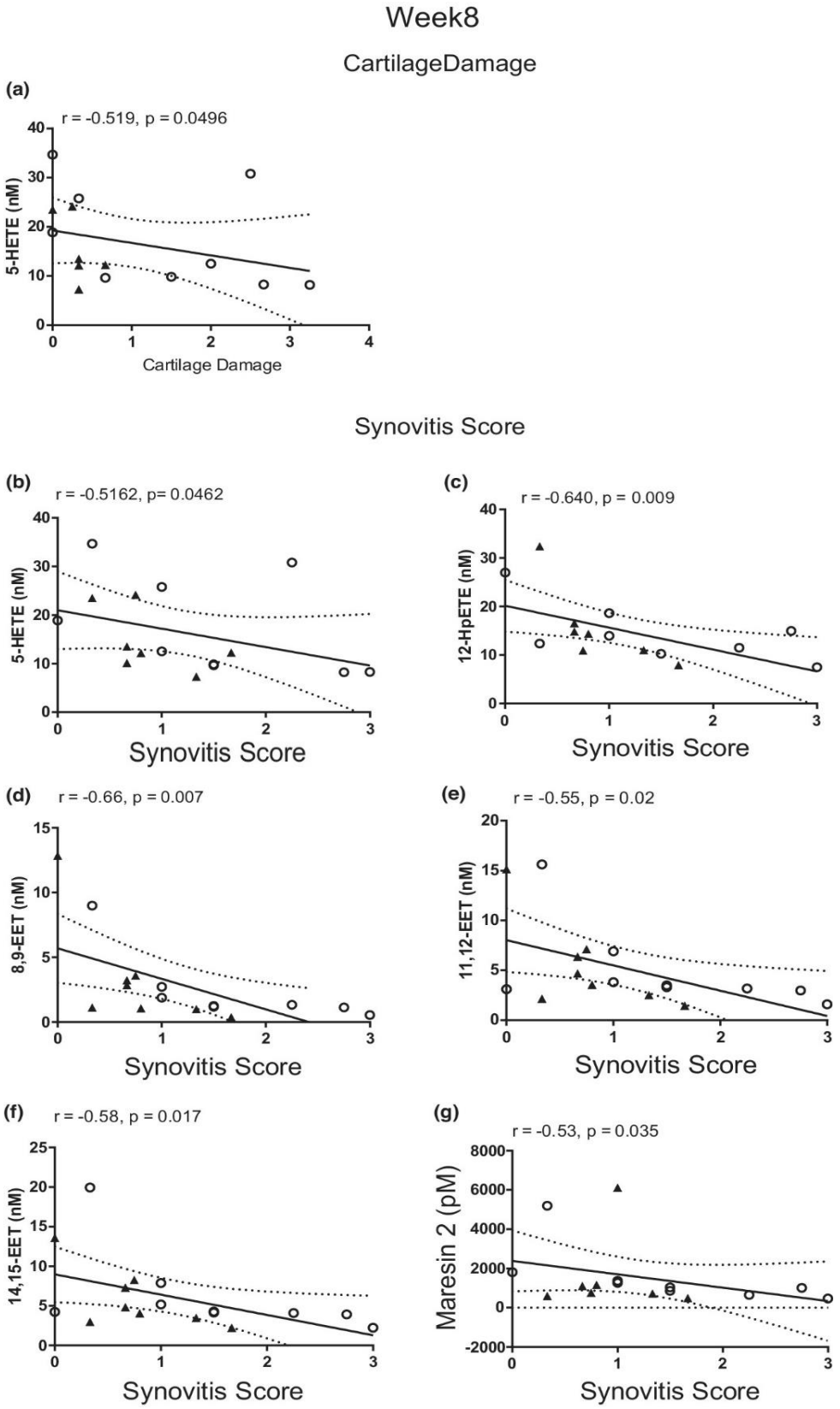

Figure 5. Correlation between cartilage damage and plasma concentrations of 5-HETE (a) at 8 weeks post-surgery. Correlation between synovitis score and plasma concentration of 5-HETE (b), 12-HpETE (c), 8,9-EET (d), 11,12-EET (e), 14,15-EET (f) and Maresin 2 (g) in mice 8 weeks post-surgery. The open circles represent DMM-operated mice, and the closed triangles represent sham-operated mice. Data analysed by Spearman's Rho.

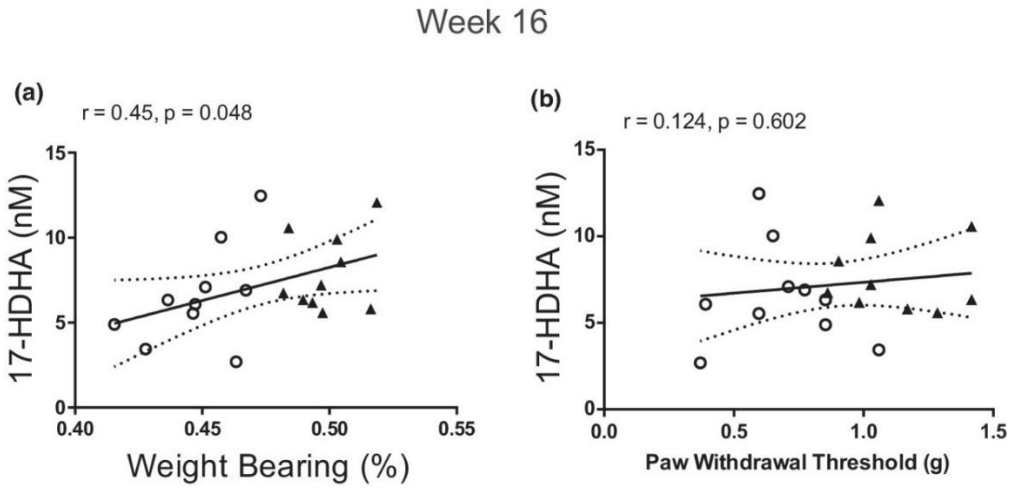

Figure 6. Correlation between weight-bearing asymmetry and plasma concentration of 17-HDHA (a) at 16 weeks post-surgery. Correlation between ipsilateral paw withdrawal thresholds and plasma concentrations of 17-HDHA (b) at 16 weeks post-surgery. The open circles represent DMM-operated mice and the triangles represent sham-operated mice. Data analysed by Spearman's Rho.

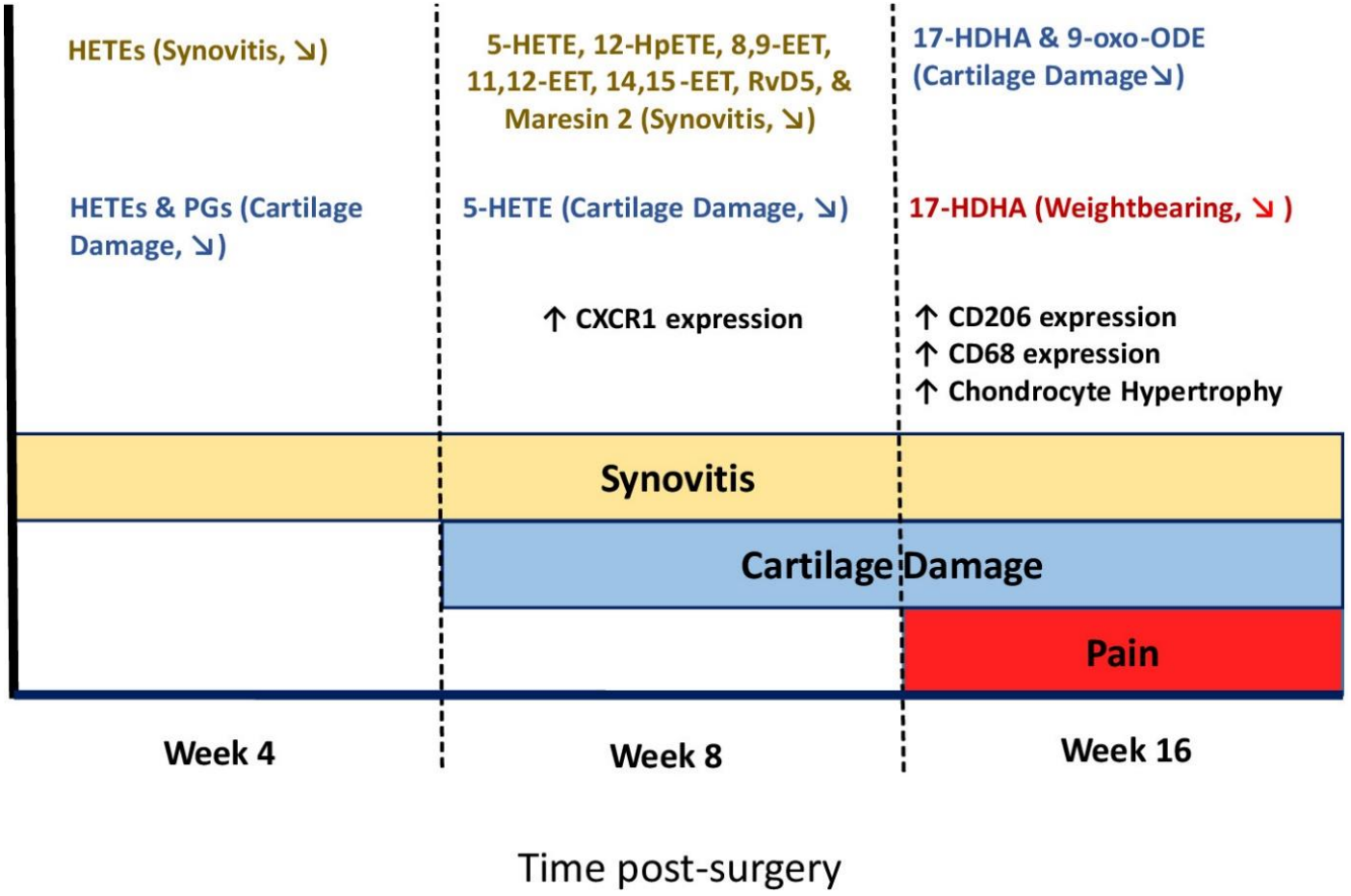

Figure 7. An illustration summarizing the changing relationships between circulating plasma lipids, joint pathology and pain behaviours in mice following DMM surgery. Synovial hyperplasia (yellow) was observed at all time-points post-surgery, cartilage damage (blue) was observed from 8 weeks post-surgery, and pain behaviours (red) were observed from 16-weeks post-surgery. The text in the illustration indicates which oxylipins were correlated with joint pathology, and/or pain behaviours at each time-point measured. The diagonal arrows indicate the direction of the correlation.

5.3.5 Targeting sEH in the DMM model

5.3.6 TPPU Reverses pain behaviour post IP injection in the DMM model of OA

This first dosing study aimed to investigate the effects of TPPU (3 mg/kg) in the DMM model when administered by IP injection. At week 16, animals were injected with vehicle (Sham, n=10, DMM, n=10) or TPPU (DMM, n=10) and their pain behaviour measured at one hour and three hours post injection. TPPU significantly reversed pain behaviour compared to measurements taken prior to injection for both weight bearing asymmetry and 50% paw withdrawal threshold (Figure 8).

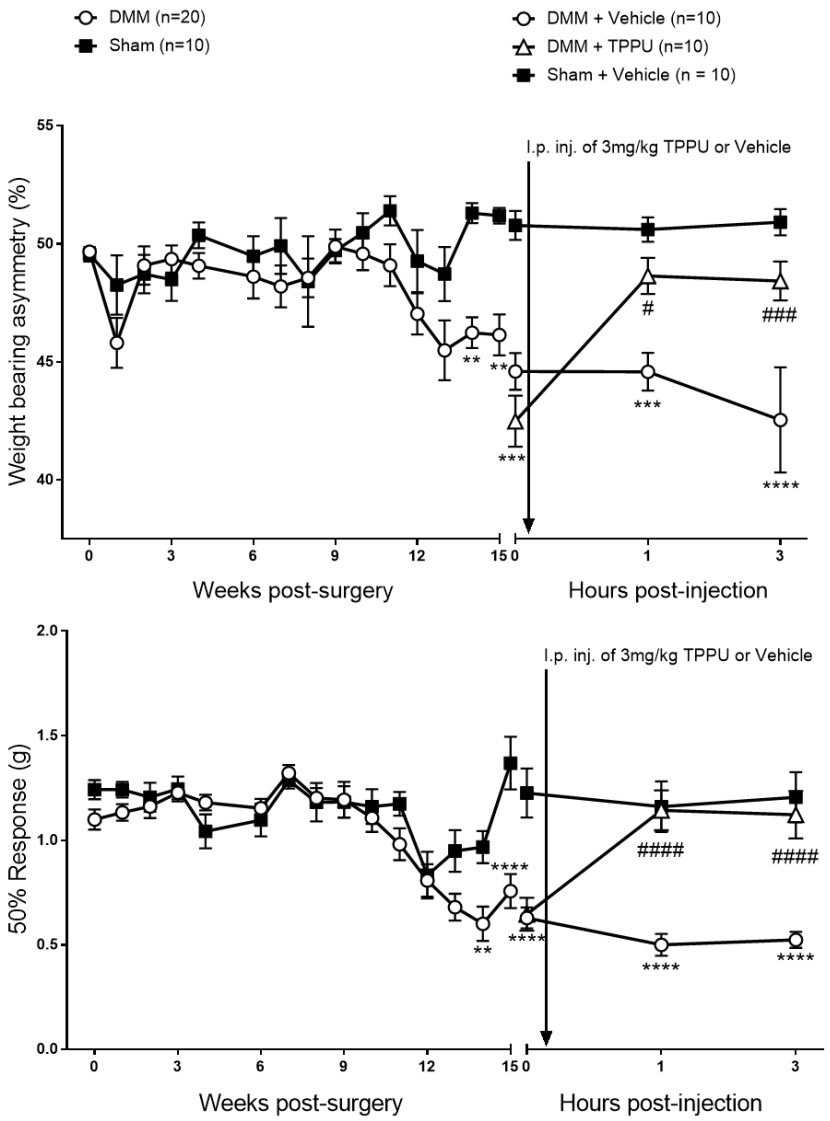

*Figure 8. Thirty adult male C57BL/6 mice underwent either DMM (n=20) or sham surgery (n=10). Data analysed by unpaired t-test, ** = p<0.01 sham vs DMM. The effects of i.p injection of TPPU (3mg/kg) or vehicle on weight-bearing asymmetry (A) and ipsilateral hind-paw withdrawal thresholds (B) were assessed at 16 weeks post-surgery. Final group sizes were DMM + Vehicle (n=10), DMM + TPPU (n=10), Sham + Vehicle (n=10). Data analysed by 2-way ANOVA with Bonferroni corrected multiple corrections, ** = p<0.01. *** = p<0.001, **** = p<0.0001 DMM + vehicle vs sham + vehicle, # = p<0.05, ### = p<0.001, #### = p<0.0001 DMM = vehicle vs DMM + TPPU.*

5.3.7 IP Injection of TPPU alters plasma levels of EETs, DHETs, and other bioactive lipids

At four hours post injection, animals were sacrificed and tissue samples were harvested. Blood plasma were also collected for measurement of circulating levels of EETs and DHETs and other lipid mediators by LC-MS/MS analysis. Figure 9 shows a representative LC-MS/MS chromatogram of a typical mouse plasma sample where EETs and DHETs can be separated by mass and retention time.

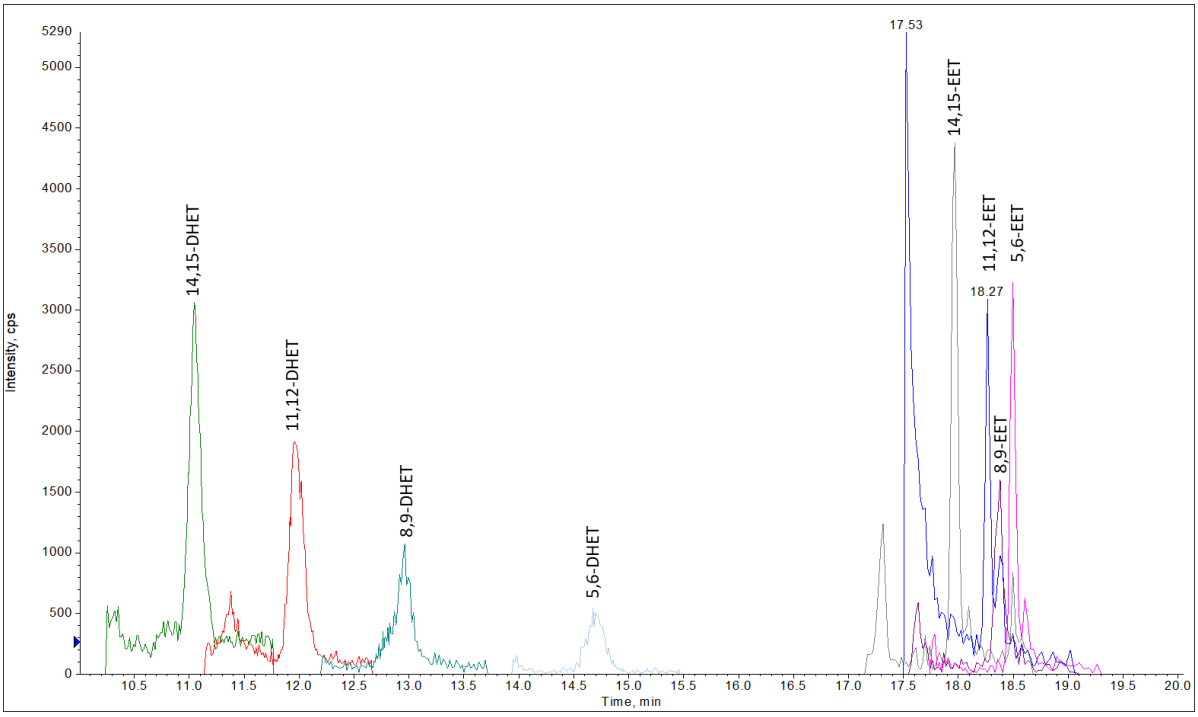

Figure 9. LC-MS/MS chromatogram of a mouse plasma sample, showing chromatographic separation of EETs and DHETs.

Levels of circulating EETs, DHETs, and their ratios were tabulated and assessed for significant changes by a two-way ANOVA in the DMM model of OA. It was found that levels of EETs were not altered between groups as expected but maintained a stable level across groups. Concentrations of 8,9-DHET (Figure 10A) and 14,15-DHET (Figure 10B) were significantly reduced in TPPU treated mice compared with vehicle treated controls. This decrease, along with the preserved levels of EETs means there was a significant increase in the EET:DHET ratios (Figure 10C-D).

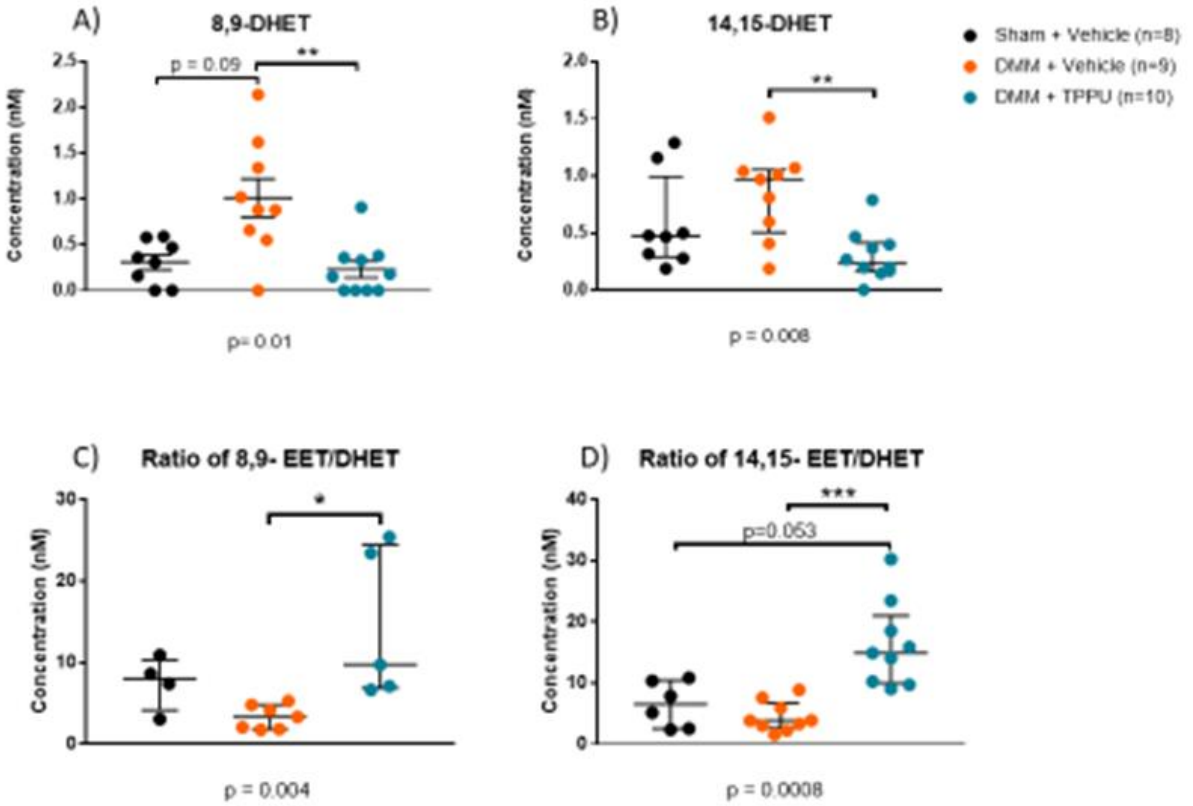

Figure 10. A) 8,9-DHET concentrations in Sham + Vehicle (n=8), DMM + Vehicle (n=9), & DMM + TPPU mice (n=10). B) 14,15-DHET concentrations in Sham + Vehicle (n=8), DMM + Vehicle (n=9), & DMM + TPPU (n=10) mice. C) Ratio of 8,9-EET/DHET ratio Sham + Vehicle (n=8), DMM + Vehicle (n=9), & DMM + TPPU (n=10) mice. D) Ratios of 14,15-EET/DHET in Sham + Vehicle (n=8), DMM + Vehicle (n=9), & DMM + TPPU (n=10) mice. Significance assessed by two way ANOVA.

Oxylipins from other pathways were also measured in plasma from the DMM study and assessed for significant changes. Decreases in levels of 11-HETE, 12-HETE, 17-HDHA, and AA in the DMM + TPPU group compared with DMM + Vehicle animals were observed (Figure 11). This adds to the evidence that sEH inhibition may have an influence over the concentration of bioactive lipids outside of the sEH pathway.

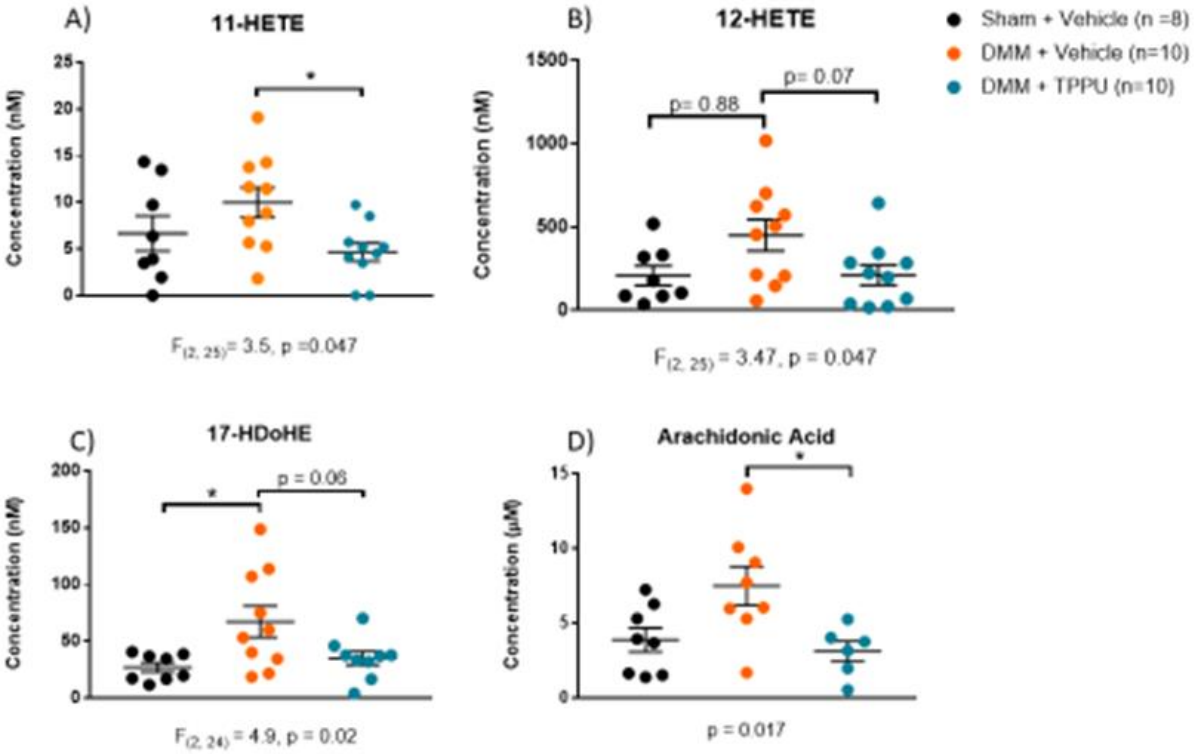

Figure 11 Lipids differentially expressed between groups: Sham + Vehicle (n=8), DMM + Vehicle (n=9) and DMM + TPPU (n=10) treatments. A) Differential expression of 11-HETE across groups. B) Differential expression of 12-HETE across groups. C) Differential expression of 17-HDHA across groups. D) Differential expression of arachidonic acid across groups. Significance assessed by two way ANOVA.

5.3.8 Repeated oral administration of TPPU shows sustained reversal of pain behaviour

During the dosing period, DMM surgery animals with access to TPPU showed significant and sustained reversal of weight bearing asymmetry (Figure 12A) and 50% paw withdrawal threshold (Figure 12B) compared with control DMM animals (Figure 10).

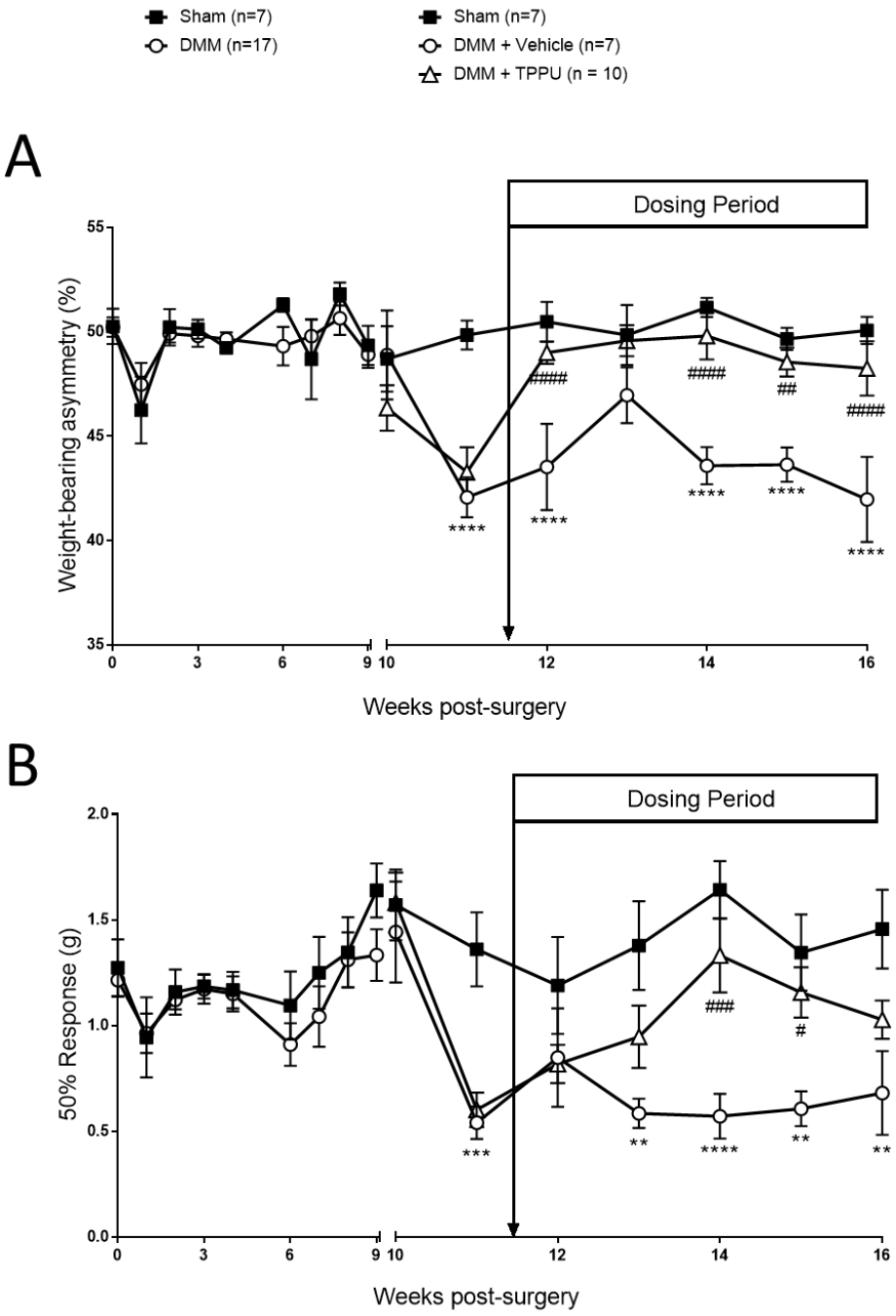

*Figure 12. Twenty-four adult male C57BL/6 mice underwent either DMM (n=17) or sham surgery (n=7). The effects of chronic administration of TPPU (3mg/kg/day) or vehicle in the drinking water on weight-bearing asymmetry (A) and ipsilateral hind-paw withdrawal thresholds (B) were assessed at 16 weeks post-surgery. The final group sizes were DMM + vehicle (n=7), DMM + TPPU (n=10), and Sham (n=7). Data analysed by 2-way ANOVA with Bonferroni corrected multiple corrections, ** = p<0.01. *** = p<0.001, **** = p<0.0001 DMM + vehicle vs sham + vehicle, # = p<0.05, ## = p<0.01, ### = p<0.001, #### = p<0.0001 DMM = vehicle vs DMM + TPPU.*

5.3.9 Repeated oral administration of TPPU increases the ratio of EETs to DHETs

Repeated oral administration of TPPU showed no effect on the circulating levels of EETs, which were comparable to vehicle treated animals. However, animals in the DMM + TPPU group had increased ratios of the EETs:DHETs, which were statistically significant for 8,9-EET:DHET and 14,15-EET:DHET compared with DMM + Vehicle animals (Figure 13). Interestingly there were no significant changes between TPPU or Vehicle treated animals that underwent sham surgery.

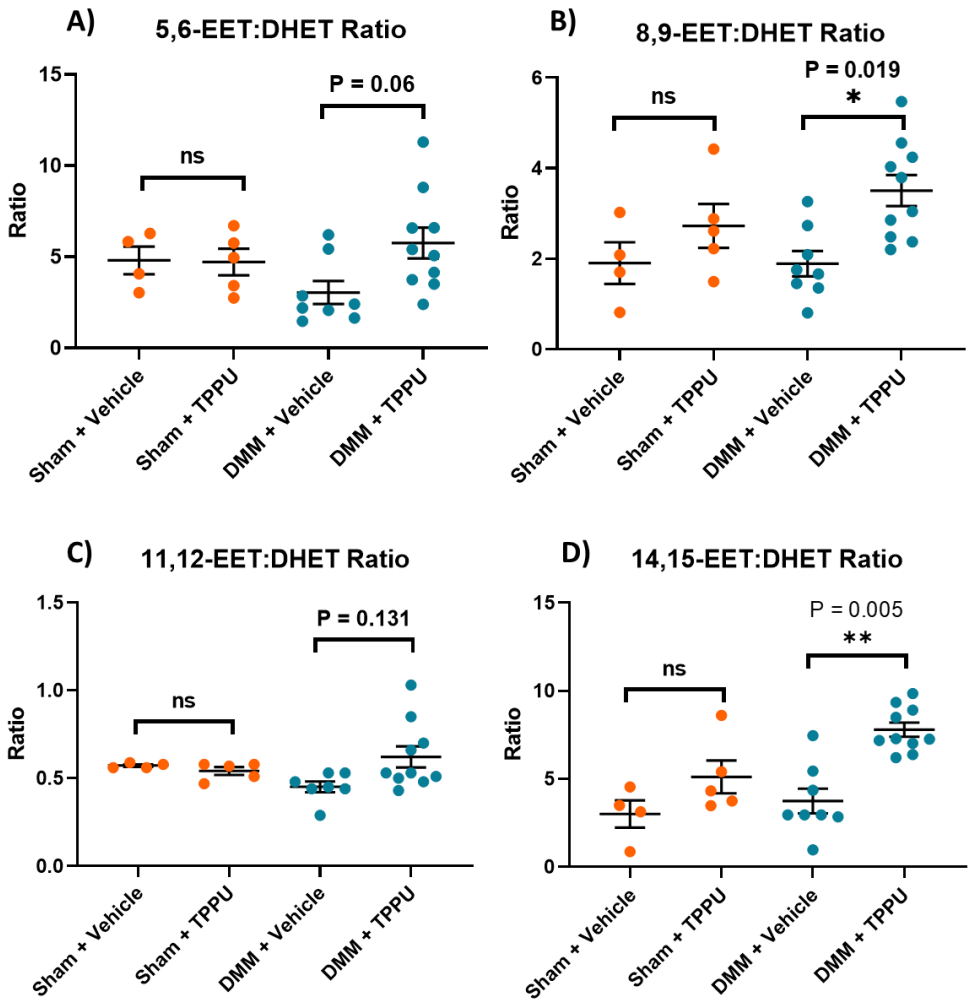

Figure 13. Levels of EETs and their corresponding were measured by LC-MS/MS and their ratios calculated DHETs A) 5,6-EET:DHET, B) 8,9-EET:DHET, C) 11,12-EET:DHET, D) 14,15-EET:DHET. Kruskal-Wallis tests were performed with multiple comparisons using Bonferroni corrections to assess changes between groups (Sham + Vehicle, n=4, Sham + TPPU, n=5, DMM + Vehicle, n= 8, and DMM + TPPU, n=10.

In this study, levels of other circulating lipids were not altered by repeated dosing of TPPU across any groups when analysed for significance using Kruskal-Wallis test with multiple comparisons (Table 2). Taken with the previous study, this could suggests that acute administration has a more widespread effect on the AA metabolites as a whole, but after repeated dosing these changes may stabilise.

Lipid	Sham + Vehicle			Sham + TPPU			DMM + Vehicle			DMM + TPPU			Correlation with pain phenotype			
	Mean Conc (nM)	±	SD	Mean Conc (nM)	±	SD	Mean Conc (nM)	±	SD	Mean Conc (nM)	±	SD	% Weight Bearing		Paw withdrawal threshold	
													R Value	P Value	R Value	P Value
5,6-EET	4.07	±	3.62	2.13	±	0.94	1.80	±	1.15	2.51	±	1.66	-0.121	0.549	0.158	0.432
5,6-DHET	0.91	±	0.89	0.51	±	0.28	0.62	±	0.15	0.41	±	0.17	-0.375	0.059	-0.100	0.626
5,6-Ratio	4.80	±	1.52	4.72	±	1.63	3.03	±	1.78	5.75	±	2.69	0.266	0.181	0.244	0.219
8,9-EET	1.87	±	1.08	1.62	±	0.84	1.53	±	0.28	1.51	±	0.62	-0.244	0.220	0.213	0.287
8,9-DHET	1.55	±	1.74	0.67	±	0.43	0.95	±	0.42	0.45	±	0.22	-0.453	0.020	-0.239	0.287
8,9-Ratio	1.90	±	0.92	2.72	±	1.08	1.89	±	0.79	3.50	±	1.08	0.217	0.278	0.233	0.239
11,12-EET	1.26	±	0.99	0.85	±	0.46	0.84	±	0.29	0.78	±	0.35	-0.204	0.318	0.016	0.242
11,12-DHET	2.17	±	1.69	1.52	±	0.73	1.67	±	0.52	1.24	±	0.49	-0.337	0.093	-0.012	0.938
11,12-Ratio	0.57	±	0.01	0.54	±	0.05	0.53	±	0.24	0.62	±	0.19	0.192	0.337	0.109	0.952
14,15-EET	2.66	±	1.25	2.54	±	1.20	2.49	±	0.45	2.39	±	0.91	-0.372	0.067	0.185	0.585
14,15-DHET	1.60	±	1.92	0.56	±	0.36	0.92	±	0.70	0.32	±	0.14	-0.171	0.395	-0.131	0.356
14,15-Ratio	3.01	±	1.54	5.11	±	2.09	3.74	±	1.98	7.79	±	1.26	0.189	0.344	0.135	0.532
17-HDHA	18.95	±	10.60	16.71	±	17.79	12.13	±	4.87	11.71	±	8.29	-0.067	0.739	0.061	0.762
TxB2	3.58	±	2.45	8.35	±	13.39	2.94	±	0.58	7.87	±	13.11	-0.166	0.408	0.127	0.526
PGE2	4.00	±	1.70	4.04	±	2.04	4.03	±	0.99	3.79	±	1.55	-0.267	0.178	0.179	0.192
PGD2	0.60	±	0.49	0.56	±	0.49	0.46	±	0.46	0.37	±	0.27	-0.165	0.410	0.259	0.371
5-HETE	1.85	±	1.66	1.12	±	0.60	1.28	±	0.55	1.09	±	0.52	-0.159	0.426	0.167	0.405
8-HETE	1.74	±	1.16	1.30	±	0.78	1.48	±	0.34	1.45	±	0.92	-0.216	0.280	0.159	0.428
9-HETE	0.91	±	0.86	0.43	±	0.22	0.63	±	0.46	0.46	±	0.27	-0.212	0.287	0.024	0.904
11-HETE	2.41	±	1.60	2.71	±	3.27	1.74	±	0.60	1.94	±	1.51	-0.088	0.663	0.082	0.683
12-HETE	217.59	±	141.42	166.90	±	153.40	188.33	±	86.30	227.12	±	187.80	-0.169	0.397	0.123	0.540
15-HETE	10.30	±	6.11	9.13	±	8.17	7.31	±	3.25	6.40	±	4.96	-0.054	0.787	0.093	0.645

Table 2. Mean values of circulating lipids with standard deviation for Sham + Vehicle, Sham + TPPU, DMM + Vehicle, and DMM + TPPU groups. R values and P values are also included for correlation analysis between each lipid and pain phenotype (all groups).

5.3.10 Correlations between lipid levels with pain phenotype and joint pathology in the DMM model (chronic dosing study).

To further explore the relationships between metabolites of the CYP450 and sEH pathway with pain phenotype, correlation analyses were performed to probe which analytes may be driving the analgesic properties of TPPU. These analyses included animals from all groups to give a range of pain phenotypes. The EETs were not correlated with either pain measurement. 8,9-DHET was significantly correlated with weight bearing asymmetry (Figure 14A) but not with 50% withdrawal thresholds (Figure 14B). Cartilage damage and synovitis were measured *ex vivo* to assess joint pathology. Although TPPU administration had no effect on joint pathology, the 8,9-EET:DHET ratio was correlated with both cartilage damage (Figure 14C) and synovitis (Figure 14D).

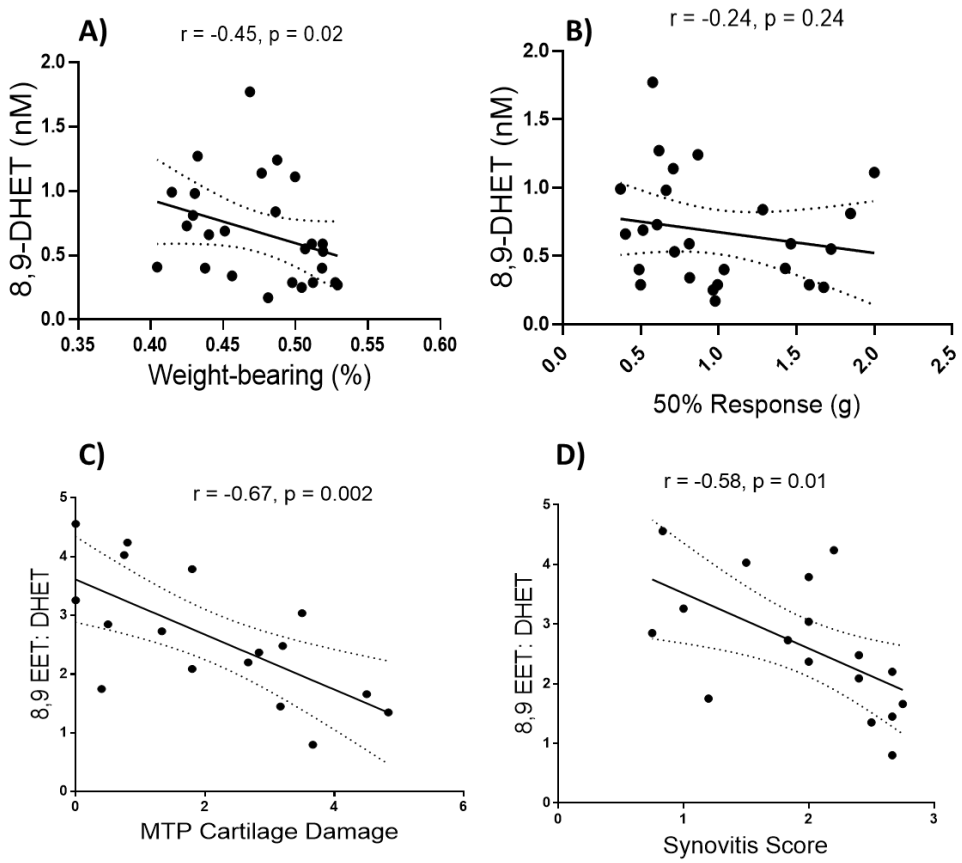

Figure 14. Levels of EETs, DHETs, and their Ratios were correlated against measured phenotypes using Pearson's correlation test. A) 8,9-DHET vs % Weight Bearing Asymmetry, B) 8,9-DHET vs 50% Paw Withdrawal Threshold, C) 8,9-EET:DHET Ratio vs MTP Cartilage Damage and D) 8,9-EET:DHET Ratio vs Synovitis Score.

5.4 Discussion

The profiling of the DMM model shows the complex changing picture of local and systemic inflammatory responses, joint pathology and pain behaviour in a murine model of OA. Sixteen weeks following DMM surgery, mice exhibited robust pain behaviour, including increased weight-bearing asymmetry, compared with sham controls. Increased weight-bearing asymmetry was significantly associated with lower plasma levels of the resolvin precursor 17-HDHA, this is consistent with previous findings from our group which identified an association between increased levels of 17-HDHA and thermal pain threshold in healthy volunteers (Valdes, Ravipati et al. 2017). At 8 weeks post-DMM surgery, before pain behaviour was evident, levels of the anti-inflammatory lipid mediators, the EETs and maresin-2, were negatively correlated with synovial hyperplasia, suggesting a possible relationship between inflammatory events in the joint and systemic inflammatory responses. The associations of lipid with features of the OA phenotype gives us confidence that the model is suitable for the study of OA. A key limitation of this work is that the model uses male mice only and is not yet established in female mice. This means there may be sex differences in the model, and that these results cannot be generalised to females. Future work is planned to establish the DMM model in female mice to address this limitation.

The data reported on targeting sEH show that TPPU does not increase levels of circulating EETs as hypothesised, however it does cause significant decreases in circulating levels of 8,9-DHET and 14,15-DHET as well as significant increase in the ratio of EETs to their diol metabolites. Epoxides 5,6-EET and 11,12-EET can also be metabolised by COX-2, which could explain why inhibition of sEH alone seems to affect these lipid levels to a lesser degree (Norwood, Liao et al. 2010) This observation makes us ask the question that if EET levels are unchanged by sEH inhibition, what are the molecular mechanisms behind the analgesic effect? Levels of EETs may be self-limiting, in that there may be a biological concentration at which EETs may inhibit their own production by CYP450, this could explain the stable levels of EETs that were seen. The ratios

of EETs:DHETs in TPPU vs Vehicle treated mice were only significantly increased in animals that received DMM surgery and not Sham surgery. This is a very interesting observation, the ratios of 5,6- and 11,12-EET:DHET appear to be the same level across both Sham groups, whereas 8,9- and 14,15-EE:DHET appear to be slightly increased in TPPU treated Sham animals compared with Vehicle treated animals. This could be explained simply in that the Sham + Vehicle group may be underpowered (n=4), or could suggest a more dependent effect of TPPU – were the levels of EETs and DHETs are only significantly altered where there is a painful or inflammatory stimuli.

Measuring the circulating levels of other bioactive lipid mediators in our assay alongside the EETs and DHETs show some curious results. In the DMM models, levels of lipid mediators other than metabolites of sEH pathway are altered in groups injected acutely with TPPU. Looking at the complexity of arachidonic metabolism, and the class shift throughout the inflammatory response it is likely that an equilibrium exists between pro and anti-inflammatory mediators. Data from the acute dosing of TPPU in the DMM model study give us further insight where levels of 11-HETE, 12-HETE, arachidonic acid, and 17-HDHA were reduced in TPPU treated animals compared with their DMM surgery controls. There is also a noticeable but non-significant increase of these analytes in DMM + vehicle compared to Sham + Vehicle animals. This suggests that the model itself causes an upregulation of these lipids and the increased ratio of EET:DHETs may reverse this effect, supporting the idea that sEH inhibitors exert a physiological response to drive tissue back to homeostasis. Altering the concentration of arachidonic acid alone would have widespread effects across the whole aracidonate pathways which include COX, LOX, and CYP450 pathways which generally are pro-inflammatory. Repeated dosing of TPPU did not show any altered levels of lipids outside of the sEH pathway. This could be explained by a gradual stabilisation of lipid levels over the dosing period. As the same level of analgesia is reached and sustained it suggests that the mechanisms by which the EETs and DHETs provide pain relief is not based on their altering of other lipid mediators. This supports previously reported data

from the Hammock group where that also see no tolerance to sEH inhibition (Wagner, Atone et al. 2020), and in a canine OA study where sEH inhibition also reduced pain behaviour. This study also performed *in vitro* cell viability assays of chondrocytes, where increased levels of EETs protected chondrocytes from inflammation induced cytotoxicity. It's suggested that EETs shielding properties here are mediated through decrease of IL-6 and TNFα, which in turn reduce inflammatory cytokine expression from chondrocytes in the joint (McReynolds, Hwang et al. 2019).

Inhibition of sEH by oral administration in our study does not significantly increase or decrease any other lipids measured. However to fully assess the specificity of TPPU, and to gain more understanding over biochemistry involved in sEH inhibition, it would be beneficial to measure other lipid products of sEH. The metabolism of linoleic acid derived epoxyoctadecenoic acids (EpOMEs) to dihydroxyoctadecenoic acis (DiHOMEs) (Yu, Hennebelle et al. 2019) may also be inhibited by TPPU, which means they could also play a part in the analgesic effect, however at the time of our studies there were no commercially available reference materials available for these analytes in the UK.

The studies reported here could suggest that DHETs may play a more important role in nociception than previously thought, and that decreases in their systemic levels by TPPU may provide analgesia. In particular, 8,9-DHET appears to be involved in both pain phenotype and joint pathology. This supports previously reported data from our group, where 8,9-DHET was correlated with radiographic progression of OA in human studies and (Valdes, Ravipati et al. 2018), and findings from Chapter Three where DHETs were associated with worse knee symptoms 2 years after acute knee injury. As 8,9-DHET is significantly decreased by TPPU, an interesting future study could look at the potential prophylactic effect of TPPU on joint pathology when dosed immediately after DMM surgery, particularly as the EETs are associated with synovial hyperplasia at 8 weeks post-surgery. It is interesting that 8,9-DHET is associated with weight bearing asymmetry and not 50% paw withdrawal threshold. This could indicate that there may be a local nociceptive effect

rather than of central sensitisation. Measurement of the EETs and DHETs in synovial fluid may provide further insight for their local roles in pain phenotype and joint pathology.

The studies detailed here show that TPPU dosed in both an acute and chronic manner, reverses pain behaviour in an established model of OA pain. This analgesic effect is sustained throughout repeated oral administration with no evidence of tolerance or adverse side effects. Measured levels of EETs remained unchanged upon treatment with TPPU, however the plasma concentrations of 8,9-DHET and 14,15-DHET were significantly reduced whereas EET:DHET ratios of 8,9- and 14,15- were significantly increased. We found significant correlations between 8,9-DHET with weight bearing asymmetry but not with paw withdrawal threshold suggesting a local nociceptive effect. Furthermore the 8,9-EET:DHET ratio was significantly associated with cartilage damage and synovitis in the joint which supports data reported from human studies. Chronic administration of TPPU did not significantly alter any of the other lipid mediators measured using our LC-MS/MS assay. These data suggest targeting the sEH enzymatic pathway to be an exciting and promising target for treating osteoarthritis pain. As these studies came to an end, another sEH inhibitor (EC5026) developed out of UC Davis' lab gained FDA approval for phase I human clinical trials late 2019 for treatment of chronic pain – this is a significant step toward assessing the efficacy of targeting sEH for treating a range of chronic diseases.

Chapter Six

Profiling of serum oxylipins in hospitalised COVID-19 patients

Acknowledgements

The work in this chapter was performed during the height of the COVID-19 pandemic, while the UK was in strict lockdown. During this time, my PhD work on OA and pain was put on hold, however due to the significant role of oxylipins in inflammation and immunity, I was able to conduct this study on samples collected from people hospitalised with COVID-19 in the QMC in Nottingham. This study was conducted in collaboration with colleagues in virology who provided clinical samples, anonymised clinical data, and data on immune response (Alex Tarr, Will Irving, and Paddy Tighe). I would like to thank Rakesh Jha for his help with the extraction and data analysis for this study, particularly the MVA. I would also like to thank the participants for their consent in using these clinical samples for research.

Data from this chapter have been peer reviewed and reported in the following manuscript:

James Turnbull, Rakesh Jha, Catherine A. Ortori, Eleanor Lunt, Patrick J. Tighe, William L. Irving, Sameer A. Gohir, Dong-Hyun Kim, Ana M. Valdes, Alexander W. Tarr, David A. Barrett, Victoria Chapman. **Serum levels of pro-inflammatory lipid mediators and specialized pro-resolving molecule pathways are greatly increased in SARS-CoV-2 patients and correlate with markers of the adaptive immune response.** Journal of Infectious Diseases. 2022. DOI: 10.1093/infdis/jiab632

Abstract

Infection with severe acute respiratory syndrome coronavirus 2 (SARS-CoV-2) is characterized by fever and cough, with more severe cases developing acute respiratory distress, acute lung injury, pneumonia, and mortality. A key driving force behind severe SARS-CoV-2 infection is uncontrolled inflammation. Specialized pro-resolution molecules (SPMs) halt the transition to chronic pathogenic inflammation. We aimed to quantify serum levels of pro- and anti-inflammatory bioactive lipids in severe acute respiratory syndrome coronavirus 2 (SARS-CoV-2) patients, and to identify potential relationships with innate responses and clinical outcome. Serum from 50 hospital admitted inpatients (22 female, 28 male) with confirmed symptomatic SARS-CoV-2 infection and 94 age- and sex-matched controls collected prior to the pandemic (SARS-CoV-2 negative), were processed for quantification of bioactive lipids and anti-nucleocapsid and anti-spike quantitative binding assays. SARS-CoV-2 serum had significantly higher concentrations of omega-6-derived proinflammatory lipids and omega-6- and omega-3-derived SPMs, compared to the age- and sex-matched SARS-CoV-2-negative group, which were not markedly altered by age or sex. There were significant positive correlations between SPMs, proinflammatory bioactive lipids, and anti-spike antibody binding. Levels of some SPMs were significantly higher in patients with an anti-spike antibody value >0.5. Levels of linoleic acid and 5,6-DHET were significantly lower in SARS-CoV-2 patients who died. SARS-CoV-2 infection was associated with increased levels of SPMs and other pro- and anti-inflammatory bioactive lipids, supporting the future investigation of the underlying enzymatic pathways, which may inform the development of novel treatments.

6.1 Introduction

Infection with severe acute respiratory syndrome coronavirus 2 (SARS-CoV-2) is characterised by fever and cough, with more severe cases developing acute respiratory distress, acute lung injury, pneumonia, and mortality (Fan, Beitler et al. 2020, Wu, Chen et al. 2020, Yang, Yu et al. 2020). The higher rates of severe SARS-CoV-2 illness and death are associated with increasing age (Ho, Petermann-Rocha et al. 2020, Jayaraj, Kumarasamy et al. 2020). SARS-CoV-2 infection is associated with changes in adaptive and innate immunity, including elevated levels of circulating neutrophils and the presence of peripherally derived macrophages in the lungs of severe cases (Merad and Martin 2020, Zhand, Saghaeian Jazi et al. 2020), reduced numbers of circulating T cells (Kenneth, Monty et al. 2021) and robust cytokine responses, which continues after clearance of the virus (Blanco-Melo, Nilsson-Payant et al. 2020). SARS-CoV-2 infection is associated with elevated levels of pro-inflammatory cytokines, including IL6, IL1β, and TNFα (Huang, Wang et al. 2020, Karaba, Jones et al. 2021), however levels of anti-inflammatory cytokines IL4 and IL10 are also elevated (Huang, Wang et al. 2020). Knowledge of the impact of SARS-CoV-2 infection on the resolution of inflammation pathways will provide crucial new mechanistic insight and potential new avenues for treatment (Panigrahy, Gilligan et al. 2020, Regidor, Santos et al. 2020, Tang, Liu et al. 2020).

Prostaglandins (PGs) and leukotrienes have essential roles in initiating acute inflammatory responses and the generation of pro-inflammatory cytokines, which sustain chronic inflammatory responses. In concert with these cyclooxygenase (COX) pathways, the lipoxygenase (LOX) pathways produce pro-inflammatory hydroxyeicosatetraenoic acids (HETEs) from arachidonic acid (AA) and hydroxyoctadecadienoic acids (HODEs) from di-homo-γ-linolenic acid (LNA). The active curtailing of inflammatory signalling is essential to restore tissue homeostasis and prevent chronic inflammatory events leading to pathology (Serhan and Levy 2018). Following the initial acute inflammatory phase, specialised pro-resolving molecules (SPMs), derived from key polyunsaturated fatty acids (PUFAs), are generated and orchestrate the resolution of inflammation by promoting macrophage mediated clearance of cellular debris and counteracting the effects of pro-inflammatory cytokines (Serhan and Levy 2018). The SPMs are derived from omega-6 (ω-6) (LNA, AA) or omega-3 (ω-3)

(eicosapentaenoic acid (EPA), docosahexaenoic acid (DHA)) substrates via the COX, LOX and cytochrome P450 pathways (Serhan and Levy 2018).

The most well characterised SPMs are the resolvins (Rvs), protectins (PDs), and maresins (MaRs), which halt the transition from acute to chronic inflammation preventing pathogenesis (Basil and Levy 2016). 17(S)-hydroxy Docosahexaenoic acid (17-HDHA), a substrate for the generation of the D series resolvins (Serhan and Levy 2018), enhances the adaptive immune response in a preclinical model of influenza(Ramon, Baker et al. 2014), both 17-HDHA and resolvin D1 enhance B cell production and promote B cell differentiation towards an antibody secreting phenotype (Ramon, Gao et al. 2012)). The epoxyeicosatrienoic acids (EETs), derived from AA via soluble epoxide hydrolase (sEH), also mediate resolution of inflammation (Tam, Quehenberger et al. 2013, Romashko, Schragenheim et al. 2016), down-regulating inflammatory transcription factors such as NF-kB (Dong, Dong et al. 2017), curtailing the induction of COX2 and production of cytokines (Bora, Steven et al. 2008).

Current knowledge of the consequences of SARS-CoV-2 infection on endogenous levels of SPMs and EETs is in its infancy. Building a comprehensive picture of the impact of SARS-CoV-2 infection upon the serum lipidomic profile will aid understanding of the therapeutic potential of resolution pathways for SARS-COV-2 infection (Darwesh, Bassiouni et al. 2020, Panigrahy, Gilligan et al. 2020, Regidor, Santos et al. 2020).

The aims were to 1) compare serum levels of a range of SPMs and pro-inflammatory bioactive lipids between patients admitted to hospital with SARS-CoV-2 infection and an age-matched control group, 2) determine the potential relationship between levels of these bioactive lipids and levels of anti-nucleocapsid and anti-spike antibody titre, markers of the production of an adaptive immune response (Tighe, Urbanowicz et al. 2020) and 3) investigate outcomes following infection.

6.2 Methods

6.2.1 Sample Collection and Preparation

Serum samples obtained from 50 inpatients admitted to Nottingham University Hospitals NHS Trust Queen's Medical Centre with symptomatic RT-PCR confirmed SARS-CoV-2 infection were collected as diagnostic specimens for clinical chemistry testing, excess sera were provided anonymously for research purposes. Review by the University of Nottingham's School of Life Sciences Ethical Review Committee deemed the study to not require full ethical review. Approval for use of anonymized clinical data was provided by the NHS Health Research Authority (HRA) and Health and Care Research Wales (HCRW) (ref. 20/HRA/4843). Samples were determined not to be Relevant Materials in line with the Human Tissue Authority. Risk assessments were approved by the UK Health and Safety Executive (ref. CBA1.470.20.1). Viral genomic sequencing of samples from a subset of these patients was performed as part of the COG-UK consortium (consortium 2020).

Baseline serum samples from the iBEAT-OA cohort study (n=94) were used as age and sex matched controls (Gohir, Greenhaff et al. 2019), which were collected prior to the SARS-CoV-2 pandemic served as a SARS-CoV-2 negative control. As collected pre-pandemic a lack of SARS-CoV-2 infection was not confirmed. The iBEAT-OA cohort had a confirmed diagnosis of osteoarthritis. Ethical approval was obtained from the University of Nottingham's Research Ethics Committee (ref: 18/EM/0154) and the NHS East Midlands (Nottingham) Health Research Authority (protocol no: 18021).

6.2.2 Lipidomic Analysis

Lipidomic analysis was performed using the methods detailed in chapter 2. Samples were extracted and analysed in a single batch alongside (n=12) QC samples.

6.2.3 Anti-Nucleocapsid & Anti-Spike Binding Assays

Anti-nucleocapsid and anti-spike quantitative binding assays were performed on serum samples using ELISA following the protocol described by Tighe et al (2020) (Tighe, Urbanowicz et al. 2020). Levels of C reactive protein (CRP) were measured in clinical diagnostic tests (mean 172.9 levels ranged from 11-489). The median time between sample collection for CRP

measurement and collection of serum for the measurement of bioactive lipids, anti-nucleocapsid and anti-spike antibody binding was 5 days.

6.2.4 Data Analysis

GraphPad Prism (Version 8.2.1) was used. In some cases, patients were stratified into three age groups (<60, 61-74, & >75 years). Groups were assessed for normal distribution using D'Agostino & Pearson test and evaluated for significant changes between groups using Kruskal-Wallis test with multiple comparisons corrected for using Dunn's test. Multivariate analysis using Metaboanalyst 4.0 (https://www.metaboanalyst.ca/)(Chong and Xia 2020) including principal component analysis (PCA) was performed. Partial least square discrimination analysis (PLS-DA) was used to identify the lipid mediator clusters. A cross validation analysis was used to validate the PLS-DA model based on accuracy, R2 and Q2 scores and a permutation test. Variable Importance in Projection (VIP) scores greater than 1 were recognized as playing a key role in cluster differentiation (Figure 4).

6.3 Results

6.3.1 Characteristics of SARS-COV-2 infection cohort and clinical features

Serum samples collected from hospital inpatients (22 female, 28 male) with confirmed diagnosis of Sars-CoV-2 (SARS-CoV-2) were studied. 30 patients recovered and were discharged, 20 died, and 25 spent time in ICU during hospitalisation (Table 1).

Table 1. Clinical characteristics of SARS-CoV-2 and control cohorts.

Clinical Characteristic	Sars-CoV-2 Negative	Sars-CoV-2
Total (n)	91	50
Sex (M/F)	30/61	28/22
Age (Mean, Range)	67 (45-85)	69.3 (35-91)
Comorbidities (n,%):		
Arthritis	65 (72%)	9 (18%)
Hypertension	19 (21%)	18 (36%)
Asthma	13 (14%)	5 (10%)
Diabetes	5 (6%)	12 (24%)
Cancer	2 (2%)	9 (18%)
Cardiac disease	2 (2%)	10 (20%)
Transient Ischaemic Attack	-	4 (8%)
Kidney disease	1 (1%)	12 (24%)
NEWS2 Score (Mean, Range)	-	6 (0-12)
Oxygen Saturation (Mean, Range)	-	94 (65-100)
Respiratory Rate (Mean, Range)	-	26 (14-65)
Temperature (Mean, Range)	-	37 (34.1-39.4)
Days between diagnosis & sample collection (Mean, Range)	-	7 (0-21)
Outcome (Recovered/Died)	-	30/20
Admitted to ICU (Y/N)	-	25/25
Required Mechanical Ventilation (Y/N)		26/23
CRP (Mean, Range)	-	172.9 (11-489)
Anti-nucleocapsid binding (Mean, Range)	-	1.81 (0.12-3.1)
Anti-spike binding (Mean, Range)	-	0.939 (0.115-3.067)

6.3.2 SARS-COV-2 serum has a distinct bioactive lipid profile

SARS-CoV-2 serum had high concentrations of ω-6 derived pro-inflammatory lipids (Table 2) and ω-6 and ω-3 derived anti-inflammatory SPM lipids (Table 2), which were significantly increased compared to age and sex matched control serum. In control serum, comparable to the healthy population, many of the anti-inflammatory SPM lipids were not detectable, or present at very low levels (Norris, Skulas-Ray et al. 2018).

Table 2. Concentrations of pro-inflammatory and anti-inflammatory bioactive lipids quantified in SARS-CoV-2 (n=50) and age and sex matched controls (n=94). Statistical analysis by Mann-Whitney Test. Where lipids were not detected in samples, an arbitrary value of 0.001 indicated by + was used for statistical analysis.

Bioactive lipids			Mean Concentration (nM) ± SD						P Value
			Control (n=94)			Sars-COV-2 (n=50)			
AA	Pro-inflammatory	µM (±SD)	47.98	±	12.75	99.61	±	60.21	<0.0001
LA			307.8	±	109.7	213.79	±	108.4	<0.001
5-HETE		nM (±SD)	0.99	±	0.40	158.33	±	159.17	<0.0001
8-HETE			0.81	±	0.57	3.52	±	3.32	<0.0001
9-HETE			0.15	±	0.05	16.27	±	19.02	<0.0001
11-HETE			1.77	±	1.34	19.84	±	19.95	<0.0001
12-HETE			160.89	±	127.54	162.41	±	137.29	0.651
15-HETE			7.14	±	4.79	135.18	±	125.42	<0.0001
16-HETE			0.20	±	0.05	0.22	±	0.08	0.4442
19-HETE			0.37	±	0.29	188.65	±	199.17	<0.0001
20-HETE			1.04	±	0.56	69.80	±	54.66	<0.0001
TXB2			21.66	±	20.33	63.20	±	80.40	<0.0001
11-dehy-TXB2			1.10	±	1.47	0.29	±	0.33	0.0001
PGE2			0.37	±	0.33	0.56	±	0.41	0.0033
PGD2			0.001+			1.12	±	1.34	<0.0001
LTB4			0.52	±	0.72	5.30	±	0.67	<0.0001
13-oxoODE			6.82	±	5.45	25.85	±	32.33	0.0001
9-oxoODE			0.85	±	0.96	7.51	±	10.28	<0.0001
9-HODE			6.14	±	3.03	225.74	±	308.14	<0.0001
13-HODE			12.44	±	5.72	263.98	±	363.04	<0.0001
DHA	Anti-inflammatory	µM (±SD)	36.96	±	17.63	39.67	±	27.01	0.7135
EPA			37.26	±	4.72	26.13	±	21.59	<0.001
17-HDHA		nM (±SD)	1.88	±	1.46	88.61	±	107.3	<0.0001
14-HDHA			55.53	±	54.4	93.11	±	69.82	0.0006
18-HEPE			0.49	±	0.32	10.27	±	14.16	<0.0001
RvD4			0.001+			4.11	±	3.94	<0.0001
Maresin 2			0.03	±	0.01	0.42	±	0.48	<0.0001
LXA4			0.001+			2.29	±	3.15	<0.0001
LXA5			0.001+			0.52	±	0.60	<0.0001
5,6-EET			0.24	±	0.38	0.30	±	0.29	<0.0001
5,6-DHET			0.38	±	0.21	2.35	±	1.73	<0.0001
5,6-Ratio			0.60	±	0.72	0.21	±	0.24	<0.0001
8,9-EET			0.21	±	0.21	0.74	±	0.88	<0.0001
8,9-DHET			0.22	±	0.07	0.47	±	0.32	<0.0001
8,9-Ratio			0.97	±	0.86	2.63	±	4.09	0.0098
11,12-EET			0.56	±	0.77	160.95	±	122.47	<0.0001
11,12-DHET			0.53	±	0.16	0.60	±	0.32	0.315
11,12-Ratio			1.09	±	1.31	363.01	±	407.70	<0.0001
14,15-EET			0.27	±	0.35	0.43	±	0.44	<0.0001
14,15-DHET			0.43	±	0.14	0.52	±	0.27	0.0672
14,15-Ratio			0.68	±	0.74	0.90	±	0.73	0.0002
2-AG			40.8	±	28.3	726.1	±	454.9	<0.0001
AEA			1.80	±	0.39	1.60	±	0.77	0.009
OEA			7.44	±	1.92	37.25	±	15.84	<0.0001
PEA			37.53	±	51.68	29.58	±	29.82	0.079

PLS-DA analysis of these lipids identified contributors to the separation between the SARS-CoV-2 and control serum (Figure 1A). 22 lipids from seven classes of lipids had a VIP score >1 and statistically underpinned the separation between the two clusters. Although serum concentrations of the PUFAs (LA, EPA and DHA) were generally not different between the SARS-CoV-2 and control serum (Figure 1B), concentrations of the down-stream bioactive lipids were markedly increased in SARS-CoV-2 serum (Figure 1B). There were substantially higher levels of the pro-inflammatory molecule PGD2, and the anti-inflammatory SPMs (17-HDHA, RvD4, LXA4, LXA5), endocannabinoids (2-AG, AEA) and, 11,12-EET in SARS-CoV-2 serum, compared to control serum (Table 1). These findings support a profound mobilisation of pro-resolving mediators following SARS-CoV-2 infection.

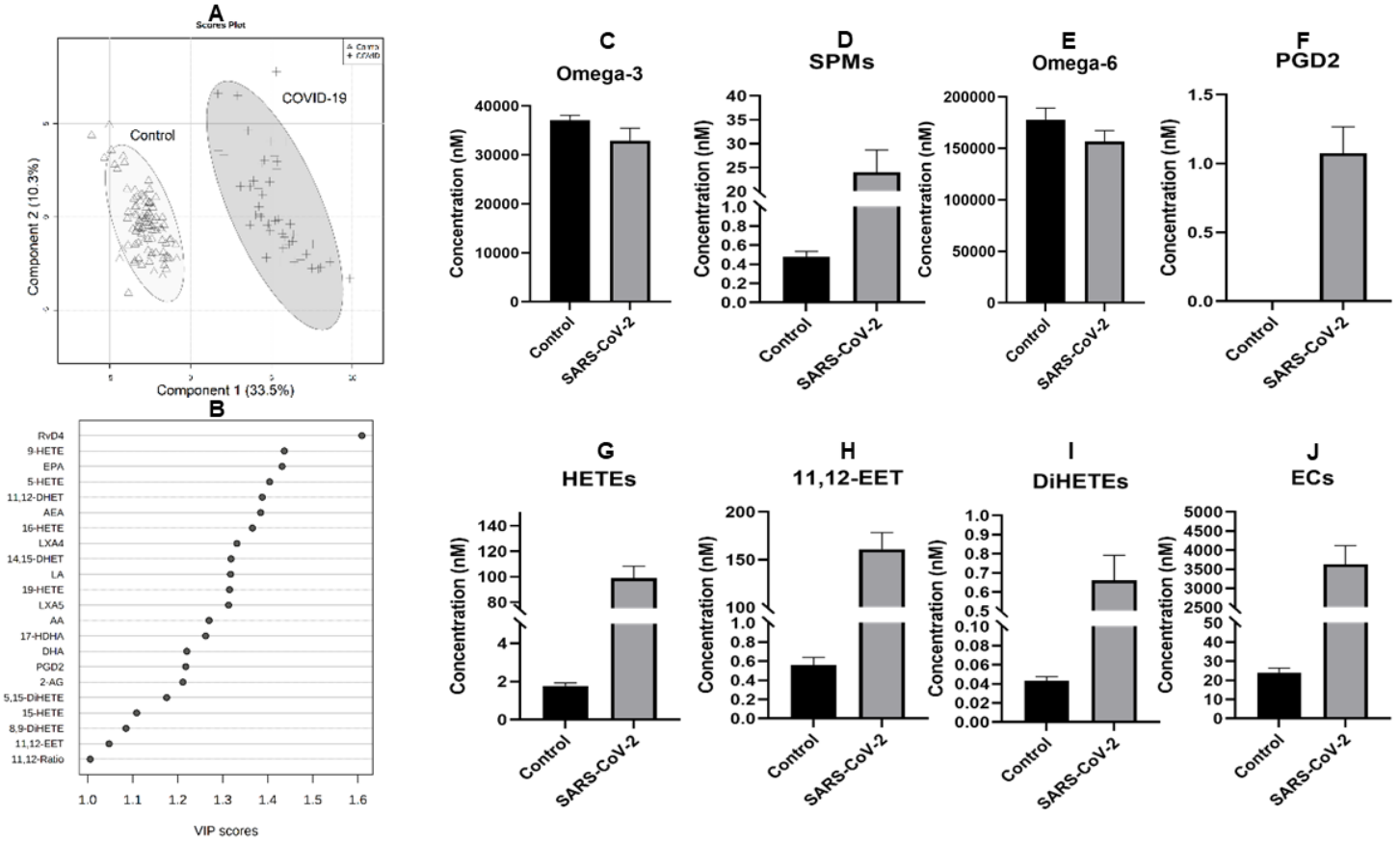

Figure 1. A, Partial least square discrimination analysis for the 44 serum lipids quantified in severe acute respiratory syndrome coronavirus 2 (SARS-CoV-2; n = 50) and age- and sex-matched controls (n = 94) with R2 = 0.944, Q2 = 0.932, and accuracy = 1.0. B, variable importance in projection (VIP) scores showing important lipid mediators (n = 22, VIP >1.0) involved in differentiation of the 2 groups (control vs SARS-CoV-2). C–J, Histograms of the highest-ranked lipid mediators, omega-3 polyunsaturated fatty acids (PUFAs; EPA, DHA), specialized proresolving molecules (17-HDHA, RvD4, LXA4, LXA5), omega-6 PUFAs (AA, LA), PGD2, HETEs (5-HETE, 9-HETE, 16-HETE, 19-HETE, 15-HETE), 11,12-EET, DiHETEs (5, 15-DiHETEs, 8, 9-DiHETEs), and endocannabinoids (2-AG, AEA). Lipid clusters are based on previously reported analysis [34]. Abbreviations: 2-AG, 2-arachidonoylglycerol; AA, arachidonic acid; AEA, N-arachidonoylethanolamine; COVID-19, coronavirus disease 2019; DHA, docosahexaenoic acid; DHET, dihydroxyeicosatrienoic acid; DiHETE, dihydroxyeicosatetraenoic acid; EC, endocannabinoids; EET, epoxyeicosatrienoic acid; EPA, eicosapentaenoic acid; HETE, hydroxyeicosatetraenoic acid; LA, linoleic acid; LXA4, Lipoxin A4; PGD2, prostaglandin D2; RvD4, resolvin D4; SARS-CoV-2, severe acute respiratory syndrome coronavirus 2; SPM, specialized proresolving molecules; VIP, variable importance in projection.

PLS-DA analysis revealed a clear separation between the SARS-CoV-2 and control serum for the three age groups (Figure 2A-C). Overall, the majority of the lipids contributing to the separation between the SARS-CoV-2 and control serum were the same for the three age groups studied (Figure 2D). This was confirmed by a univariate analysis (Figure 2). Overall, the ability to mount a pro-resolution response was not markedly altered by age in this study.

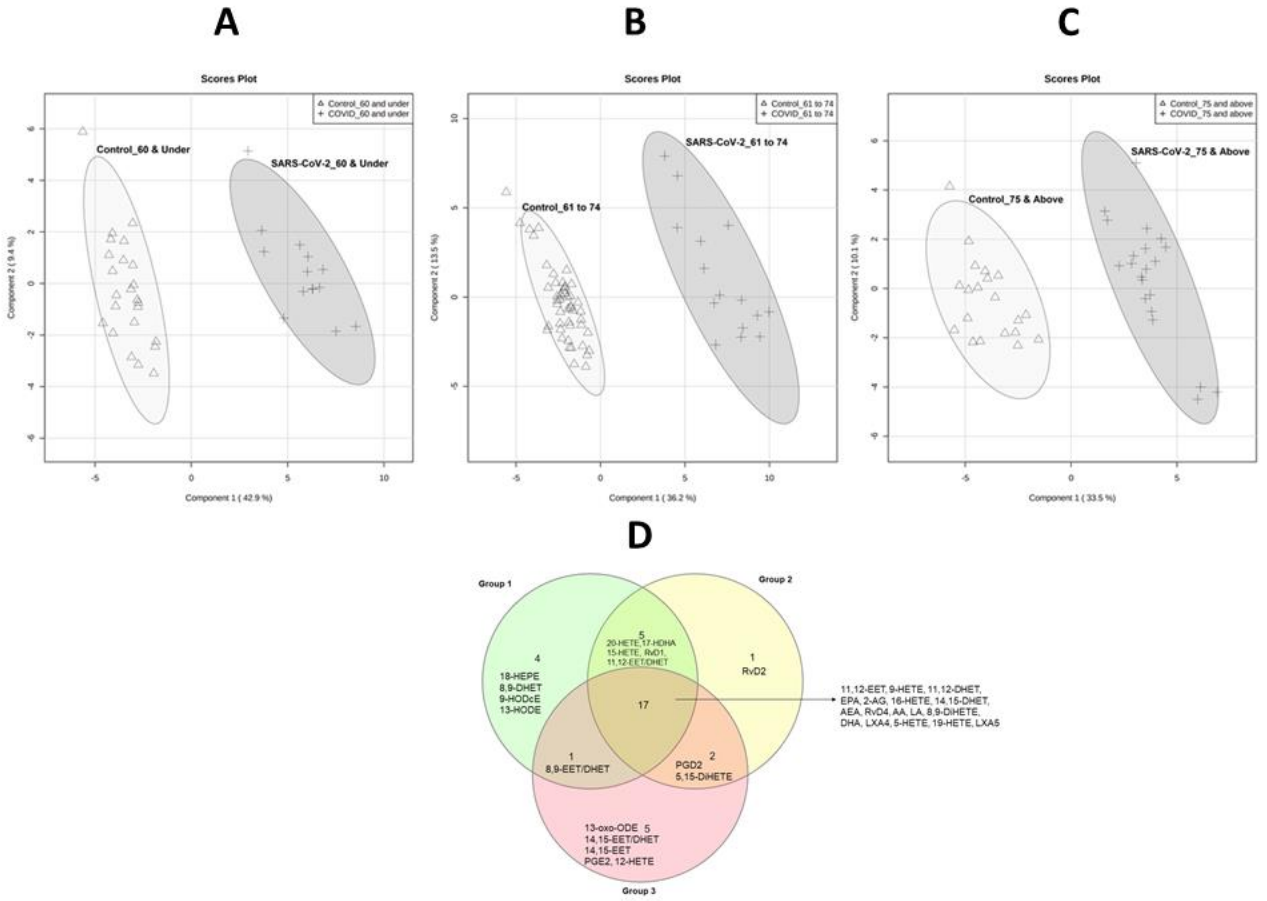

Figure 2. Partial least square discrimination analysis (PLS-DA) for the 44 serum lipids quantified in SARS-CoV-2 (n=50) and age and sex matched controls (n=94), stratified by age. A: Group 1 (60 and under) with R2 = 0.966, Q2 = 0.941 and Accuracy = 1.0; B: Group 2 (61 to 74) with R2 = 0.986, Q2 = 0.969 and Accuracy = 1.0; C: Group 3 (75 and above) with R2 = 0.952, Q2 = 0.928 and Accuracy = 1.0. D: Venn diagram showing the common versus unique lipid mediators obtained from PLS-DA analysis (VIP>1) of the age stratified samples.

Changes in the flux through enzymatic pathways generating SPMs may provide insight into novel treatments for Sars-CoV-2 infection. Serum levels of DHA and the downstream metabolites, 17-HDHA and 14-HDHA, were correlated in both SARS-CoV-2 and control serum (Figure 3A-B). However, levels of EPA and 18-HEPE were correlated in SARS-CoV-2 serum but not control serum, suggesting a potential upregulation of the E series resolving pathway following infection (Figure 3C).

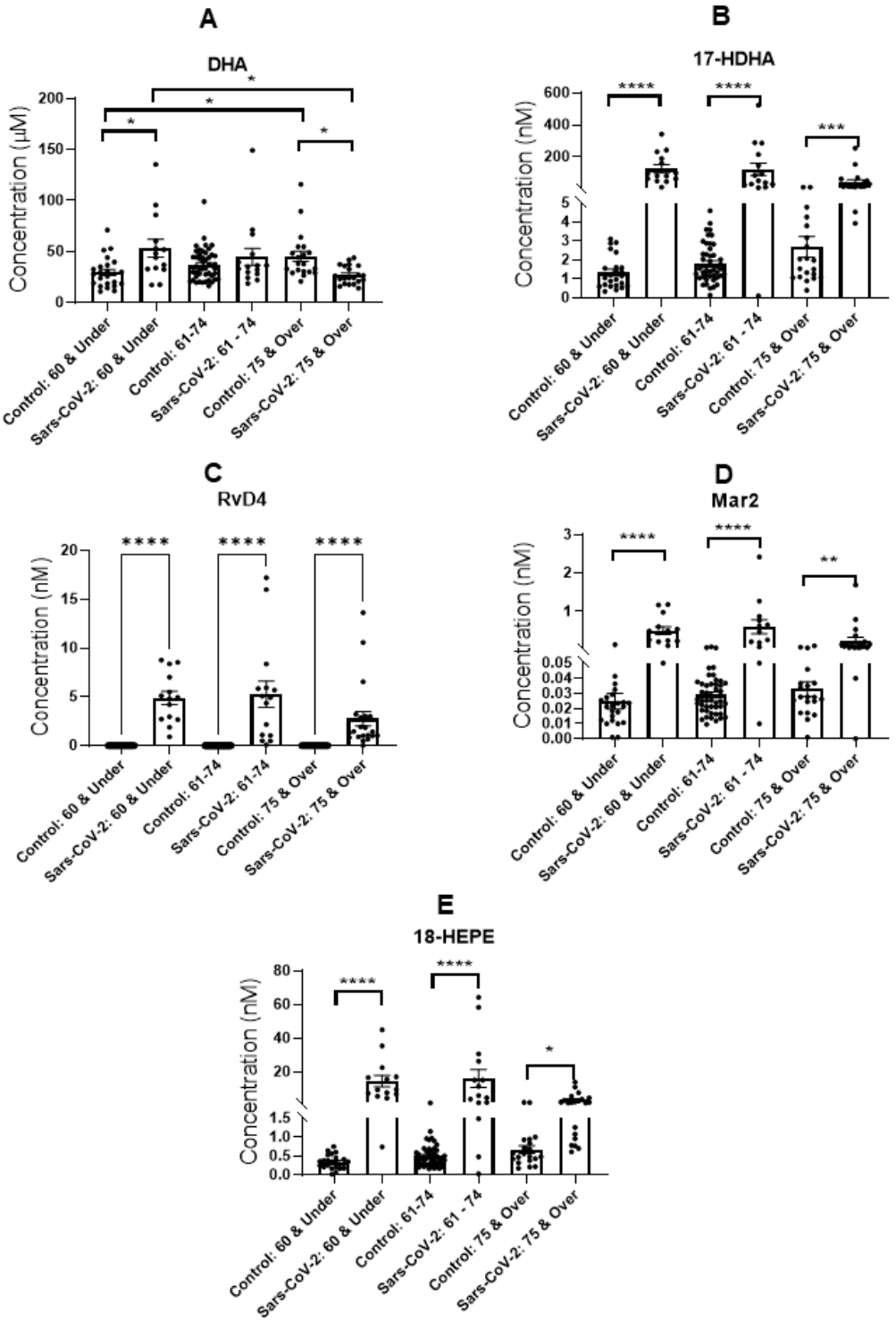

*Figure 3. Serum concentrations of docosahexaenoic acid (DHA; A), 17-hydroxydocosahexaenoic acid (17-HDHA; B), resolvin D4 (RvD4; C), maresin 2 (MaR2; D), and 18-hydroxyeicosapentaenoic acid (18-HEPE; E) in severe acute respiratory syndrome coronavirus 2 (n = 50) and age- and sex-matched control sera (n = 94), stratified by age group. Groups were assessed for normal distribution using D'Agostino–Pearson test. Significance was assessed using Kruskal–Wallis test correcting for multiple comparisons using Dunn test. *P ≤ .05, **P ≤ .01, ***P ≤ .001, ****P ≤ .0001.*

Serum levels of AA were within a healthy range in the control group (Abdelmagid, Clarke et al. 2015), but were elevated in SARS-CoV-2 serum across all age groups (Table 2). Levels of the anti-inflammatory EETs and the downstream metabolites (DHETs) are presented both individually and as a ratio to reflect the activity of the sEH pathway (Table 2). The ratio of 11,12-EET:11,12-DHET was significantly increased in SARS-CoV-2 serum, compared to matched control serum. There were some differences in the ratios of 8,9-EET:8,9-DHET and 14,15-EET:14,15-DHET but these were less consistent across the age groups for the two groups (Table 2). In the SARS-CoV-2 serum, levels of AA were correlated with all EETs, whereas in the control serum AA was only correlated with 8,9-EET and 11,12-EET (Figure 4B & 4C). These data suggest changes in the flux through the sEH pathway following SARS-CoV-2 infection, worthy of further future investigation.

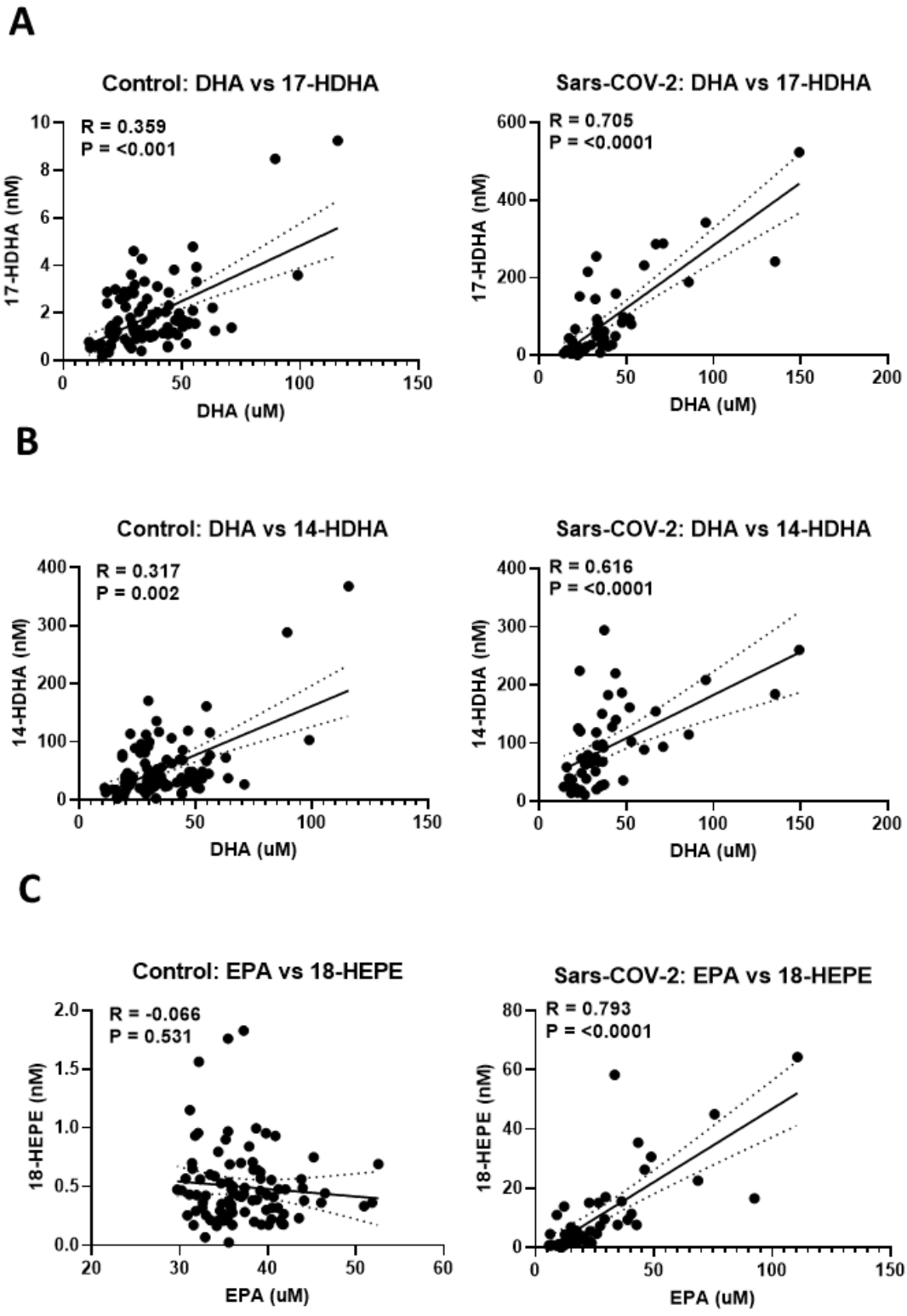

Figure 4. Correlation analysis of docosahexaenoic acid (DHA) and eicosapentaenoic acid (EPA) and relevant downstream specialized proresolving molecule pathway metabolites 17-hydroxydocosahexaenoic acid (17-HDHA; A), 14-hydroxydocosahexaenoic acid (14-HDHA; B), and 18-hydroxyeicosapentaenoic acid (18-HEPE; C) in severe acute respiratory syndrome coronavirus 2 (SARS-CoV-2; n = 50) and age- and sex-matched controls (n = 94). Data analyzed by Spearman ρ.

6.3.3 Associations between adaptive immune responses to SARS-COV-2 infection and serum levels of bioactive lipids

Anti-SARS-CoV-2 antibody binding to the nucleocapsid protein was interrogated using a reference antigen. Viral sequence data, where available, confirmed that the variants circulating in this cohort were either the Hu-1 strain, or the variant defining the 20B lineage (defined by the spike D614G variant), with no variability in nucleocapsid amino acid sequence (Tighe, Urbanowicz et al. 2020). There was a range of levels of anti-nucleocapsid (0.15 to 3.11 OD450) and anti-spike antibody (0.115-3.067 OD450) in the SARS-CoV-2 group (Table 3). Based on the range of anti-spike antibody binding, patients were separated into two groups: low (<0.5, n=26) and high (>0.5, n=26), the subset of patients who died had significantly lower levels of anti-spike antibody binding (Figure 5). Levels of 18-HEPE, 17-HDHA, RvD4 and 14,15-EET were significantly higher in patients with an anti-spike antibody value >0.5 (Figure 6). There were statistically significant positive correlations between these lipids and anti-spike antibody binding for the entire group of patients (Table 4).

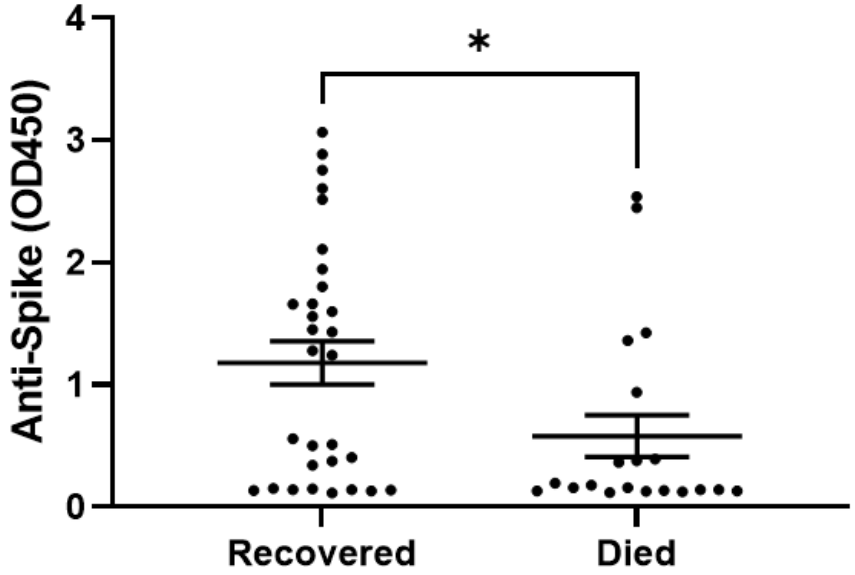

*Figure 5. Levels of anti-spike antibody binding in SARS-CoV-2 patients stratified by clinical outcome, recovered (n=30) and died (n=20). Statistical analysis by Mann-Whitney test showed lower levels of anti-spike antibody binding in those patients who died compared to those who survived. *p=<0.05.*

Table 3. Correlation analysis between concentrations of bioactive lipid with anti-nucleocapsid & anti-spike antibody response in SARS-CoV-2 (n=50). Data analysed by Spearman's Rho.

Bioactive lipids	Correlation Analysis of Lipids vs Antibody binding			
	Anti-Nucleocapsid		Anti-Spike	
	R Value	P Value	R Value	P Value
AA	0.326	**0.021**	0.352	**0.012**
LA	0.249	0.081	0.382	**0.006**
DHA	0.369	**0.009**	0.337	**0.017**
EPA	0.419	**0.002**	0.540	**<0.0001**
17-HDHA	0.269	0.059	0.537	**<0.0001**
18-HEPE	0.366	**0.009**	0.410	**0.003**
14-HDHA	0.434	**0.002**	0.293	**0.039**
RvD4	0.211	0.142	0.449	**0.001**
Maresin 2	0.282	0.055	0.343	**0.018**
LXA4	0.051	0.723	0.324	**0.022**
LXA5	0.222	0.133	0.436	**0.002**
5-HETE	0.093	0.52	0.361	**0.010**
8-HETE	0.404	**0.004**	0.419	**0.002**
9-HETE	0.27	0.058	0.469	**0.001**
11-HETE	0.279	**0.05**	0.464	**0.001**
12-HETE	0.231	0.106	0.084	0.563
15-HETE	0.259	0.069	0.407	**0.003**
16-HETE	0.245	0.097	0.045	0.756
19-HETE	0.138	0.344	0.314	**0.028**
20-HETE	0.234	0.101	0.099	0.494
TxB2	-0.26	0.071	-0.052	0.722
PGE2	0.049	0.744	0.275	0.056
PGD2	0.113	0.445	0.283	0.052
LTB4	-0.041	0.776	0.326	**0.021**
5,6-EET	0.357	**0.011**	0.271	0.057
5,6-DHET	0.024	0.867	0.310	**0.029**
5,6-Ratio	0.243	0.089	-0.018	0.904
8,9-EET	0.099	0.494	0.185	0.198
8,9-DHET	0.063	0.663	-0.104	0.474
8,9-Ratio	0.064	0.664	0.164	0.257
11,12-EET	0.239	0.093	0.084	0.564
11,12-DHET	0.109	0.452	-0.041	0.779
11,12-Ratio	0.15	0.297	0.114	0.431
14,15-EET	0.302	**0.033**	0.334	**0.018**
14,15-DHET	0.023	0.874	-0.194	0.178
14,15-Ratio	0.339	**0.016**	0.443	**0.001**
13-oxo-ODE	0.202	0.169	0.447	**0.002**
9-oxo-ODE	0.243	0.154	0.482	**0.003**
9-HODE	0.265	0.063	0.505	**0.0002**
13-HODE	0.268	0.059	0.488	**0.0003**
AEA	0.017	0.907	-0.216	0.131
PEA	-0.071	0.626	-0.083	0.567
OEA	0.063	0.666	-0.060	0.679

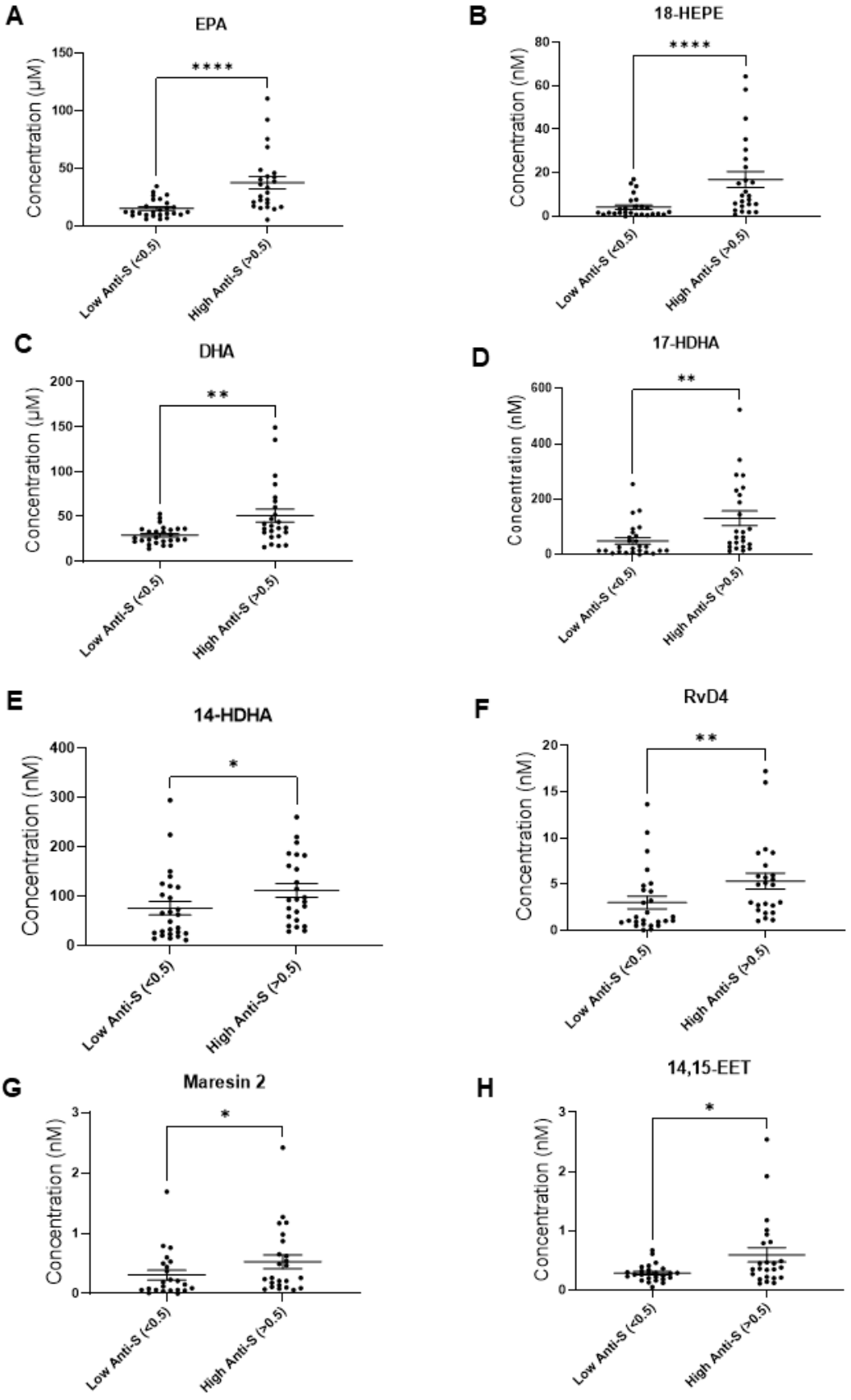

Figure 6. Serum concentration of significantly altered proresolution lipid mediators eicosapentaenoic acid (EPA; A), 18-hydroxyeicosapentaenoic acid (18-HEPE; B), docosahexaenoic acid (DHA; C), 17-

hydroxydocosahexaenoic acid (17-HDHA; D), 14-hydroxydocosahexaenoic acid (14-HDHA; E), resolvin D4 (RvD4; F), maresin 2 (G), and 14,15-Epoxyeicosa-5,8,11-trienoic Acid (14,15-EET; H) based on the anti-spike antibody response (low group <0.5, n = 26; high group >0.5, n = 24) in patients with severe acute respiratory syndrome coronavirus 2. Groups were assessed for normal distribution using D'Agostino–Pearson test. Significance was assessed using Mann–Whitney test. ∗P ≤ .05, ∗∗P ≤ .01, ∗∗∗∗P ≤ .0001.

6.3.4 Predictors of clinical outcomes

Analysis of serum levels of bioactive lipids early in the infection and the clinical outcome identified that levels of LA and 5,6-DHET were significantly lower in SARS-CoV-2 infected patients who died (Figure 7A-B), and the ratio of 5,6-EET:5,6-DHET was higher in those patients that died compared to those that survived (Figure 7C). Receiver operating characteristic curves were also able to significantly differentiate between patient who recovered and those who died based on serum concentrations of LA (AUC =0.72, 95% CI = 0.57–0.87), 5,6-DHET (AUC = 0.74, 95% CI = 0.60–0.89), and 5,6-EET:DHET (AUC = 0.67, 95% CI=0.52-0.82) (Figure 7 A-B). Comparison of oxylipin levels between patients who went on to spend time in ICU and those who remained on the wards also found higher levels of many of the oxylipins in those patients spent time in ICU (Table 4). These differences were seen across all sub-groups of oxylipins both pro- and anti-inflammatory, with the exception of the endocannabinoids.

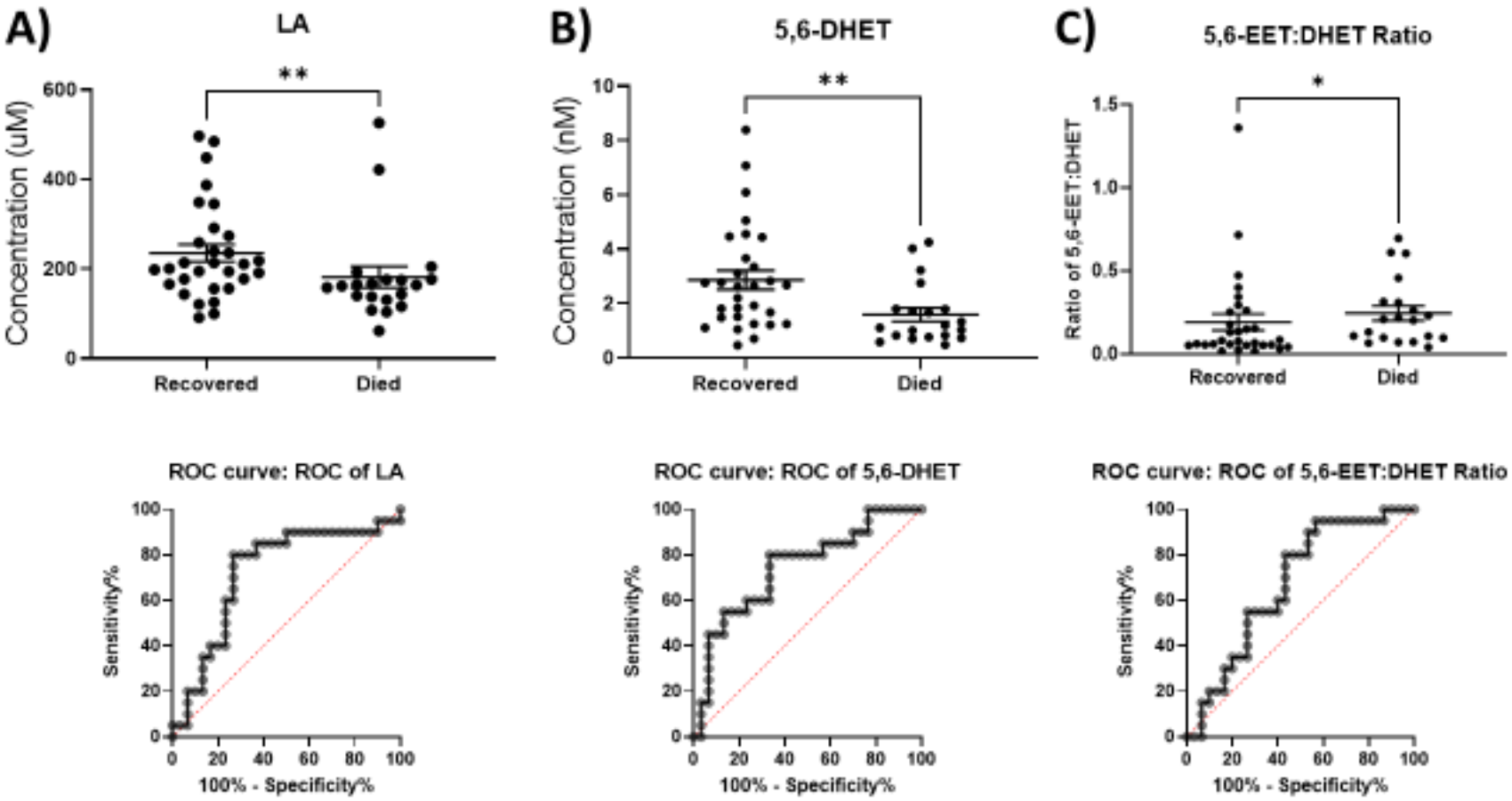

Figure 7. Comparison of the serum levels of A) LA; B) 5,6-DHET; and C) 5,6-EET:DHET ratio between COVID-19 patients who went on to recover, and who died. Associated receiver operating characteristic (ROC) curves are presented to illustrate the diagnostic ability of each oxylipin. Groups were assessed for normal distribution using D'Agostino–Pearson test. Significance was assessed using Mann–Whitney test. $*P \leq .05$, $**P \leq .01$

Table 4. Mean concentration of oxylipins in people who later went on to either be admitted to ICU or not. Significance was assessed using Mann-Whitney Test

Lipid	No ICU			ICU			P value
	Mean	±	SD	Mean	±	SD	
5-HETE	150.48	±	192.82	170.71	±	119.09	0.0611
8-HETE	2.29	±	2.17	4.82	±	3.74	0.0011
9-HETE	9.60	±	12.84	23.23	±	21.59	0.0011
11-HETE	12.77	±	13.27	27.33	±	22.59	0.0035
12-HETE	171.61	±	157.52	159.55	±	113.55	0.8197
15-HETE	90.06	±	81.36	182.91	±	142.79	0.0056
16-HETE	0.20	±	0.07	0.23	±	0.09	0.3623
19-HETE	189.32	±	248.53	194.21	±	141.21	0.0907
20-HETE	72.20	±	61.43	69.96	±	46.86	0.7587
TxB2	87.20	±	103.62	43.09	±	41.95	0.0948
PGE2	0.49	±	0.41	0.62	±	0.41	0.1862
PGD2	1.16	±	1.56	1.13	±	1.13	0.1901
LTB4	5.12	±	0.68	5.50	±	0.61	0.0213
5,6-EET	0.20	±	0.08	0.41	±	0.38	0.0066
5,6-DHET	2.39	±	1.50	2.08	±	1.51	0.4597
5,6-Ratio	0.13	±	0.11	0.30	±	0.30	0.0083
8,9-EET	0.49	±	0.36	1.00	±	1.13	0.3276
8,9-DHET	0.54	±	0.28	0.37	±	0.30	0.0129
8,9-Ratio	1.29	±	1.40	4.06	±	5.30	0.0084
11,12-EET	168.72	±	140.64	158.90	±	101.07	0.8352
11,12-DHET	0.57	±	0.20	0.57	±	0.29	0.9226
11,12-Ratio	317.99	±	248.98	420.24	±	512.64	0.6991
14,15-EET	0.26	±	0.14	0.61	±	0.56	0.0007
14,15-DHET	0.51	±	0.20	0.50	±	0.28	0.4068
14,15-Ratio	0.54	±	0.28	1.28	±	0.84	<0.0001
13-oxo-ODE	12.48	±	15.54	39.45	±	38.58	0.0014
9-oxo-ODE	2.28	±	1.82	11.15	±	12.12	0.0008
9-HODE	89.12	±	110.07	363.62	±	374.43	<0.0001
13-HODE	104.78	±	131.93	424.80	±	441.71	0.0002
18-HEPE	3.13	±	3.30	17.50	±	16.91	<0.0001
17-HDHA	42.17	±	55.61	136.17	±	124.44	0.0003
14-HDHA	81.41	±	74.92	107.62	±	61.25	0.0459
PEA	27.83	±	10.36	26.49	±	11.33	0.5030
AEA	1.80	±	0.79	1.43	±	0.70	0.0961
OEA	37.45	±	15.97	37.38	±	15.94	0.9803
AA	74.96	±	28.88	125.03	±	71.71	0.0003
LA	164.27	±	51.93	262.25	±	127.15	0.0052
DHA	27.63	±	9.28	51.78	±	32.91	0.0004
EPA	13.68	±	5.88	38.62	±	24.25	<0.0001
LXA4	2.78	±	3.72	3.14	±	2.51	0.0590
LXA5	0.22	±	0.26	0.81	±	0.69	<0.0001
Maresin 2	0.26	±	0.36	0.58	±	0.53	0.0034
RvD4	2.97	±	3.47	5.33	±	4.04	0.0033

6.4 Discussion

SARS-CoV-2 infection was associated with robust increases in both ω-6 and ω-3 derived bioactive lipids which have well characterized roles in both pro- and anti-inflammatory responses (Gilroy and Bishop-Bailey 2019). Significant increases in serum levels of pro-inflammatory lipids included PGE2, TBXB2 and LTB4 and a range of bioactive lipids with well-established roles in dampening down / resolving inflammatory processes were evident in the SARS-CoV-2 group, compared to the age matched control group. Of particular note was the 47-fold increase in levels of the SPM precursor 17-HDHA and the SPMs RvD4 and Mar2, serum levels of which are normally close to, or below, the limits of detection in the healthy population (Colas, Shinohara et al. 2014). Substantial increases in levels of some EETs and endocannabinoids also support a concerted anti-inflammatory response via multiple enzymatic pathways following SARS-CoV-2 infection. The demonstration of a robust activation of the resolution pathways following SARS-CoV-2 infection, irrespective of patient age, points to a complex pathophysiological response which may be amenable to pharmacological intervention and provide new targets for treatment.

There was a broad range of anti-nucleocapsid and anti-spike responses in the SARS-CoV-2 group, indicative of adaptive immune response to infection. Consistent with a larger study, increased anti-spike responses were associated with improved clinical outcome (Tighe, Urbanowicz et al. 2020). SARS-CoV-2 patients with higher anti-spike responses (>0.5) had significantly increased levels of a number anti-inflammatory and resolution molecules as well as some pro-inflammatory lipids. The statistically altered bioactive lipids represent clusters of SPMs, lipoxins and EETs which either directly mediate resolution of inflammation or are metabolites in the resolution pathways and are generated by COX, LOX and CYP pathways. Levels of PUFA substrates were not substantially altered by SARS-CoV-2 infection or age, thus it is unlikely that substrate and therefore diet is a major determining factor in the resolution response to SARS-CoV-2 infection. The strong correlations between PUFAs and their downstream SPM pathway metabolites in the SARS-CoV-2 infection group suggests that these enzymatic pathways are upregulated by this infection, particularly evident for the E series pathway. These findings support future studies of the relationship between the antibody response to SARS-CoV-2 infection, activation of the resolution pathways and clinical outcome in a larger cohort of patients.

These findings are consistent with the recent report of an elevation of plasma and serum SPMs and increased expression of related enzymatic pathways in peripheral blood monocyte subsets in 19 patients infected with SARS-CoV-2 (Koenis, Beegun et al. 2021) and findings by Archambault et al (2020)(Archambault, Zaid et al. 2021). In addition, increased levels of pro-inflammatory bioactive lipids and anti-inflammatory SPMs, including RvD4, D5, D2, D1 and PDX have been reported in bronchoalveolar lavage from SARS-CoV-2 patient (Schwarz, Sharma et al. 2020). SPMs are already known to modulate acute lung injury and respiratory distress syndrome (Sandhaus and Swick 2021), supporting these findings following SARS-CoV-2 infection. Antibodies generated by B cells are critical to anti-viral immunity. The D series precursors and resolvins, including 17-HDHA, enhance human B cell antibody production by promoting differentiation towards an anti-body secreting phenotype (Ramon, Gao et al. 2012). In a pre-clinical murine model of influenza immunization, 17-HDHA treatment increased antigen specific antibody responses and protected against live influenza virus infection (Ramon, Baker et al. 2014). These data suggest that a robust generation of 17-HDHA following infection not only acts to counter pro-inflammatory responses but may also facilitate the response of B cells to mount an antibody response. To date, there are no studies of the effects of the SPMs on SARS-CoV-2 infection in patients, however, it has been reported that both RvD1 and RvD2 have beneficial effects on inflammatory responses in SARS-CoV-2 infected macrophages (Recchiuti, Patruno et al. 2021).

Current evidence suggests that treatments for SARS-CoV-2 infection, alongside vaccinations, will remain a priority in the immediate future. Identification of the critical steps involved in the up-regulation of these anti-inflammatory pathways may be instructive for the development of interventions aimed at dampening the inflammatory response or promoting the clearance of the inflammation arising from SARS-CoV-2 infection. Dexamethasone has been identified as an important treatment to promote recovery from SARS-CoV-2 infection. Dexamethasone has been shown to increase SPM levels in a small number of SARS-CoV-2 infected patients (Koenis, Beegun et al. 2021), healthy volunteers (Barden, Phillips et al. 2018) and in allergic airway inflammation (Pyrillou, Chairakaki et al. 2018). Future investigation of the potential contribution of SPMs to the beneficial effects of dexamethasone in patients with SARS-CoV-2 infection in a larger cohort will improve further our understanding of the potential mechanisms of action of this treatment.

The differences in the LA and 5,6-DHET at the time of admission to hospital between patients who recovered and patients who died is an extremely interesting finding. As samples were collected on admission to hospital, and clinical outcomes were not know for days/weeks after admission, the ability to predict clinical outcome based on the levels of several oxylipins in a sample taken on hospital admission is particularly useful. As levels of LA and 5,6-DHET are fairly easy to measure, a basic LC-MS/MS method could be used to measure these in the clinical lab, and could provide further information to clinicians when making clinical decisions, and could help identify those people at the most risk of death. The differences in the levels of oxylipin in people who went on to spend time in ICU vs those who did not, is less straightforward. It is interesting that a high number of oxylipins are higher in those people who went on to be admitted to ICU, which include many of the anti-inflammatory and pro-resolution lipids. However, the admission criteria to ICU is based on a range of factors including age, frailty, and availability of space. Therefore predicting this outcome based on a oxylipin measures is difficult to interpret. However the increase in levels of those who do go on to spend time is ICU could point toward dysregulated inflammatory signalling and attempted resolution, consistent with other groups' findings (McReynolds, Cortes-Puch et al. 2021, Palmas, Clarke et al. 2021, Karu, Kindt et al. 2022).

There are a number of study limitations. Serum samples were collected from patients hospitalised with SARS-CoV-2 for clinical diagnostic tests during the first wave of the pandemic in the UK. Due to the clinical pressures within the system at the time some clinical data, such as BMI, were not collected. It is known that levels of SPMs are decreased with increased BMI, which could potentially contribute to SARS-CoV-2 related morbidities and mortalities (Pal, Gowdy et al. 2020). Serum samples were collected within the first few days of hospital admission and represent a snapshot of the anti-nucleocapsid and anti-spike response and the lipid levels at a point in time. It is important to note that levels of antibodies change over time, however we do not have matched longitudinal data. The anti-nucleocapsid and anti-spike signal provides an indication of the potency of the adaptive immune response following infection. The viral genome sequencing data available for these patients indicated that the nucleocapsid amino acid sequence was completely conserved between infections. While it is possible that there may be mismatches between the antigen used in our assay and the strain of infecting virus that mean that antibodies are present which are undetected by

our assay, at the time of sampling there was minimal genetic diversity in UK isolates [www.nextrstrain.org]. To mitigate against this, ELISAs were used against two antigens.

In summary, these findings highlight that SARS-CoV-2 infection can lead to very robust activation of the pathways that generate the specialised pro-resolving molecules and other anti-inflammatory bioactive lipids. This new knowledge supports the future investigation of these pathways which may inform the development of novel anti-inflammatory treatments for SARS-CoV-2 infection. Furthermore, these new datasets provide us opportunities to explore further the underlying molecular pathways that regulate the resolution pathways in humans, with the goal of identifying novel approaches for the development of new therapeutics for other infections and chronic inflammatory diseases.

Chapter Seven

General Discussion

The work in this thesis has used clinically relevant cohorts of participants to identify potential biomarkers for chronic pain and joint pathology, as well as pharmacologically targetable pathways to treat chronic pain in OA. The soluble epoxide hydrolase pathway was identified in independent cohorts as being associated with pain and knee symptoms, and targeting this pathway in a rodent model of OA showed effective analgesia. Future work on this pathway will aim to assess the prophylactic potential of targeting sEH in the early stages of OA pathogenesis to prevent pain and pathology from developing. Although the pandemic brought many challenges to research, it also allowed me to study oxylipins in people hospitalised with COVID-19. This provided evidence of some of the SPMs in a clinical cohort, and associations with measures of adaptive immune response.

7.1 Suitability of methods for clinical samples and further developments

The targeted LC-MS/MS method developed for these clinical and pre-clinical studies has been robust and provided valuable and reliable quantitative measurements of oxylipins in study samples. The balance between the throughput of the method, and the quality of chromatograms generated was fit for purpose for the amount of samples generated from these studies. The method has also been used for studies not documented in this thesis such as trauma, dietary intervention studies, cell based experiments, and other pre-clinical models of disease. Taking the method forward will involve adding novel lipid as and when commercial standards are available, for example the CYP450 epoxides and sEH diols of other PUFAS, and continuing to ensure the method is optimised for current throughput of samples. For example, currently it would not be possible to use this method to perform analysis of oxylipins in large scale epidemiological studies involving thousands of samples, due to the 25 minute run time of the instrument. Future development of the extraction procedure and increasing the throughput of sample preparation will increase the utility of this method. This could be achieved through a combination of reducing the required volume of sample and extraction solvents, with the potential of transferring the extraction from tubes to in-plate. This would need to be validated to ensure the sensitivity and reliability was not compromised.

The method is highly complex and requires a great deal of planning and care when performing. With the aim of identifying clinical biomarkers of future OA, to move to a clinical environment the method would need to be simplified down to the key oxylipins and made compatible to NHS instrumentation and workflows. For example, in chapter three it was

shown that levels of 5-HETE + 8,9-EET were predictive of future pain scores – to deliver this as a test routinely in a clinical environment the LC-MS/MS method would need to be re-optimised to reduce the chromatographic run time and only include the oxylipins of interest. A key challenge in translating oxylipin measurements to the clinical laboratory will be in defining healthy ranges for their levels, as these can influenced by various individual differences and sample collection methods. Advances in MS technologies will likely drive this method forward. Future work to investigate the role of oxylipins mechanistically, could use imaging MS platforms such as MALDI and DESI imaging, and 3D-OrbiSIMS to investigate the spatial distribution of oxylipins in OA joint tissue. These could be integrated with traditional histology techniques to give a more comprehensive picture of the joint during disease.

7.2 Reliability of measuring SPMs in biological samples

Further work is needed across the field to increase the reliability of measuring SPMs in biological samples, which is the subject of current academic debate. In this thesis, SPMs were generally not detected. The sensitivity of the method to spiked QCs containing the SPMs was reliable down to the low pM range, therefore it was expected that these could be detected in study samples. This could be due to several reasons such as profiling of plasma/serum rather than tissue/tissue fluid where levels would be expected to be higher. It is possible that in OA/knee pain any SPMs produced would be from immune cells acting at the site of tissue injury and that these pro-resolution signals would be diluted when entering circulation and below the limits of detection of the LC-MS/MS. The study involving the hospitalised COVID-19 participants, who had high levels of systemic inflammation, provided the opportunity to measure several of these SPMs in serum. The results reported were consistent with others also investigating oxylipins following COVID-19 infection. The confirmation of the observed chromatograms with enhanced product ion scans gave confidence in the allocation of lipid identities reported. Interestingly, across multiple studies I have observed that the MRM transitions used for the SPMs generate extremely variable chromatograms between individuals compared to other oxylipins. Particularly variable are the levels of baseline noise observed, and the presence/absence of multiple peaks. Future work could use untargeted analyses on high resolution MS to identify these unknown peaks which may provide further understanding to why these SPMs are particularly difficult to measure. The lack of reproducibility in the measurement of the SPMs across labs means that currently they are not

ideal candidates for biomarkers of disease, however mechanistic studies focused on defining their biological functions are particularly interesting.

The balance between understanding the mechanistic role of the oxylipins versus identifying clinically relevant biomarkers is also something to be considered with the choice of matrix. In this thesis, studies have used plasma/serum, which are indicative of circulating levels of oxylipins in blood. The limitation of this is that the circulating concentrations may not reflect the levels in the joint, and therefore it is difficult to interpret the mechanistic role of the oxylipin in the pathogenesis of disease at the tissue level. The benefits of using plasma/serum are that these samples are readily accessible and much more suitable for biomarker discovery and the future translation to identify people at high risk of future OA and OA pain is much more achievable in a clinical test which uses blood compared to one which required a tissue biopsy or extraction of synovial fluid. Future studies are planned to compare the levels of oxylipins in synovial fluid and serum and to see whether these levels correlate.

7.3 Variability in clinical data

Currently, clinical studies involving people with OA pain generally use subjective measures of pain such as self-reported questionnaires and scoring. This inevitably introduces individual variability into datasets and is a key limitation in interpreting data. How participants score their pain on the day is likely to be influenced by a variety of factors such as mood, recent activities, and circadian rhythms. Quantitative sensory testing, including pressure pain thresholds, are often used in combination with self-reported pain assessments. This is where participants have gradual pressure applied to their painful joint and press a button when they feel pain. Generally this is a less subjective measure of pain, however there have been association reported between depression, pain catastrophizing, and physical activity level with several QST measures (Othman, Jayakaran et al. 2021). In order to fully understand the relationship between oxylipins and pain sensitisation, it is argued that objective methods must be developed which are not influenced by external factors. However, the opposing argument would be that experience of pain is extremely subjective, and using methods which take into account all these external factors give the best overall response to what someone with pain is experiencing. Clinical research also can risk introducing recruitment bias to study cohorts, which could result in participants being recruited who have worse knee pain, or are generally more proactive about managing their pain. This must be considered before

observations from clinical studies are generalised to the general population of people with OA. Improvement is required across the field to improve the standardisation of sample and storage of clinical samples. Particularly relevant to this thesis is the preparation of blood into plasma and serum samples, which can vary from study to study depending on the protocol. This introduced variation to the datasets and makes comparison across cohorts particularly difficult as well as assigning 'normal' ranges to the oxylipins.

The majority of studies also recruit participants to studies who are presenting with symptoms and have a clinical diagnosis of disease. This is extremity useful in studying the role of oxylipins in disease, however it means that the early stages of disease before symptoms are present can be overlooked. In order to address this the profiling of the KICK cohort samples was performed for people who are at high risk of developing OA in the future. Hopefully, the data collected in chapter 3 will be used in the future to see if levels of oxylipins after injury are able to identify people who will go on to develop OA in the future. Another possible avenue to explore is the use of biobanks, where participants have been followed longitudinally over time and where repeated samples collected prior to diagnosis could be available from people who have gone on to develop OA. This would allow biomarkers identified in studies with people with established OA to be validated in samples collected from early disease stages.

These studies show a translational approach of identifying potential targets using targeted lipidomic analysis of clinically relevant human samples, and targeting these in appropriate animal model of disease. This approach means that prior to animal work, targets are known to be clinically relevant in humans. This strengthens the overall findings as studies in rodent are often underpowered to identify these targets without excessive numbers of animals.

7.4 Soluble Epoxide Hydrolase and Lipoxygenase

The results of the studies in this thesis point towards soluble epoxide hydrolase as a strong potential target for OA pain. The KICK cohort showed association of DHETs with worse knee symptoms only 2 years post-injury, and not immediately and 3 months post-injury. What this could suggest is that this pathway is associated with chronic pain rather than acute pain, which would make it a more appropriate target compared to current analgesics. The dosing of an sEH inhibitor in a preclinical model of post-traumatic OA further supports this as a suitable treatment for OA. Although the drug did not improve the joint pathology, it was

observed that 8,9-EET:DHET was associated with cartilage degradation. In the pre-clinical model, the drug was administered from week 12, where pain and joint pathology had been established. Future studies could investigate whether dosing from an earlier time point, such as immediately after induction of the model, had any effect on preventing the development of joint pathology. An inhibitor for sEH is currently undergoing clinical trials in the US for neuropathic pain, which if approved, will show a clinical pipeline for sEH inhibitors to market for other diseases. Targeting sEH as a treatment for chronic pain could further be optimised through personalised medicine approaches. Where levels of sEH and sEH activity are quantified to identify which people would likely benefit most from treatments targeting this enzyme. Another pathway to investigate further is the LOX pathway. It was observed in Chapter 4 that levels of LOX metabolites were associated with radiographic knee OA. The literature suggests that the LOX pathway generally has a protective role in the joint but can become dysregulated leading to uncontrolled inflammation that drives the pathophysiology further. The term 'dysregulated lipid metabolism' is often used, particularly when describing disease pathology driven by underlying inflammation, however there is currently no general consensus as to what constitutes regulated and dysregulated levels of oxylipins or the activity of the enzymes that produce them.

7.5 Conclusions

The work presented in this thesis highlight key oxylipins associated with clinical features of osteoarthritis and chronic pain, and show that pharmacologically targeting soluble epoxide hydrolase provides analgesia in a rodent model of OA. These studies will inform future research into these pathways which will hopefully lead to novel therapeutics and biomarkers to treat osteoarthritis and chronic pain.

8.0 References

Abate, K. H., Z. Abebe, O. Z. Abil, A. Afshin, M. B. Ahmed, F. Alahdab, K. Alam, S. M. Alavian, A. a. Alkerwi, F. Alla, Y. A. Amoako, N. H. Anber, M. D. Animut, B. Armoon, H. Badali, B. T. Baune, K. M. Cercy, Y. Chaiah, F. J. Charlson, J. Coresh, Z. El-Khatib, A. Y. Endries, V. Fallah Omrani, M. Faramarzi, M. Fareed, I. Filip, F. G. Gankpe, A. L. Garcia-Basteiro, M. Ghimire, A. C. Goulart, G. Grosso, H. C. Gugnani, T. Gupta, N. Hafezi-Nejad, H. L. Harb, M. K. Hole, O. S. Ilesanmi, C. M. S. Irvine, S. M. S. Islam, M. Jürisson, A. Karch, G. M. Kassa, T. D. Kassa, B. Khafaei, Y. J. Kim, J. M. Kocarnik, T. Kolola, G. A. Kotsakis, A. Lafranconi, J. V. Lazarus, S. Liu, T. C. D. Lucas, S. Ma, A. Majeed, M. B. Marzan, M. R. Mathur, K. M. Mehta, B. Miazgowski, A. H. Mokdad, M. Molokhia, K. B. Mruts, U. O. Mueller, C. Nagata, A. Naheed, J. W. Ngunjiri, S. Nomura, I.-H. Oh, M. O. Owolabi, N. Perico, A. Pourshams, D. Prabhakaran, M. Rahman, G. A. Roth, P. S. Sachdev, A. Sahebkar, K. Saleem, J. A. Salomon, M. M. Santric Milicevic, B. P. Sao Jose, M. Sawhney, I. J. C. Schneider, D. C. Schwebel, M. Sekerija, A. Shafieesabet, M. Shamsizadeh, M. Sharif, E. L. N. Slepak, M. Soofi, D. O. Sylte, H. Temesgen, D. Tsoi, M. S. Usman, F. Weldegebreal, T. Wijeratne, A. S. Winkler, Y.-C. Wu, A. Yadollahpour, P. Yip, E. Yisma and I. Zucker (2018). "Global, regional, and national incidence, prevalence, and years lived with disability for 354 diseases and injuries for 195 countries and territories, 1990–2017: a systematic analysis for the Global Burden of Disease Study 2017." The Lancet (British edition) **392**(10159): 1789-1858.

Abdelmagid, S. A., S. E. Clarke, D. E. Nielsen, A. Badawi, A. El-Sohemy, D. M. Mutch and D. W. L. Ma (2015). "Correction: Comprehensive profiling of plasma fatty acid concentrations in young healthy Canadian adults." PloS one **10**(5): e0128167-e0128167.

Ackermann, J. A., K. Hofheinz, M. M. Zaiss and G. Krönke (2017). "The double-edged role of 12/15-lipoxygenase during inflammation and immunity." BIOCHIMICA ET BIOPHYSICA ACTA-MOLECULAR AND CELL BIOLOGY OF LIPIDS **1862**(4): 371-381.

Akundi, R. S., E. Candelario-Jalil, S. Hess, M. Hüll, K. Lieb, P. J. Gebicke-Haerter and B. L. Fiebich (2005). "Signal transduction pathways regulating cyclooxygenase-2 in lipopolysaccharide-activated primary rat microglia." Glia **51**(3): 199-208.

Allen, B. L., K. Montague-Cardoso, R. Simeoli, R. A. Colas, S. Oggero, B. Vilar, P. A. McNaughton, J. Dalli, M. Perretti, E. Sher and M. Malcangio (2020). "Imbalance of proresolving lipid mediators in persistent allodynia dissociated from signs of clinical arthritis." Pain (Amsterdam) **161**(9): 2155-2166.

Araldi, D., L. F. Ferrari, C. M. Lotufo, A. S. Vieira, M. C. P. Athié, J. G. Figueiredo, D. B. Duarte, C. H. Tambeli, S. H. Ferreira and C. A. Parada (2013). "Peripheral inflammatory

hyperalgesia depends on the COX increase in the dorsal root ganglion." Proceedings of the National Academy of Sciences - PNAS **110**(9): 3603-3608.

Archambault, A. S., Y. Zaid, V. Rakotoarivelo, C. Turcotte, É. Doré, I. Dubuc, C. Martin, O. Flamand, Y. Amar, A. Cheikh, H. Fares, A. El Hassani, Y. Tijani, A. Côté, M. Laviolette, É. Boilard, L. Flamand and N. Flamand (2021). "High levels of eicosanoids and docosanoids in the lungs of intubated COVID-19 patients." The FASEB journal **35**(6): e21666-n/a.

Asahara, M., N. Ito, T. Yokomizo, M. Nakamura, T. Shimizu and Y. Yamada (2015). "The Absence of the Leukotriene B4 Receptor BLT1 Attenuates Peripheral Inflammation and Spinal Nociceptive Processing Following Intraplantar Formalin Injury." Molecular pain **11**: 11-11.

Ashraf, S., M. Radhi, P. Gowler, J. J. Burston, R. D. Gandhi, G. J. Thorn, A. M. Piccinini, D. A. Walsh, V. Chapman and C. H. de Moor (2019). "The polyadenylation inhibitor cordycepin reduces pain, inflammation and joint pathology in rodent models of osteoarthritis." Scientific reports **9**(1): 4696.

Ashraf, S., M. Radhi, P. Gowler, J. J. Burston, R. D. Gandhi, G. J. Thorn, A. M. Piccinini, D. A. Walsh, V. Chapman and C. H. de Moor (2019). "The polyadenylation inhibitor cordycepin reduces pain, inflammation and joint pathology in rodent models of osteoarthritis." Scientific Reports **9**(1).

Attiq, A., J. Jalil, K. Husain and W. Ahmad (2018). "Raging the war against inflammation with natural products." Frontiers in pharmacology **9**: 976-976.

Attur, M., S. Krasnokutsky, A. Statnikov, J. Samuels, Z. Li, O. Friese, M. P. Hellio Le Graverand-Gastineau, L. Rybak, V. B. Kraus, J. M. Jordan, C. F. Aliferis and S. B. Abramson (2015). "Low-Grade Inflammation in Symptomatic Knee Osteoarthritis: Prognostic Value of Inflammatory Plasma Lipids and Peripheral Blood Leukocyte Biomarkers." Arthritis & rheumatology (Hoboken, N.J.) **67**(11): 2905-2915.

Banchet, G. S., A. Scholze and H. G. Schaible (2003). "Prostaglandin E2 increases the expression of the neurokinin1 receptor in adult sensory neurones in culture: a novel role of prostaglandins." British journal of pharmacology **139**(3): 672-680.

Bang, S., Y.-K. Xie, Z.-J. Zhang, Z. Wang, Z.-Z. Xu and R.-R. Ji (2018). "GPR37 regulates macrophage phagocytosis and resolution of inflammatory pain." The Journal of clinical investigation **128**(8): 3568-3582.

Barden, A., M. Phillips, L. M. Hill, E. M. Fletcher, E. Mas, P. S. Loh, M. A. French, K. M. Ho, T. A. Mori and T. B. Corcoran (2018). "Antiemetic doses of dexamethasone and their

effects on immune cell populations and plasma mediators of inflammation resolution in healthy volunteers." Prostaglandins, leukotrienes and essential fatty acids **139**: 31-39.

Basil, M. C. and B. D. Levy (2016). "Specialized pro-resolving mediators: endogenous regulators of infection and inflammation." Nature reviews. Immunology **16**(1): 51-67.

Beiche, F., S. Scheuerer, K. Brune, G. Geisslinger and M. Goppelt-Struebe (1996). "Up-regulation of cyclooxygenase-2 mRNA in the rat spinal cord following peripheral inflammation." FEBS letters **390**(2): 165-169.

Bernando, A. and L. Minghetti (2006). "PPAR-γ Agonists as Regulators of Microglial Activation and Brain Inflammation." Current pharmaceutical design **12**(1): 93-109.

Bijlsma, J. W. J. P., F. M. D. Berenbaum and F. P. J. G. P. Lafeber (2011). "Osteoarthritis: an update with relevance for clinical practice." The Lancet (British edition) **377**(9783): 2115-2126.

Blaker, C. L., E. C. Clarke and C. B. Little (2017). "Using mouse models to investigate the pathophysiology, treatment, and prevention of post-traumatic osteoarthritis: MOUSE MODELS OF POST-TRAUMATIC OSTEOARTHRITIS." Journal of orthopaedic research **35**(3): 424-439.

Blanco-Melo, D., B. E. Nilsson-Payant, W.-C. Liu, S. Uhl, D. Hoagland, R. Møller, T. X. Jordan, K. Oishi, M. Panis, D. Sachs, T. T. Wang, R. E. Schwartz, J. K. Lim, R. A. Albrecht and B. R. tenOever (2020). "Imbalanced Host Response to SARS-CoV-2 Drives Development of COVID-19." Cell (Cambridge) **181**(5): 1036-1045.e1039.

Bora, I., L. J. Steven, U. Arzu, M. H. Christine, G. Katrin, R. S. Kara, W. Karen, D. J. Paul, M. Christophe and D. H. Bruce (2008). "Soluble Epoxide Hydrolase and Epoxyeicosatrienoic Acids Modulate Two Distinct Analgesic Pathways." Proceedings of the National Academy of Sciences - PNAS **105**(48): 18901-18906.

Brenneis, C., M. Sisignano, O. Coste, K. Altenrath, M. J. Fischer, C. Angioni, I. Fleming, R. P. Brandes, P. W. Reeh, C. J. Woolf, G. Geisslinger and K. Scholich (2011). "Soluble Epoxide Hydrolase Limits Mechanical Hyperalgesia during Inflammation." Molecular pain **7**(1): 78-78.

Bressan, E., R. C. Farges, P. Ferrara and C. R. Tonussi (2003). "Comparison of two PBR ligands with classical antiinflammatory drugs in LPS-induced arthritis in rats." Life sciences (1973) **72**(23): 2591-2601.

Briggs, K. K., J. R. Steadman, C. J. Hay and S. L. Hines (2009). "Lysholm Score and Tegner Activity Level in Individuals With Normal Knees." The American journal of sports medicine **37**(5): 898-901.

Bryk, M., J. Chwastek, M. Kostrzewa, J. Mlost, A. Pędracka and K. Starowicz (2020). "Alterations in anandamide synthesis and degradation during osteoarthritis progression in an animal model." International journal of molecular sciences **21**(19): 1-19.

Burleigh, A., A. Chanalaris, M. D. Gardiner, C. Driscoll, O. Boruc, J. Saklatvala and T. L. Vincent (2012). "Joint immobilization prevents murine osteoarthritis and reveals the highly mechanosensitive nature of protease expression in vivo." Arthritis and rheumatism **64**(7): 2278-2288.

Burnett, B. P. and R. M. Levy (2012). "5-Lipoxygenase Metabolic Contributions to NSAID-Induced Organ Toxicity." Advances in therapy **29**(2): 79-98.

Bystrom, J., S. J. Thomson, J. Johansson, M. L. Edin, D. C. Zeldin, D. W. Gilroy, A. M. Smith and D. Bishop-Bailey (2013). "Inducible CYP2J2 and Its Product 11,12-EET Promotes Bacterial Phagocytosis: A Role for CYP2J2 Deficiency in the Pathogenesis of Crohn's Disease?" PloS one **8**(9): e75107.

Bystrom, J., J. A. Wray, M. C. Sugden, M. J. Holness, K. E. Swales, T. D. Warner, M. L. Edin, D. C. Zeldin, D. W. Gilroy and D. Bishop-Bailey (2011). "Endogenous epoxygenases are modulators of monocyte/macrophage activity." PloS one **6**(10): e26591-e26591.

Chen, X., Z. Li, B. Zhang, R. Hu, J. Li, M. Feng, W. Yao, C. Zhang, L. Wan and Y. Zhang (2019). "Alleviation of Mechanical Allodynia by 14,15-Epoxyeicosatrienoic Acid in a Central Poststroke Pain Model: Possible Role of Allopregnanolone and δ-Subunit-Containing Gamma-Aminobutyric Acid A Receptors." The journal of pain **20**(5): 577-591.

Chiang, N., J. Dalli, R. A. Colas and C. N. Serhan (2015). "Identification of resolvin D2 receptor mediating resolution of infections and organ protection." J Exp Med **212**(8): 1203-1217.

Chiurchiù, V., A. Leuti and M. Maccarrone (2018). "Bioactive lipids and chronic inflammation: Managing the fire within." Frontiers in immunology **9**: 38-38.

Chong, J. and J. Xia (2020). "Using MetaboAnalyst 4.0 for Metabolomics Data Analysis, Interpretation, and Integration with Other Omics Data." Computational Methods and Data Analysis for Metabolomics **2104**: 337-360.

Chopra, B., S. Giblett, J. G. Little, L. F. Donaldson, S. Tate, R. J. Evans and B. D. Grubb (2000). "Cyclooxygenase-1 is a marker for a subpopulation of putative nociceptive neurons in rat dorsal root ganglia." The European journal of neuroscience **12**(3): 911-920.

Colas, R. A., M. Shinohara, J. Dalli, N. Chiang and C. N. Serhan (2014). "Identification and signature profiles for pro-resolving and inflammatory lipid mediators in human tissue." American Journal of Physiology: Cell Physiology **307**(1): C39-C54.

consortium, T. C.-G. U. C.-U. (2020). "An integrated national scale SARS-CoV-2 genomic surveillance network." The Lancet Microbe **1**(3): e99-e100.

Culley, K. L., C. L. Dragomir, J. Chang, E. B. Wondimu, J. Coico, D. A. Plumb, M. Otero and M. B. Goldring (2014). Mouse Models of Osteoarthritis: Surgical Model of Posttraumatic Osteoarthritis Induced by Destabilization of the Medial Meniscus. Methods Mol Biol. New York, NY, New York, NY: Springer New York. **1226:** 143-173.

da Costa, B. R., T. V. Pereira, P. Saadat, M. Rudnicki, S. M. Iskander, N. S. Bodmer, P. Bobos, L. Gao, H. D. Kiyomoto, T. Montezuma, M. O. Almeida, P.-S. Cheng, C. A. Hincapié, R. Hari, A. J. Sutton, P. Tugwell, G. A. Hawker and P. Jüni (2021). "Effectiveness and safety of non-steroidal anti-inflammatory drugs and opioid treatment for knee and hip osteoarthritis: network meta-analysis." BMJ (Online) **375**: n2321-n2321.

Dall'Acqua, M. C., I. J. M. Bonet, A. R. Zampronio, C. H. Tambeli, C. A. Parada and L. Fischer (2014). "The contribution of transient receptor potential ankyrin 1 (TRPA1) to the in vivo nociceptive effects of prostaglandin E-2." Life sciences (1973) **105**(1-2): 7-13.

Dalli, J., J. M. Sanger, A. R. Rodriguez, N. Chiang, B. W. Spur and C. N. Serhan (2016). "Identification and actions of a novel third maresin conjugate in tissue regeneration: MCTR3." PloS one **11**(2): e0149319-e0149319.

Dalli, J. and C. N. Serhan (2019). "Identification and structure elucidation of the pro-resolving mediators provides novel leads for resolution pharmacology." British journal of pharmacology **176**(8): 1024-1037.

Dannhardt, G. and W. Kiefer (2001). Cyclooxygenase inhibitors – current status and future prospects. **36:** 109-126.

Darwesh, A. M., W. Bassiouni, D. Sosnowski and J. M. Seubert (2020). "Can N-3 polyunsaturated fatty acids be considered a potential adjuvant therapy for COVID-19-associated cardiovascular complications?" Pharmacology & therapeutics (Oxford): 107703-107703.

de Gaetano, M., E. Butler, K. Gahan, A. Zanetti, M. Marai, J. Chen, A. Cacace, E. Hams, C. Maingot, A. McLoughlin, E. Brennan, X. Leroy, C. E. Loscher, P. Fallon, M. Perretti, C. Godson and P. J. Guiry (2019). "Asymmetric synthesis and biological evaluation of imidazole- and oxazole-containing synthetic lipoxin A4 mimetics (sLXms)." European journal of medicinal chemistry **162**: 80-108.

Deng, B., C.-W. Wang, H. H. Arnardottir, Y. Li, C.-Y. C. Cheng, J. Dalli and C. N. Serhan (2014). "Maresin biosynthesis and identification of maresin 2, a new anti-inflammatory and pro-resolving mediator from human macrophages." PloS one **9**(7): e102362-e102362.

Domenichiello, A. F., M. R. Sapio, A. J. Loydpierson, D. Maric, T. Goto, M. S. Horowitz, G. S. Keyes, Z.-X. Yuan, S. F. Majchrzak-Hong, A. J. Mannes, M. J. Iadarola and C. E. Ramsden (2021). "Molecular Pathways Linking Oxylipins to Nociception in Rats." The journal of pain **22**(3): 275-299.

Dong, L., L. Dong, Y. Zhou, Y. Zhou, Z.-Q. Zhu, Z.-Q. Zhu, T. Liu, T. Liu, J.-X. Duan, J.-X. Duan, J. Zhang, J. Zhang, P. Li, P. Li, B. D. Hammcok, B. D. Hammcok, C.-X. Guan and C.-X. Guan (2017). "Soluble Epoxide Hydrolase Inhibitor Suppresses the Expression of Triggering Receptor Expressed on Myeloid Cells-1 by Inhibiting NF-kB Activation in Murine Macrophage." Inflammation **40**(1): 13-20.

Dua, R. and W. Cho (1994). "Inhibition of human secretory class II phospholipase A2 by heparin." European journal of biochemistry **221**(1): 481-490.

Dusting, G. J. and A. G. Stewart (1990). "Overview of eicosanoid metabolism and relationship to platelet-activating factor." Reproduction fertility and development **2**(5): 417-421.

Dyall, S. C., L. Balas, N. G. Bazan, J. T. Brenna, N. Chiang, F. da Costa Souza, J. Dalli, T. Durand, J.-M. Galano, P. J. Lein, C. N. Serhan and A. Y. Taha (2022). "Polyunsaturated fatty acids and fatty acid-derived lipid mediators: Recent advances in the understanding of their biosynthesis, structures, and functions." Progress in lipid research **86**: 101165-101165.

Ebersberger, A., B. D. Grubb, H. L. Willingale, N. J. Gardiner, J. Nebe and H. G. Schaible (1999). "The intraspinal release of prostaglandin E2 in a model of acute arthritis is accompanied by an up-regulation of cyclo-oxygenase-2 in the spinal cord." Neuroscience **93**(2): 775-781.

Ebersberger, A., G. Natura, A. Eitner, K.-J. Halbhuber, R. Rost and H.-G. Schaible (2011). "Effects of prostaglandin D2 on tetrodotoxin-resistant Na + currents in DRG neurons of adult rat." Pain (Amsterdam) **152**(5): 1114-1126.

Eguchi, N., T. Minami, N. Shirafuji, Y. Kanaoka, T. Tanaka, A. Nagata, N. Yoshida, Y. Urade, S. Ito and O. Hayaishi (1999). "Lack of Tactile Pain (Allodynia) in Lipocalin-Type Prostaglandin D Synthase-Deficient Mice." Proceedings of the National Academy of Sciences - PNAS **96**(2): 726-730.

England, S., S. Bevan and R. J. Docherty (1996). "PGE2 modulates the tetrodotoxin-resistant sodium current in neonatal rat dorsal root ganglion neurones via the cyclic AMP-protein kinase A cascade." The Journal of physiology **495**(Pt 2): 429-440.

Fan, E., J. R. Beitler, L. Brochard, C. S. Calfee, N. D. Ferguson, A. S. Slutsky and D. Brodie (2020). "COVID-19-associated acute respiratory distress syndrome: is a different approach to management warranted?" The Lancet Respiratory Medicine **8**(8): 816-821.

Fattori, V., F. A. Pinho-Ribeiro, L. Staurengo-Ferrari, S. M. Borghi, A. C. Rossaneis, R. Casagrande and W. A. Verri (2019). "The specialised pro-resolving lipid mediator maresin 1 reduces inflammatory pain with a long-lasting analgesic effect." British journal of pharmacology **176**(11): 1728-1744.

FDA (2018). Bioanalytical Method Validation

Guidance for Industry

Availability. Washington, Washington: Federal Information & News Dispatch, LLC. **83:** 23690.

Fernandes, G. S., A. Sarmanova, S. C. Warner, H. Harvey, K. Akin-Akinyosoye, H. Richardson, N. Frowd, L. Marshall, J. Stocks, M. Hall, A. M. Valdes, D. A. Walsh, W. Zhang and M. Doherty (2017). "Knee pain and related health in the community study (KPIC): a cohort study protocol."

Fiorucci, S., E. Distrutti, G. Cirino and J. L. Wallace (2006). "The Emerging Roles of Hydrogen Sulfide in the Gastrointestinal Tract and Liver." Gastroenterology (New York, N.Y. 1943) **131**(1): 259-271.

Fleming, I. (2007). "DiscrEET regulators of homeostasis: epoxyeicosatrienoic acids, cytochrome P450 epoxygenases and vascular inflammation." Trends in pharmacological sciences (Regular ed.) **28**(9): 448-452.

Fonseca, F. C. S., R. M. Orlando, R. M. M. Turchetti-Maia and J. N. de Francischi (2017). "Comparative effects of the ω3 polyunsaturated fatty acid derivatives resolvins E1 and D1 and protectin DX in models of inflammation and pain." Journal of inflammation research **10**: 119-133.

Fowler, J. C., W. F. Wonderlin and D. Weinreich (1985). "Prostaglandins block a Ca 2+-dependent slow spike afterhyperpolarization independent of effects on Ca 2+ influx in visceral afferent neurons." Brain research **345**(2): 345-349.

Funk, K., A. Woitecki, C. Franjic-Würtz, T. Gensch, F. Möhrlen and S. Frings (2008). "Modulation of Chloride Homeostasis by Inflammatory Mediators in Dorsal Root Ganglion Neurons." Molecular pain **4**(1): 32-32.

Garriga C, G. M., Paterson E, Hrusecka R, Hamid B, Alderson J, Leyland K, Honeyfield L, Greenshields L, Satchithananda K, Lim A, Arden NK, Judge A, Williams A, Vincent TL, Watt

FE (2021). "Clinical and molecular associations with outcomes at 2 years after acute knee injury: a longitudinal study in the Knee Injury Cohort at the Kennedy (KICK)." Lancet Rheumatol **3(9)**.

Gaur, K., M. Kori, L. Tyagi, V. Singh, R. Nema, P. Tripathi and C. Sharma (2009). "Licofelone- novel analgesic and anti-inflammatory agent for osteoarthritis: An overview." Journal of young pharmacists **1**(1): 67.

Gijón, M. A. and C. C. Leslie (1999). "Regulation of arachidonic acid release and cytosolic phospholipase A2 activation." Journal of leukocyte biology **65**(3): 330-336.

Gill, L. and S. Contag (2022). "Lipidomics provides therapeutic and diagnostic potential, but needs standardisation." BJOG : an international journal of obstetrics and gynaecology **129**(6): 889-889.

Gilroy, D. W. and D. Bishop-Bailey (2019). "Lipid mediators in immune regulation and resolution." British journal of pharmacology **176**(8): 1009-1023.

Gohir, S. A., P. Greenhaff, A. Abhishek and A. M. Valdes (2019). "Evaluating the efficacy of Internet-Based Exercise programme Aimed at Treating knee Osteoarthritis (iBEAT-OA) in the community: a study protocol for a randomised controlled trial." BMJ open **9**(10): e030564-e030564.

Gowler, P. R. W., P. I. Mapp, J. J. Burston, M. Shahtaheri, D. A. Walsh and V. Chapman (2020). "Refining surgical models of osteoarthritis in mice and rats alters pain phenotype but not joint pathology." PloS one **15**(9): e0239663-e0239663.

Gowler, P. R. W., J. Turnbull, M. Shahtaheri, S. Gohir, T. Kelly, C. McReynolds, J. Yang, R. R. Jha, G. S. Fernandes, W. Zhang, M. Doherty, D. A. Walsh, B. D. Hammock, A. M. Valdes, D. A. Barrett and V. Chapman (2022). "Clinical and Preclinical Evidence for Roles of Soluble Epoxide Hydrolase in Osteoarthritis Knee Pain." Arthritis & rheumatology (Hoboken, N.J.) **74**(4): 623-633.

Gregus, A. M., S. Doolen, D. S. Dumlao, M. W. Buczynski, T. Takasusuki, B. L. Fitzsimmons, X.-Y. Hua, B. K. Taylor, E. A. Dennis and T. L. Yaksh (2012). "Spinal 12-lipoxygenase-derived hepoxilin A3 contributes to inflammatory hyperalgesia via activation of TRPV1 and TRPA1 receptors." Proceedings of the National Academy of Sciences - PNAS **109**(17): 6721-6726.

Habouri, L., F. E. El Mansouri, Y. Ouhaddi, B. Lussier, J. P. Pelletier, J. Martel-Pelletier, M. Benderdour and H. Fahmi (2017). "Deletion of 12/15-lipoxygenase accelerates the development of aging-associated and instability-induced osteoarthritis." Osteoarthritis and cartilage **25**(10): 1719-1728.

Haeggstrom, J. Z. (2018). "Leukotriene biosynthetic enzymes as therapeutic targets." The Journal of clinical investigation **128**(7): 2680-2690.

Hains, B. C. and S. G. Waxman (2006). "Activated Microglia Contribute to the Maintenance of Chronic Pain after Spinal Cord Injury." The Journal of neuroscience **26**(16): 4308-4317.

Hame, S. L. and R. A. Alexander (2013). "Knee osteoarthritis in women." Current reviews in musculoskeletal medicine **6**(2): 182-187.

Hamilton, S. G., A. Wade and S. B. McMahon (1999). "The effects of inflammation and inflammatory mediators on nociceptive behaviour induced by ATP analogues in the rat." British journal of pharmacology **126**(1): 326-332.

Hammock, B. D., C. B. McReynolds, K. Wagner, A. Buckpitt, I. Cortes-Puch, G. Croston, K. S. S. Lee, J. Yang, W. K. Schmidt and S. H. Hwang (2021). "Movement to the Clinic of Soluble Epoxide Hydrolase Inhibitor EC5026 as an Analgesic for Neuropathic Pain and for Use as a Nonaddictive Opioid Alternative." Journal of medicinal chemistry **64**(4): 1856-1872.

Hartling, I., A. Cremonesi, E. Osuna, P.-H. Lou, E. Lucchinetti, M. Zaugg and M. Hersberger (2021). "Quantitative profiling of inflammatory and pro-resolving lipid mediators in human adolescents and mouse plasma using UHPLC-MS/MS." Clinical chemistry and laboratory medicine **59**(11): 1811-1823.

He, J., C. Wang, Y. Zhu and D. Ai (2016). Soluble epoxide hydrolase: A potential target for metabolic diseases. **8:** 305-313.

Ho, F. K., F. Petermann-Rocha, S. R. Gray, B. D. Jani, S. Vittal Katikireddi, C. L. Niedzwiedz, H. Foster, C. E. Hastie, D. F. Mackay, J. M. R. Gill, C. O'Donnell, P. Welsh, F. Mair, N. Sattar, C. A. Celis-Morales and J. P. Pell (2020). "Is older age associated with COVID-19 mortality in the absence of other risk factors? General population cohort study of 470,034 participants." PloS one **15**(11): e0241824-e0241824.

Hu, S., Q.-L. Mao-Ying, J. Wang, Z.-F. Wang, W.-L. Mi, X.-W. Wang, J.-W. Jiang, Y.-L. Huang, G.-C. Wu and Y.-Q. Wang (2012). "Lipoxins and aspirin-triggered lipoxin alleviate bone cancer pain in association with suppressing expression of spinal proinflammatory cytokines." Journal of neuroinflammation **9**(1): 278-278.

Huang, C., Y. Wang, X. Li, L. Ren, J. Zhao, Y. Hu, L. Zhang, G. Fan, J. Xu, X. Gu, Z. Cheng, T. Yu, J. Xia, Y. Wei, W. Wu, X. Xie, W. Yin, H. Li, M. Liu, Y. Xiao, H. Gao, L. Guo, J. Xie, G. Wang, R. Jiang, Z. Gao, Q. Jin, J. Wang and B. Cao (2020). "Clinical features of patients infected with 2019 novel coronavirus in Wuhan, China." The Lancet (British edition) **395**(10223): 497-506.

Huang, J., J. J. Burston, L. Li, S. Ashraf, P. I. Mapp, A. J. Bennett, S. Ravipati, P. Pousinis, D. A. Barrett, B. E. Scammell and V. Chapman (2017). "Targeting the D-series resolvin receptor system for the treatment of osteoarthritic pain."

Huang, J., J. J. Burston, L. Li, S. Ashraf, P. I. Mapp, A. J. Bennett, S. Ravipati, P. Pousinis, D. A. Barrett, B. E. Scammell and V. Chapman (2017). "Targeting the D Series Resolvin Receptor System for the Treatment of Osteoarthritis Pain." Arthritis & rheumatology (Hoboken, N.J.) **69**(5): 996-1008.

Huang, L., C.-F. Wang, C. N. Serhan and G. Strichartz (2011). "Enduring prevention and transient reduction of postoperative pain by intrathecal resolvin D1." Pain (Amsterdam) **152**(3): 557-565.

Hulse, R. P., N. Beazley-Long, J. Hua, H. Kennedy, J. Prager, H. Bevan, Y. Qiu, E. S. Fernandes, M. V. Gammons, K. Ballmer-Hofer, A. C. Gittenberger de Groot, A. J. Churchill, S. J. Harper, S. D. Brain, D. O. Bates and L. F. Donaldson (2014). "Regulation of alternative VEGF-A mRNA splicing is a therapeutic target for analgesia." Neurobiology of Disease **71**(1): 245-259.

Hwang, S.-M., G. Chung, Y. H. Kim and C.-K. Park (2019). "The role of maresins in inflammatory pain: Function of macrophages in wound regeneration." International journal of molecular sciences **20**(23): 5849.

Hwang, S. H., K. Wagner, J. Xu, J. Yang, X. Li, Z. Cao, C. Morisseau, K. S. S. Lee and B. D. Hammock (2017). "Chemical synthesis and biological evaluation of ω-hydroxy polyunsaturated fatty acids." Bioorganic & medicinal chemistry letters **27**(3): 620-625.

Hwang, S. W., H. Cho, J. Kwak, S.-Y. Lee, C.-J. Kang, J. Jung, S. Cho, K. H. Min, Y.-G. Suh, D. Kim and U. Oh (2000). "Direct Activation of Capsaicin Receptors by Products of Lipoxygenases: Endogenous Capsaicin-Like Substances." Proceedings of the National Academy of Sciences - PNAS **97**(11): 6155-6160.

Inceoglu, B., A. Bettaieb, C. A. Trindade Da Silva, K. S. S. Lee, F. G. Haj and B. D. Hammock (2015). "Endoplasmic reticulum stress in the peripheral nervous system is a significant driver of neuropathic pain." Proceedings of the National Academy of Sciences - PNAS **112**(29): 9082-9087.

Inceoglu, B., S. L. Jinks, K. R. Schmelzer, T. Waite, I. H. Kim and B. D. Hammock (2006). "Inhibition of soluble epoxide hydrolase reduces LPS-induced thermal hyperalgesia and mechanical allodynia in a rat model of inflammatory pain." Life sciences (1973) **79**(24): 2311-2319.

Inceoglu, B., S. L. Jinks, A. Ulu, C. M. Hegedus, K. Georgi, K. R. Schmelzer, K. Wagner, P. D. Jones, C. Morisseau and B. D. Hammock (2008). "Soluble epoxide hydrolase and epoxyeicosatrienoic acids modulate two distinct analgesic pathways." Proceedings of the National Academy of Sciences - PNAS **105**(48): 18901-18906.

Inceoglu, B., K. R. Schmelzer, C. Morisseau, S. L. Jinks and B. D. Hammock (2007). "Soluble epoxide hydrolase inhibition reveals novel biological functions of epoxyeicosatrienoic acids (EETs)." Prostaglandins & other lipid mediators **82**(1): 42-49.

Inceoglu, B., K. Wagner, N. H. Schebb, C. Morisseau, S. L. Jinks, A. Ulu, C. Hegedus, T. Rose, R. Brosnan and B. D. Hammock (2011). "Analgesia mediated by soluble epoxide hydrolase inhibitors is dependent on cAMP." Proceedings of the National Academy of Sciences - PNAS **108**(12): 5093-5097.

Ishikawa, M., K. Maekawa, K. Saito, Y. Senoo, M. Urata, M. Murayama, Y. Tajima, Y. Kumagai and Y. Saito (2014). "Plasma and serum lipidomics of healthy white adults shows characteristic profiles by subjects' gender and age." PloS one **9**(3): e91806-e91806.

Jang, Y., M. Kim and S. W. Hwang (2020). "Molecular mechanisms underlying the actions of arachidonic acid-derived prostaglandins on peripheral nociception." Journal of neuroinflammation **17**(1): 30-30.

Jayaraj, R., C. Kumarasamy, S. S. Shetty, R. Ram M and P. Shaw (2020). "Clinical and conceptual comments on "Risk factors of critical & mortal COVID-19 cases: A systematic literature review and meta-analysis"." The Journal of infection **81**(4): 647-679.

Ji, R.-R., J. Y. Park, C. N. Serhan, T. Liu, R. Yang, Z.-Z. Xu, L. Zhang and T. Berta (2010). "Resolvins RvE1 and RvD1 attenuate inflammatory pain via central and peripheral actions." Nature medicine **16**(5): 592-597.

Jin, J., Y. Xie, C. Shi, J. Ma, Y. Wang, L. Qiao, K. Li and T. Sun (2020). "Corrigendum: Lipoxin A4 Inhibits NLRP3 Inflammasome Activation in Rats With Non-compressive Disc Herniation Through the JNK1/Beclin-1/PI3KC3 Pathway." Frontiers in neuroscience **14**: 608184-608184.

Johnson, V. L. B. A. S. H. and D. J. Hunter (2014). "The epidemiology of osteoarthritis." Best practice & research. Clinical rheumatology **28**(1): 5-15.

Kanda, H., K. Kobayashi, H. Yamanaka and K. Noguchi (2013). "COX-1-dependent prostaglandin D2 in microglia contributes to neuropathic pain via DP2 receptor in spinal neurons." Glia **61**(6): 943-956.

Karaba, S. M., G. Jones, T. Helsel, L. L. Smith, R. Avery, K. Dzintars, A. B. Salinas, S. C. Keller, J. L. Townsend, E. Klein, J. Amoah, B. T. Garibaldi, S. E. Cosgrove and V. Fabre

(2021). "Prevalence of Co-infection at the Time of Hospital Admission in COVID-19 Patients, A Multicenter Study." Open forum infectious diseases **8**(1): ofaa578-ofaa578.

Karu, N., A. Kindt, L. Lamont, A. J. van Gammeren, A. A. M. Ermens, A. C. Harms, L. Portengen, R. C. H. Vermeulen, W. A. Dik, A. W. Langerak, V. H. J. van der Velden and T. Hankemeier (2022). "Plasma Oxylipins and Their Precursors Are Strongly Associated with COVID-19 Severity and with Immune Response Markers." Metabolites **12**(7): 619.

Kashfi, K., M. Chattopadhyay and R. Kodela (2015). "NOSH-sulindac (AVT-18A) is a novel nitric oxide- and hydrogen sulfide-releasing hybrid that is gastrointestinal safe and has potent anti-inflammatory, analgesic, antipyretic, anti-platelet, and anti-cancer properties." Redox biology **6**: 287-296.

Kaza, M., M. Karaźniewicz-Łada, K. Kosicka, A. Siemiątkowska and P. J. Rudzki (2019). "Bioanalytical method validation: new FDA guidance vs. EMA guideline. Better or worse?" Journal of pharmaceutical and biomedical analysis **165**: 381-385.

Kelly, S., R. J. Chapman, S. Woodhams, D. R. Sagar, J. Turner, J. J. Burston, C. Bullock, K. Paton, J. Huang, A. Wong, D. F. McWilliams, B. N. Okine, D. A. Barrett, G. J. Hathway, D. A. Walsh and V. Chapman (2015). "Increased function of pronociceptive TRPV1 at the level of the joint in a rat model of osteoarthritis pain." Annals of the rheumatic diseases **74**(1): 252-259.

Kenneth, E. R., M. Monty, A. S. David, H. E. Ali, H. W. Andrew, U. Jacqueline, M. B. Teresa, A. M. Philip, J. Y. Daehan, A. M. Daniel, F. O. Dale, R. S. Martin, J. A. Nitin, P. B. James, B. Jane, M. D. Anne, C. C. Charles, R. T. Isaiah, C. B. Scott, L. M. Lyle and S. H. Richard (2021). "Severe immunosuppression and not a cytokine storm characterizes COVID-19 infections." JCI insight **5**(17).

Khasabova, I. A., S. G. Khasabov, J. K. Olson, M. L. Uhelski, A. H. Kim, A. M. Albino-Ramírez, C. L. Wagner, V. S. Seybold and D. A. Simone (2019). "Pioglitazone, a PPARγ agonist, reduces cisplatin-evoked neuropathic pain by protecting against oxidative stress." Pain (Amsterdam) **160**(3): 688-701.

Kodela, R., M. Chattopadhyay, C. A. Velázquez-Martínez and K. Kashfi (2015). "NOSH-aspirin (NBS-1120), a novel nitric oxide- and hydrogen sulfide-releasing hybrid has enhanced chemo-preventive properties compared to aspirin, is gastrointestinal safe with all the classic therapeutic indications." Biochemical pharmacology **98**(4): 564-572.

Koelmel, J. P., C. Z. Ulmer, C. M. Jones, R. A. Yost and J. A. Bowden (2017). "Common cases of improper lipid annotation using high-resolution tandem mass spectrometry data and corresponding limitations in biological interpretation." BIOCHIMICA ET BIOPHYSICA ACTA-MOLECULAR AND CELL BIOLOGY OF LIPIDS **1862**(8): 766-770.

Koenis, D. S., I. Beegun, C. C. Jouvene, G. A. Aguirre, P. R. Souza, M. Gonzalez-Nunez, L. Ly, K. Pistorius, H. M. Kocher, W. Ricketts, G. Thomas, M. Perretti, G. Alusi, P. Pfeffer and J. Dalli (2021). "Disrupted Resolution Mechanisms Favor Altered Phagocyte Responses in Covid-19." Circulation research.

Köfeler, H. C., T. O. Eichmann, R. Ahrends, J. A. Bowden, N. Danne-Rasche, E. A. Dennis, M. Fedorova, W. J. Griffiths, X. Han, J. Hartler, M. Holčapek, R. Jirásko, J. P. Koelmel, C. S. Ejsing, G. Liebisch, Z. Ni, V. B. O'Donnell, O. Quehenberger, D. Schwudke, A. Shevchenko, M. J. O. Wakelam, M. R. Wenk, D. Wolrab and K. Ekroos (2021). "Quality control requirements for the correct annotation of lipidomics data." Nature communications **12**(1): 1-4.

Köfeler, H. C., A. Fauland, G. N. Rechberger and M. Trötzmüller (2012). "Mass spectrometry based lipidomics: An overview of technological platforms." Metabolites **2**(1): 19-38.

Kronke, G., J. Katzenbeisser, S. Uderhardt, M. M. Zaiss, C. Scholtysek, G. Schabbauer, A. Zarbock, M. I. Koenders, R. Axmann, J. Zwerina, H. W. Baenckler, W. van den Berg, R. E. Voll, H. Kuhn, L. A. B. Joosten and G. Schett (2009). "12/15-Lipoxygenase Counteracts Inflammation and Tissue Damage in Arthritis." The Journal of immunology (1950) **183**(5): 3383-3389.

Kundu, S., T. Roome, A. Bhattacharjee, K. A. Carnevale, V. P. Yakubenko, R. Zhang, S. H. Hwang, B. D. Hammock and M. K. Cathcart (2013). "Metabolic products of soluble epoxide hydrolase are essential for monocyte chemotaxis to MCP-1 in vitro and in vivo." Journal of lipid research **54**(2): 436.

Lakkappa, N., P. T. Krishnamurthy, B. D. Hammock, D. Velmurugan and M. M. S. Bharath (2016). "Possible role of Epoxyeicosatrienoic acid in prevention of oxidative stress mediated neuroinflammation in Parkinson disorders." Medical Hypotheses **93**: 161-165.

Lawrence, T. and D. W. Gilroy (2007). "Chronic inflammation: a failure of resolution?" International journal of experimental pathology **88**(2): 85-94.

Lazaar, A. L., L. Yang, R. L. Boardley, N. S. Goyal, J. Robertson, S. J. Baldwin, D. E. Newby, I. B. Wilkinson, R. Tal-Singer, R. J. Mayer and J. Cheriyan (2016). "Pharmacokinetics, pharmacodynamics and adverse event profile of GSK2256294, a novel soluble epoxide hydrolase inhibitor." British journal of clinical pharmacology **81**(5): 971-979.

Lazzaroni, M. and G. Bianchi Porro (2004). "Gastrointestinal side-effects of traditional non-steroidal anti-inflammatory drugs and new formulations." Alimentary pharmacology & therapeutics **20**(2): 48-58.

Li, Q., Y. Tian, Z. F. Wang, S. B. Liu, W. L. Mi, H. J. Ma, G. C. Wu, J. Wang, J. Yu and Y. Q. Wang (2013). "Involvement of the spinal NALP1 inflammasome in neuropathic pain and aspirin-triggered-15-epi-lipoxin A4 induced analgesia." Neuroscience **254**: 230-240.

Liakh, I., A. Pakiet, T. Sledzinski and A. Mika (2020). "Methods of the analysis of oxylipins in biological samples." Molecules (Basel, Switzerland) **25**(2): 349.

Lieberthal, J., N. Sambamurthy and C. R. Scanzello (2015). "Inflammation in joint injury and post-traumatic osteoarthritis." Osteoarthritis and cartilage **23**(11): 1825-1834.

Liebisch, G., C. S. Ejsing and K. Ekroos (2015). "Identification and annotation of lipid species in metabolomics studies need improvement." Clinical chemistry (Baltimore, Md.) **61**(12): 1542-1544.

Lima-Garcia, J. F., R. C. Dutra, K. da Silva, E. M. Motta, M. M. Campos and J. B. Calixto (2011). "The precursor of resolvin D series and aspirin-triggered resolvin D1 display anti-hyperalgesic properties in adjuvant-induced arthritis in rats." British journal of pharmacology **164**(2): 278-293.

Liu, P., A. Okun, J. Ren, R.-c. Guo, M. H. Ossipov, J. Xie, T. King and F. Porreca (2011). "Ongoing pain in the MIA model of osteoarthritis." Neuroscience letters **493**(3): 72-75.

Liu, X., Z.-Y. Qian, F. Xie, W. Fan, J. W. Nelson, X. Xiao, S. Kaul, A. P. Barnes and N. J. Alkayed (2017). "Functional screening for G protein-coupled receptor targets of 14,15-epoxyeicosatrienoic acid." Prostaglandins and Other Lipid Mediators **132**: 31-40.

Liu, Y., Y. Zhang, K. Schmelzer, T.-S. Lee, X. Fang, Y. Zhu, A. A. Spector, S. Gill, C. Morisseau, B. D. Hammock and J. Y. J. Shyy (2005). "The Antiinflammatory Effect of Laminar Flow: The Role of PPARγ, Epoxyeicosatrienoic Acids, and Soluble Epoxide Hydrolase." Proceedings of the National Academy of Sciences - PNAS **102**(46): 16747-16752.

Long, H., Q. Liu, H. Yin, K. Wang, N. Diao, Y. Zhang, J. Lin and A. Guo (2022). "Prevalence Trends of Site-Specific Osteoarthritis From 1990 to 2019: Findings From the Global Burden of Disease Study 2019." Arthritis & rheumatology (Hoboken, N.J.) **74**(7): 1172-1183.

Lu, Y., S. Hong, E. Tjonahen and C. N. Serhan (2005). "Mediator-lipidomics: databases and search algorithms for PUFA-derived mediators." Journal of lipid research **46**(4): 790-802.

Luo, X., Y. Gu, X. Tao, C. N. Serhan and R.-R. Ji (2019). "Resolvin D5 Inhibits Neuropathic and Inflammatory Pain in Male But Not Female Mice: Distinct Actions of D-Series Resolvins in Chemotherapy-Induced Peripheral Neuropathy." Frontiers in pharmacology **10**: 745-745.

Luria, A., A. Bettaieb, Y. Xi, G. Shieh, H. C. Liu, H. Inoue, H. Tsai, J. D. Imig, F. Haj and B. D. Hammock (2011). "Soluble epoxide hydrolase deficiency alters pancreatic islet size and improves glucose homeostasis in a model of insulin resistance." Proceedings Of The National Academy Of Sciences Of The United States Of Ame **108**(22): 9038-9043.

Ma, W. and R. Quirion (2005). "Up-regulation of interleukin-6 induced by prostaglandin E2 from invading macrophages following nerve injury: an in vivo and in vitro study." Journal of neurochemistry **93**(3): 664-673.

Mahmoudian, A., L. S. Lohmander, A. Mobasheri, M. Englund and F. P. Luyten (2021). "Early-stage symptomatic osteoarthritis of the knee — time for action." Nature reviews. Rheumatology **17**(10): 621.

Mainka, M., C. Dalle, M. Pétéra, J. Dalloux-Chioccioli, N. Kampschulte, A. I. Ostermann, M. Rothe, J. Bertrand-Michel, J. W. Newman, C. Gladine and N. H. Schebb (2020). "Harmonized procedures lead to comparable quantification of total oxylipins across laboratories." Journal of lipid research **61**(11): 1424-1436.

Majewski, M., H. Susanne and S. Klaus (2006). "Epidemiology of athletic knee injuries: A 10-year study." The knee **13**(3): 184-188.

Mansouri, M. T., B. Naghizadeh, B. Ghorbanzadeh, H. Rajabi and M. Pashmforoush (2017). "Pharmacological evidence for systemic and peripheral antinociceptive activities of pioglitazone in the rat formalin test: Role of PPARγ and nitric oxide." European journal of pharmacology **805**: 84-92.

Martini, A. C., T. Berta, S. Forner, G. Chen, A. F. Bento, R.-R. Ji and G. A. Rae (2016). "Lipoxin A4 inhibits microglial activation and reduces neuroinflammation and neuropathic pain after spinal cord hemisection." Journal of neuroinflammation **13**(1): 75-75.

McReynolds, C. B., I. Cortes-Puch, R. Ravindran, I. H. Khan, B. G. Hammock, P.-a. B. Shih, B. D. Hammock and J. Yang (2021). "Plasma Linoleate Diols Are Potential Biomarkers for Severe COVID-19 Infections." Frontiers in physiology **12**: 663869-663869.

McReynolds, C. B., S. H. Hwang, J. Yang, D. Wan, K. Wagner, C. Morisseau, D. Li, W. K. Schmidt and B. D. Hammock (2019). "Pharmaceutical Effects of Inhibiting the Soluble Epoxide Hydrolase in Canine Osteoarthritis." Frontiers in Pharmacology **10**(MAY).

McReynolds, C. B., S. H. Hwang, J. Yang, D. Wan, K. Wagner, C. Morisseau, D. Li, W. K. Schmidt and B. D. Hammock (2019). "Pharmaceutical effects of inhibiting the soluble epoxide hydrolase in canine osteoarthritis." Frontiers in pharmacology **10**(MAY): 533-533.

Meesawatsom, P., J. Burston, G. Hathway, A. Bennett and V. Chapman (2016). "Inhibitory effects of aspirin-triggered resolvin D1 on spinal nociceptive processing in rat pain models." Journal of neuroinflammation **13**(1): 233-233.

Merad, M. and J. C. Martin (2020). "Pathological inflammation in patients with COVID-19: a key role for monocytes and macrophages." Nature reviews. Immunology **20**(6): 355-362.

Momin, A., H. Cadiou, A. Mason and P. A. McNaughton (2008). "Role of the hyperpolarization-activated current Ih in somatosensory neurons." The Journal of physiology **586**(24): 5911-5929.

Moren, X., M. Lhomme, A. Bulla, J.-C. Sanchez, A. Kontush and R. W. James (2016). "Proteomic and lipidomic analyses of paraoxonase defined high density lipoprotein particles: Association of paraoxonase with the anti-coagulant, protein S." Proteomics. Clinical applications **10**(3): 230-238.

Morgenweck, J., O. S. Abdel-aleem, K. C. McNamara, R. R. Donahue, M. Z. Badr and B. K. Taylor (2010). "Activation of peroxisome proliferator-activated receptor γ in brain inhibits inflammatory pain, dorsal horn expression of Fos, and local edema." Neuropharmacology **58**(2): 337-345.

Morgenweck, J., R. B. Griggs, R. R. Donahue, J. E. Zadina and B. K. Taylor (2013). "PPARγ activation blocks development and reduces established neuropathic pain in rats." Neuropharmacology **70**: 236-246.

Morin, C., M. Sirois, V. Echave, M. M. Gomes and E. Rousseau (2008). "EET displays anti-inflammatory effects in TNF-alpha stimulated human bronchi: putative role of CPI-17." American journal of respiratory cell and molecular biology **38**(2): 192.

Morisseau, C. and B. D. Hammock (2013). "Impact of Soluble Epoxide Hydrolase and Epoxyeicosanoids on Human Health." Annual Review of Pharmacology and Toxicology **53**(1): 37-58.

Morisseau, C., B. Inceoglu, K. Schmelzer, H.-J. Tsai, S. L. Jinks, C. M. Hegedus and B. D. Hammock (2010). "Naturally occurring monoepoxides of eicosapentaenoic acid and docosahexaenoic acid are bioactive antihyperalgesic lipids[S]." Journal of lipid research **51**(12): 3481-3490.

Moriyama, T., T. Higashi, K. Togashi, T. Iida, E. Segi, Y. Sugimoto, T. Tominaga, S. Narumiya and M. Tominaga (2005). "Sensitization of TRPV1 by EP1 and IP Reveals Peripheral Nociceptive Mechanism of Prostaglandins." Molecular pain **1**(1): 3-3.

Murray, C. J. L., R. M. Barber, K. J. Foreman, A. A. Ozgoren, F. Abd-Allah, S. F. Abera, V. Aboyans, J. P. Abraham, I. Abubakar, L. J. Abu-Raddad, N. M. Abu-Rmeileh, T. Achoki, I. N. Ackerman, Z. Ademi, A. K. Adou, J. C. Adsuar, A. Afshin, E. E. Agardh, S. S. Alam, D. Alasfoor, M. I. Albittar, M. A. Alegretti, Z. A. Alemu, R. Alfonso-Cristancho, S. Alhabib, R. Ali, F. Alla, P. Allebeck, M. A. Almazroa, U. Alsharif, E. Alvarez, N. Alvis-Guzman, A. T. Amare, E. A. Ameh, H. Amini, W. Ammar, H. R. Anderson, B. O. Anderson, C. A. T. Antonio, P. Anwari, J. Arnlov, V. S. A. Arsenijevic, A. Artaman, R. J. Asghar, R. Assadi, L. S. Atkins, M. A. Avila, B. Awuah, H. W. Hoek and A. Singh (2015). "Global, regional, and national disability-adjusted life years (DALYs) for 306 diseases and injuries and healthy life expectancy (HALE) for 188 countries, 1990-2013: quantifying the epidemiological transition." The Lancet (British edition) **386**(10009): 2145-2191.

Mustonen, A.-M. and P. Nieminen (2021). "Fatty Acids and Oxylipins in Osteoarthritis and Rheumatoid Arthritis—a Complex Field with Significant Potential for Future Treatments." Current rheumatology reports **23**(6): 41.

Narumiya, S. and G. A. FitzGerald (2001). "Genetic and pharmacological analysis of prostanoid receptor function." The Journal of clinical investigation **108**(1): 25-30.

Needleman, P., J. Truk, B. A. Jakschik, A. R. Morrison and J. B. Lefkowith (1986). "Arachidonic Acid Metabolism." Annual review of biochemistry **55**(1): 69-102.

Node, K., Y. Huo, X. Ruan, B. Yang, M. Spiecker, K. Ley, D. C. Zeldin and J. K. Liao (1999). "Anti-Inflammatory Properties of Cytochrome P450 Epoxygenase-Derived Eicosanoids." Science (American Association for the Advancement of Science) **285**(5431): 1276-1279.

Norris, P. C., A. C. Skulas-Ray, I. Riley, C. K. Richter, P. M. Kris-Etherton, G. L. Jensen, C. N. Serhan and K. R. Maddipati (2018). "Identification of specialized pro-resolving mediator clusters from healthy adults after intravenous low-dose endotoxin and omega-3 supplementation: a methodological validation." Scientific reports **8**(1): 18050-18013.

Norwood, S., J. Liao, B. D. Hammock and G.-Y. Yang (2010). "Epoxyeicosatrienoic acids and soluble epoxide hydrolase: potential therapeutic targets for inflammation and its induced carcinogenesis." American journal of translational research **2**(4): 447.

Okubo, M., H. Yamanaka, K. Kobayashi and K. Noguchi (2010). "Leukotriene synthases and the receptors induced by peripheral nerve injury in the spinal cord contribute to the generation of neuropathic pain." Glia **58**(5): 599-610.

Pal, A., K. M. Gowdy, K. J. Oestreich, M. Beck and S. R. Shaikh (2020). "Obesity-Driven Deficiencies of Specialized Pro-resolving Mediators May Drive Adverse Outcomes During SARS-CoV-2 Infection." Frontiers in immunology **11**: 1997.

Palmas, F., J. Clarke, R. A. Colas, E. A. Gomez, A. Keogh, M. Boylan, N. McEvoy, O. J. McElvaney, O. McElvaney, R. Alalqam, N. G. McElvaney, G. F. Curley and J. Dalli (2021). "Dysregulated plasma lipid mediator profiles in critically ill COVID-19 patients." PloS one **16**(8): e0256226-e0256226.

Panigrahy, D., M. M. Gilligan, S. Huang, A. Gartung, I. Cortés-Puch, P. J. Sime, R. P. Phipps, C. N. Serhan and B. D. Hammock (2020). "Inflammation resolution: a dual-pronged approach to averting cytokine storms in COVID-19?" Cancer and metastasis reviews **39**(2): 337-340.

Park, C.-K., N. Lü, Z.-Z. Xu, T. Liu, C. N. Serhan and R.-R. Ji (2011). "Resolving TRPV1- and TNF-α-mediated spinal cord synaptic plasticity and inflammatory pain with neuroprotectin D1." The Journal of neuroscience **31**(42): 15072-15085.

Park, C.-K., Z.-Z. Xu, T. Liu, N. Lü, C. N. Serhan and R.-R. Ji (2011). "Resolvin D2 is a potent endogenous inhibitor for transient receptor potential subtype V1/A1, inflammatory pain, and spinal cord synaptic plasticity in mice: Distinct roles of resolvin D1, D2, and E1." The Journal of neuroscience **31**(50): 18433-18438.

Park, J., J. Choi, D.-D. Kim, S. Lee, B. Lee, Y. Lee, S. Kim, S. Kwon, M. Noh, M.-O. Lee, Q.-V. Le and Y.-K. Oh (2021). "Bioactive lipids and their derivatives in biomedical applications." Biomolecules & therapeutics **29**(5): 465-482.

Penzo, D., V. Petronilli, A. Angelin, C. Cusan, R. Colonna, L. Scorrano, F. Pagano, M. Prato, F. Di Lisa and P. Bernardi (2004). "Arachidonic Acid Released by Phospholipase A2 Activation Triggers Ca2+-dependent Apoptosis through the Mitochondrial Pathway." The Journal of biological chemistry **279**(24): 25219-25225.

Pettipher, R. (2008). "The roles of the prostaglandin D 2 receptors DP 1 and CRTH2 in promoting allergic responses." British journal of pharmacology **153**(1): S191-S199.

Pitchford, S. and J. D. Levine (1991). "Prostaglandins sensitize nociceptors in cell culture." Neuroscience letters **132**(1): 105-108.

Pomonis, J. D., J. M. Boulet, S. L. Gottshall, S. Phillips, R. Sellers, T. Bunton and K. Walker (2005). "Development and pharmacological characterization of a rat model of osteoarthritis pain." Pain (Amsterdam) **114**(3): 339-346.

Pyrillou, K., A.-D. Chairakaki, C. Tamvakopoulos and E. Andreakos (2018). "Dexamethasone induces ω3-derived immunoresolvents driving resolution of allergic airway inflammation." Journal of allergy and clinical immunology **142**(2): 691-695.e694.

Qiu, H., N. Li, J. Liu, T. Harris, B. D. Hammock and N. Chiamvimonvat (2011). "Soluble Epoxide Hydrolase Inhibitors and Heart Failure." Cardiovascular Therapeutics **29**(2): 99-111.

Quan-Xin, F., F. Fan, F. Xiang-Ying, L. Shu-Jun, W. Shi-Qi, L. Zhao-Xu, Z. Xu-Jie, Z. Qing-Chuan and W. Wei (2012). "Resolvin D1 reverses chronic pancreatitis-induced mechanical allodynia, phosphorylation of NMDA receptors, and cytokines expression in the thoracic spinal dorsal horn." BMC gastroenterology **12**(1): 148-148.

Ramon, S., S. F. Baker, J. M. Sahler, N. Kim, E. A. Feldsott, C. N. Serhan, L. Martínez-Sobrido, D. J. Topham and R. P. Phipps (2014). "The specialized proresolving mediator 17-HDHA enhances the antibody-mediated immune response against influenza virus: a new class of adjuvant?" The Journal of immunology (1950) **193**(12): 6031-6040.

Ramon, S., F. Gao, C. N. Serhan and R. P. Phipps (2012). "Specialized proresolving mediators enhance human B cell differentiation to antibody-secreting cells." The Journal of immunology (1950) **189**(2): 1036-1042.

Rand, A. A., B. Barnych, C. Morisseau, T. Cajka, K. S. S. Lee, D. Panigrahy and B. D. Hammock (2017). "Cyclooxygenase-derived proangiogenic metabolites of epoxyeicosatrienoic acids." Proceedings of the National Academy of Sciences - PNAS **114**(17): 4370-4375.

Recchiuti, A., S. Patruno, D. Mattoscio, E. Isopi, A. Pomilio, A. Lamolinara, M. Iezzi, R. Pecce and M. Romano (2021). "Resolvin D1 and D2 reduce SARS-CoV-2-induced inflammatory responses in cystic fibrosis macrophages." The FASEB journal **35**(4): e21441-n/a.

Recchiuti, A. and C. N. Serhan (2012). "Pro-resolving lipid mediators (SPMs) and their actions in regulating miRNA in novel resolution circuits in inflammation." Frontiers in immunology **3**: 298-298.

Regidor, P.-A., F. G. Santos, J. M. Rizo and F. M. Egea (2020). "Pro resolving inflammatory effects of the lipid mediators of omega 3 fatty acids and its implication in SARS COVID-19." Medical hypotheses **145**: 110340-110340.

Ricciotti, E. and G. A. FitzGerald (2011). "Prostaglandins and Inflammation." Arteriosclerosis, thrombosis, and vascular biology **31**(5): 986-1000.

Robertson-Plouch, C., J. R. Stille, P. Liu, S. Malcolm, D. Brown, M. Warner and M. J. Fisher (2017). "SAT0502 A randomized, placebo-controlled, proof-of-concept efficacy study of a microsomal prostaglandin e synthase-1 (MPGES1) inhibitor and a prostaglandin E receptor

(EP4) antagonist in the treatment of canine osteoarthritis pain." Annals of the rheumatic diseases **76**(Suppl 2): 965.

Robinson, W. H., C. M. Lepus, Q. Wang, H. Raghu, R. Mao, T. M. Lindstrom and J. Sokolove (2016). "Low-grade inflammation as a key mediator of the pathogenesis of osteoarthritis." Nature reviews. Rheumatology **12**(10): 580-592.

Rodriguez, A. R. and B. W. Spur (2015). "First total synthesis of the macrophage derived anti-inflammatory and pro-resolving lipid mediator Maresin 2." Tetrahedron letters **56**(1): 256-259.

Rodríguez, L. A. G., A. Lanas, M. Soriano-Gabarró, P. Vora and L. C. Soriano (2020). "Effect of proton pump inhibitors on risks of upper and lower gastrointestinal bleeding among users of low-dose aspirin: A population-based observational study." Journal of clinical medicine **9**(4): 928.

Roman, R. J. (2002). "P-450 Metabolites of Arachidonic Acid in the Control of Cardiovascular Function." Physiological reviews **82**(1): 131-185.

Romashko, M., J. Schragenheim, N. G. Abraham and J. A. McClung (2016). "Epoxyeicosatrienoic Acid as Therapy for Diabetic and Ischemic Cardiomyopathy." Trends in pharmacological sciences (Regular ed.) **37**(11): 945-962.

Roos, E. M., H. P. Roos, L. S. Lohmander, C. Ekdahl and B. D. Beynnon (1998). "Knee Injury and Osteoarthritis Outcome Score (KOOS) - Development of a self-administered outcome measure." The journal of orthopaedic and sports physical therapy **28**(2): 88-96.

Rose, T. E., C. Morisseau, J.-Y. Liu, B. Inceoglu, P. D. Jones, J. R. Sanborn and B. D. Hammock (2010). "1-Aryl-3-(1-acylpiperidin-4-yl)urea inhibitors of human and murine soluble epoxide hydrolase: structure-activity relationships, pharmacokinetics, and reduction of inflammatory pain." Journal of medicinal chemistry **53**(19): 7067.

Rose, T. E., C. Morisseau, J.-Y. Liu, B. Inceoglu, P. D. Jones, J. R. Sanborn and B. D. Hammock (2010). "1-Aryl-3-(1-acylpiperidin-4-yl)urea Inhibitors of Human and Murine Soluble Epoxide Hydrolase: Structure−Activity Relationships, Pharmacokinetics, and Reduction of Inflammatory Pain." Journal of medicinal chemistry **53**(19): 7067-7075.

Rund, K. M., F. Nolte, J. Doricic, R. Greite, S. Schott, R. Lichtinghagen, F. Gueler and N. H. Schebb (2020). "Clinical blood sampling for oxylipin analysis - effect of storage and pneumatic tube transport of blood on free and total oxylipin profile in human plasma and serum." Analyst (London) **145**(6): 2378-2388.

Sagar, D. R., J. J. Burston, G. J. Hathway, S. G. Woodhams, R. G. Pearson, A. J. Bennett, D. A. Kendall, B. E. Scammell and V. Chapman (2011). "The Contribution of Spinal Glial

Cells to Chronic Pain Behaviour in the Monosodium Iodoacetate Model of Osteoarthritic Pain." Molecular Pain **7**(1).

Sala, A., G. Folco and R. C. Murphy (2010). "Transcellular biosynthesis of eicosanoids." Pharmacol Rep **62**(3): 503-510.

Salmon, J. A. and G. A. Higgs (1987). "Prostaglandins and leukotrienes as inflammatory mediators." British medical bulletin **43**(2): 285-296.

Samokhvalov, V., J. Vriend, K. L. Jamieson, M. K. Akhnokh, R. Manne, J. R. Falck and J. M. Seubert (2014). "PPARÎ³ signaling is required for mediating EETs protective effects in neonatal cardiomyocytes exposed to LPS." Frontiers in pharmacology **5**.

Sandhaus, S. and A. G. Swick (2021). "Specialized proresolving mediators in infection and lung injury." BioFactors (Oxford) **47**(1): 6-18.

Sasaki, F. and T. Yokomizo (2019). "The leukotriene receptors as therapeutic targets of inflammatory diseases." International immunology **31**(9): 607-615.

Schmelzer, K. R., L. Kubala, J. W. Newman, I.-H. Kim, J. P. Eiserich and B. D. Hammock (2005). "Soluble Epoxide Hydrolase Is a Therapeutic Target for Acute Inflammation." Proceedings of the National Academy of Sciences - PNAS **102**(28): 9772-9777.

Schnitzer, T. J. M. D. P., M. C. M. D. M. P. H. Hochberg, C. E. M. D. Marrero, B. M. D. Duquesroix, H. M. Frayssinet and M. M. D. P. Beekman (2011). "Efficacy and Safety of Naproxcinod in Patients with Osteoarthritis of the Knee: A 53-Week Prospective Randomized Multicenter Study." Seminars in arthritis and rheumatism **40**(4): 285-297.

Schwarz, B., L. Sharma, L. Roberts, X. Peng, S. Bermejo, I. Leighton, A. C. Massana, S. Farhadian, A. I. Ko, I. T. Yale, C. S. D. Cruz and C. M. Bosio (2020). "Severe SARS-CoV-2 infection in humans is defined by a shift in the serum lipidome resulting in dysregulation of eicosanoid immune mediators." medRxiv.

Sekiguchi, M., K. Otoshi, S.-I. Kikuchi and S.-I. Konno (2011). "Analgesic effects of prostaglandin E2 receptor subtype EP1 receptor antagonist: Experimental study of application of nucleus pulposus." Spine (Philadelphia, Pa. 1976) **36**(22): 1829-1834.

Serhan, C. N. (2017). "Treating inflammation and infection in the 21st century: new hints from decoding resolution mediators and mechanisms." The FASEB journal **31**(4): 1273-1288.

Serhan, C. N., J. Dalli, S. Karamnov, A. Choi, C. K. Park, Z. Z. Xu, R. R. Ji, M. Zhu and N. A. Petasis (2012). "Macrophage proresolving mediator maresin 1 stimulates tissue regeneration and controls pain." The FASEB journal **26**(4): 1755-1765.

Serhan, C. N., K. Gotlinger, S. Hong, Y. Lu, J. Siegelman, T. Baer, R. Yang, S. P. Colgan and N. A. Petasis (2006). "Anti-Inflammatory Actions of Neuroprotectin D1/Protectin D1 and Its Natural Stereoisomers: Assignments of Dihydroxy-Containing Docosatrienes." Journal of Immunology **176**(3): 1848-1859.

Serhan, C. N., S. Hong, K. Gronert, S. P. Colgan, P. R. Devchand, G. Mirick and R.-L. Moussignac (2002). "Resolvins: A family of bioactive products of omega-3 fatty acid transformation circuits initiated by aspirin treatment that counter proinflammation signals." The Journal of experimental medicine **196**(8): 1025-1037.

Serhan, C. N. and B. D. Levy (2018). "Resolvins in inflammation: emergence of the pro-resolving superfamily of mediators." The Journal of clinical investigation **128**(7): 2657-2669.

Serhan, C. N. and N. A. Petasis (2011). "Resolvins and Protectins in Inflammation Resolution." Chemical reviews **111**(10): 5922-5943.

Serhan, C. N. and B. Samuelsson (1988). "Lipoxins: a new series of eicosanoids (biosynthesis, stereochemistry, and biological activities)." Adv Exp Med Biol **229**: 1-14.

Serhan, C. N., R. Yang, K. Martinod, K. Kasuga, P. S. Pillai, T. F. Porter, S. F. Oh and M. Spite (2009). "Maresins: Novel macrophage mediators with potent antiinflammatory and proresolving actions." The Journal of experimental medicine **206**(1): 15-23.

Sharma, A., P. Kudesia, Q. Shi and R. Gandhi (2016). "Anxiety and depression in patients with osteoarthritis: Impact and management challenges." Open access rheumatology: research and reviews **8**: 103-113.

Shen, T. Y. (1972). "Perspectives in Nonsteroidal Anti-inflammatory Agents." Angewandte Chemie (International ed.) **11**(6): 460-472.

Sisignano, M., C. Angioni, N. Ferreiros, C.-D. Schuh, J. Suo, Y. Schreiber, J. M. Dawes, A. Antunes-Martins, D. L. H. Bennett, S. B. McMahon, G. Geisslinger and K. Scholich (2013). "Synthesis of lipid mediators during UVB-induced inflammatory hyperalgesia in rats and mice." PloS one **8**(12): e81228-e81228.

Smirnov, D., P. Mazin, M. Osetrova, E. Stekolshchikova and E. Khrameeva (2021). "The hitchhiker's guide to untargeted lipidomics analysis: Practical guidelines." Metabolites **11**(11): 713.

Spector, A. A., X. Fang, G. D. Snyder and N. L. Weintraub (2004). Epoxyeicosatrienoic acids (EETs): metabolism and biochemical function. **43:** 55-90.

Spector, A. A. and H. Kim (2015). "Cytochrome P-450 epoxygenase pathway of polyunsaturated fatty acid metabolism." Biochimica Et Biophysica Acta-Molecular And Cell Biology Of Lipids **1851**(4): 356-365.

Strassburg, K., A. M. L. Huijbrechts, K. Kortekaas, J. Lindeman, T. L. Pedersen, J. W. Newman, A. Dane, R. Berger, A. Brenkman, T. Hankemeier, J. P. M. van Duynhoven, E. Kalkhoven and R. Vreeken (2012). "Quantitative Profiling of Oxylipins through Comprehensive LC-MS/MS Analysis: Application in cardiac surgery." Analytical and bioanalytical chemistry **404**(5): 1413-1426.

Sullivan, L. C., T. A. Chavera, X. Gao, M. M. Pando and K. A. Berg (2017). "Regulation of δ opioid receptor-mediated signaling and antinociception in peripheral sensory neurons by arachidonic acid-dependent 12/15-lipoxygenase metabolites." The Journal of pharmacology and experimental therapeutics **362**(1): 200-209.

Swain, S., A. Kamps, J. Runhaar, A. Dell'Isola, A. Turkiewicz, D. Robinson, V. Strauss, C. Mallen, C.-F. Kuo, C. Coupland, M. Doherty, A. Sarmanova, D. Prieto-Alhambra, M. Englund, S. M. A. Bierma-Zeinstra and W. Zhang (2022). "Comorbidities in osteoarthritis (ComOA): a combined cross-sectional, case–control and cohort study using large electronic health records in four European countries." BMJ open **12**(4): e052816-e052816.

Swain, S., A. Sarmanova, C. Mallen, C. F. Kuo, C. Coupland, M. Doherty and W. Zhang (2020). "Trends in incidence and prevalence of osteoarthritis in the United Kingdom: findings from the Clinical Practice Research Datalink (CPRD)." Osteoarthritis and cartilage **28**(6): 792-801.

Taiwo, Y. O., L. K. Bjerknes, E. J. Goetzl and J. D. Levine (1989). "Mediation of primary afferent peripheral hyperalgesia by the cAMP second messenger system." Neuroscience **32**(3): 577-580.

Tam, Vincent C., O. Quehenberger, Christine M. Oshansky, R. Suen, Aaron M. Armando, Piper M. Treuting, Paul G. Thomas, Edward A. Dennis and A. Aderem (2013). "Lipidomic Profiling of Influenza Infection Identifies Mediators that Induce and Resolve Inflammation." Cell (Cambridge) **154**(1): 213-227.

Tang, S., M. Wan, W. Huang, R. C. Stanton and Y. Xu (2018). "Maresins: Specialized Proresolving Lipid Mediators and Their Potential Role in Inflammatory-Related Diseases." Mediators of inflammation **2018**: 2380319-2380318.

Tang, Y., J. Liu, D. Zhang, Z. Xu, J. Ji and C. Wen (2020). "Cytokine Storm in COVID-19: The Current Evidence and Treatment Strategies." Frontiers in immunology **11**: 1708-1708.

Teixeira, J. M., H. B. Abdalla, R. T. Basting, B. D. Hammock, M. H. Napimoga and J. T. Clemente-Napimoga (2020). "Peripheral soluble epoxide hydrolase inhibition reduces hypernociception and inflammation in albumin-induced arthritis in temporomandibular joint of rats." International immunopharmacology **87**: 106841-106841.

Thakare, R., Y. S. Chhonker, N. Gautam, A. Nelson, R. Casaburi, G. Criner, M. T. Dransfield, B. Make, K. K. Schmid, S. I. Rennard and Y. Alnouti (2018). "Simultaneous LC–MS/MS analysis of eicosanoids and related metabolites in human serum, sputum and BALF." Biomedical chromatography **32**(3): e4102-n/a.

Thomson, S. J., A. Askari and D. Bishop-Bailey (2012). "Anti-Inflammatory Effects of Epoxyeicosatrienoic Acids." International journal of vascular medicine **2012**: 605101-605107.

Tian, Y., M. Liu, Q.-L. Mao-Ying, H. Liu, Z.-F. Wang, M.-T. Zhang, J. Wang, Q. Li, S.-B. Liu, W.-L. Mi, H.-J. Ma, G.-C. Wu and Y.-Q. Wang (2015). "Early single Aspirin-triggered Lipoxin blocked morphine anti-nociception tolerance through inhibiting NALP1 inflammasome: Involvement of PI3k/Akt signaling pathway." Brain, behavior, and immunity **50**: 63-77.

Tighe, P. J., R. A. Urbanowicz, C. L. Fairclough, C. P. McClure, B. J. Thomson, N. Gomez, J. G. Chappell, T. Tsoleridis, M. Loose, M. Carlile, C. Moore, N. Holmes, F. Sang, D. Hrushikesh, G. Clark, N. Temperton, T. Brooks, J. K. Ball, W. L. Irving and A. W. Tarr (2020). "Potent anti-SARS-CoV-2 Antibody Responses are Associated with Better Prognosis in Hospital Inpatient COVID-19 Disease." MedRxiv

Turnbull, R. E., K. N. Sander, J. Turnbull, D. A. Barrett and A. H. Goodall (2022). "Profiling oxylipins released from human platelets activated through the GPVI collagen receptor." Prostaglandins & other lipid mediators **158**: 106607-106607.

Ulu, A., S. Appt, C. Morisseau, S. Hwang, P. Jones, T. Rose, H. Dong, J. Lango, J. Yang, H. Tsai, C. Miyabe, C. Fortenbach, M. Adams and B. Hammock (2012). "Pharmacokinetics and in vivo potency of soluble epoxide hydrolase inhibitors in cynomolgus monkeys." British Journal of Pharmacology **165**(5): 1401-1412.

Valdes, A. M., S. Ravipati, C. Menni, A. Abhishek, S. Metrustry, J. Harris, A. Nessa, F. M. K. Williams, T. D. Spector, M. Doherty, V. Chapman and D. A. Barrett (2017). "Association of the resolvin precursor 17-HDHA, but not D- or E- series resolvins, with heat pain sensitivity and osteoarthritis pain in humans."

Valdes, A. M., S. Ravipati, C. Menni, A. Abhishek, S. Metrustry, J. Harris, A. Nessa, F. M. K. Williams, T. D. Spector, M. Doherty, V. Chapman and D. A. Barrett (2017). "Association

of the resolvin precursor 17-HDHA, but not D-or E-series resolvins, with heat pain sensitivity and osteoarthritis pain in humans." Scientific reports **7**(1): 10748-10748.

Valdes, A. M., S. Ravipati, P. Pousinis, C. Menni, M. Mangino, A. Abhishek, V. Chapman, D. A. Barrett and M. Doherty (2018). "Omega-6 oxylipins generated by soluble epoxide hydrolase are associated with knee osteoarthritis." Journal of lipid research **59**(9): 1763.

Valdes, A. M., S. Ravipati, P. Pousinis, C. Menni, M. Mangino, A. Abhishek, V. Chapman, D. A. Barrett and M. Doherty (2018). "Omega-6 oxylipins generated by soluble epoxide hydrolase are associated with knee osteoarthritis."

Wagner, K., B. Inceoglu, H. Dong, J. Yang, S. H. Hwang, P. Jones, C. Morisseau and B. D. Hammock (2013). "Comparative efficacy of 3 soluble epoxide hydrolase inhibitors in rat neuropathic and inflammatory pain models." European journal of pharmacology **700**(1-3): 93-101.

Wagner, K., J. Yang, B. Inceoglu and B. D. Hammock (2014). "Soluble Epoxide Hydrolase Inhibition Is Antinociceptive in a Mouse Model of Diabetic Neuropathy." The journal of pain **15**(9): 907-914.

Wagner, K. M., J. Atone and B. D. Hammock (2020). "Soluble epoxide hydrolase inhibitor mediated analgesia lacks tolerance in rat models." Brain research **1728**: 146573-146573.

Wallace, J. L., P. Nagy, T. D. Feener, T. Allain, T. Ditrói, D. J. Vaughan, M. N. Muscara, G. Nucci and A. G. Buret (2020). "A proof-of-concept, Phase 2 clinical trial of the gastrointestinal safety of a hydrogen sulfide-releasing anti-inflammatory drug." British journal of pharmacology **177**(4): 769-777.

Wan, D., J. Yang, C. B. McReynolds, B. Barnych, K. M. Wagner, C. Morisseau, S. H. Hwang, J. Sun, R. Blöcher and B. D. Hammock (2019). "In vitro and in vivo Metabolism of a Potent Inhibitor of Soluble Epoxide Hydrolase, 1-(1-Propionylpiperidin-4-yl)-3-(4-(trifluoromethoxy)phenyl)urea." Frontiers in Pharmacology **10**(MAY).

Wang, C., G.-W. Li and L.-Y. M. Huang (2007). "Prostaglandin E2 Potentiation of P2X3 Receptor Mediated Currents in Dorsal Root Ganglion Neurons." Molecular pain **3**(1): 22-22.

Wang, Y. Y., A. A. Armando, O. O. Quehenberger, C. C. Yan and E. A. E. A. Dennis (2014). "Comprehensive Ultra Performance Liquid Chromatographic Separation and Mass Spectrometric Analysis of Eicosanoid Metabolites Suitable for Human Materials." Journal of chromatography. A **1359**: 60-69.

Washio, E., M. Esaki, Y. Maehata, M. Miyazaki, H. Kobayashi, H. Ishikawa, T. Kitazono and T. Matsumoto (2016). "Proton Pump Inhibitors Increase Incidence of Nonsteroidal Anti-

Inflammatory Drug–Induced Small Bowel Injury: A Randomized, Placebo-Controlled Trial." Clinical gastroenterology and hepatology **14**(6): 809-815.e801.

Watt, F. E. (2021). "Posttraumatic osteoarthritis: what have we learned to advance osteoarthritis?" Current opinion in rheumatology **33**(1): 74-83.

Watt, F. E., H. M. Ismail, A. Didangelos, M. Peirce, T. L. Vincent, R. Wait and J. Saklatvala (2013). "Src and fibroblast growth factor 2 independently regulate signaling and gene expression induced by experimental injury to intact articular cartilage." Arthritis and rheumatism **65**(2): 397-407.

Watt, F. E., E. Paterson, A. Freidin, M. Kenny, A. Judge, J. Saklatvala, A. Williams and T. L. Vincent (2016). "Acute Molecular Changes in Synovial Fluid Following Human Knee Injury: Association With Early Clinical Outcomes." Arthritis & rheumatology (Hoboken, N.J.) **68**(9): 2129-2140.

Wen, H., J. Östman, K. J. Bubb, C. Panayiotou, J. V. Priestley, M. D. Baker and A. Ahluwalia (2012). "20-Hydroxyeicosatetraenoic Acid (20-HETE) Is a Novel Activator of Transient Receptor Potential Vanilloid 1 (TRPV1) Channel." The Journal of biological chemistry **287**(17): 13868-13876.

Wolfer, A. M., M. Gaudin, S. D. Taylor-Robinson, E. Holmes and J. K. Nicholson (2015). "Development and Validation of a High-Throughput Ultrahigh-Performance Liquid Chromatography–Mass Spectrometry Approach for Screening of Oxylipins and Their Precursors." Analytical chemistry (Washington) **87**(23): 11721-11731.

Wong, A., D. R. Sagar, C. A. Ortori, D. A. Kendall, V. Chapman and D. A. Barrett (2014). "Simultaneous tissue profiling of eicosanoid and endocannabinoid lipid families in a rat model of osteoarthritis." Journal of lipid research **55**(9): 1902-1913.

Wu, C.-L., D. Jain, J. N. McNeill, D. Little, J. A. Anderson, J. L. Huebner, V. B. Kraus, R. M. Rodriguiz, W. C. Wetsel and F. Guilak (2015). "Dietary fatty acid content regulates wound repair and the pathogenesis of osteoarthritis following joint injury." Annals of the rheumatic diseases **74**(11): 2076-2083.

Wu, C., X. Chen, Y. Cai, J. Xia, X. Zhou, S. Xu, H. Huang, L. Zhang, X. Zhou, C. Du, Y. Zhang, J. Song, S. Wang, Y. Chao, Z. Yang, J. Xu, X. Zhou, D. Chen, W. Xiong, L. Xu, F. Zhou, J. Jiang, C. Bai, J. Zheng and Y. Song (2020). "Risk Factors Associated With Acute Respiratory Distress Syndrome and Death in Patients With Coronavirus Disease 2019 Pneumonia in Wuhan, China." JAMA Intern Med **180**(7): 934-943.

Xie, C. and D. H. Wang (2011). "Inhibition of Renin Release by Arachidonic Acid Metabolites, 12(s)-HPETE and 12-HETE: Role of TRPV1 Channels." Endocrinology (Philadelphia) **152**(10): 3811-3819.

Xu, T., C. Hu, Q. Xuan and G. Xu (2020). "Recent advances in analytical strategies for mass spectrometry-based lipidomics." Analytica chimica acta **1137**: 156-169.

Xu, X., X. Zhang and D. Wang (2011). "The roles of CYP450 epoxygenases and metabolites, epoxyeicosatrienoic acids, in cardiovascular and malignant diseases." Advanced Drug Delivery Reviews **63**(8): 597-609.

Xu, Z.-Z., T. Berta and R.-R. Ji (2013). "Resolvin E1 Inhibits Neuropathic Pain and Spinal Cord Microglial Activation Following Peripheral Nerve Injury." Journal of neuroimmune pharmacology **8**(1): 37-41.

Xu, Z.-Z., X.-J. Liu, T. Berta, C.-K. Park, N. Lü, C. N. Serhan and R.-R. Ji (2013). "Neuroprotectin/protectin D1 protects against neuropathic pain in mice after nerve trauma." Annals of neurology **74**(3): 490-495.

Yamaguchi, A., L. Stanger, C. J. Freedman, M. Standley, T. Hoang, R. Adili, W. C. Tsai, C. Hoorebeke, T. R. Holman and M. Holinstat (2021). "DHA 12-LOX-derived oxylipins regulate platelet activation and thrombus formation through a PKA-dependent signaling pathway." Journal of thrombosis and haemostasis **19**(3): 839-851.

Yang, X., Y. Yu, J. Xu, H. Shu, J. a. Xia, H. Liu, Y. Wu, L. Zhang, Z. Yu, M. Fang, T. Yu, Y. Wang, S. Pan, X. Zou, S. Yuan and Y. Shang (2020). "Clinical course and outcomes of critically ill patients with SARS-CoV-2 pneumonia in Wuhan, China: a single-centered, retrospective, observational study." The Lancet Respiratory Medicine **8**(5): 475-481.

Yekkirala, A. S., D. P. Roberson, B. P. Bean and C. J. Woolf (2017). "Breaking barriers to novel analgesic drug development." Nature reviews. Drug discovery **16**(8): 544-563.

Yu, D., M. Hennebelle, D. Sahlas, J. Ramirez, F. Gao, M. Masellis, H. Cogo-Moreira, R. Swartz, N. Herrmann, P. Chan, J. Pettersen, D. Stuss, S. Black, A. Taha and W. Swardfager (2019). "Soluble Epoxide Hydrolase-Derived Linoleic Acid Oxylipins in Serum Are Associated with Periventricular White Matter Hyperintensities and Vascular Cognitive Impairment." Translational Stroke Research **10**(5): 522-533.

Yu, Z., F. Xu, L. M. Huse, C. Morisseau, A. J. Draper, J. W. Newman, C. Parker, L. Graham, M. M. Engler, B. D. Hammock, D. C. Zeldin and D. L. Kroetz (2000). "Soluble Epoxide Hydrolase Regulates Hydrolysis of Vasoactive Epoxyeicosatrienoic Acids." Circulation research **87**(11): 992-998.

Zeldin, D. C. (2001). "Epoxygenase Pathways of Arachidonic Acid Metabolism." The Journal of biological chemistry **276**(39): 36059-36062.

Zeldin, D. C., C. R. Moomaw, N. Jesse, K. B. Tomer, J. Beetham, B. D. Hammock and S. Wu (1996). "Biochemical Characterization of the Human Liver Cytochrome P450 Arachidonic Acid Epoxygenase Pathway." Archives of biochemistry and biophysics **330**(1): 87-96.

Zhand, S., M. Saghaeian Jazi, S. Mohammadi, R. Tarighati Rasekhi, G. Rostamian, M. R. Kalani, A. Rostamian, J. George and M. W. Douglas (2020). "COVID-19: The Immune Responses and Clinical Therapy Candidates." International journal of molecular sciences **21**(15): 5559.

Zhang, J.-H., T. Pearson, B. Matharoo-Ball, C. A. Ortori, A. Y. Warren, R. Khan and D. A. Barrett (2007). "Quantitative profiling of epoxyeicosatrienoic, hydroxyeicosatetraenoic, and dihydroxyeicosatetraenoic acids in human intrauterine tissues using liquid chromatography/electrospray ionization tandem mass spectrometry." Analytical biochemistry **365**(1): 40-51.

Zhang, W., W. B. Robertson, J. Zhao, W. Chen and J. Xu (2019). Emerging Trend in the Pharmacotherapy of Osteoarthritis. **10**.

Zhao, P., S. G. Waxman and B. C. Hains (2007). "Extracellular Signal-Regulated Kinase-Regulated Microglia-Neuron Signaling by Prostaglandin E2 Contributes to Pain after Spinal Cord Injury." The Journal of neuroscience **27**(9): 2357-2368.

Appendix

Analyte	Structure	Full Name	HMDB Code
AA-d8	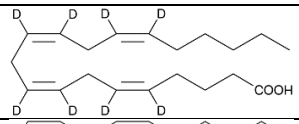	Arachidonic Acid-d8	-
AA	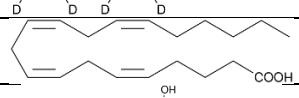	Arachidonic Acid	HMDB0001043
TBX B2	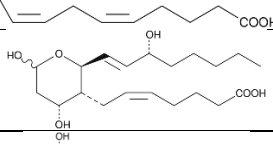	Thromboxane B2	HMDB0003252
11-dehydro-TBX B2	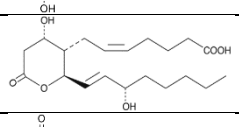	11-Dehydro-thromboxane B2	HMDB0004242
PGE2	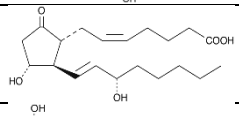	Prostaglandin E2	HMDB0001220
PGD2	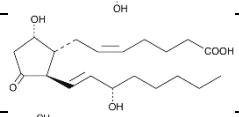	Prostaglandin D2	HMDB0001403
6-Keto-PG-F1α	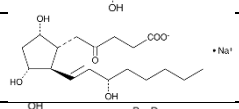	6-Keto-prostaglandin F1a	HMDB0002886
PGD2-d4	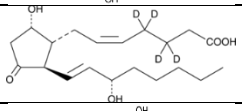	Prostaglandin D2-d4	-
LTE4	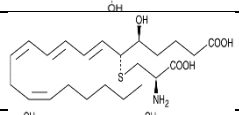	Leukotriene E4	HMDB0002200
LTB4	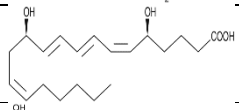	Leukotriene B4	HMDB0001085
6-trans-LTB4	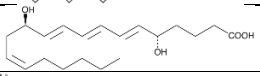	6-trans-Leukotriene B4	HMDB0005087
6-trans-12-epi-LTB4	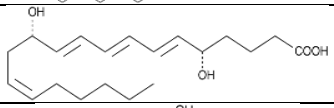	6-trans-12-epi-Leukotriene B4	HMDB0005088
5-HETE	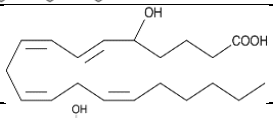	5-hydroxyeicosatetraenoic acid	HMDB0011134
8-HETE	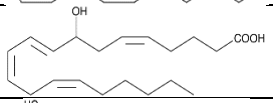	8-hydroxyeicosatetraenoic acid	HMDB0004679
9-HETE	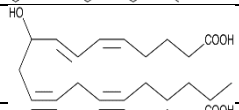	9-hydroxyeicosatetraenoic acid	HMDB0010222
11-HETE	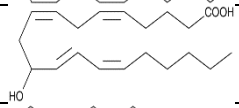	11-hydroxyeicosatetraenoic acid	HMDB0004682
12-HETE	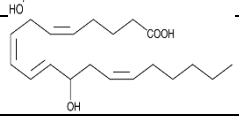	12-hydroxyeicosatetraenoic acid	HMDB0006111

15-HETE	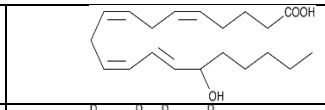	15-hydroxyeicosatetraenoic acid	HMDB0003876
15-HETE-d8	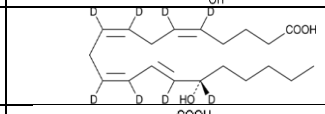	15-hydroxyeicosatetraenoic acid-d8	-
16-HETE	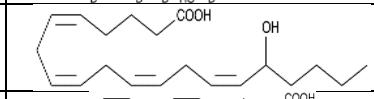	16-hydroxyeicosatetraenoic acid	HMDB0004680
19-HETE	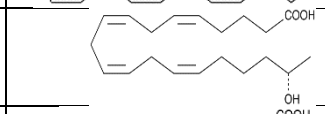	19-hydroxyeicosatetraenoic acid	HMDB0011136
20-HETE	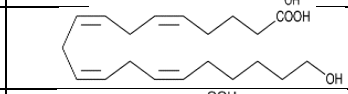	20-hydroxyeicosatetraenoic acid	HMDB0005998
5-HpETE	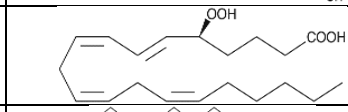	5-Hydroperoxyicosatetraenoic acid	HMDB0011135
12-HpETE	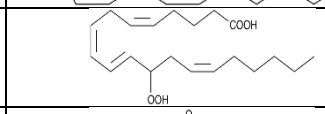	12-Hydroperoxyicosatetraenoic acid	HMDB0004243
5,6-EET	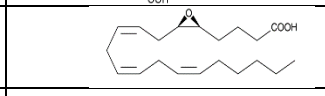	5,6-epoxyeicosatrienoic acid	HMDB0002190
8,9-EET	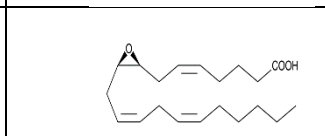	8,9-epoxyeicosatrienoic acid	HMDB0002232
11,12-EET	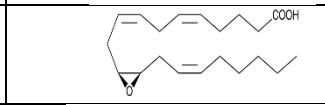	11,12-epoxyeicosatrienoic acid	HMDB0004673
14,15-EET	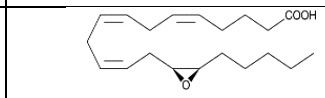	14,15-epoxyeicosatrienoic acid	HMDB0004264
5,6-DHET	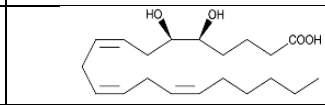	5,6-Dihydroxyeicosatrienoic acid	HMDB0002343
8,9-DHET	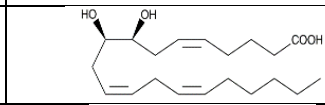	8,9-Dihydroxyeicosatrienoic acid	HMDB0002311
11,12-DHET	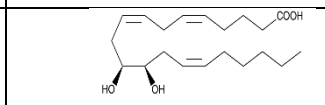	11,12-Dihydroxyeicosatrienoic acid	HMDB0002314
14,15-DHET	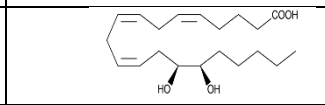	14,15-Dihydroxyeicosatrienoic acid	HMDB0002265
5(S),6(R)-DiHETE	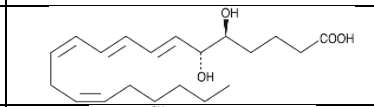	5,6-dihydroxyeicosatetraenoic acid	N/A
5,12-DiHETE	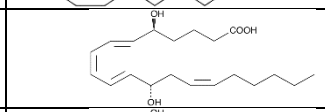	5,12-dihydroxyeicosatetraenoic acid	HMDB0062409
5,15-DiHETE	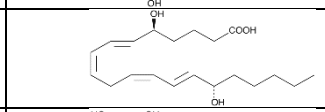	5,15-dihydroxyeicosatetraenoic acid	HMDB0010216
8,9-DiHETE	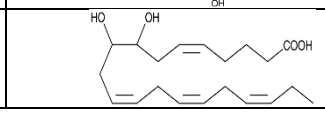	8,9-dihydroxyeicosatetraenoic acid	HMDB0002311

8,15-DiHETE	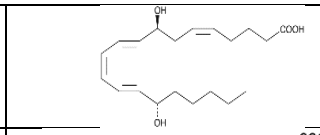	8,15-dihydroxyeicosatetraenoic acid	HMDB0010219
LA	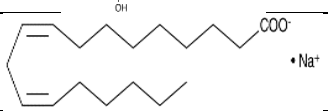	Linoleic Acid	HMDB0000673
18-HEPE	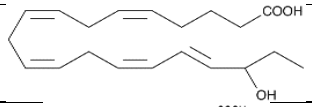	18-Hydroxyeicosapentaenoate	HMDB0012611
9-HODE	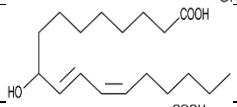	9-Hydroxyoctadecadienoic acid	HMDB0062652
13-HODE	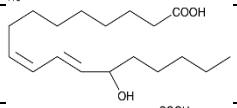	13-Hydroxyoctadecadienoic acid	HMDB0004667
9-oxoODE	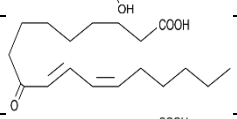	9-oxooctadecadienoic acid	HMDB0004669
13-oxoODE	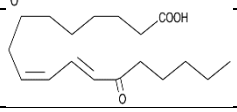	13-oxooctadecadienoic acid	HMDB0004668
17-HDHA	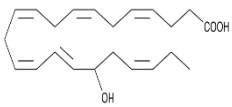	17-hydroxydocosahexaenoic acid (Historically known as 17-HDoHE)	HMDB0010213
10,17-DiHDHA	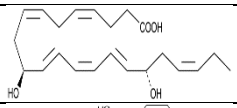	10,17-dihydroxy-docosahexaenoic acid	N/A
RvD1	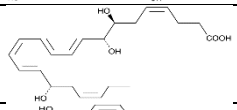	Resolvin D1	HMDB0003733
RvD2	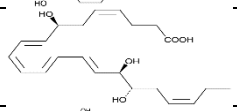	Resolvin D2	HMDB0002294
RvD3	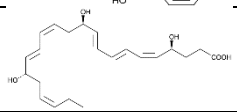	Resolvin D3	N/A
RvD4	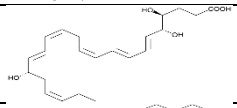	Resolvin D4	N/A
RvD5	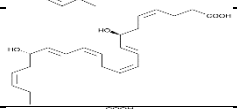	Resolvin D5	HMDB0004038
RvD2-d5	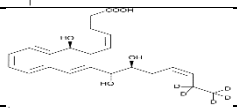	Resolvin D2-d5	N/A
PD1	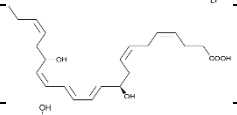	Protectin D1 (Historically known as Neuroprotectin)	HMDB0003689
RvE1	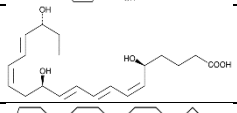	Resolvin E1	HMDB0010410
17-oxoDHA	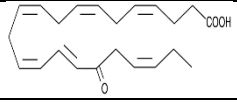	17-oxo-Docosahexaenoic Acid	N/A

LXA4	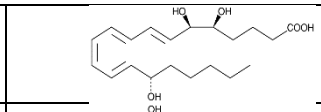	Lipoxin A4	HMDB0004385
LXB4	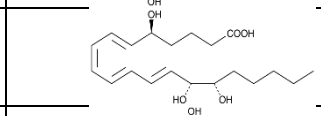	Lipoxin B4	HMDB0005082
LXA5	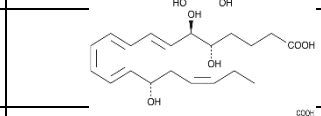	Lipoxin A5	N/A
MaR1	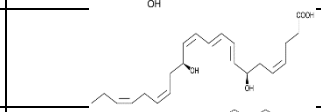	Maresin 1	HMDB0254335
MaR2	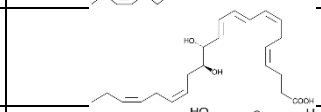	Maresin 2	N/A
PEA	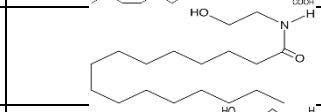	Palmitoylethanolamide	HMDB0002100
OEA	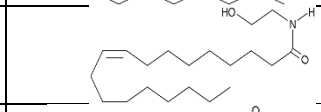	Oleoylethanolamide (also known as NOE)	HMDB0002088
2-AG		2-Arachidonyl Glycerol ether	HMDB0013657
AEA	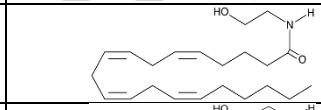	Anandamide (also known as arachidonoylethanolamide)	HMDB0004080
AEA-d8	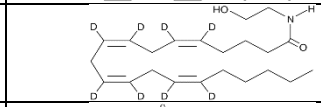	Anandamide-d8	N/A
MCTR1	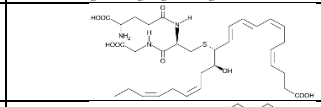	Maresin Conjugates in Tissue Regeneration 1	N/A
MCTR2	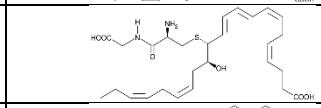	Maresin Conjugates in Tissue Regeneration 2	N/A
MCTR3	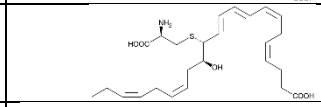	Maresin Conjugates in Tissue Regeneration 3	N/A
EPA	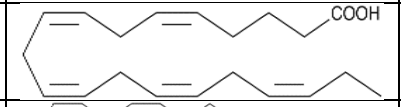	Eicosapentaenoic acid	HMDB0001999
14-HDHA	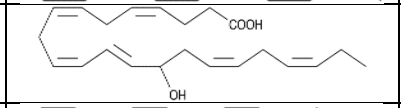	17-hydroxydocosahexaenoic acid	HMDB0060044
DHA	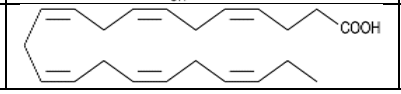	Docosahexaenoic acid	HMDB0002183

SPM Chromatograms and Enhanced Product Ion Scans – Matched spectra between reference standard and pooled biological sample

RvD4 RT 6.8 – m/z transition 375/100

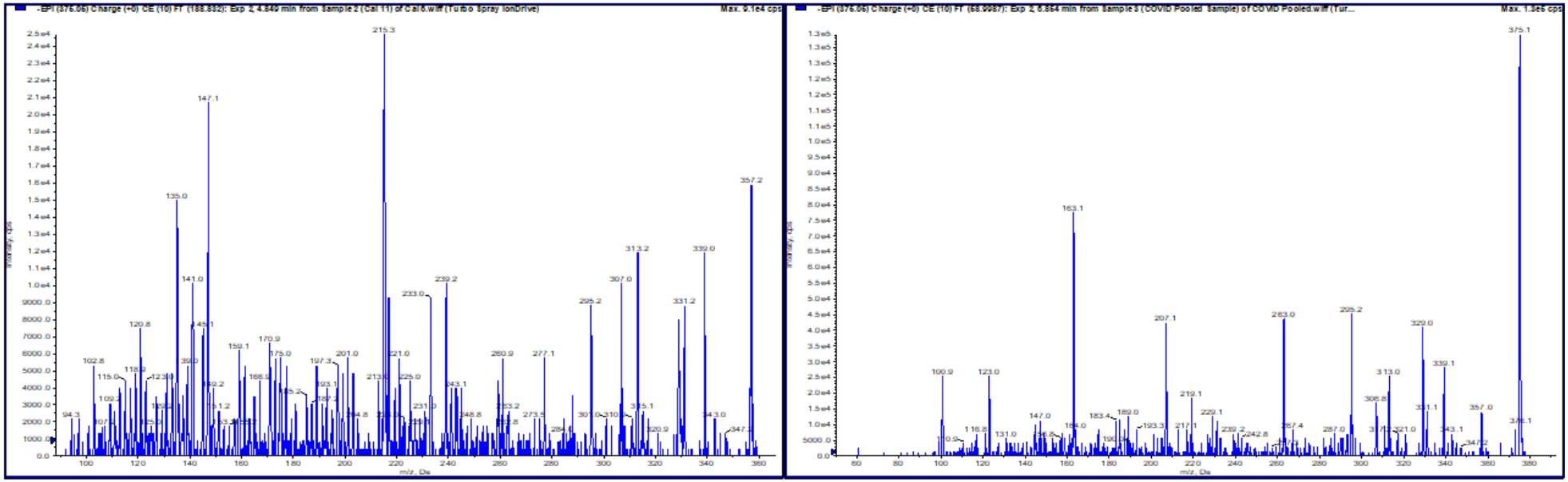

Maresin 2 RT 10 m/z 359/221

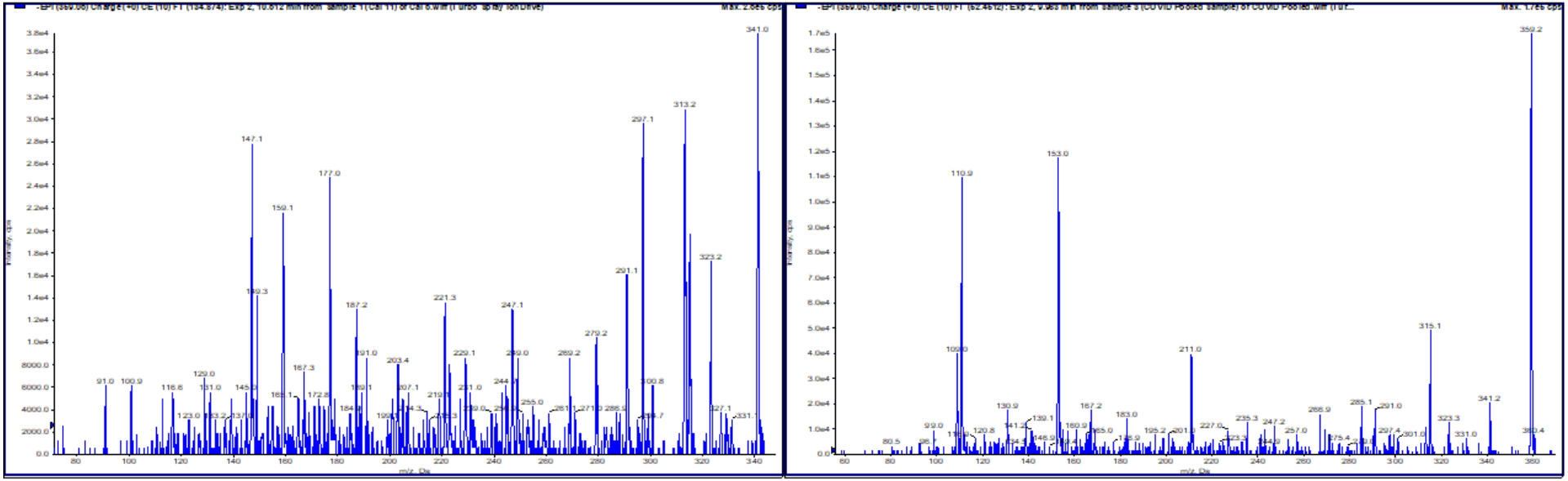

LXA4 RT: 7.1 m/z: 351/115

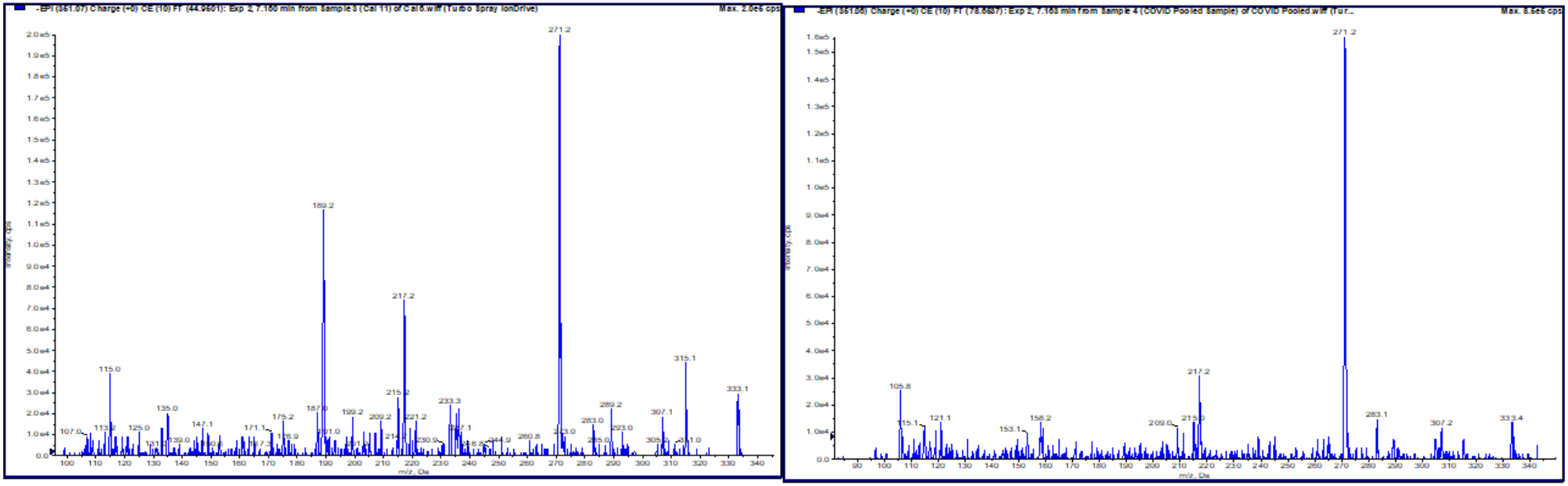

Resolvin D4

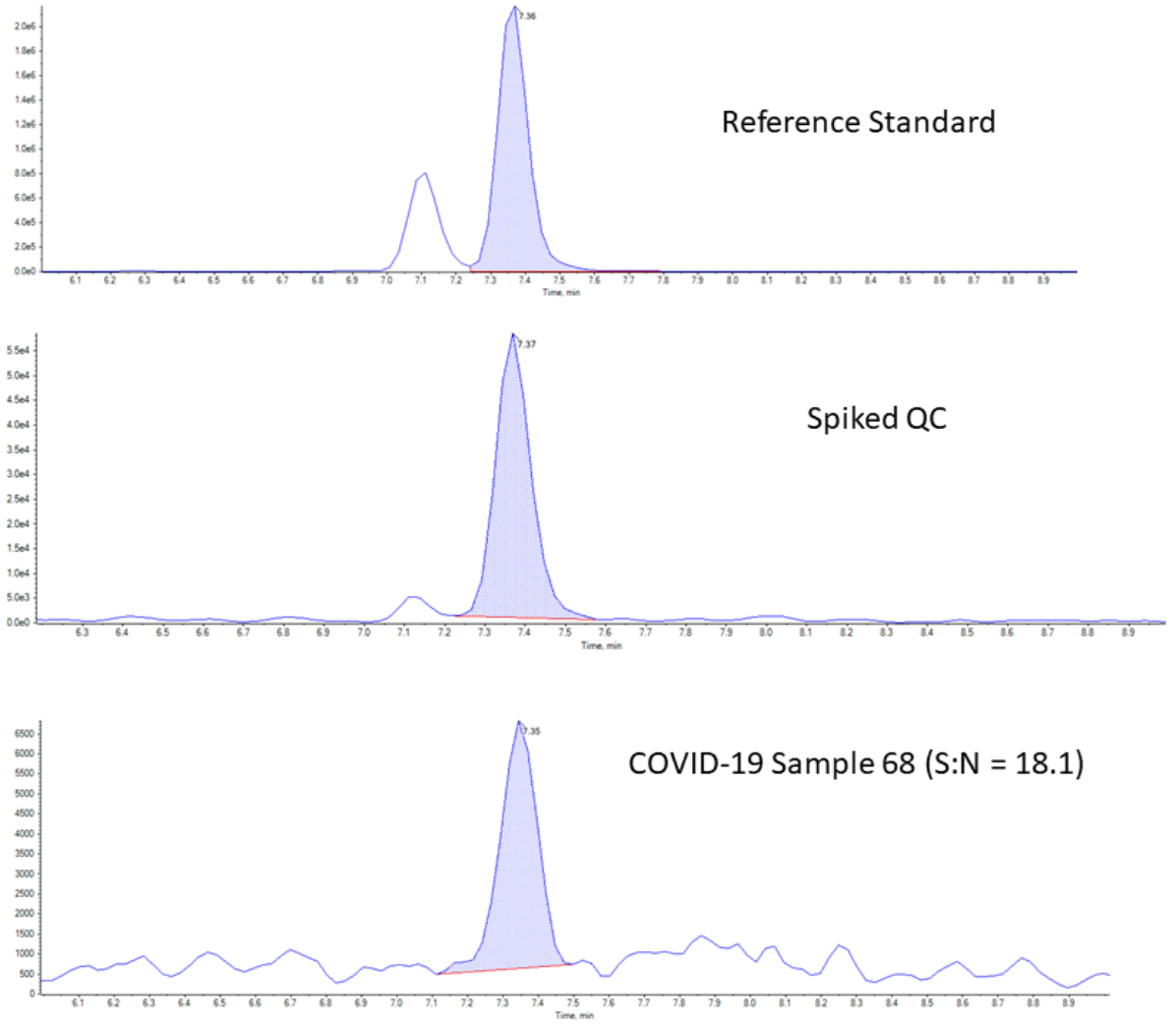
Reference Standard
Spiked QC
COVID-19 Sample 68 (S:N = 18.1)
Time, min

Lipoxin A4

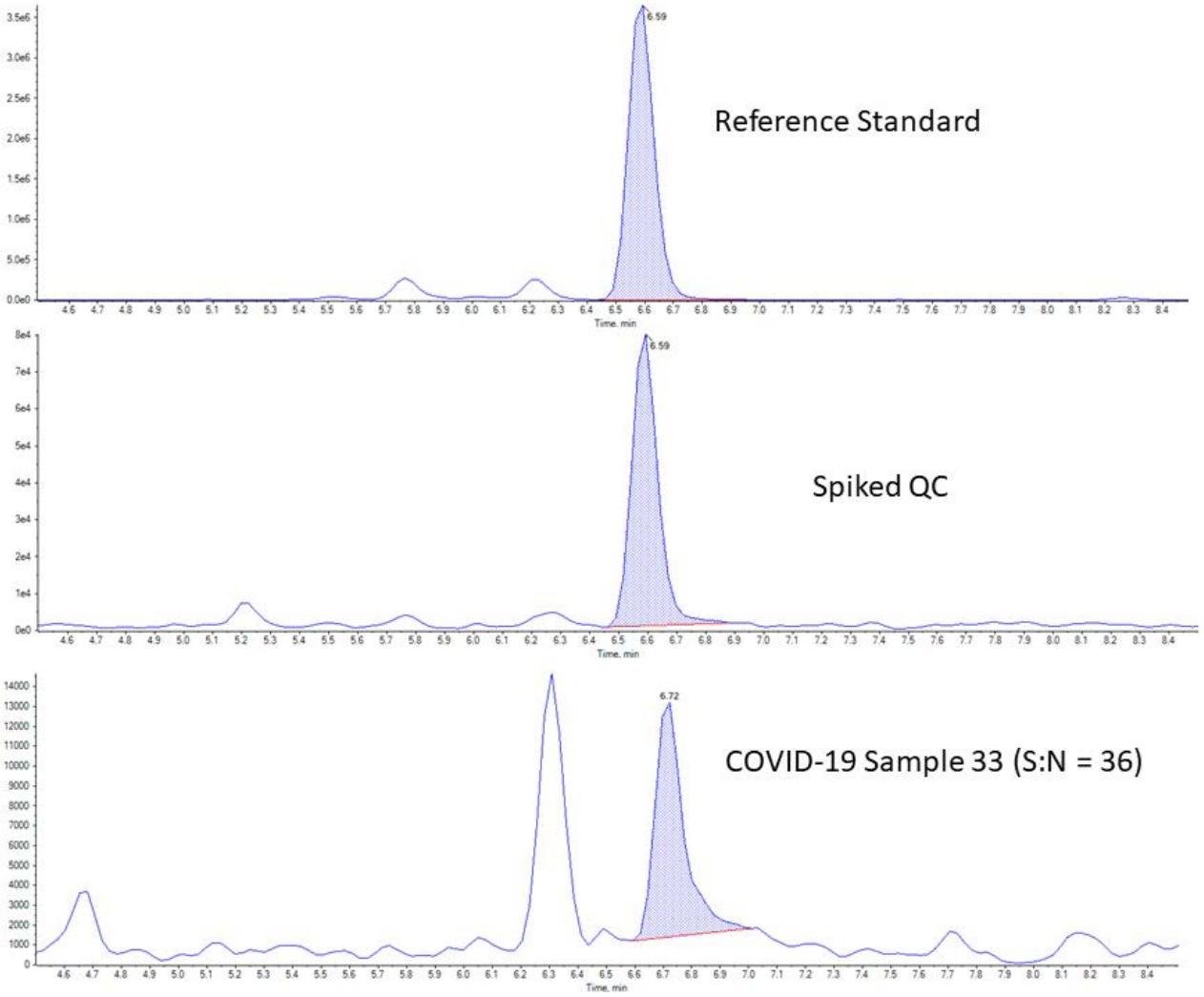
6.59
Reference Standard
6.59
Spiked QC
6.72
COVID-19 Sample 33 (S:N = 36)
Time, min

Maresin 2

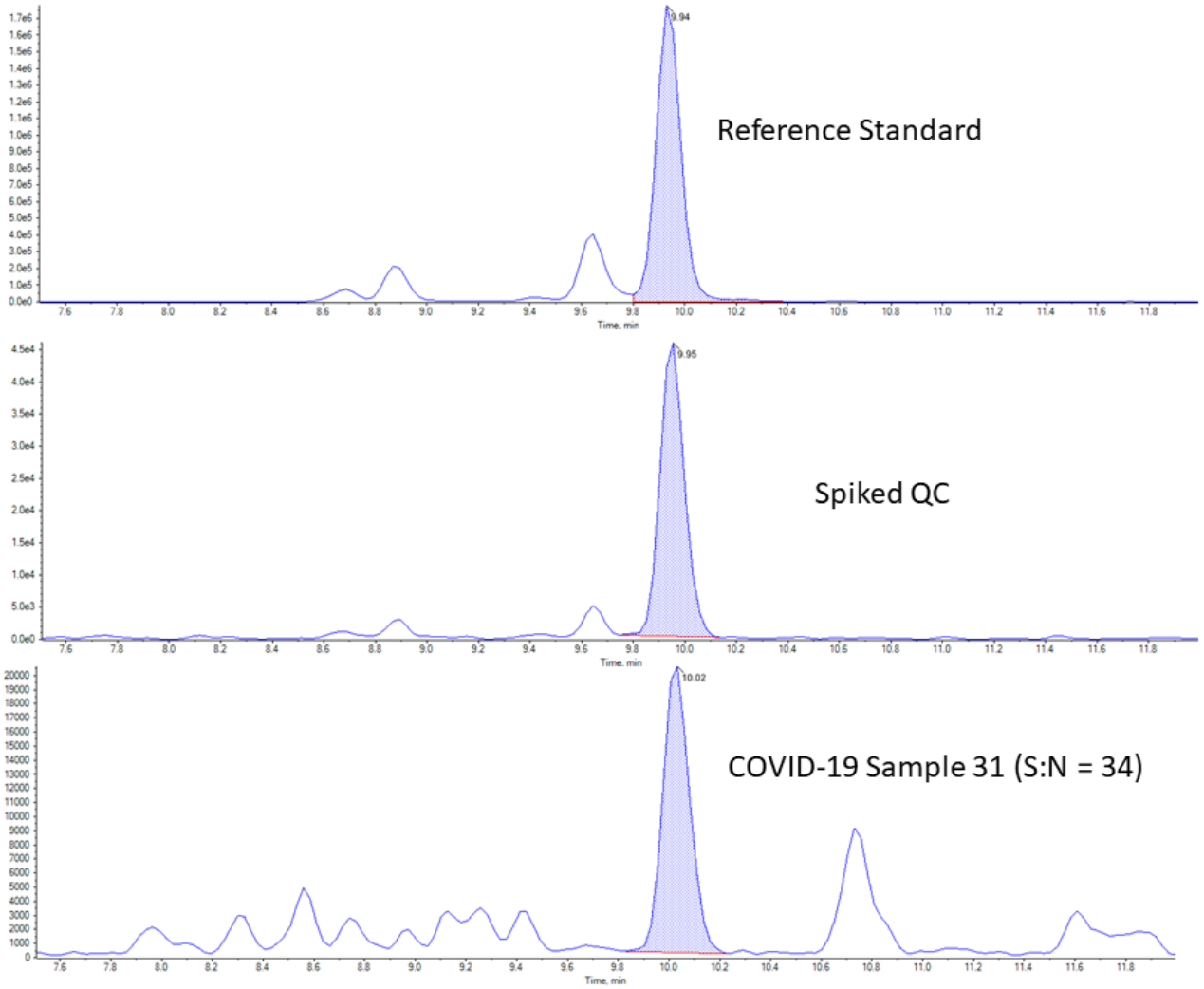
9.94
Reference Standard
Time, min
9.95
Spiked QC
Time, min
10.02
COVID-19 Sample 31 (S:N = 34)
Time, min